



HAL
open science

Thermodynamic analysis of gasification and pyrolysis of lignocellulosic biomass: parametric study, energy/exergy balance and kinetic modelling

Luis César Reyes Alonzo

► To cite this version:

Luis César Reyes Alonzo. Thermodynamic analysis of gasification and pyrolysis of lignocellulosic biomass: parametric study, energy/exergy balance and kinetic modelling. Chemical and Process Engineering. Normandie Université, 2020. English. NNT : 2020NORMIR23 . tel-03272426

HAL Id: tel-03272426

<https://theses.hal.science/tel-03272426>

Submitted on 28 Jun 2021

HAL is a multi-disciplinary open access archive for the deposit and dissemination of scientific research documents, whether they are published or not. The documents may come from teaching and research institutions in France or abroad, or from public or private research centers.

L'archive ouverte pluridisciplinaire **HAL**, est destinée au dépôt et à la diffusion de documents scientifiques de niveau recherche, publiés ou non, émanant des établissements d'enseignement et de recherche français ou étrangers, des laboratoires publics ou privés.



Normandie Université

THÈSE

Pour obtenir le diplôme de doctorat

Spécialité Génie des Procédés

Préparée au sein de « l'Institut National des Sciences Appliquées de Rouen Normandie »

Thermodynamic analysis of gasification and pyrolysis of lignocellulosic biomass: Parametric study, energy/exergy balance and kinetic modelling.

**Présentée et soutenue par
Luis César REYES ALONZO**

**Thèse soutenue publiquement le 10 décembre 2020
devant le jury composé de**

M. Anthony DUFOUR	Chargé de Recherche, CNRS, LRGP, Nancy	Rapporteur
M. Abdeslam MENIAI	Professeur, Université Constantine 3, Algérie	Rapporteur
Mme. Capucine DUPONT	Lecturer, IHE Delft, Pays Bas.	Examinatrice
M. Aïssa OULD-DRIS	Professeur des Universités, Université de Compiègne	Examineur
M. Alexis COPPALLE	Professeur des Universités, INSA de Rouen Normandie	Examineur
M. Lokmane ABDELOUAHED	MCF, INSA Rouen Normandie	Co-Encadrant de thèse
M. Jean-Christophe BUVAT	MCF, INSA Rouen Normandie	Co-Encadrant de thèse
M. Bechara TAOUK	Professeur des Universités, INSA Rouen Normandie	Directeur de thèse

Thèse dirigée par Bechara TAOUK et co-encadrée par Lokmane ABDELOUAHED et Jean-Christophe BUVAT, laboratoire de Sécurité des Procédés Chimiques- LSPC



Acknowledgments

I want to express my deepest appreciation to all the people who participated in the creation and development of this CALIOPE project, especially to the Ministry of Higher Education Science and Technology of my beloved Dominican Republic. I also wish to thank Dr. Anthony Dufour and Professor Abdeslam Meniai for having agreed to be the reviewers of my thesis. Furthermore, Dr. Capucine Dupont, Professor Aissa Ould-Dris and Professor Alexis Coppalle, I wish to thank all of you for accepting the role and taking the time in this complicated period to be part of my jury.

To my thesis director, Bechara Taouk, sincerely there are no words to express my sincere gratitude to you: since day one, your help and attention were always there for me. I am so grateful to be part of the history of the number people that you have worked with. It has been an honour working with you sir. I also wish to warmly thank Dr. Jean-Christophe Buvat for your help and presence in my thesis. To my dear colleague, professor, supervisor and friend, Lokmane, I think the word “thanks” is not enough to describe how great and valuable was your presence in my thesis. Man, you were my mentor! I am so proud of the team Bechara-Lokmane-Chetna-Luis. You will never be forgotten. A special word to my friend Chetna: thank you very much for introducing me to this beautiful subject; your help to my thesis and adaptation to this new environment was immeasurable: inside, outside and beyond you were always a friend.

To all the people that were always there for me in the laboratory (LSPC) to help in the development of my thesis, especially Sylvie, Emmanuelle, Catherine, Maria, Rafael, Jeremy, Axelle, Abdellah, Christine, and Fatima, thank you. A special word to Bruno: without you, nothing, would have been done, my friend. I also want to thank all the current and past Ph.D. students and interns for all the moments of science and joy that we have shared.

To my CALIOPE I friends, thanks, all of you. Today this journey comes to an end. Beyond work, sharing moments with you was crucial for my thesis, and big mentions go to Silvia, Lilivet, Milly and Wilson. Maxwell, my friend and sports coach, thanks for your friendship: our discussions about science were very important for writing my work, and this journey was easier alongside to you. I also want to thank all my family for and wife family for their support and motivation through this process, my dad, my mom, my big brother and aunts. You have always been my strongest motivation. Final words to my eternal partner and love, Léa, I just cannot imagine doing this thesis without your dedication and motivation. Thank you very much for being the electricity for my motor. We started as two and now we are three with Gabrielle. There is still a long way to go. I love you both.

Symbol and abbreviations

Symbols

A_0	Pre-exponential factor [$s^{-1} atm^{-n}$]
C.	Carbon [wt. %]
C_p	Heat Capacity [MJ/kmol K]
D_p	Particle diameter (mm)
E_a	Activation energy [kJ/kmol]
\dot{E}_n	Energy rate [MJ/kg _{biomass}]
\dot{E}_x	Exergy rate [MJ/kg _{biomass}]
$e_{x, ch}$	Standard chemical exergy [kJ/kmol]
$f(X)$	Consumption mechanism of char [-]
H	Hydrogen [wt. %]
H/C	Hydrogen/Carbon molar ratio [-]
$(h-h^\circ)$	Specific enthalpy difference [kJ/kmol]
I	Exergy destruction term [MJ/kg _{biomass}]
k	Apparent reaction constant [s^{-1}]
LHV_{fuel}	Low heating Value of fuel [MJ/kg _{biomass}]
LHV_{syngas}	Low heating Value of syngas [MJ/kg]
m	Mass [g]
m_0	Initial mass [g]
m_t	Mass at time (t) [g]
m_{f-af}	Final mass-ash free [g]
Mw	Molecular weight [g/mol]
n	Mol flow rate [mol/kg _{biomass}]
N.	Nitrogen [wt. %]
O/C	Oxygen/Carbon molar ratio [-]

P_i	Partial pressure [atm]
P°	Reference pressure [atm]
\dot{Q}_{loss}	Loss energy rate [MJ/kg _{biomass}]
$E_{X_{\text{loss}}}$	Loss exergy rate [MJ/kg _{biomass}]
r	Reaction rate [s ⁻¹]
r_{50}	Reaction rate at 50% conversion [s ⁻¹]
R	Gas constant [8.314 J/K mol]
S_i	Sulfur [wt. %]
$(s-s^\circ)$	Specific entropy difference [kJ/kmol]
t	Time [min]
T°	Reference Temperature [°C]
T	Temperature [°C]
T_w	Temperature of walls [°C]
x	Molar fraction [%]
X	Conversion [-]

Subscripts

Ch	Chemical.
in	inlet
i	i th species.
Ki	Kinetic.
out	outlet
Ph	Physical.
Po	Potential.

Abbreviations

A.C.	Ash content [wt. %]
AC	Aromatic compounds

C.G.E.	Cold Gas efficiency [%]
F.C.	Fixed Carbon [wt. %]
FBR	Fluidized bed reactor
HAC	Heterocyclic aromatic compounds
HPAH	High poly-aromatic hydrocarbons
M.	Moisture [wt. %]
V.M.	Volatile matter [wt. %]
VM	Volumetric Model
LHV	Low Heating Value [MJ/kg _{biomass}]
LPAH	Light poly-aromatic compounds
PLM	Power Law Model
SCM	Shrinking Core Model
TGA	Thermogravimetric Analyzer

Greek letters

Δh	Enthalpy change [kJ/kmol]
β	Non-conventional fuels exergy factor [-]
η	Energy efficiency [%]
Ψ	Exergy efficiency [%]
τ	Residence time of vapors (s)

Abstract

The detailed thermodynamic analysis of biomass conversion by pyrolysis and gasification was studied in this thesis work. The analysis was based on the calculation of the energy balance and exergy evaluation according to the operating conditions. The presence of a catalyst, the temperature and the gasification agent effect were studied in the case of gasification in a fluidized bed reactor. It was observed that energy demand increases with the temperature as well as the exergy destruction rate. It was also found that high-temperature pyrolysis requires less energy than gasification with carbon dioxide. In addition, the use of a biochar catalytic bed for gasification increases the exergy destruction rate but also increases the exergetic efficiency of the syngas. Comparison between the two gasification agents, steam and carbon dioxide, showed that steam gasification was thermodynamically more efficient, as less entropy was generated and less energy was required.

Study of the biomass pyrolysis in a semi-continuous reactor coupled with catalytic deoxygenation was also carried out. It was found that deoxygenation in the presence of the HZSM-5 catalyst decreases the exergy destruction rate of the process, while the energy requirements were roughly doubled. The thermodynamic analysis of the catalytic and non-catalytic pyrolysis of biomass components (cellulose, hemicellulose and lignin) was also performed, the analysis showing that the pyrolysis of individual components required less heat input than the pyrolysis of biomass. Also, less irreversibility was observed during the conversion of pseudo-components compared to that of biomass.

The last part of the thesis concerns kinetic modelling of the gasification reaction of biochar with carbon dioxide in a fluidized bed reactor. The kinetic model was compared to that developed for a thermogravimetric study. The results showed that despite the use of identical gasification conditions in both systems, the kinetic model developed differs from one case to another. The difference was attributed to the fact that the heat and mass transfer process is not the same in the two cases.

Résumé

L'analyse thermodynamique détaillée de la conversion de la biomasse par pyrolyse et gazéification a été étudiée dans ce travail de thèse. Cette analyse est basée sur le calcul des bilans énergétiques et exergétiques en fonction des paramètres opératoires. L'effet de la présence d'un catalyseur, de la température et de l'agent de gazéification ont été étudiés dans le cas de la gazéification en réacteur à lit fluidisé. Il a été observé que la demande énergétique augmentait avec la température, ainsi que le taux de destruction de l'exergie. Il a aussi été mis en évidence que la pyrolyse à haute température nécessitait moins d'énergie que la gazéification avec le dioxyde de carbone. De plus, l'utilisation d'un lit catalytique de biocharbon pour la gazéification augmente le taux de destruction d'exergie, mais augmente aussi l'efficacité exergetique du gaz de synthèse. La comparaison entre les deux agents de gazéifications, la vapeur d'eau et le dioxyde de carbone, a révélé que la gazéification avec la vapeur d'eau est thermodynamiquement plus efficace, en effet moins d'entropie est générée et moins d'énergie est requise.

L'étude de la pyrolyse de la biomasse en réacteur semi-continu couplée à une désoxygénation catalytique a été également menée. Il a été constaté que la désoxygénation en présence du catalyseur HZSM-5 fait diminuer le taux de destruction exergétique du procédé alors que la demande énergétique est multipliée approximativement par deux. L'analyse thermodynamique de la pyrolyse catalytique et non catalytique des composants de la biomasse (cellulose, hémicellulose et lignine) a été enfin réalisée. Cette analyse a montré que la pyrolyse des composants séparés nécessitait moins d'énergie que la pyrolyse de la biomasse. Aussi, moins d'irréversibilité est notée lors de la conversion des pseudo-composants comparée à celle de la biomasse.

La dernière partie de la thèse concerne la modélisation cinétique de la réaction de gazéification du biochar avec le dioxyde de carbone dans un réacteur à lit fluidisé. Le modèle cinétique a été comparé à celui développé pour l'analyse thermogravimétrique ATG. Les résultats ont montré que malgré l'utilisation de conditions identiques de gazéification dans les deux systèmes, le modèle cinétique développé diffère d'un cas à l'autre. Cette différence a été attribuée au fait que le processus de transfert de matière et de chaleur n'est pas identique dans les deux cas.

Table of contents

Acknowledgments	2
Symbol and abbreviations	3
Abstract.....	5
Résumé.....	6
General introduction	20
Literature review.....	26
1. Biomass.....	27
1.1. Lignocellulosic biomass.....	27
2. Thermochemical conversion of biomass	29
2.1. Pyrolysis.....	29
2.1.1 Pyrolysis heat requirement.....	31
2.1.2 Catalytic pyrolysis heat requirements.....	32
2.2 Gasification	34
2.2.1 Steam gasification.....	35
2.2.2 CO ₂ gasification.....	36
2.2.3 Gasification heat requirement	36
3. Thermodynamic efficiency	40
3.1 Energy efficiency	40
3.2 Cold gas efficiency	40
3.3 Exergetic efficiency.....	41
4. Kinetic modelling of gasification	41
5. Conclusion.....	44
Material, methods and set-ups.	46
1. Materials used	47
1.1 Biomasses.....	47
1.2 Woody pseudo-components.....	47
1.3 Catalysts used.....	48
1.4 Biochar preparation	49
2. Experimental set-ups	49

2.1 Semi-continuous reactor.....	49
2.2 Fluidized bed reactor.....	50
2.3 Thermogravimetric analyzer.....	53
3. Analytical set-up and methods.....	54
3.1 Gaseous products.....	54
3.2 Liquid products.....	54
3.3 Pyrolysis oil classification.....	55
3.4 Tar classification.....	56
4. Energy balance.....	58
5. Exergy evaluation.....	61
6. Efficiency calculation.....	63
6.1 Energy efficiency (η).....	63
6.2 Cold gas efficiency (CGE).....	63
6.3 Exergetic efficiency (Ψ).....	63
Thermodynamic analysis of biomass and pseudo-components pyrolysis in a semi-continuous reactor.....	64
1. Pyrolysis of beech wood and flax shives.....	66
1.1 Energetic and exergetic evaluation of biomass pyrolysis products.....	68
1.2 Heat for pyrolysis and exergy destruction rate.....	71
2. Catalytic pyrolysis of beech wood and flax shives.....	73
2.1 Energetic and exergetic evaluation of catalytic pyrolysis on products.....	76
2.2 Heat for pyrolysis and exergy destruction rate.....	78
3. Pyrolysis of biomass pseudo-components.....	80
3.1 Energetic and exergetic evaluation of pseudo-components pyrolysis on products.....	81
3.2 Heat for pyrolysis and exergy destruction.....	86
4. Catalytic pyrolysis of biomass pseudo-components.....	87
4.1 Energetic and exergetic evaluation of catalytic pyrolysis of biomass pseudo-components.....	89
4.2 Heat for pyrolysis and exergy destruction rate.....	92

4. Conclusions	93
Thermodynamic analysis of biomass gasification in a fluidized bed reactor	95
1. Biomass gasification with carbon dioxide	97
1.1 Effect of gasification temperature on energy and exergy rate of products.....	102
1.2 Heat requirement.....	105
2.1 Comparison of pyrolysis and gasification with CO ₂ of biomass in terms of energy and exergy rate of products.....	107
2.2 Heat requirement.....	111
3. Steam and CO ₂ gasification of biomass with biochar as a bed material	112
3.1 Effect of varying gasification agent in terms of energy and exergy rate of products	114
3.2 Heat requirement.....	117
4. Thermodynamic efficiency	119
4.1 Cold gas efficiency- CGE.....	119
4.2 Exergetic efficiency.....	120
5. Conclusion.....	122
Development of a kinetic model of biochar gasification with CO ₂	124
1. Effects of gasification temperature on biochar consumption.....	125
2. Effect of partial pressure on biochar consumption.....	128
3. Effect of CO ₂ /C ratio on biochar consumption	130
4. Development and selection of the kinetic model.....	131
4.1 Kinetic models studied.....	132
4.1.1 Volumetric Model (VM).....	132
4.1.2 Shrinking Core Model (SCM)	132
4.1.3 Power-law Model (PLM).....	132
4.2 Kinetic model for TG analysis.	133
4.3 Kinetic model in fluidised bed reactor	137
4.4 Further discussion	141
5. Conclusion.....	145

General conclusions and perspectives	146
Conclusions	147
Perspectives	149
References.....	151
Appendix	173
Appendix A1	174
Appendix A.2	188
Appendix A3	189
Appendix A4	215

Table of figures

Figure i. Thesis development scheme.	24
Figure ii. Proposed scheme for simulation in Aspen plus, determination of the overall energy and exergy of the process.	149
Figures Chapter 1.	
Figure 1.1. Biomass structural composition [14].	28
Figure 1.2. Biomass pyrolysis common schema.	29
Figure 1.3. Biomass pyrolysis products evolution with temperature [19].	30
Figure 1.4. Bio-oil molecules deoxygenation schema (adapted from Kay Lup et al. [48]).	33
Figure 1.5. Gasification of solid fuels scheme (adapted from Higman et al. [58]).	35
Figure 1.6. Major gases obtained from gasification.	37
Figures Chapter 2.	
Figure 2.1. Experimental set-up (fixed bed reactor)	49
Figure 2.2. Fluidized bed reactor set-up.	50
Figure 2.3. Thermogravimetric analyzer set-up.	54
Figure 2.4. Chromatogram GC-MS of tar obtained from gasification with CO ₂	57
Figure 2.5. Streams input and output from the reactor.	59
Figures Chapter 3.	
Figure 3.1. Energy distribution of products from biomasses at 500°C, a) MJ/kg _{biomass} b) MJ/kg _{phase}	66
Figure 3.2. Exergy distribution of products from biomasses at 500°C, a) MJ/kg _{biomass} b) MJ/kg _{phase}	68
Figure 3.3. Energy distribution of gases from biomasses at 500°C, a) MJ/kg _{biomass} b) MJ/kg _{phase}	70
Figure 3.4. Energy and b) Exergy distribution of chemical families in bio-oil from beech wood and flax shives at 500°C.	71
Figure 3.5. Heat for pyrolysis and exergy destruction b) exergetic efficiency of beech wood and flax shives pyrolysis at 500°C.	72
Figure 3.6. Energy product distribution for beech wood b) MJ/kg _{Biomass} , b) MJ/kg _{Phase} at 500°C.	74
Figure 3.7. Exergy product distribution for beech wood b) MJ/kg _{Biomass} , b) MJ/kg _{Phase} at 500°C.	74
Figure 3.8. Energy product distribution for flax shives b) MJ/kg _{Biomass} , b) MJ/kg _{Phase} at 500°C.	75

Figure 3.9. Exergy product distribution for flax shives b) MJ/kg _{Biomass} , b) MJ/kg _{Phase} at 500°C.	75
Figure 3.10. Energy product distribution of gases for a) beech wood and b) flax shives at 500°C.	77
Figure 3.11. Energy product distribution of bio-oil families for a) beech wood (MJ/kg _{Biomass}), b) flax shives (MJ/kg _{Biomass}), c) beech wood (MJ/kg _{Bio-oil}) and d) flax shives (MJ/kg _{Bio-oil}) at 500°C.	78
Figure 3.12. Energy Heat for pyrolysis and exergy destruction for a) beech wood and b) flax shives with and without catalyst treatment at 500°C.	79
Figure 3.13. Energy distribution of pyrolysis products, for cellulose, hemicellulose and lignin at 500°C.	80
Figure 3.14. Exergy distribution of pyrolysis products, for cellulose, hemicellulose and lignin at 500°C.	81
Figure 3.15. Exergy distribution of gaseous components, for cellulose, hemicellulose and lignin at 500°C.	83
Figure 3.16. a) Energy and b) exergy distribution of chemical families in bio-oil, for cellulose, hemicellulose and lignin at 500°C.	85
Figure 3.17. Heat for pyrolysis and exergy destruction, b) exergetic efficiency of biomass components at 500°C.	87
Figure 3.18. a) Energy balance, b) exergy evaluation for catalytic pyrolysis of cellulose at 500°C.	88
Figure 3.19. a) Energy balance, b) exergy evaluation for catalytic pyrolysis of hemicellulose at 500°C.	88
Figure 3.20. a) Energy balance, b) exergy evaluation for catalytic pyrolysis of lignin at 500°C.	89
Figure 3.21. Energy distribution of gaseous components for catalytic pyrolysis of lignin at 500°C.	90
Figure 3.22. Energy distribution of gaseous components for catalytic pyrolysis of cellulose (up) and hemicellulose (down) at 500°C.	90
Figure 3.23. Heat for pyrolysis and exergy destruction with the catalytic treatment of biomass components at 500°C.	93

Figures Chapter 4.

Figure 4.1. Effect of temperature on energy/exergy products distribution of gasification with CO ₂	97
Figure 4.2. Chemical and physical exergy products distribution of gasification with CO ₂	101
Figure 4.3. Energy and exergy difference for biochar and biomass, gasification with CO ₂ . .	102

Figure 4.4. Syngas energy and exergy value evolution with temperature, gasification with CO ₂ .	104
Figure 4.5. Effect of temperature on a) energy, b) exergy distribution of syngas components, gasification with CO ₂ .	105
Figure 4.6. Effect of temperature in the heat input for CO ₂ gasification.	106
Figure 4.7. Energy a) and exergy b) products distribution for pyrolysis and gasification with CO ₂ at 800°C and 900°C.	107
Figure 4.8. Energy distribution of syngas components for pyrolysis and gasification with CO ₂ at 800°C and 900°C.	110
Figure 4.9. Exergy distribution of syngas components for pyrolysis and gasification with CO ₂ at 800°C and 900°C.	110
Figure 4.10. Heat for pyrolysis vs heat for gasification with CO ₂ at 800°C and 900°C.	111
Figure 4.11. Energy distribution of products for a) CO ₂ and b) Steam gasification with biochar bed.	112
Figure 4.12. Chemical and physical exergy distribution of products for a) steam and b) CO ₂ gasification with biochar bed.	113
Figure 4.13. Exergy destruction for steam and CO ₂ gasification with biochar bed.	114
Figure 4.14. Syngas components energy distribution for a) CO ₂ and b) Steam gasification with biochar bed.	116
Figure 4.15. Syngas components exergy distribution for a) Steam and b) CO ₂ gasification with biochar bed.	117
Figure 4.16. Heat input for steam and CO ₂ gasification with biochar bed.	118

Figures Chapter 5.

Figure 5.1. Comparison between TGA and FBR results. Effect of reaction temperature on biochar conversion: pressure 0.67 atm and CO ₂ /C ratio 7.05.	126
Figure 5.2. Effect of temperature on r ₅₀ for TGA and FBR: pressure 0.67 atm and CO ₂ /C ratio: 7.05.	128
Figure 5.3. Comparison between TGA and FBR. Effect of CO ₂ partial pressure on biochar conversion: Temperature 1000°C and CO ₂ /C ratio 7.05.	129
Figure 5.4. Effect of the partial pressure of CO ₂ on r ₅₀ for TGA and FBR: Temperature 1000°C and CO ₂ /C ratio 7.05.	130
Figure 5.5. Effect of CO ₂ /C ratio on biochar conversion for TGA: Temperature 1000°C and pressure of CO ₂ 0.67 atm.	131
Figure 5.6. Reaction models data plots in reduced times for isothermal solid conversion (adapted from Vyazovkin et al. [16]).	133

Figure 5.7. Fitting results between $\ln r$ and $\ln P_{CO_2}$, reaction order determination. Temperature 1000°C and CO_2/C 7.01.	134
Figure 5.8. Fitting results between $\ln k(T)$ as a function of $1/T$: kinetic parameter determination for TGA. CO_2 pressure 0.67 atm and CO_2/C 7.01.....	135
Figure 5.9. Conversion curves for biochar gasification and calculated conversion with the selected models for TGA: CO_2 pressure 0.67 atm and CO_2/C 7.01.	137
Figure 5.10. Fitting results between $\ln r$ and $\ln P_{CO_2}$, reaction order determination for FBR. Temperature: 1000°C and $CO_2/C/$ 7.01.	138
Figure 5.11. Fitting results of $\ln k (T)$ as a function of $1/T$, kinetic parameters determination for FBR. CO_2 pressure: 0.67 atm and CO_2/C : 7.01.	139
Figure 5.12. Conversion curves for biochar gasification and calculated conversion with selected model for FBR. CO_2 pressure: 0.67 and CO_2/C : 7.01.	140
Figure 5.13. Validation of conversion curves of experimental test and shrinking core model (SCM), partial pressure effect. Temperature: 1000°C and CO_2/C : 7.01.	140
Figure 5.14. Hypothetical mechanism of biochar gasification in TGA (up) and FBR (down).	142
Figure 5.15. Biochar gasification kinetic model comparison with the literature at fixed conditions, for TGA. Temperature: 1000°C and CO_2 pressure: 1 atm.....	143
Figure 5.16. Biochar gasification kinetic model comparison with the literature at fixed conditions, for FBR. Temperature: 1000°C and CO_2 pressure: 1 atm.	144

Figures Appendix 1.

Figure A1.1. Products yield from the pyrolysis of beech wood and flax shives at 500°C.	177
Figure A1.2. The volumetric flow of individual gases from the pyrolysis of biomasses at 500°C.	179
Figure A1.3. The molar fraction of individual chemical families in bio-oil at 500°C.....	180
Figure A1.4. Mass balance of the pyrolysis of biomass components, cellulose, hemicellulose and lignin at 500°C.....	181
Figure A1.5. The volumetric flow of individual gases from the pyrolysis of cellulose, hemicellulose and lignin at 500°C.....	182
Figure A1. 6. The molar fraction of individual chemical families in bio-oil, from cellulose, hemicellulose and lignin at 500°C.....	183
Figure A1.7. Mass balance of the obtained products from the catalytic treatment of beech wood at 500°C.	184
Figure A1.8. Mass balance of the obtained products from the catalytic treatment of flax shives at 500°C.	184

Figure A1.9. Oxygen content in bio-oil after catalytic treatment of beech wood and flax shives at 500°C.	185
Figure A1.10. Mass balance of catalytic treatment of cellulose at 500°C.	186
Figure A1.11. Mass balance of catalytic treatment of hemicellulose at 500°C.	186
Figure A1.12. Mass balance of catalytic treatment of lignin at 500°C.....	187
Figure A1.13. Oxygen content of pseudo-components after catalytic treatment at 500°C...188	

Figures Appendix 3.

Figure A3.1. Effect of temperature in product yields obtained from gasification with CO ₂ . ..	190
Figure A3.2. Effect of temperature in the volumetric flow of individual syngas components. Gasification with CO ₂	191
Figure A3.3. Effect of temperature in syngas molar concentration of individual gas components. Gasification with CO ₂	192
Figure A3.4. Effect of temperature in tar concentration in the syngas. Gasification with CO ₂	193
Figure A3.5. Effect of temperature in the concentration distribution of tars. Gasification with CO ₂	194
Figure A3.6. Evolution with the temperature of the major tar compounds. Gasification with CO ₂	194
Figure A3. 7. Fluidized bed regimes for solid particles (adapted from Levenspiel et al. [6]).	195
Figure A3.8. Effect of the residence time of gases in the mass balance of products. Gasification with CO ₂	196
Figure A3.9. Mass balance comparison from high-temperature pyrolysis and gasification with CO ₂ at 800°C and 900°C.....	197
Figure A3.10. Volumetric flow rate comparison with pyrolysis and gasification with CO ₂ at 800°C and 900°C.	198
Figure A3.11. a) syngas molar concentration, b) H ₂ /CO ratio evolution for pyrolysis, and gasification with CO ₂ at 800°C and 900°C.	199
Figure A3.12. Tar concentration organized by class type for pyrolysis and CO ₂ gasification at 800°C and 900°C.	200
Figure A3.13. Effect of biomass particle size in product distribution in gasification with CO ₂ at 900°C.	201
Figure A3.14. Example of gasification atmosphere for low and high particle size.	202
Figure A3.15. Effect of biomass particle size in the volumetric flow rate of syngas components. Gasification with CO ₂ at 900°C.	203
Figure A3.16. Schematic of biomass particle structure.	203

Figure A3.17. Effect of particle size in tar concentration in syngas.	204
Figure A3.18. Effect of particle size in tar classification distribution. Gasification with CO ₂ at 900°C.	204
Figure A3.19. Effect of biochar bed quantity in product distribution. Gasification with CO ₂ at 900°C.	205
Figure A3.20. Effect of biochar bed quantity in syngas components molar fraction. Gasification with CO ₂ at 900°C.	207
Figure A3.21. Effect of biochar bed quantity in syngas components volumetric flow rate. Gasification with CO ₂ at 900°C.	207
Figure A3.22. Effect of biochar bed quantity in tar concentration and conversion. Gasification with CO ₂ at 900°C.	208
Figure A3.23. Effect of temperature in gasification with CO ₂ using biochar as bed material.	210
Figure A3.24. Effect of temperature in gasification with steam using biochar as bed material.	210
Figure A3.25. Effect of temperature in syngas components molar concentration with steam and CO ₂ using biochar as bed material.	212
Figure A3.26. Effect of temperature in tar concentration for CO ₂ and steam gasification. ...	213
Figure A3.27. Effect of temperature in the conversion of tar molecules for steam and CO ₂ gasification.	214

Figures Appendix 4.

Figure A4.1. Validation of conversion curves of experimental test and power-law model (PLM), partial pressure effect, Temperature 1000°C and CO ₂ /C ratio 10.5.	215
Figure A4.2. Validation of conversion curves of experimental test and power-law model (PLM), partial pressure effect, Temperature 1000°C and CO ₂ /C ratio 3.5.	215

Table of tables

Table i. Fuels consumption shares and contributions to growth in 2019–2020 Q1 [1].	21
Tables Chapter 1.	
Table 1.1. Mass balance product distribution of pyrolysis at 500°C.	31
Table 1.2. Typical gasification reactions and heat requirements [41].	35
Table 1.3. Average gaseous components yield in gasification.	37
Tables Chapter 2.	
Table 2.1. Proximate and elemental analysis of raw materials*	48
Table 2.2. Proximate and elemental analysis of produced chars*.	48
Table 2.3. Experimental conditions summarized.	51
Table 2.4. Experimental conditions for gasification Fluidized bed reactor.	52
Table 2.5. Chemical families classification for bio-oil molecules.	55
Table 2.6. Tar classification and details for calibration.	58
Tables Chapter 3.	
Table 3.1. Results of energy balance and exergy evaluation of biomasses pyrolysis.	67
Table 3.2. Results of energy balance and exergy evaluation of pseudo-components pyrolysis.	67
Table 3.3. Energy rates of chemical families with catalytic treatment (MJ/kg _{bio-oil}).	92
Tables Chapter 4.	
Table 4.1. Results of mass, energy balance and exergy evaluation of biomass gasification using fluidized bed reactor in this study.	98
Table 4.2. Results of Energy balance and product composition of experimental runs of gasification.	99
Table 4.3. Results of Exergy evaluation and product composition of experimental runs of gasification.	100
Table 4.4. LHV, cold gas efficiency (CGE), and exergetic efficiency ψ of syngas.	119
Tables Chapter 5.	
Table 5.1. Kinetic parameters obtained for each gasification model.	136
Tables Appendix A1.	
Table A1.1. Thermodynamics properties of gaseous compounds.	174
Table A1.2. Specific enthalpy, entropy and chemical standard exergy for gases.	174
Table A1.3. Thermodynamics properties of bio-oil major compounds.	175
Table A1.4. Chemical standard exergy for major bio-oil compounds.	175
Table A1.5. Thermodynamics properties of major tar compounds.	176
Table A1.6. Chemical standard exergy for tars.	176
Table A1.7. Mass balance of results in a semi-continuous reactor.	178

Tables Appendix A2.

Table A2. 1. Energy product distribution of gases for beech wood and flax shives with catalytic treatment (MJ/kg_{gas}) at 500°C.....189

Tables Appendix A3.

Table A3.1. Effect of biochar bed quantity in tar groups concentration (g/Nm³) in syngas. Gasification with CO₂ at 900°C.....209

Table A3.2. Effect of temperature in H₂/CO ration for CO₂ and steam gasification.....212

Tables Appendix A4.

Table A4. 1. Kinetic models for biochar gasification with CO₂, in TGA and FBR.216

GENERAL INTRODUCTION

General introduction

Since day one, human beings have been since day 1 using different sources of energy in order to satisfy their needs. The energy application has always been linked to the stage of worldwide development. The global definition of energy by the scientific community is the ability to do or perform work. It is true that energy has accompanied to powered the development of society since the first written articles and nowadays it is vital in powering the industrial production of consumer goods, homes, transportation, and countless processes. Energy sources can be classified into renewable and non-renewable. Non-renewable sources are mainly represented by petroleum, natural gas, and coal, commonly known as fossil fuels. The major types of renewable energy are solar energy, wind energy, hydropower and biomass. Amid all the available sources, oil and coal are the most consumed ones. **Table i** shows the global energy composition chart of energy sources until the first quarter of 2020 [1].

Table i. Fuels consumption shares and contributions to growth in 2019–2020 Q1 [1].

Fuel type	Consumption (10 ⁸ Joules)	Annual change (10 ⁸ Joules)	Share of primary energy (%)	Change from 2018–2019 (%)
Oil	193.0	1.6	33.1	-0.2
Gas	141.5	2.8	24.2	+0.2
Coal	157.9	-0.9	27.0	-0.5
Renewables	66.6	3.5	11.4	+0.5
Nuclear	24.9	0.8	4.3	+0.1

Unfortunately, the global consumption of oil and coal dominates that from renewable sources, though the energetic dependency from fossil fuels is slightly reduced from previous years (2018–2019). Governments have highly encouraged the energy production from renewable sources as a solution to reduce fossil fuel dependency and to decrease greenhouse effect and emissions. These measures have been taken into serious consideration. the European Union reported at the end of 2019 that approximately 8–10% of the primary energy came from biomass treatments [2].

Nowadays, biomass seems to be one of the most attractive energy sources available on our planet. This is due to its abundance and high energy potential. Most of the investigations into biomass thermal conversion focus on detailing mass balance and product distribution. Meanwhile, as the mass balance is not enough to explain biomass conversion sustainability, the use of thermodynamic analysis might support comprehension the process. In order to simplify the thermodynamic analysis, researchers focus on energy and exergy process

calculations. This analysis is able to measure the process performance of energy and its degradation [3].

The law of conservation of energy explains that energy cannot be created nor destroyed. Under this principle, energy balance details where the energy entering a system is distributed or transformed. In thermodynamics [4], energy balance is the most conventional way to study the energy usage in any operational process. Nevertheless, the analysis is not able to quantify or qualify the degradation of the energy. The “exergy” is mostly employed to describe the useful part of the energy or work. The non-profitable part of the energy is called waste or exergy destroyed, which corresponded to the process irreversibility (entropy generation).

The thermodynamic evaluation of biomass pyrolysis and gasification, with or without catalytic treatment, allows users to give clear statements about the energy/exergy process upgrading. This upgrading considers not only mass balance evaluation, but also involves how much heat might be required to increase product quality and how much exergy could be destroyed under each condition. The details obtained from thermodynamics coupled with mass balance, process modelling, economy and environment study complete the chemical engineering cycle for design and selection of the most appropriate biomass thermochemical conditions.

Biomass gasification involves a very large and complex number of reactions, demanding a deep comprehension of the mechanism and behaviour. The development of a kinetic model has provided researchers with a mechanism to emulate and validate gasification results by applying kinetics principles of particle consumption and reaction mechanism. Biomass gasification in general comprises a large number of chemical reactions that separately present an individual kinetic behaviours: for this reason, the most appropriate and accurate conduct is to select individual reactions to develop kinetic models. In this study, only the kinetic investigation of biochar-CO₂ gasification is discussed.

It is well known that when discussing biomass gasification, biochar is the main intermediary product that suffers heterogenous transformation with the used agent. As a result, the investigation of kinetic modelling of char transformation contributes to a better comprehension of the biomass conversion process, together with the mass and thermodynamics study.

Thesis Scope

The objective of the thesis is to evaluate the energy performance of two types of thermochemical conversion of woody biomass: pyrolysis and gasification. The aim of the study is to compare the energy balance and exergy evaluation of the processes after both are exposed to different operating conditions, such as use of a catalyst in situ or ex-situ, temperature variation and gas carrier variation. The problematics surrounding this topic are

the following: “How advantageous is the biomass decomposition process from a thermodynamic point of view, when the variation of operating conditions is employed to upgrade mass balance and product quality? Does the biomass conversion process increase its energetic/exergetic quality with the variations in experimental conditions beyond the upgrading of chemical properties of principal products?”.

In order to answer these questions as accurately as possible, the experiments involved the strict study of two experimental setups: a semi-continuous fixed bed reactor and a fluidized bed reactor. In the fixed bed reactor, the pyrolysis of biomass and its pseudo-components was performed with the objective of studying the influence of each component in the energetic and exergetic evaluation. Also, the influence in the thermodynamic balance was studied using catalysts commonly employed to optimize bio-oil properties. In the fluidized bed reactor, the energetic and exergetic quality of biomass gasification was evaluated, varying the operating conditions. In addition, the influence in thermodynamic analysis of the use of a catalyst for pyrolysis was investigated.

The particularity of this work lies in the comparison of each operating condition using the same experimental set-up (reactor). A strict comparison of biomass thermal conditions in varying operating conditions is rarely found in the literature and a wide ambiguity is present when the process is evaluated thermodynamically, making a proper comparison difficult from a thermodynamic aspect.

In order to deepen the investigation of the thermochemical reaction of biomass the development of a kinetic model of the gasification of biochar with CO₂ was included. This was performed with the purpose of contributing complementary details to the concepts of mass, energy balance and exergy evaluation of the process.

Figure i illustrates the path of the work in this thesis, which was developed in three steps. The first step involved the literature review, followed by experimental runs, in order to evaluate the influence of common operating conditions in pyrolysis and gasification reaction. The second step of the thesis was the wide thermodynamic study of the experimental results. Finally, the last step was the development of kinetic modelling for the gasification reaction.

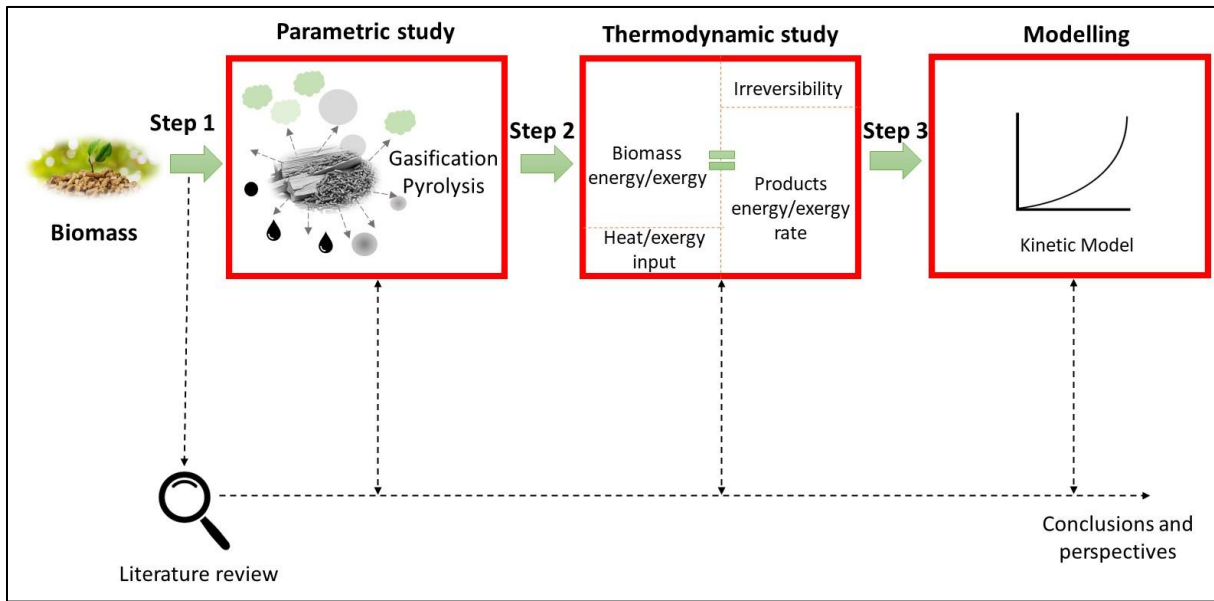


Figure i. Thesis development scheme.

This work was divided into 5 different chapters. A concise explanation of the information contained in each chapter is given below.

Chapter 1. The first chapter presents an extensive literature review of the principal features of biomass and its conversion techniques, focused on pyrolysis and mainly gasification. The most important available findings regarding the thermodynamic evaluations of biomass conversion are also presented, involving the catalytic and non-catalytic pyrolysis of biomass and its pseudo-components, and the gasification of biomass. Finally, a short review of char gasification kinetics modelling is presented.

Chapter 2. The second chapter details the materials used for this investigation. This section includes the raw materials used, the experimental set-ups, the experimental procedure, the analytical procedures and the equipment for each experimental run. The development of mathematic equations for the thermodynamic and kinetic modelling are also presented in this chapter.

Chapter 3. The third chapter presents the thermodynamic evaluation of the pyrolysis in the semi-continuous fixed bed reactor of beech wood and flax shives and their pseudo-components (cellulose, hemicellulose and lignin). This evaluation involves a comparison of both biomasses, as well as a comparison when the pyrolysis of their individual components is carried out. In addition, thermodynamic analysis of the catalytic treatment of bio-oil is analysed in this chapter and compared with the results of the non-catalytic treatment.

Chapter 4. The fourth chapter presents the thermodynamic evaluation of the gasification in the fluidized bed reactor. The energy balance and exergy evaluation of various operating

General introduction

conditions are evaluated in this chapter, such as the variation of reaction temperature, bed material, and gasification agent. The pyrolysis and gasification of biomass are compared in order to evaluate which process was thermodynamically more efficient.

Chapter 5. The fifth and final chapter presents a comparison of the kinetic study and model development of the gasification of biochar with carbon dioxide in a thermogravimetric analyser and a fluidized bed reactor. The gasification reaction was evaluated in a temperature range from 800°C to 1000°C and a partial pressure from 0.33 atm to 1 atm. The use of structural particle models such as volumetric, shrinking core and power-law models is investigated in this chapter, in order to validate the experimental results with the appropriated kinetic model.

Chapter 1:
LITERATURE REVIEW

Introduction

This chapter involves a literature review of the available and most important findings regarding the thermodynamic evaluations of biomass conversion, involving: the catalytic and non-catalytic pyrolysis of biomass and its pseudo-components and the gasification of biomass. Also, the investigation of the kinetic modelling of the char gasification with carbon dioxide in the fluidized bed reactor and thermogravimetric analyzer.

1. Biomass

Biomass is defined as any mass of living organisms or organic matter from animal or vegetal origin, including residues and organic waste, susceptible to be exploited energetically. Biomass on land is mainly represented in the forest which holds between 70% to 90% of the total above-ground resources [5], accounting for approximately 800 to 1300 Pg. Others defined biomass as any derivative fuel from plants, this definition including wood, crops, crop residues and animal waste [6]–[8].

Meanwhile, biomass definition varies as researches day by day justifies its classification and approach. Despite this, one invariable detail of biomass is the consideration of a renewable energy source. Biomass contains stored energy, as chemical energy capable to be transformed into other energy forms, such as electricity, mechanical and kinetic. Biomass is not only obtained as a residue form; it can also be harvested for later use as an energy source.

There is not a universal way to classify biomass as the difference in composition and origin is so wide that some authors prefer to group them in two groups according to the function, final products and origin [9]. The first group classifies biomass based on the existing form in nature (this includes the type of flora and biology). The second group is based on its application and use as a potential fuel feedstock. Based on their origin, source and biological variety Vassilev et al. [10] classed biomass in the following groups: Lignocellulosic biomass (woody), aquatic biomass, human and animal wastes, industrial biomass wastes, agricultural and mixtures of the previous classifications.

1.1. Lignocellulosic biomass

Lignocellulosic biomass is considered the most abundant and economical renewable resource and often can be considered less expensive than crude [11], [12]. The term lignocellulosic comes from its structural composition, woody biomass is mainly composed of polysaccharides cellulose (33-51%), hemicellulose (19-34%) and biopolymer lignin (20-30%) [13]. These compounds give biomass its structural form and hardness. **Figure 1.1** illustrates the location of these compounds in woody biomass.

Woody biomass along with plant biomass are the two types of resources most used in energy production, because of its abundance and high energetic values of the obtained products, regardless of the thermochemical process used.

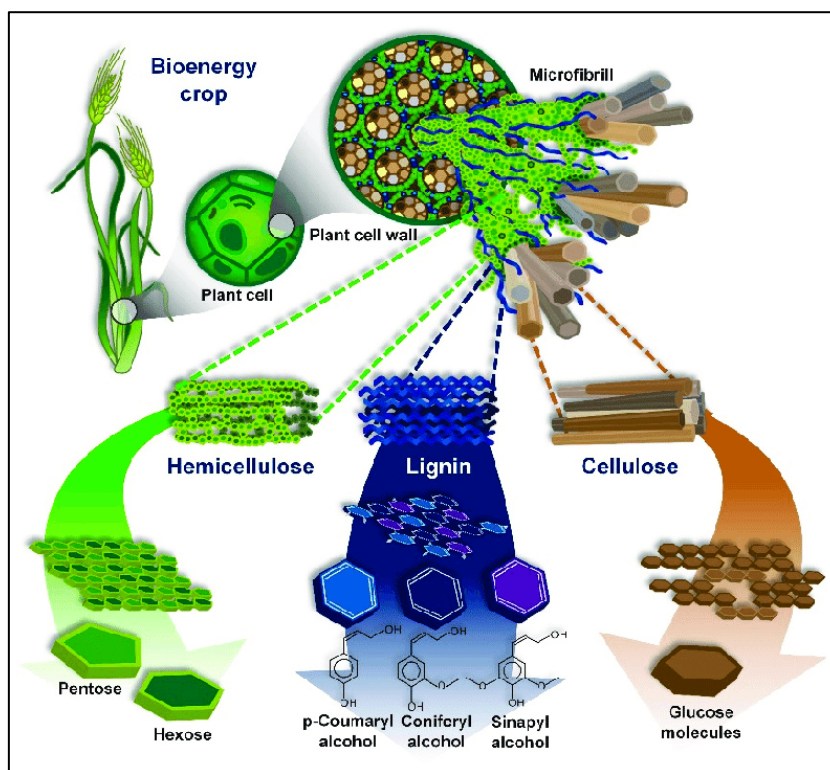


Figure 1.1. Biomass structural composition [14].

Cellulose: it has the highest mass constituent in biomass. It is composed of polysaccharide formed by the interconnection of glucose bonds (D-glucose), its chemical formula is $(C_6H_{10}O_5)_n$. It has a linear monopolymer of glucopyranose related to a beta-1,4-glycosidic bond [14]. These hydrogen bonds are connected one to the other to form a very long cellulose structure forming fibrils [15].

Hemicellulose: unlike cellulose, hemicellulose has more than a mono-sugar unit (known as heteropolysaccharides). These polysaccharides are constructed of D-glucose, D-galactose, D-xylose and other pentoses and hexoses. Hemicellulose is not as ordered as cellulose, and it has a molecular weight inferior to cellulose. For this reason, it can be rapidly hydrolyzed, compared with cellulose. Hemicellulose makes an important contribution to the quality of wood fiber and is mainly composed of xylan [16].

Lignin: wood hardness is attributed to the presence of lignin. It affords wood resistance against microbial occurrences. It is composed of three phenols, including sinapyl, p-coumaryl alcohol and coniferyl. Lignin is considered the second most abundant polymer of natural origin [17]. In

a very straight definition, lignin is known to be not soluble in water and it operates as a potential “glue” that links hemicellulose and cellulose.

All three polymers: cellulose, hemicellulose and lignin mainly represent woody biomass or lignocellulosic biomass. The mass distribution of these compounds may vary depending on the biomass type. Due to this reason degradation from biomass to another could be directly affected by the mass distribution of these three compounds and products as well.

2. Thermochemical conversion of biomass

Biomass can be converted into valuable and concentrated products with high energy value and chemical utility. The conversion techniques of biomass depend majorly on the basic conditions and properties of the used raw material. For dry biomass, the most common thermochemical conversions are pyrolysis, gasification and combustion.

2.1. Pyrolysis

Pyrolysis of biomass is one of the different alternatives to convert this organic matter into a profitable energetic product. The pyrolysis is done at high temperatures ($>200^{\circ}\text{C}$, the temperature where organic matter begins to devolatilize) in an inert atmosphere. This condition makes organic matter to decompose and release volatile matters (including permanent gases and chemical compounds in vapors form) and charcoal (or biochar, as it is known in the scientific community). The condensation of the chemical vapors evidences the presence of a high viscosity liquid, commonly known as bio-oil. The latest one is a dark brown oil that represents a promising source to reduce fossil fuel dependency. **Figure 1.2** illustrates the sequential step of pyrolysis and product formation. Pyrolysis products vary depending on the operation conditions and variation of the lignocellulosic biomass used.

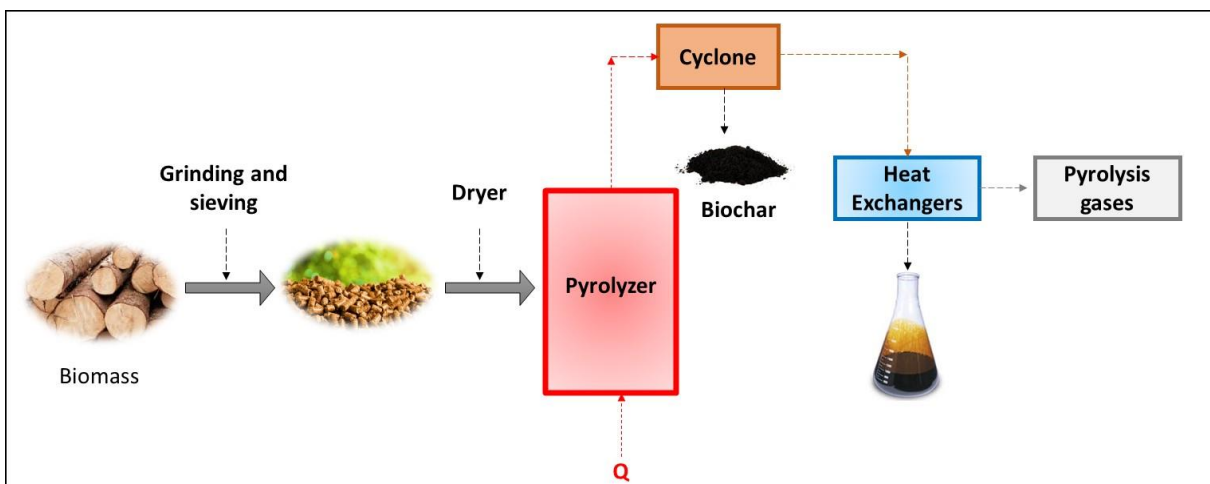


Figure 1.2. Biomass pyrolysis common schema.

Balat et al. [18] studied the pyrolysis of black alder wood in a lab-scale fixed bed reactor, in a temperature range from 200°C to 500°C, different residence time and heating rates were tested. The authors concluded that the temperature range from 375°C to 500°C showed to be the most interesting temperature range having a significant impact on pyrolysis products. The highest biomass conversion was obtained at 500°C for a maximum of 71% of the introduced biomass feed.

The products obtained after the pyrolysis of biomass can be varied as devolatilization conditions and biomass characteristics are very diversified. Meanwhile, at temperatures around 500°C, bio-oil and biochar tend to be the highest product yields. **Figure 1.3** shows the evolution of pyrolysis products as a function of temperature.

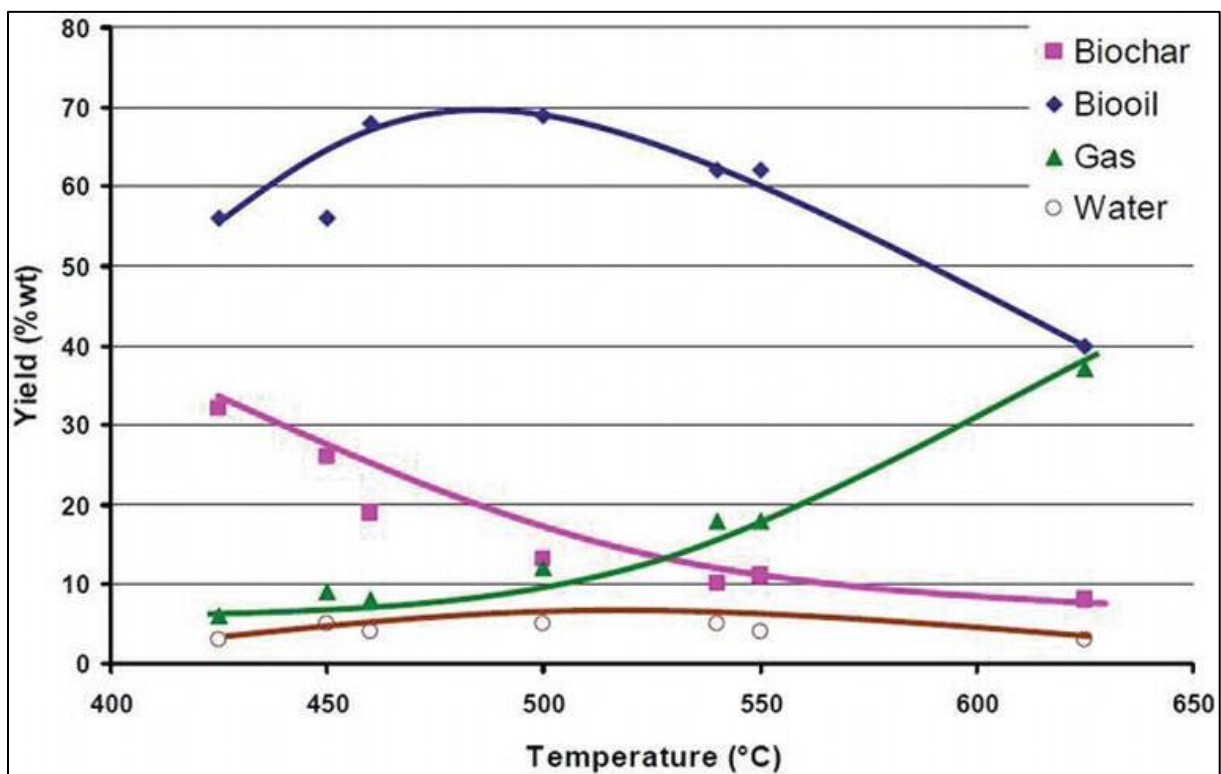


Figure 1.3. Biomass pyrolysis products evolution with temperature [19].

As for biomass pyrolysis, the products obtained from the pyrolysis of biomass constituents may vary depending on the operation conditions. Cellulose and hemicellulose are known to have similar properties as biomass, meanwhile, biochar is more related in the scientific community to lignin [20]. Ansari et al. [21] observed the fast pyrolysis of the three biomass constituents in a pyrolyzer, in a temperature range of 200°C to 550°C. The authors concluded that the majority of biomass bio-oil comes from cellulose and hemicellulose. On the other hand, biochar characteristics were represented by lignin hardness and thermal resistance.

Table 1.1 shows the mass balance obtained by several investigations about the pyrolysis of biomass constituents. It is observed that the bio-oil average to be the product with the highest yield in the mass balance. Inside bio-oil, phenols, alcohols, ketones and acids claim to be the oxygenated compounds with the highest yields [14], [21]–[24]. The mass balance distribution of the conversion of biomass and its pseudo components can change depending the mineral distribution in the sample. These inorganic minerals can impact the conversion rate, specially transition metals (Ni, Fe), alkaline earth and alkali metals (Ca, Mg, Sr, Ba, Li, Na, K, Rb) [25]. Hognon et al. [26] discussed that among all the inorganic elements, potassium had the most confirmed catalytic role in carbonaceous compounds gasification, meanwhile phosphorus and silicon showed to be promote inhibition of the gasification reaction.

Table 1.1. Mass balance product distribution of pyrolysis at 500°C.

	Cellulose	Hemicellulose	Lignin	*Reference
Gas – biochar –	7.04 - 8.79 - 84.99	4.40 - 16.25 - 55.38	4.23 - 43.83 - 29.58	[21]
bio-oil (wt. %)	11.84 - 12.5 - 75.66	8.58 - 12.87 - 78.55	10.59 - 56.62 - 32.78	[27]
	22.0 - 30.0 - 48.0	18.0 - 32.0 - 50.0	17.0 - 44.0 - 39.0	[28]
	20.5 - 16.0 - 63.5	38.0 - 25.9 - 36.1	16.0 - 48.6 - 35.4	[29]

*Dry basis.

2.1.1 Pyrolysis heat requirement

The pyrolysis is considered high energy demanding, as required more than 0.43 MJ/kg of heat in order to take place [30]. Throughout pyrolysis, a high amount of reactions take place in series and parallel, such as; depolymerization, isomerization, aromatization, carbonization, dehydration, polymerization, and others [31], [32].

Pyrolysis of biomass and its pseudo components is known as an endothermic reaction for some researchers [24], [33], [34]. Di Blasi et al. [34] explained that primary pyrolysis reactions are endothermic whilst secondary reactions are exothermic. Explaining that the pyrolysis endothermicity can decrease as a function of formed char yield in the process. Atsonios et al. [35] investigated the energy balance of beech wood in a bench-scale pyrolysis reactor. Their results showed that 1.12 MJ per kg of dry beech wood was needed in order to perform pyrolysis at 500°C. In addition to this, the authors explained that this value could be varied between 2.7 and 6.5% depending on the operating conditions. This heat needed to perform the reaction is called heat for pyrolysis [36].

Other researchers found values of heat for pyrolysis for woody biomass ranging from 0.5 to 2.5 MJ/kg of biomass [37]–[39]. Milosavljevic et al. [40] explained that these variations on the heat for pyrolysis were due to the difference in heating rates in pyrolysis and the volatiles release rate as well. The authors also discussed the importance of studying the heat for

pyrolysis of the biomass components in order to better understand and reduce inconsistencies in energy balance conclusions. For cellulose, the author found values of heat of 0.536 MJ per kg of volatiles released from pyrolysis. As it was for biomass, the heat for pyrolysis of cellulose and hemicellulose were very diverse in literature, from exothermic values to endothermic, -1.02 to 2.51 MJ/kg [41]–[43]. For lignin, Franck et al. [44] summarized values of heat for pyrolysis as a function of temperature, at a temperature range from 200 to 800°C, values were approximately from 0.7 to 1.8 MJ/kg.

Arbelàez et al. [45] performed a parametric study review of the pyrolysis of lignocellulosic biomass in order to find agreement in biomass pyrolysis statements. The authors concluded that between 400°C and 500°C an energetic optimum of pyrolysis is achieved. As the main objective of pyrolysis is to produce biochar and bio-oil with an energetic interest, the increase in pyrolysis temperature would promote cracking reactions of volatile matter. The latest would be translated into a reduction of the bio-oil quantity [46], while it would increase products heating values and energy requirements.

Authors have debated thermodynamics [47], and reported that energy balance is the most conventional way to study the energy usage in any operational process. Nevertheless, energy analysis is not able to quantify or qualify its degradation. The term “exergy” is mostly employed to describe the useful part of the energy or work. In thermochemical process, thermodynamic analysis is mainly employed for the permanent gases exiting the reactor. Keedy et al. [48] found that approximately 93% of the total exergy could be recovered in the output exergy stream of the pyrolyzer, as only 7% of the total exergy was destroyed, in pyrolysis of woody biomass at temperatures between 450 and 500°C. Meanwhile, Peters et al. [49], [50] showed that between 30 and 40% of the total exergy entering the pyrolysis process was destroyed. The author used a simulator to estimate all the consecutive steps of pyrolysis in order to calculate global process exergy destruction.

Boateng et al. [51] explained the reasons for the variation of energy and exergy values in biomass pyrolysis. They attributed this to uncertainty in mass balance calculations, in which errors lead to deviations around 15 to 40% of thermodynamic values. Despite the thermal conditions of biomass which required a heat input in order to take place, the obtained bio-oil heating values evidenced the biomass pyrolysis energetic potential. Bio-oil heating values oscillate between 16 and 18 MJ per kilogram of bio-oil [52].

2.1.2 Catalytic pyrolysis heat requirements

The interest in maximizing bio-oil quantity make researches to look for pyrolysis conditions that can unfortunately reduce bio-oil quality. Garcia-Perez et al. [53] investigated the effects of

temperature on the pyrolysis products yields, but at the same time, the quality was also observed. The authors concluded that the fact of maximizing bio-oil yield led to the formation of oligomers in bio-oil, for this fact it degrades its quality by increasing its viscosity.

Bio-oil is a mixture of hydrocarbons and oxygenated molecules, its quality is a subject of discussion as contains a high oxygen content >30%. Acids, phenols, alcohols, BTXs, and sugars are some of the chemical families present in bio-oil. As bio-oil can be considered as fuel, there is interest in increasing its heating values. The latest can be done if the pyrolysis temperature is increased. Despite this, a post-treatment has to be done in order to increase quality and avoid undesirable reactions, this post-treatment can be the deoxygenation process.

The catalytic pyrolysis of biomass comprises the use of catalyst in-situ or ex-situ in order to treat the pyrolysis vapors to increase bio-oil quality. The net bio-oil obtained from the pyrolysis of woody biomass has some disadvantageous properties that limit its use in combustion motors and also limits its mixture with conventional fuels. Due to this, the use of a deoxygenation catalyst is strongly suggested. **Figure 1.4** shows a common example of the deoxygenation routine of bio-oil.

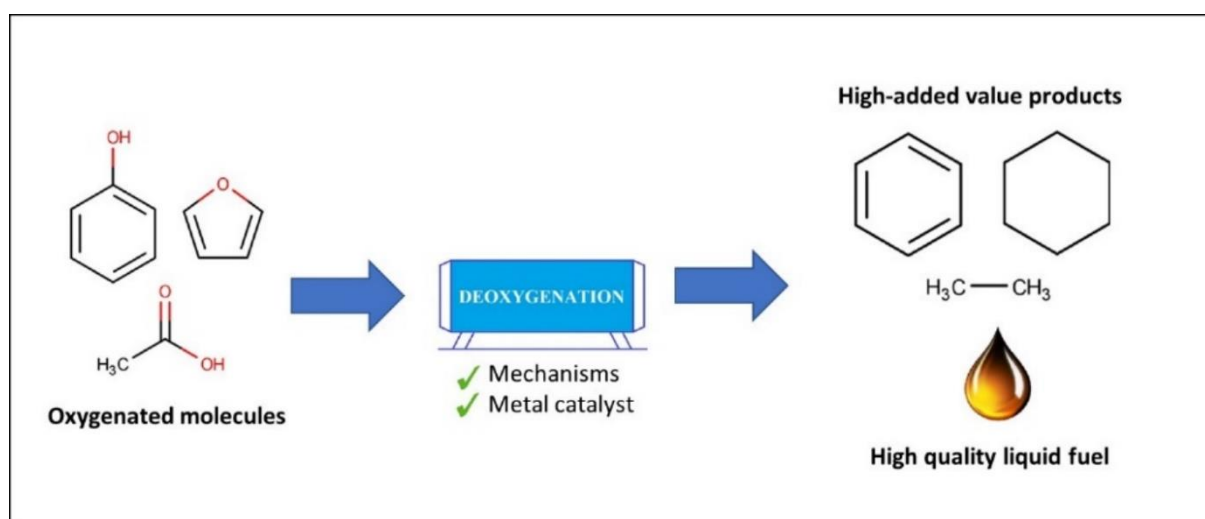


Figure 1.4. Bio-oil molecules deoxygenation schema (adapted from Kay Lup et al. [48]).

Mohabeer et al. [54] studied the effect zeolites (HZSM-5 and H-Y) and their respective iron modifications (Fe-HZSM-5 and Fe-H-Y), metallic and bimetallic catalyst supported with alumina ($\text{Pt}/\text{Al}_2\text{O}_3$ and $\text{Co-Mo}/\text{Al}_2\text{O}_3$) over pyrolytic oil obtained from the pyrolysis of beech wood and flax shives. The used reactor was a fixed bed at a temperature of 500°C , and a residence time of 10 min. The authors concluded that HZSM-5 and its iron modification were the most efficient catalysts, by reducing oxygen content of bio-oil from 33.8 % to 14.5% for Fe-HZSM-5 and 18.8% for HZSM-5.

The bio-oil heating values are approximately between 16 and 19 MJ/kg, when the moisture content is in the range from 15% to 30%. These values are increased by using a catalyst, in order to approach bio-oil properties to the ones presented by diesel and other petroleum fuels. The reduction of the oxygen content with the use of a catalyst such as zeolites and alumina supported metals is one of the most employed upgrading technics in pyrolysis [22], [54]. The use of catalysts increases bio-oil heating values by 30 to 50%, because of reducing oxygen content and concentrating carbon and hydrogen yields in the oil [55], [56].

The advantage of increasing bio-oil heating value could be counteracted by the fact that bio-oil upgrading reactions (deoxygenation or hydrodeoxygenation) are known to increase process endothermicity, hence more heat is required to be afforded in order to perform pyrolysis. Meanwhile, the process available work (exergy) is increased with the use of a catalyst in pyrolysis [57] and in some investigations, the total process exergetic efficiency was increased [52]. Other researchers showed a contrary statement about the exergetic efficiency of catalytic pyrolysis [50], [57], [58]. It was shown that the presence of catalyst increased internal process entropy generation, hence more exergy was destroyed in the reaction and the overall exergetic efficiency decreased.

The energy degradation is strictly linked with the entropy changes of the process, both energy and exergy calculations are dependent on the system entropy values [59]. Authors [60] claimed that the presence of a catalyst (HZSM-5 and metal-supported catalyst) improves the process conversion velocity, this resulted in a higher reactivity consequently system entropy would increase. The latest fact according to the authors decreased pyrolysis global energetic and exergetic efficiency.

Since different statements are found in the literature about the effect in energy and exergy rates of the catalytic pyrolysis of biomass, uncertainties revolve around this subject and a clear explanation on the behavior of catalytic pyrolysis of biomass is lacking in the literature.

2.2 Gasification

The biomass gasification process (**Figure 1.5**) has majorly three principal steps [61]; drying, devolatilization and char gasification. The gasification involves a complex and large number of chemical reactions, exothermic and endothermic and with heterogeneous and homogeneous character. **Table 1.2** shows the typical biomass gasification reactions. The reactions can be favored by operation conditions and heat and mass transfer issues. Gasification is employed nowadays as an alternative solution to produce high energetic valuable products as syngas, because of its high heating values. In addition, gasification is used to treat hazardous waste with high thermal stability [62].

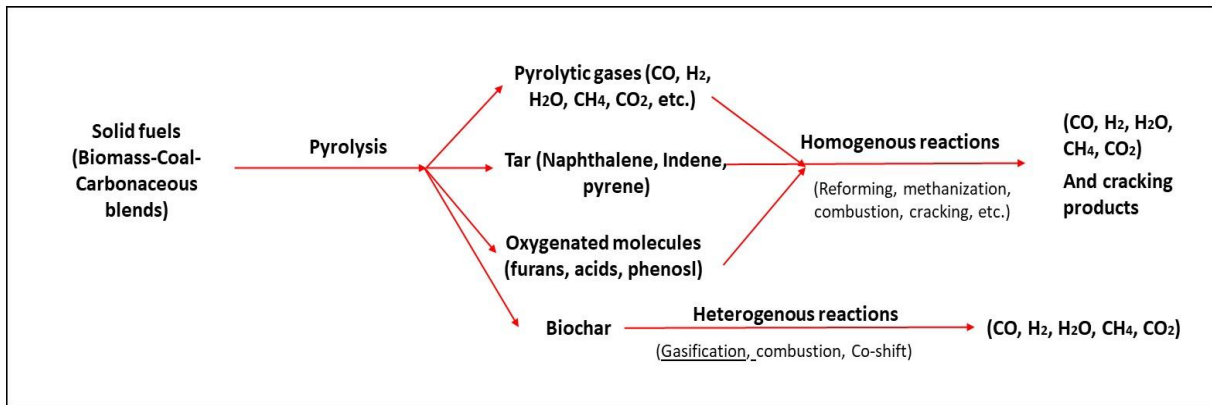


Figure 1.5. Gasification of solid fuels scheme (adapted from Higman et al. [58]).

The authentic definition for syngas or synthesis gas in scientific community is that is a mixture of gases mainly carbon monoxide and hydrogen, with important quantities of carbon dioxide, methane and water. Gasification takes place when a carbonaceous compound, mainly the char reacts with a controlled amount of oxidant in a process between pyrolysis and combustion. Different gasification methods or mechanisms are depending the oxidant agent used to convert char into profitable gaseous products, such as: air gasification also known as partial oxidation, dry reforming or CO₂-gasification, steam reforming or H₂O-gasification and finally hydrogasification known as H₂-gasification.

Table 1.2. Typical gasification reactions and heat requirements [41].

Reaction Name	Balanced equation
Biochar reaction	$C + CO_2 \leftrightarrow 2CO + 172 \text{ KJ/mol}$
	$C + H_2O \leftrightarrow CO + H_2 + 131 \text{ KJ/mol}$
	$C + 2H_2 \leftrightarrow CH_4 - 74.8 \text{ KJ/mol}$
	$C + 0,5 O_2 \rightarrow CO - 111 \text{ KJ/mol}$
Oxidation reactions	$C + O_2 \rightarrow CO_2 - 394 \text{ KJ/mol}$
	$C + 0.5 O_2 \rightarrow CO_2 - 284 \text{ KJ/mol}$
	$CH_4 + 2O_2 \leftrightarrow CO_2 + 2H_2O - 803 \text{ KJ/mol}$
	$H_2 + 0,5 O_2 \rightarrow 2H_2O - 242 \text{ KJ/mol}$
Shift reactions	$CO + H_2O \leftrightarrow CO_2 + H_2 - 41,2 \text{ KJ/mol}$
Methanation reactions	$2CO + 2H_2 \rightarrow CH_4 + CO_2 - 247 \text{ KJ/mol}$
	$CO + 3H_2 \leftrightarrow CH_4 + H_2O - 206 \text{ KJ/mol}$
	$2CO_2 + 4H_2 \rightarrow CH_4 + 2H_2O - 165 \text{ KJ/mol}$
Reforming reactions	$CH_4 + H_2O \leftrightarrow CO + 3H_2 + 206 \text{ KJ/mol}$
	$CH_4 + 0,5O_2 \rightarrow CO + 2H_2 - 36 \text{ KJ/mol}$

2.2.1 Steam gasification

The gasification of fuels with steam is also known as reforming. As for air gasification, the reforming of fuels is a very economical process due to the use of water vapor as a non-expensive agent. Steam gasification involves the transformation of carbon into two high energy gases H_2 and CO , generally done at atmospheric pressure. In recent decades steam gasification has been very attractive due to the high formation of hydrogen which has a modest price in the chemical industry [63]–[65].

The selection of the gasification agent depends on the final interest of the users. Most of the time, an economic/energetic factor is the decisional character. Guizani et al. [66] discussed that among all the possible gasification agents, steam presents the highest reactivity with char compared to others.

2.2.2 CO_2 gasification

Dry reforming gasification or CO_2 gasification involves the use of carbon dioxide as an agent to convert carbon into carbon monoxide, via the Boudouard reaction. Cheng et al. [67] defined CO_2 gasification as a very promising technique able to contribute to the reduction of emissions of the principal gas causing the greenhouse effect. The authors also studied the gasification of biomass using CO_2 in a fluidized bed reactor, the aim of their work was to perform a parametric study of this reaction. It was concluded that with a partial pressure of 0.6 atm of CO_2 , maximum values of CO and methane were obtained. It was also discussed that the increase in gasification agent flow rate increased the heating value of the syngas produced and the cold gas efficiency.

Sadhwani et al. [68] studied the gasification of lignocellulosic biomass in a fluidized bed reactor. The temperature range was from $700^\circ C$ to $935^\circ C$, and varying the CO_2 /Carbon ratio from 0.5 to 2.5 (wt./wt.). The authors compared CO_2 and air gasification in terms of mass and energy balances. It was established that syngas obtained from CO_2 gasification had a lower yield (51.42 wt.% - 76.5 wt.%) than air gasification (73.06 wt.% - 79.4 wt.%). Despite this, the authors concluded that the heating value of syngas from CO_2 gasification (8.0 MJ/NM^3) was higher than that from air gasification (5.51 MJ/NM^3).

2.2.3 Gasification heat requirement

Among the gasification products and sub-products, researchers mainly focus on syngas due to its economic and energetic value [69]–[72]. Furthermore, it has been proven that the biomass gasification plant (integrated gasification combined cycle, IGCC) has a lower cost of electricity and heat requirements production than combustion and gas engine plants [73], [74]. The quality of syngas depends on how much CO and H_2 it contains to the detriment of other gaseous molecules present. The heating value of syngas is approximately 50% of the

energetic density of natural gas. **Figure 1.6** illustrates the individual gaseous components in the production of syngas with different gasification agents.

Higher heating values of syngas were found in literature, approximately 4.5 to 9.7 MJ/NM³, in a temperature range from 800°C to 1000°C [75]–[77], Authors reported that syngas heating values increased with gasification temperature. Other such as Zhai et al. [78] also corroborated this statement but added that from 600°C to 800°C syngas production decreased due to the high methane yield at low temperatures, in the case of steam gasification. Authors also concluded that H₂ yield decreases slightly (38 wt.% to 35 wt.%) with the increase of temperature, hence CO yield highly increases (10 wt.% to 27 wt.%). **Table 1.3** shows the typical gas composition and heating values obtained from diverse gasification techniques.

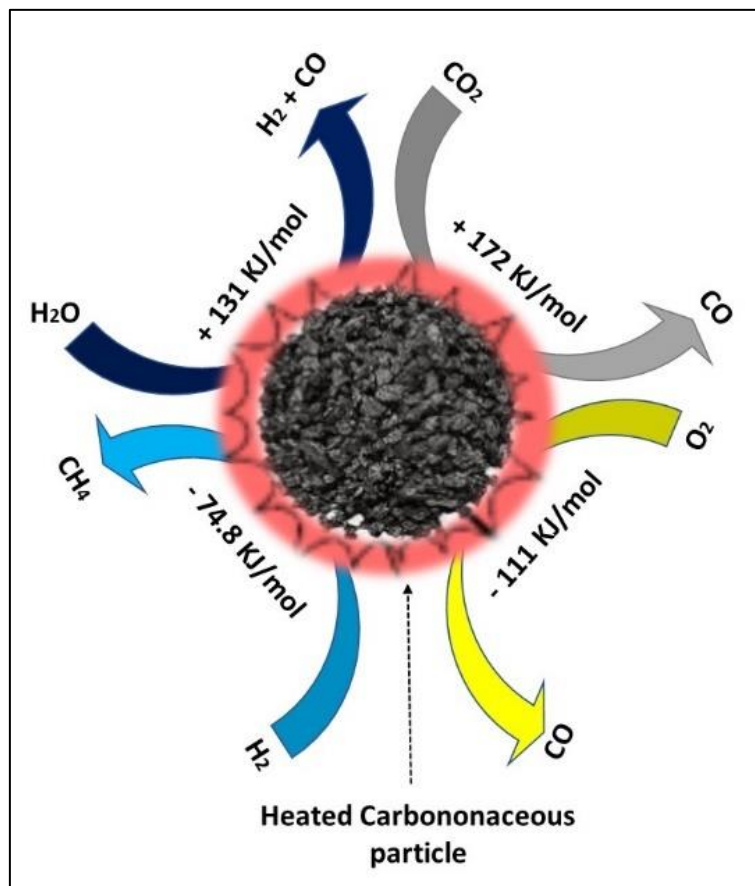


Figure 1.6. Major gases obtained from gasification.

Table 1.3. Average gaseous components yield in gasification.

Gasification Agent	Gases composition (vol/vol %)*				HHV (MJ/NM ³)	Reference
	H ₂	CO	CH ₄	CO ₂		
**Air	32.7	40.4	1.9	25.0	5.7	[74]
	23.4	51.0	6.4	19.2	5.5	
	27.6	36.7	6.9	28.8	***N.A.	[79]
O ₂	33.0	50.0	2.0	15.0	10.4	[74]
Steam	35.9	28.6	11.7	23.8	12.5	[80]
	52.0	27.2	7.0	18.0	13.0	[81]
CO ₂	31.5	38.4	7.5	22.8	11.08	[82]

*Dry basis, ** Normalized without N₂ content. *** Not available

Gasification is generally performed with controlled amounts of air, pure oxygen, steam, or carbon dioxide. The latter agent has been less studied [83], [84] in comparison to the former ones. The reason why CO₂ is less studied includes the need of an external heat source that has to be added to the system because no partial combustion of the biomass is reached like it is for air and oxygen gasification. The calculations of external heat sources depend on the mass and energy balances, which involve thermodynamics notions and analysis. Thermochemical conversions as gasification and pyrolysis are highly endothermic [85]–[87]. The use of the term endothermic did not mean that only endothermic reactions take place. As gasification is known as an intermediate step between pyrolysis and combustion, exothermic reactions are also present in the process. Methane formation, water-gas shift and methanation reactions are some of the exothermic reactions taking place in the entire process [88]. These reactions energetically help to sustain the gasification process, despite this, the required energy amount to perform gasification remains elevated. Consequently, the global process is considered endothermic.

A thermodynamic analysis is usually performed in gasification systems in order to provide detailed information on the energy of gasification products, as well as to provide information about the design, optimization and performance prediction of gasification systems [89]. Parvez and colleagues [90] compared thermodynamic values obtained from CO₂ and steam gasification; the latter was referred to in his work as conventional gasification. The author used computational software to simulate the gasification installation and perform energy calculations, showing that CO₂ gasification provided higher energetic values than steam gasification. It is noteworthy that in his work, only syngas was evaluated from the output streams of the system. As the gasification system in his study was a combination of several operation units, including a decomposer and a solid separator, only syngas was the final product.

As the main aim of gasification processes is to produce syngas for power generation, the direct focus of thermodynamic analysis is syngas. Tar represents an important issue, due to the complexity of its removal from syngas. The use of biochar as a catalyst has been employed to reduce tar and boost syngas production [91]. Other authors [92] evaluated the steam gasification of biomass integrated with a biochar catalytic bed in a simulated two-stage gasifier. The energy analyses were performed at different temperatures and equivalence ratios. The author demonstrated the relevance of using biochar as a catalytic treatment for tar, showing the increase in thermodynamic efficiency of the syngas produced.

Zhang and colleagues [93] compared exergy from steam gasification and the partial oxidation of biomass. Their work provided detailed information about the products of all streams exiting the reactor, including biochar, tar and syngas. The results favored steam gasification over the partial oxidation of biomass in terms of exergetic values for all tested temperatures and system conditions. Unfortunately, no information was available for the type of reactor used in their work. The authors explained that when temperatures increased from 800°C to 1200°C, the exergetic efficiency of gases increased, while it decreased for both steam and air gasification of tar.

On the contrary, Tang and colleagues [94] revealed that the exergy of syngas increased as a function of temperature, but that exergy values declined above 650°C due to the strengthened partial oxidation reactions. The reactor used for the study was a laboratory-scale fluidized bed. The authors also included tar exergy calculation using a liquid fuel exergy equation based on their elemental composition [95]. Wu et al. [96] used the same procedure to calculate tar exergy, and remarked the importance of including tar exergy in exergy destruction calculations, even though this only represented between 4 and 8% of the total exergy values for some gasification systems at high temperatures.

Chen et al. [97] studied the effect of temperature and the equivalent ratio of biomass steam intermittent gasification. The authors concluded that both chemical and physical exergy of syngas was increased with temperature. Also, syngas exergy efficiency was increased as a function of temperature. The tested temperatures ranged from 875°C to 975°C in a steam atmosphere. The temperature effect over gases exergy is a subject of discussion, different statements are found in the literature. Sreejith et al. [98] mentioned that biomass typology was one of the most important factors affecting the irreversible nature of gasification processes, as a variety of exergy statements as a function of temperature from one biomass type to another could be found.

Energy and exergy calculations are generally performed by considering all unit operations in the process [99]–[101]; this consideration is disputable only if the syngas exiting the gasifier

needs to be analyzed and compared to other processes where syngas cleaning or post-treatment is not used. Energy and exergy comparisons were performed by several researchers under different gasification conditions [98], [102], even though the operating conditions and gasification set-up were not entirely the same in several cases. This issue makes proper comparisons more complex.

3. Thermodynamic efficiency

The thermodynamic efficiency of biomass conversion involves the calculation of the energy or exergy feed rate of the process related to the individual thermal contribution of an individual stream. The efficiency can be calculated by three parameters: energy, cold gas and exergetic efficiency.

3.1 Energy efficiency

The energy balance is the instrument to indicate the heat distribution of products of a process. Meanwhile, the energetic efficiency (η), is employed to quantify the process performance of all streams. This term is used as an indicator to express the quality of energy changes [103]. The energetic efficiency depends on the same factors associated with the optimization of thermal conversions, the operations conditions, type of installation and in some cases the thermal isolation.

Based on literature data Panepinto et al. [104] expressed that the energetic efficiency of pyrolysis and gasification of biomass is in the range of 55 and 75%. The authors also expressed that additional percentage points could be added to these values by the optimization of the heat recovery system. The energetic efficiency comparisons were found in the literature concerning gasification technologies [105]. The Authors compared energy balance and process efficiency of three types of gasifiers, such as entrained flow, fluidized bed and allothermal reactor. It was concluded that allothermal and fluidized bed reactors were more energetically efficient (67% and 59%, respectively) than the entrained flow gasifier (54%). The authors attributed this difference to the advantage in heat transfer and reactor gasification routines.

3.2 Cold gas efficiency

The cold gas efficiency (CGE) is defined as the ratio between the chemical energy value of the product gas concerning the fuel energy value (lower heating value of gas/lower heating value of biomass). This calculation is mainly applied to the thermochemical process where gaseous streams are the major product, as it is the case for gasification of biomass. Chaiwatanodom et al. [106] studied the energy balance of the gasification of biomass with carbon dioxide using Aspen plus with results obtained from Renganathan et al. study [107]. It was concluded that

CGE efficiency was increased by the increase of CO₂ feed rate, however, the authors concluded that CGE calculations do not account energy requirements into consideration, only syngas efficiency is evaluated. Due to this reason, the authors proposed to use energetic efficiency to calculate system overall efficiency.

The CGE values vary as a function of the conversion technique, equivalence ratio, type of biomass, and operation conditions. Rao and colleagues [108] compared wood chips with municipal and sun-dried soybean straw residues gasification in a fixed-bed reactor. They concluded that residues showed similar CGE values of 73%, meanwhile wood chips CGE was 65%. Besides this fact, the global energy content of the produced syngas from residues and wood chips was very close, approximately 12.2 MJ/kg.

3.3 Exergetic efficiency

The exergetic efficiency (Ψ_{syngas}) in thermochemical process is mainly employed for the produced gas. It is defined as the ratio between the physical and chemical exergy of the gas and the chemical value of the biomass. For power generation, syngas is the desired product of gasification. Due to this fact exergy efficiency is calculated taking into consideration only syngas and biomass exergy. It is reported in the literature [109], [110] that the maximum exergy efficiency values for biomass gasification varies between 65.5% and 71%, for the overall process.

Wang et al. [111] showed that between 53% and 61% of the syngas exergy efficiency came from the devolatilization (pyrolysis) step only, which could increase as gasification reactions take place. Experiments were performed in a fixed bed reactor using rice husk as biomass. The authors also concluded that between 900°C and 1000°C syngas exergy achieved a maximum in its increasing value. The same biomass was tested by Zhang et al. [112] using an entrained flow reactor. The authors concluded that the highest exergy amounts of syngas were obtained at 900°C and 1000°C, syngas exergy was increased from 6.6 MJ/kg_{Biomass} to approximately 10.1 MJ/kg_{Biomass}.

4. Kinetic modelling of gasification

Biomass gasification involves a very large and complex number of reactions, which demands a deep comprehension of the mechanism and behavior. The development of a kinetic model gives researchers a mechanism to emulate and validate gasification results by applying kinetics principles of particle consumption and reaction mechanism. Biomass gasification, in general, comprises a large number of chemical reactions that separately present an individual kinetic behavior, due to this reason the most appropriate and accurate conduct is the selection

of individual reactions to develop kinetic models [113]–[115]. For this reason, in the following section, only the literature review of biochar-CO₂ gasification is discussed.

It is found in literature a significant number of articles reviewing gasification technology and models with char [116]–[119]. Most of these reviews focus on partial oxidation and steam gasification of chars, leaving aside carbon dioxide gasification. Despite this, the use of CO₂ as a gasification agent, still trending in the research community but with less impact than steam gasification. Some of the reasons for the low use of CO₂ as a gasification agent in laboratories and industries are the highly endothermic Boudouard reaction ($\Delta_rH^\circ = 172.3 \text{ kJ/mol}$) and hence high energy requirements [107]. Also, the use of steam evidenced a reaction rate of 2-5 times higher than CO₂ gasification and syngas with higher heating values [120].

Di Blasi and colleagues [116] summarized the investigations of combustion and gasification rates of lignocellulosic chars. The authors discussed that some of the main parameters affecting char reactivity were the volatiles amount in chars, the volatile release rate and the ash content. As the volatile compounds could interact with char and also secondary reactions take place, this could inhibit at some point the gasification rate by reducing its reactivity. They also added that char structure plays an important role in gasification kinetics and the transformation behaves differently between chars. For this reason, the authors described a variety of structural models that could be applied for char gasification. These models were only linked to the particle structure and conversion parameters.

Models of char reactivity are usually detailed as volumetric and structural types. Structural models define an internal solid matrix (grain model) or an internal pore structure (random pore model) [121] throughout conversion, with a constant reaction surface rate. For volumetric type models, the variations in the pore structure during char conversion can be defined by empirical correlations where porosity does not appear in an explicit form (only conversion X , is represented as a variable in the majority of this type of models).

Nguyen et al. [122] studied the kinetics of rice husk char isothermal gasification using a CO₂ atmosphere. The set-up used was a macro-thermogravimetric reactor and the experiments were conducted in a temperature range of 900 to 1000°C. The char was prepared in an N₂ atmosphere at 600°C with a heating rate of 20°C/min. The authors represented the rice husk char transformation rate as a function of the conversion process, using a volumetric model. The kinetics parameters found for the study n , E_a and A for reaction order, activation energy and pre-exponential factor were 0.36, 193.4 kJ/mol and $1.80 \times 10^5 \text{ s}^{-1} \text{ atm}$, the kinetic equation was; $r = A \exp(-E_a/RT) (1-X)$. Yuan et al [123] also studied CO₂ gasification of rice husk. A thermogravimeter analyzer was used and biochar was prepared in situ at a temperature of

800°C. It was used the random pore model and kinetics parameters were $A = 3.937 \times 10^7 \text{ s}^{-1}$ and 238.3 kJ/mol, the kinetic equation was; $r = A \exp(-E_a/RT) (1-X) (1-12.6 \ln(1-x))^2$.

Morin et al. [124] discussed that ash content catalyzes gasification reaction, claiming that the conversion mechanism of the char particle can be affected because of ash content and distribution. The authors observed that the ash content of chars could vary from one char to another, even though both chars have the same origins but different preparations. It was also added that regardless of this, the effect on gasification kinetics of ash content is not well-established yet as more of the investigations focus on char structure as it plays a more dominant role in reactivity. Nowicki et al. [125] expressed in their study that the differences that could be found in char reactivity and kinetic parameter values are due to the variation of ash content in chars. The authors performed gasification with CO_2 of char derived from sewage sludge using a thermo-balance reactor.

Despite ash content, biochar preparation method, reaction temperature, partial pressure and other parameters that affect biochar reaction rate, the reaction kinetics do not depend on the reactor dynamic of type, as it can be found in literature different studies comparing char gasification rate and kinetics in different reactors [126]–[128]. This statement is purely theoretical, as at some point the dynamic of a reactor could influence mass and heat transfer of particles, and this could potentially aggravate diffusional limitations if they are present obviously.

In order to identify the presence of diffusional limitations, the calculation of the characteristic times of the main external and internal phenomena is strongly recommended for biochar thermal conversion in the scientific community. Dupont et al. [129]–[131] calculated the external and internal heat transfer times by conduction, convection and radiation for biochar gasification and showed that for biochar particles size superior to 100 μm , the reaction could be controlled by both physical and chemical kinetics. The authors also explained that convection gas to particle heat transfer is the most significant diffusional phenomena for large particle sizes.

Gomez and colleagues [132], [133] studied the diffusional effects of a single char particle using a thermogravimetric analyzer (TGA). The authors expressed that kinetic studies of char gasification with CO_2 are highly criticized and surveyed due to the incoherence in a general criterion for kinetic model selection. It was also added that reaction rate of char determined in TGA equipment may deviate from the observed in bench-scale equipment, due to reasons as the high heating rate and operation control conditions.

Mueller et al. [134] compared CO₂-char gasification using biomass, brown coal and industrial petcoke char in a small-scale fluidized bed reactor (FBR) and a thermogravimetric analyser (TGA). The main difference between both set-ups was the fuel bed configuration. The temperature range, partial pressure and batch fuel samples were the same in both reactors. As was observed char gasification with FBR showed a much rapid gasification rate than TGA. The authors attributed this to the particle local boundary conditions. As in the FBR experiments, the particles were in better heat and mass transfer conditions in a quasi-homogeneous gas atmosphere while for TGA it had a fixed bed configuration type.

Chen et al. [135] also performed CO₂-char gasification in TGA and FBR reactors. The study was focused on comparing different chars with gasification agents to estimate a suitable kinetic model. Meanwhile, it was observed that TGA and FBR reactors had a similar exponential conversion curve, but FBR showed a faster gasification rate compared to TGA. Unfortunately, no clear information was given about this behavior, as it was only known that TGA and FBR configurations were different.

The selection of a kinetic model in both isothermal and non-isothermal gasification depends eventually on the conversion path that char particle undergoes. Vyazovkin et al. [136] summarized the kinetic analysis of conversion curves which fitted with known kinetic models. The authors showed that conversion curves from gasification could vary from linear to exponential forms. The reaction models that were accounted in the study showed power law, contracting sphere, contracting cylinder and Mampel first order, as the most employed ones, as they better fit with char degradation.

Summarizing literature of the kinetic modelling of gasification of biochar with carbon dioxide, it can be detailed that the election of the most appropriated set-up to perform model development can also be a significant factor to take into account. As it is found, information that describes that under the same operating conditions, kinetic model parameters might vary from one type of reactor to another. Due to the aggravation of diffusional effects and difference in particle consumption dynamic.

5. Conclusion

The first chapter of this investigation focused on the presentation of the most appropriate literature review according to the goal of this work. It was evidenced the interest of studying essential details of pyrolysis of biomass and pseudo-components and biomass gasification, in order to proceed in the comprehension of thermodynamic balances. It was found that rather only focusing thermodynamic analysis on energy balance, its quality and degradation might be included, by performing an exergetic analysis of the process. The latest would be able to

Chapter 1

determine process feasibility and efficiency. It is well worth mentioning that studies have been approached in the scientific community about these topics, but many of these works compared and criticized results without having even identically operation conditions and set-ups. This investigation is intended as a contribution to a much clear comprehension of these topics.

According to the literature review, it was found a wide range of energy requirements for pyrolysis and gasification of biomass and components, which involves conditions from exothermicity to endothermicity. These statements comprise some of the ambiguities found in literature concerning the biomass thermochemical process. It was also evidenced in the literature that liquid products (bio-oil and tar) are rarely accounted for thermodynamic analysis due to the complexity and a high number of molecules present in the stream. Due to this fact, most of the energy balance and exergy evaluation focuses only on gaseous products. Also, it was found in literature contradictory statements concerning the effect on the energy balance and exergy evaluation with the variation of operating conditions. The operating conditions used to upgrade products chemical quality apparently could increase global process exergetic efficiency for some authors, while for others it decreases.

It is worth saying that the Information concerning the exergy destruction comparison of thermochemical conversion of biomass pseudo-components was not found in the literature review, meaning that this work would afford a significant novelty in thermodynamic aspects.

Chapter 2:
MATERIAL, METHODS AND SET-UPS.

Introduction

This chapter describes the materials, the analytical and experimental setups used for this thesis work, and the mathematic equation development for the thermodynamic and kinetic modelling. For each reactor used, the experimental procedure is detailed, including the analytical equipment employed for the quantification and identification of the products.

1. Materials used

1.1 Biomasses

The biomasses used for the investigation of pyrolysis in the semi-continuous reactor were beech wood and flax shives. Beech wood with a particle size of approximately 0.4 mm was obtained from ETS Lignex. The flax shives were supplied by La Cooperative Terre de Lin. Before pyrolysis, the flax shives were ground and sieved in the laboratory for a particle size of less than 0.5mm. For the case of the gasification runs, the biomass used was also beech wood, but obtained from Ooni Corporation London, UK in pellet form (6 x 100 mm). It was also ground and crushed to obtain an average particle size of 6 x 10 mm. The bed material—washed sand with a particle size of approximately 150 μm and a density of 1.60 g/cm^3 at 20°C — was obtained from Alfa Aesar. All biomasses were dried in an oven at 100°C for one hour before utilization.

1.2 Woody pseudo-components

The cellulose was obtained from Merck, with a density of 1.5 g/cm^3 . Hemicellulose was represented by Xylan and was obtained from Tokyo Chemical Company Co. Ltd. The lignin was obtained in its alkaline form from Sigma-Aldrich. All raw materials were dried for one hour in an oven at 100°C before utilization.

Table 2.1 and **Table 2.2** present the elemental and proximate analysis of the raw materials and the collected biochar, respectively. The elemental analysis of the individual biochar of each raw material was also included in this study, to be used for energy and exergy calculations in **chapters 3** and **4**. The variables, C, H, N, O, M., V.M., F.C., and A.C., corresponded to the carbon, hydrogen, nitrogen, oxygen, moisture, volatile matter, fixed carbon and ash content of the samples, respectively.

Table 2.1. Proximate and elemental analysis of raw materials*.

Material	^a Elemental analysis (wt. %)				Proximate Analysis (wt. %) ^b			
	C	H	N	O ^a	M. [%]	V.M. [%]	F.C. [%]	A.C. [%]
Beech wood (Powder)	49.35	6.25	<0.01	44.40	6.23	75.4	17.54	0.83
Flax Shives	45.70	5.77	0.41	48.12	8.28	69.22	19.97	2.53
Beech wood (pellets)	46.70	5.57	<0.01	47.72	7.44	74.19	17.52	0.85
Cellulose	41.74	6.08	<0.01	52.18	6.23	90.26	3.51	<0.01
Xylan	41.47	6.48	<0.01	52.05	6.47	74.99	18.31	0.23
Lignin	57.04	4.76	<0.01	38.21	10.25	61.41	22.31	6.03

* Standard deviation \pm 1%. ^a Obtained by difference. ^b Based on TGA experiments according to the method established by Garcia et al. [137]

Table 2.2. Proximate and elemental analysis of produced chars*.

Material	Elemental analysis (wt. %)				Proximate Analysis (wt. %) ^b		
	C	H	N	O ^a	V.M.	F.C.	A.C.
Beech wood char (powder)	78.24	3.13	0.00	18.63	1.59	93.83	4.58
Flax Shives char	75.87	3.20	1.21	19.73	1.67	81.61	16.72
Beech wood char (pellets)	85.76	2.59	<0.00	11.65	1.31	94.16	4.53
Cellulose char	81.40	3.25	0.00	15.35	0.39	99.25	0.37
Xylan char	71.19	3.20	0.00	25.61	0.74	98.83	0.43
Lignin char	58.04	2.65	0.0	39.3	2.75	71.67	25.58

* Standard deviation \pm 1%. ^a Obtained by difference. ^b Based on TGA experiments according to the method established by Garcia et al. [137]

1.3 Catalysts used

The catalysts used for the study of the deoxygenation reaction were HZSM-5 and Fe-HZSM-5. The zeolite HZSM-5 was obtained commercially from ACS Material, with a SiO₂/Al₂O₃ ratio of approximately 38. Modification of these catalysts was carried out by the impregnation method aqueous solution of Fe (NO₃)₃·9H₂O, known as Iron (III) nitrate nonahydrate. After impregnation, the catalyst was calcined at 500°C for four hours in air. The iron content in the catalyst was 1.4 wt.%. The iron-modified catalyst was Fe-HZSM-5. The surface area of the catalyst used was 285.7 m²/g for HZSM-5 and 220.8 m²/g for Fe-HZSM-5.

Before utilization, these catalysts were introduced to an oven at 100°C for one hour in order to reduce their humidity.

1.4 Biochar preparation

The biomass used to prepare the biochar was beech wood (pellets). The biomass was introduced in the fluidized bed reactor and was heated at 3°C/min to 900°C and maintained there for one hour in order to ensure that no volatile matter was present after the devolatilization process. A nitrogen flow rate of 0.5 L/min was used as the carrier gas. The biochar was recovered from the reactor and then sieved to a particle size of approximately 450 μm , with a bulk density of 0.33 g/cm³ at 20°C. This biochar was used for catalytic gasification as bed material and kinetic modelling development runs.

2. Experimental set-ups

2.1 Semi-continuous reactor

The pyrolysis reaction was performed in a spoon reactor (**Figure 2.1**). The reactor was in quartz and had two sections—the pyrolysis section and the catalyst section. The total length of the reactor was 1050 mm, where 760 mm corresponded to the pyrolysis section and 290 mm to the catalyst section. The reactor was heated at 500°C under an N₂ flow of 0.5 L/min as a gas carrier. Once the reaction temperature was achieved, the selected raw material was introduced to the reactor using a stainless-steel spoon. Around 3 g of raw materials were used for each experiment. The reaction time was about five minutes for each test. For the experiments where the catalyst was used, 12 g of catalyst was placed in the catalytic zone before launching the reaction. The products were collected at the end of the reaction after the temperature went down, and then analysed with the most suitable instrument.

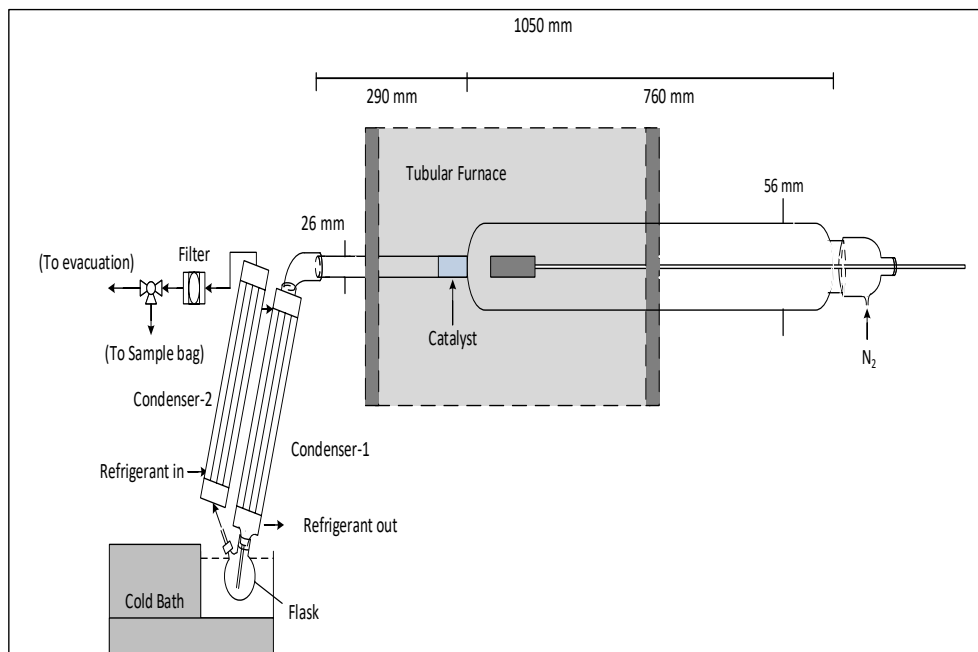


Figure 2.1. Experimental set-up (fixed bed reactor)

2.2 Fluidized bed reactor

The gasification runs were performed in a fluidized bed reactor (**Figure 2.2**). The reactor and its oven were obtained from MTI Corporation (Ref. OTF-1200X-S-FB); the reactor material wall was stainless steel, with an inner diameter of 22 mm and an external diameter of 25 mm. The gasification agent CO₂ and carrier gas N₂ were fed from the bottom of the reactor. Steam was fed into the reactor through an automatic syringe driver (Ref. AP14 ASCOR). The gasification process was isothermal. The bed materials were introduced in the reactor and then heated to the desired operating temperature. A constant flow of N₂ was used to maintain an inert atmosphere; when the desired temperature was reached, the gasification agent was added. The biomass was fed from the top of the reactor to the centre of the bed through a stainless-steel tube. The gaseous products exited from the top of the reactor through a separate tube. Finally, two condensers and a flask were placed in a cold bath at -10°C to collect all liquid products. Non-condensable gases passed through a cotton filter in order to retain all possible solid particles.

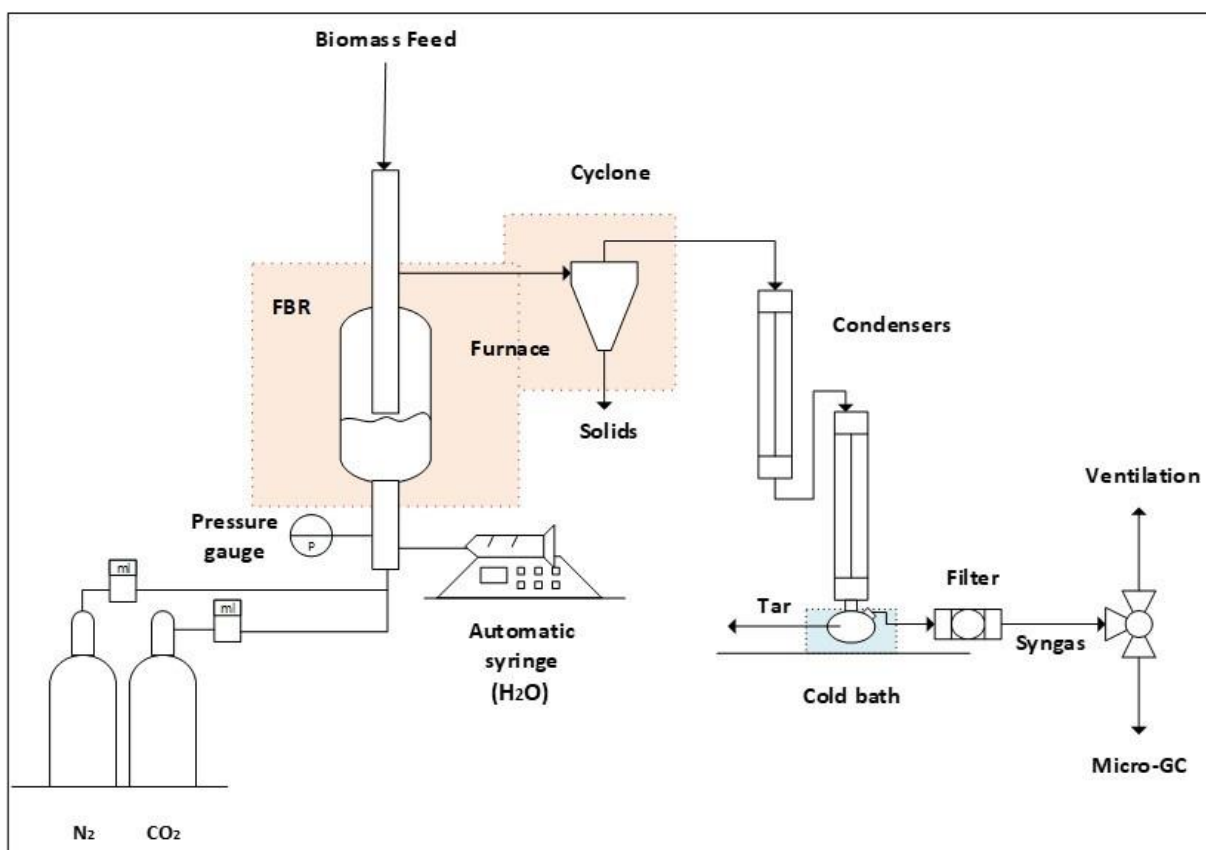


Figure 2.2. Fluidized bed reactor set-up.

Chapter 2

The gasification experiments were conducted at temperatures ranging from 600°C to 900°C. The biomass feed rate was 1 g/min. The washed sand or biochar, as bed materials, were placed inside the reactor before each run, with a height of 40 mm. The partial pressure of gases was $P_{N_2} = 0.05$ atm and 0.95 atm for the gasification agent (CO₂ or H₂O, respectively). N₂ was used as an internal standard for gas flow rate calculations. The total flow rate of the gasification agent entering the gasifier was 1.15 L/min. In order to keep the same fluidization conditions, the same flow rate of the entering gas was kept for pyrolysis, while only N₂ was introduced into the system. For product collection, solid particles were obtained from the reactor and the cyclone after each experiment, while liquid products, such as tar and water, were collected from condensers and the flask using an organic solvent (acetone, 99.98 % purity) and then analysed using gas chromatography. **Table 2.3** summarizes the experimental conditions used for this study.

Table 2.3. Experimental conditions summarized.

Thermal condition	Gasification Agent	Temperature range (°C)	Bed Material	Partial pressure (atm)
Pyrolysis	N ₂	[800 – 900]	Sand	1
CO ₂ gasification	CO ₂	[600 – 900]	Sand and biochar.	CO ₂ = 0.95 - N ₂ = 0.05
Steam gasification	H ₂ O	[600 – 900]	Sand and biochar.	H ₂ O = 0.95 - N ₂ = 0.05

For the isothermal biochar gasification tests, approximately 100 mg of biochar was introduced into the reactor with 10 g of washed sand, with a mass ratio of approximately 1/100. An N₂ flow was introduced in the reactor for approximately 15 minutes in order to create an inert atmosphere before heating. The reactor was then heated at 9°C/min in the N₂ flow; when the desired temperature was achieved, the gasification agent was introduced into the reactor. The reaction time was approximately two hours. **Table 2.4** shows the used experimental conditions for the fluidized bed gasifier tests.

Table 2.4. Experimental conditions for gasification Fluidized bed reactor.

Condition	Temperature	Atmosphere	*CO ₂ /C ratio	
1	800°C	67%CO ₂ - 33%N ₂	7.5	
2	900°C			
3	1000°C		33%CO ₂ – 67%N ₂	10.5
4				
5			100%CO ₂ – 0%N ₂	3.5
6				
7				
8		33%CO ₂ – 67%N ₂	7.5	
9				
10			10.5	
11				

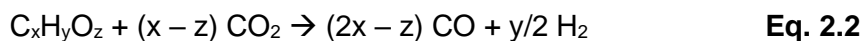
*The CO₂/C ratio was done by varying the gas flow rate from 715 to 2142 mL/min for the fluidized bed reactor for 2 hours of experiment duration.

The methodology to determine the biochar conversion in the fluidized bed gasifier was based on the carbon monoxide produced according to a derived Boudouard reaction. In literature [138]–[140], researchers consider that char or biochar is fully conformed of carbon molecules without considering its initial chemical structure: this is generally done because of the hypothesis of no volatile matter being released at high temperatures.

The commonly used Boudouard reaction is expressed as:



Using the dry reforming equation for solid fuel hydrocarbons proposed by Kaltschmitt et al. [141], biochar conversion with CO₂ can be expressed as:



Where x, y and z are the molar content of carbon, hydrogen and oxygen in the biochar, respectively. Substituting the molar values in **equation 2.2**, it was turned into,

Ref **Eq. 2.3**

The previous equation was used to calculate the conversion of biochar in this study, by stoichiometry. In order to do this, a specific amount of one of the product gases (CO or H₂) was required to calculate through the chemical equation the required amount of biochar for the

specified quantity. Using a micro-gas chromatograph, obtained from Chemlys corporation (Ref. PN 074-594-P1E), gaseous components were determined every two minutes.

The variation of biochar mass was determined as follows:

$$X = dm/dt \quad \text{Eq. 2.4}$$

$$dm/dt = [(m_0 - m_t)/(m_0 - m_{f-af})]/(t_f - t_0), \quad \text{Eq. 2.5}$$

$$m_t = (Mw_{\text{biochar}} * m_{t,\text{CO}})/(1.86 * Mw_{\text{CO}}) \quad \text{Eq. 2.6}$$

Substituting, **equation 2.6** in **equation 2.4**, it was obtained

$$X = dm/dt = (m_0 - [(Mw_{\text{biochar}} * m_{t,\text{CO}})/(1.86 * Mw_{\text{CO}}]))/(m_0 - m_{f-af}) / [(t_f - t_0)] \quad \text{Eq. 2.7}$$

where, X, m_0 , m_t , and m_{f-af} were the mass derivate and the initial, instant t and final (ash-free) mass of biochar.

The gasification rate (r) can be expressed by the following equation,

$$r = dX/dt \quad \text{Eq. 2.8}$$

The gasification rate represents the rapidity at which the reagents were consumed—in this study, the biochar samples. In order to quantify the reaction rate of biochar, a half-reaction index of r_{50} was selected. This index reported the reaction rate of biochar samples at a fixed value of conversion, in this case 50%. This common technique has been used in the literature [142] in order to present reaction rate values for a given conversion and time and to compare results. The r_{50} equation can be expressed as:

$$r_{50} = X_{(0-0.5)}/t_{0-0.5} \quad \text{Eq. 2.9}$$

where $X_{(0-0.5)}$ and $t_{0-0.5}$ represent the variation of conversion from 0 to 0.5 and the required time to reach conversion value of $X = 0.5$.

2.3 Thermogravimetric analyzer

The analyser used for this experiment was a TG SDT Q600-TA obtained from TA Instruments (USA), equipped with an aluminium oxide sample pan. The gases CO₂ and N₂ were connected into a mixer in order to provide a homogeneous stream; a pressure valve assured the volumetric flow entering the analyser. **Figure 2.3** shows the installation setup for gasification in the TG analyser. The biochar samples were introduced into the equipment with an average weight of 7.0 ± 0.1 mg. Once the sample was loaded, an N₂ flow was introduced in the equipment to create an inert atmosphere for approximately 15 minutes. Then the heating process began, with a heating rate of 9°C/min; when the operating temperature was reached, the N₂ flow was changed to CO₂ to start gasification. The iso-thermal gasification was

performed for approximately two hours for all samples. The experimental conditions were the same as for the gasification of biochar in the fluidized bed reactor shown in **Table 2.4**. For the TGA, the CO_2/C ratio was obtained by varying the gas flow rate from 50 to 150 ml/min.

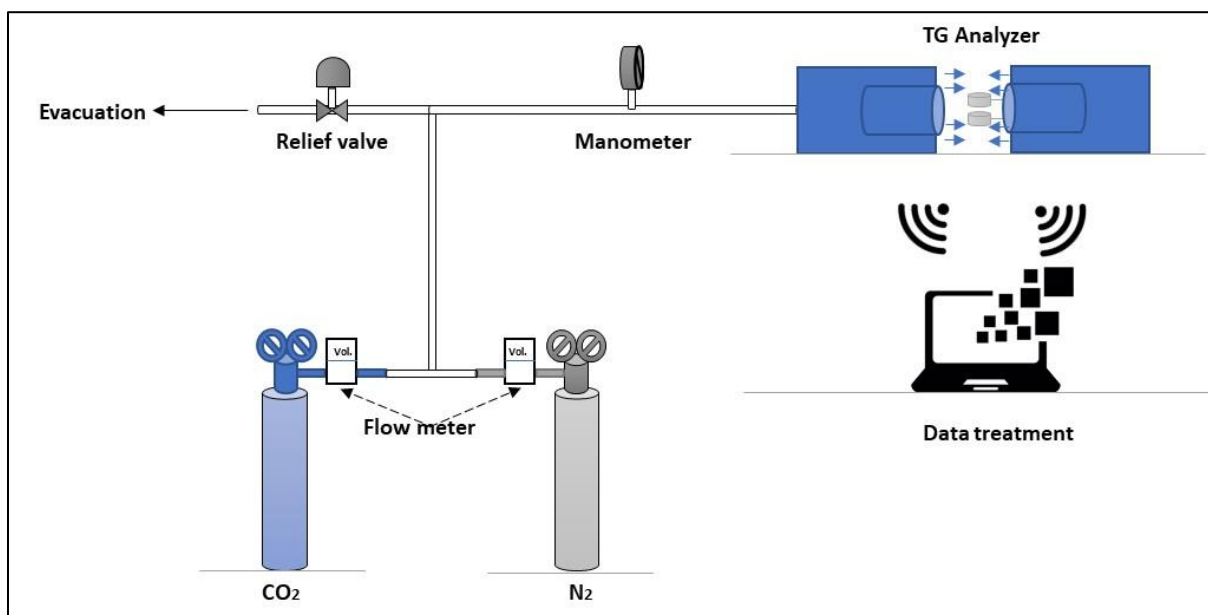


Figure 2.3. Thermogravimetric analyzer set-up.

The data acquired from the TG analyser was directly transmitted to a computer system and analysed using the software Trios from Universal TG Instruments. Once the variation in the mass of the sample was obtained, **Eq. 5** was used in order to determine the biochar conversion.

3. Analytical set-up and methods

3.1 Gaseous products

For the semi-continuous reactor, the gaseous products or non-condensable gases were collected in a sample bag and then analysed in gas chromatography (GC) using Claurus 580 from Perkin Elmer, equipped with a temperature conductivity detector (TCD) and a flame ionization detector (FID). The equipment was also equipped with a methanizer in order to detect CO and CO₂ compounds. For the gasification runs, the gaseous components were analysed continuously using a micro-gas chromatograph obtained from Chemlys Corporation (Ref. PN 074-594-P1E).

3.2 Liquid products

The liquids products were recovered from the condensers and flask using an organic solvent (ketone, purity 99.98%). A gas chromatograph mass spectrometer (GC-MS, Varian 3900 Saturn 2100T) was used to identify oil and tar molecules using the NIST library. For the

quantification of oil and tar molecules, a gas chromatograph (GC-FID Scion 456 Bruker instrument) was used. In order to determine the water content, a Karl Fisher titration equipment was used (KF Titrino Plus Metrohm 870 KF).

3.3 Pyrolysis oil classification

In this section, the analytic process developed for the identification and quantification of the bio-oil components is described. As is known, bio-oil contains more than 300 chemical molecules. In order to lighten the calculation task, the major compound was chosen for each chemical family identified in the bio-oil. A total of 12 families were identified, in which the major compound selected from each chemical family was the one with the highest mass percentage or abundance. Once these compounds were identified in the GC-MS, calibration curves were developed using the GC-FID by preparing samples of different concentrations and obtaining the respective mathematical equation. For calibration, reference compounds were used which represented a similar chemical structure to the major compounds identified. Both major compounds and reference compounds for calibration belonged to the selected chemical family. **Table 2.5** shows the selected compound for each chemical family and the values for the coefficient of determination (R^2).

The selected chemical families represented the common classification used for bio-oil quantification at temperatures between 450°C and 550°C [143]. Biomass bio-oil is mainly composed of a range of oxygenated molecules in which acetic acids, phenols, aldehydes and esters represent the most abundant components, whilst the major components of the bio-oil obtained from the biomass (cellulose, hemicellulose and lignin) showed a different distribution of molecules. Cellulose bio-oil was mainly represented by sugars and phenolic compounds, while hemicellulose bio-oil showed a high concentration of acids, alcohols and ketones. Finally, lignin bio-oil was mainly composed of phenolic compounds, acids and alkenes.

Table 2.5. Chemical families classification for bio-oil molecules.

Chemical Family	Major compound		Reference compound		R ²
Acids	C ₂ H ₄ O ₂	Acetic Acid	C ₂ H ₄ O ₂	Acetic acid	0.9933
Alcohols	C ₆ H ₆ O ₂	Catechol	C ₆ H ₆ O ₂	Catechol	0.9673
Aldehydes	C ₅ H ₄ O ₂	Furfural	C ₅ H ₄ O ₂	Furfural	0.9876
Alkanes	C ₉ H ₂₀	Nonane	C ₉ H ₂₀	Nonane	0.9867
Alkenes	C ₆ H ₆ , C ₇ H ₈ , C ₅ H ₁₀	Benzene, Toluene, cyclopentene	C ₆ H ₆ , C ₇ H ₈ , C ₈ H ₁₀	Benzene, Toluene, P-xylene	0.9989, 0.9988, 0.9982
Amides	C ₄ H ₉ NO	Butyramide	C ₇ H ₇ NO	Benzamide	0.9847
Esters	C ₂ H ₃ O ₂	Acetate	C ₇ H ₁₂ O ₂	Allyl butyrate	0.9872
Furans	C ₄ H ₄ O	Furan	C ₄ H ₄ O	Furan	0.9809
Guaiacols	C ₉ H ₁₂ O ₂	4-Ethyl guaiacol	C ₇ H ₈ O ₂	4-Methylcatechol	0.9823
Ketones	C ₅ H ₄ O ₂ , C ₆ H ₆ O ₃	Pyrane-2-one, levoglucosenone	C ₅ H ₆ O	2-Cyclopenten-1-one	0.9946
Phenols	C ₇ H ₈ O, C ₆ H ₆ O	o-cresol, phenol	C ₆ H ₆ O	Phenol	0.9952
Sugars	C ₆ H ₁₀ O ₅	Levoglucosan	C ₆ H ₁₀ O ₅	Levoglucosan	0.9954

3.4 Tar classification

The most common classification method for tar molecules was proposed by the Energy Research Centre of the Netherlands (ECN), where tars are classed based on the physical properties of polarity, dew point and the number of aromatic rings. Another method proposed by Wolfesberget et al. [144] is to classify tar into substance groups. In our work, a hybrid method from these two classifications was adopted to classify tar into chemical substance groups.

The first step in tar classification was to identify the principal chemical families present in the tar. The first tar samples from the gasification of biomass with CO₂ were analysed in the GC-MS to identify the major compounds. **Figure 2.4** shows the results of tar identification in GC-MS. The obtained compounds were gathered in eight substance groups: from these substances, the principal compounds were selected in order to create a calibration curve for the GC-FID analysis. This was done to have an accurate value of the tar obtained from the

gasification. **Table 2.6** shows the major compounds selected for tar calibration in gas chromatography.

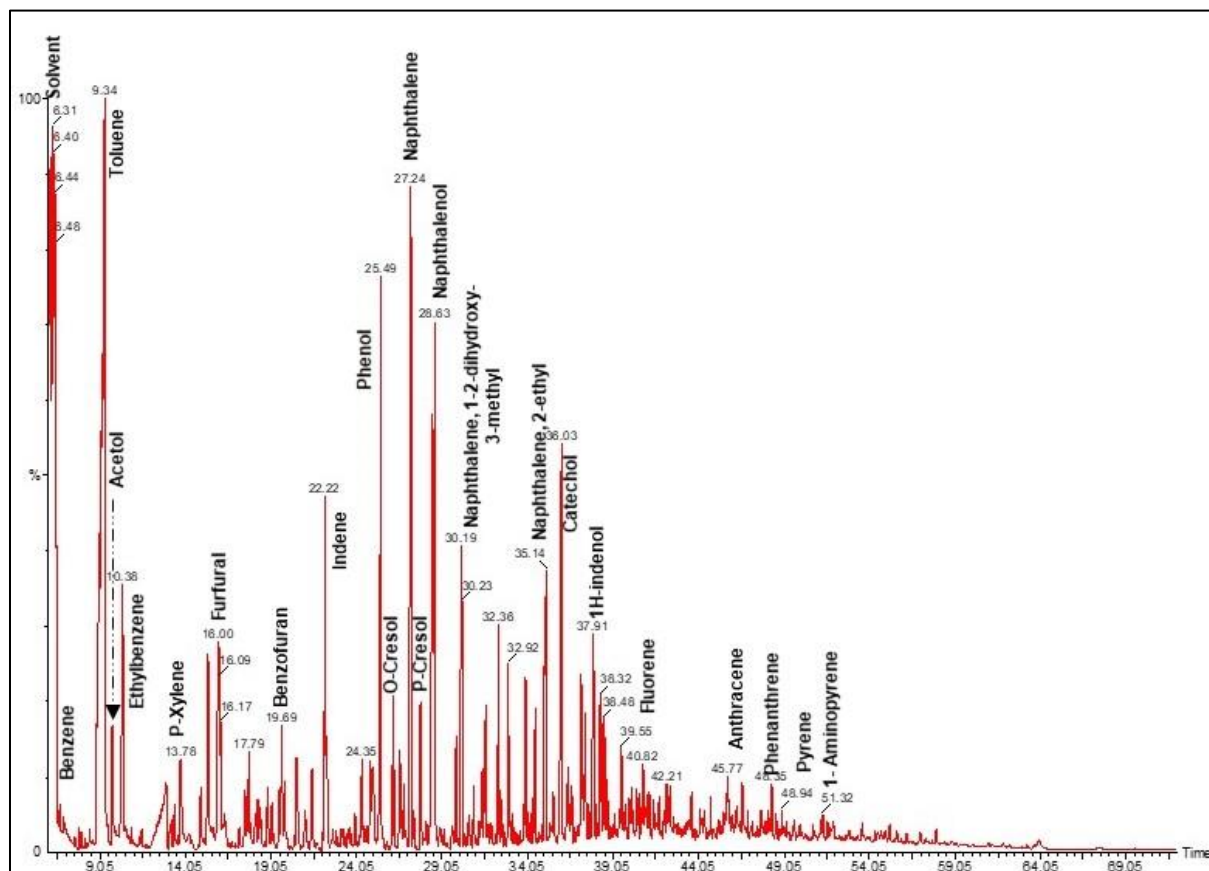


Figure 2.4. Chromatogram GC-MS of tar obtained from gasification with CO₂.

As can be observed in **Table 2.6**, the hybrid method used in this work divided ECN tar classification into several chemical groups. Class 2 was divided into compounds with a phenolic origin, furans and other heterocyclic aromatic compounds with high solubility in water. Class 3 was retained as the common definition of light aromatic hydrocarbons with one ring. In class 4, a modification was made due to the high compounds of naphthalene origin: thus this classification was divided into naphthalene origin compounds and light poly-aromatic hydrocarbons (LPAH) with two or three aromatic rings. Class 5 was represented by the heavy poly-aromatic hydrocarbons (HPAH) with four or more aromatic rings and heavy molecular weight. Finally, an additional group called others was included in the classification, which represented traces of single-chain aliphatic compounds like acids, esters and alcohols, and heterocyclic non-aromatic compounds such as cyclohexanol, 2-cyclopenten-1-one and others.

Table 2.6. Tar classification and details for calibration.

Substance groups	Major Components	Compound selected for calibration	ECN Tar Classification ^a
Phenols	Phenols, Phenol, 3-ethyl-5-methyl-, Phenol, 3-ethoxy-	Phenol	Class 2
Furans	Benzofuran, Furan-2-carbaldehyde	Furan	
Heterocyclic aromatic compounds (HAC)	O,M,P-Cresol, 1H-Indenol	O-Cresol	
Aromatic hydrocarbon compounds (AC)	Benzene, Toluene, O,P-Xylene, Ethylbenzene	Benzene, Toluene, P-Xylene	Class 3
Naphthalenes	Naphthalene, Naphthalene,1,2-dihydro-4-methyl-, Acenaphthylene,	Naphthalene	Class 4
Light poly-aromatic hydrocarbons (LPAH)	Indene, Fluorene, Anthracene, Phenanthrene	Indene, phenanthrene	
Heavy poly-aromatic hydrocarbons (HPAH)	Pyrene, 1-Aminopyrene	Benzo-Pyrene	Class 5
Others	Aliphatic compounds as acetic acid, ethers, aldehydes Heterocyclics non-aromatics: cyclopentene	Acetic acid, Allyl butyrate	N/A

^a Class 1, designed for non-detectable compounds in chromatography

4. Energy balance

The energy balance of the system was done by isolating the reactor from other units (cyclone, condensers, etc.) and considering only its energy input and output streams (**Figure. 2.5**). In pyrolysis and gasification, it was considered that a steady stage was reached in order to employ the selected equations. Following the first law of thermodynamics, energy is conserved. Applying an energy balance to the thermochemical decomposition of the biomass system, as shown in the figure, it turns into:

$$\sum \dot{E}_{in} = \sum \dot{E}_{out} \quad \text{Eq. 2.10}$$

$$\dot{E}_{biomass} + \dot{E}_{agent/gas_carrier} + \dot{Q}_{Heat} = \dot{E}_{gas} + \dot{E}_{tar/bio-oil} + \dot{E}_{biochar} + \dot{Q}_{loss} \quad \text{Eq. 2.11}$$

For this study, the heat loss through the walls of the reactor was neglected, then $\dot{Q}_{\text{loss}} = 0$.

\dot{E}_{biomass} , $\dot{E}_{\text{agent/gas_carrier}}$, \dot{E}_{gas} , $\dot{E}_{\text{tar/bio-oil}}$ and \dot{E}_{biochar} were the energy rates of biomass, gasification agent (for gasification) or gas carrier (for pyrolysis), gases, tar (for gasification) or bio-oil (for pyrolysis) and biochar, respectively, and \dot{Q}_{Heat} was the specific additional heat input introduced into the system to perform gasification or pyrolysis at a specified temperature. Since no heat loss was taken into account, then $\dot{Q}_{\text{Heat}} = \dot{Q}_{\text{gasification}}$ or $\dot{Q}_{\text{pyrolysis}}$

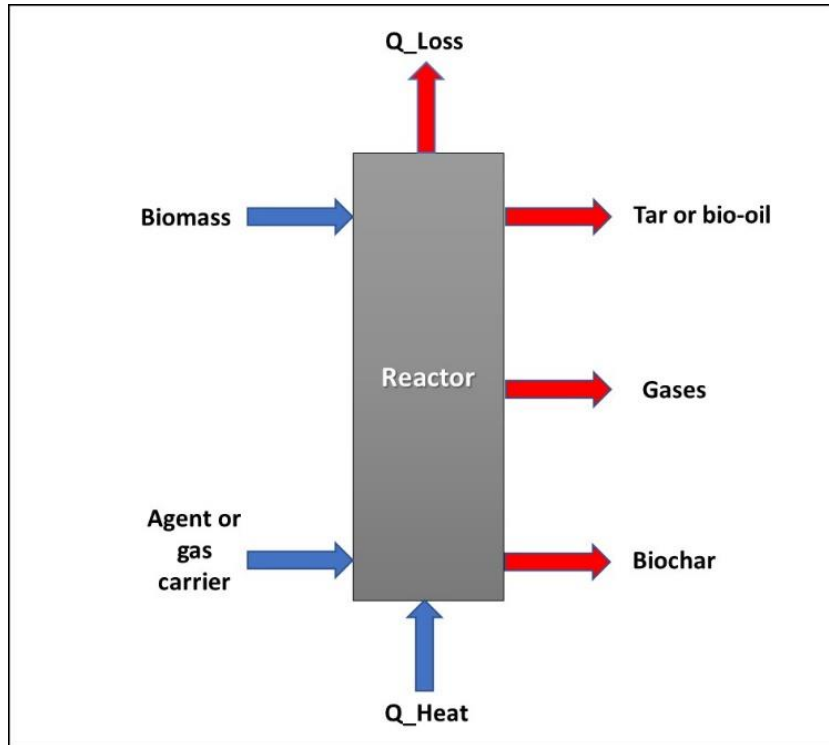


Figure 2.5. Streams input and output from the reactor.

The energy rate of a stream can be calculated as follows:

$$\dot{E}_n = \dot{E}_{n_{ph}} + \dot{E}_{n_{ch}} + \dot{E}_{n_{po}} + \dot{E}_{n_{ki}} \quad \text{Eq. 2.12}$$

The subscripts ph, ch, po and ki were the physical, chemical, potential and kinetic energy rates, respectively. Potential and kinetic energies of streams were considered to be very small when compared to physical and chemical [112], and were hence neglected. Therefore, **Eq. 2.12** is expressed as:

$$\dot{E}_n = \dot{E}_{n_{ph}} + \dot{E}_{n_{ch}} \quad \text{Eq. 2.13}$$

Substituting each energy term with its definition, it is found that physical energy (sensible heat) was defined as follows:

$$\dot{E}_{n_{ph}} = n_i \int C_{p_i} dT \quad \text{Eq. 2.14}$$

Meanwhile, the chemical energy (enthalpy of formation) was defined as follows,

$$\dot{E}_{\text{ch}} = \sum_i n_i h_{f,i}^{\circ} \quad \text{Eq. 2.15}$$

Substituting **Eq. 2.14** and **Eq. 2.15** in **Eq. 2.13**, it turned into

$$\dot{E}_n = n_i \left(\int C_{p,i} dT + \sum_i n_i h_{f,i}^{\circ} \right) \quad \text{Eq. 2.16}$$

For solids

For non-conventional fuel (e.g. biochar and biomass), the enthalpy of formation was calculated based on their combustion reaction [35]:

$$h_{f,\text{fuel}}^{\circ} = \alpha h_{f,\text{CO}_2}^{\circ} + \beta h_{f,\text{H}_2\text{O}}^{\circ} + \text{LHV}_{\text{fuel}} \quad \text{Eq. 2.17}$$

where α , β , $h_{f,\text{CO}_2}^{\circ}$, and $h_{f,\text{H}_2\text{O}}^{\circ}$ were the stoichiometric coefficient and enthalpies of formation of CO_2 and H_2O , respectively. LHV was the lower heating value of a compound at 15°C .

The above **Eq. 2.17** was believed to provide the chemical energy for non-conventional fuels. The physical energy of biomass was difficult to calculate because of the occurrence of a devolatilization reaction. Consequently, the researchers only used the chemical energy; otherwise, they calculate the physical energy at a temperature just before the devolatilization reaction [102], [145].

In this study, the energy equation used for biomass and biochar was:

$$\dot{E}_{\text{fuel}} = \dot{n}_{\text{fuel}} * (\text{LHV}_{\text{fuel}} + \Delta h_{\text{sensible}}) = \dot{n}_{\text{fuel}} * (\text{LHV}_{\text{fuel}} + \int C_{p,\text{fuel}} dT) \quad \text{Eq. 2.18}$$

In the case of biomass, T was the devolatilization temperature; while for biochar, T was the operating temperature. The LHV of the fuels was calculated using the Dulong formula:

$$\text{LHV}_{\text{fuel}} = (33.80 x_{\text{C}} + 144.20 x_{\text{H}} - 18.03 x_{\text{O}}) \quad \text{Eq. 2.19}$$

where, x_{C} , x_{H} and x_{O} were the carbon, hydrogen and oxygen composition (wt. %), obtained for each fuel from the elemental analysis.

For gases

For gaseous streams (e.g. syngas or pyrolysis gases), the energy rate was described as follows:

$$\dot{E}_{\text{gas}} = \sum_i n_i \left(\int C_{p,i} dT + \text{LHV}_i \right) \quad \text{Eq. 2.20}$$

In **Eq. 2.20**, n_i , $C_{p,i}$, and LHV_i were the molar flow rate, heat capacity at constant pressure and LHV of gases, respectively.

For tar or bio-oil

In order to calculate the tar/bio-oil energy rate, only the major compounds of each substance group were taken into consideration. As the number of tar/bio-oil molecules was very elevated (>200 compounds), it was necessary to choose the major compound in terms of quantity for each substance group. This was done to simplify calculation. The enthalpy for phase change of compounds was also taken into consideration. The energy equation for tar/bio-oil was described as follows:

$$\dot{E}_{n_{tar/bio-oil}} = \sum_i n_i (\int C_{p_i} dT + \Delta h_{phase_change} + LHV_i) \quad \text{Eq. 2.21}$$

Coefficients of heat capacity along with other thermodynamic properties for tar and gaseous species are shown in **Appendix A1**.

5. Exergy evaluation

The exergy evaluation of the process was done with the same concept as the energy balance, isolating the reactor from other equipment and considering only its exergy input and output streams. Following the first and second thermodynamic laws, the exergy evaluation might be described as follows:

$$\sum \dot{E}x_{in} = \sum \dot{E}x_{out} + I \quad \text{Eq. 2.22}$$

where $\sum \dot{E}x_{in}$, $\sum \dot{E}x_{out}$ and I were the sum of all exergy streams entering and exiting the reactor and the exergy destruction rate, respectively. The exergy destruction rate for a system can be defined as the sum of internal and external irreversibilities, as follows:

$$I = I_{internal} + I_{external} \quad \text{Eq. 2.23}$$

The internal irreversibility is the term associated with the entropy generation due to the heat and mass transfer, substance flow and chemical reactions inside the reactor. The external irreversibility represents the exergy loss due to interaction with the external environment, and can be represented as:

$$I_{external} = Q_{loss} * (1 - T^o/T_w) \quad \text{Eq. 2.24}$$

where T_w represents the reactor walls' temperature. Since no heat loss was found in this study ($Q_{loss} = 0$), external irreversibility was neglected. Therefore, the exergy destruction rate was represented by the internal irreversibilities.

Defining the streams entering and exiting the reactor, **Eq. 2.22** is expressed as:

$$\dot{E}x_{biomass} + \dot{E}x_{agent/gas_carrier} + \dot{E}x_{Heat} = \dot{E}x_{gas} + \dot{E}x_{tar/bio-oil} + \dot{E}x_{biochar} + I \quad \text{Eq. 2.25}$$

where $\dot{E}x_{biomass}$, $\dot{E}x_{agent/gas_carrier}$, $\dot{E}x_{gas}$, $\dot{E}x_{tar/bio-oil}$ and $\dot{E}x_{biochar}$ are the exergy rates of biomass, gasification agent (CO_2 or H_2O for gasification) or gas carrier (N_2 for pyrolysis), gas, tar (for

gasification) or bio-oil (for pyrolysis), and biochar, respectively, and $\dot{E}x_{Heat}$ is the exergy value of the additional heat introduced into the system to perform gasification or pyrolysis. It was assumed that the input of exergy was equal to the electrical energy input [146]. Considering that the entropy of electricity was very low, $\dot{E}x_{Heat} = \dot{Q}_{Heat_input}$. In other words, this was the electricity energy taking into account the thermal loss.

The exergy rate of a stream can be calculated as follows:

$$\dot{E}x = \dot{E}x_{ph} + \dot{E}x_{ch} + \dot{E}x_{po} + \dot{E}x_{ki} \quad \text{Eq. 2.26}$$

where the subscripts ph, ch, po and ki are the physical, chemical, potential and kinetic exergy rates, respectively. As for energy calculations, the potential and kinetic exergies of streams were considered to be very small when compared to physical and chemical exergies. Consequently, the exergy of a stream was reduced to:

$$\dot{E}x = \dot{E}x_{ph} + \dot{E}x_{ch} \quad \text{Eq. 2.27}$$

For gases

The chemical exergy for gaseous streams was defined as:

$$\dot{E}x_{ch,gas} = \sum_i n_i ((ex_{ch,i}) - RT^\circ \ln(x_i)) \quad \text{Eq. 2.28}$$

where, $ex_{ch,i}$ and x_i were the chemical standard exergy and the molar concentration of gas ith, respectively.

The physical exergy for gaseous streams was expressed as follows,

$$\dot{E}x_{ph,gas} = \sum_i n_i ((h-h^\circ)_i - T^\circ(S-S^\circ)_i) \quad \text{Eq. 2.29}$$

where the terms $(h-h^\circ)_i$ and $(S-S^\circ)_i$ represent the specific enthalpy and entropy difference of the ith gas. This can be expressed as:

$$(h-h^\circ)_i = \int Cp_i dT \quad \text{Eq. 2.30}$$

$$(S-S^\circ)_i = [(\int Cp_i/T dT) - R \ln (P_i/P^\circ)] \quad \text{Eq. 2.31}$$

Substituting **Eq. 2.30** and **Eq. 2.31** into **Eq. 2.29**, the final equation for the calculation of the exergy rate of gases is:

$$\dot{E}x_{ph,gas} = \sum_i n_i (\int Cp_i dT - T^\circ [(\int Cp_i/T dT) - R \ln (P_i/P^\circ)]) \quad \text{Eq. 2.32}$$

For tar and bio-oil

The exergy for tar/bio-oil was calculated using the same procedure, from **Eq. 2.28** to **Eq. 2.32**, but taking into account the phase change enthalpy for different components.

The final equation to calculate the tar/bio-oil exergy rate was described as follows:

$$\dot{E}_{x_{\text{tar/bio-oil}}} = \sum_i n_i \left(\int C_{p_{\text{tar/bio-oil}}} dT + \Delta h_{\text{phase_change}} - T^{\circ} \left[\int C_{p_{\text{tar/bio-oil}}} / T dT - R \ln (P_i / P^{\circ}) \right] \right) \quad \text{Eq. 2.33}$$

The thermodynamics data used for the calculation of chemical exergy, heat capacity, and entropy are presented in **Appendix A1**.

For solids

For solids, the exergy calculation varies from a gaseous stream, and empirical equations have to be used due to the lack of thermodynamic data for non-conventional fuels. For biomass and biochar, only chemical exergy can be calculated because of the difficulty in calculating their entropy. Using the Szargut method [147], the exergies of biomass and biochar were calculated as:

$$\dot{E}_{x_{\text{ch,fuel}}} = \beta * \text{LHV}_{\text{Fuel}} \quad \text{Eq. 2.34}$$

$$\beta = \{1.0414 + 0.0177 *(H/C) - 0.3328 (O/C) [1 + 0.0537 *(H/C)]\} / [1 - 0.0421 *(O/C)] \quad \text{Eq. 2.35a}$$

For, $0.5 < (O/C) < 2$

$$\beta = 1.0438 + 0.0158 *(H/C) - 0.0813 (O/C) \quad \text{Eq. 2.35b}$$

For, $(O/C) < 0.5$

6. Efficiency calculation

6.1 Energy efficiency (η)

To evaluate the energetic efficiency of the system, the following equation was employed:

$$\eta = E_{n_i} / E_{n_{\text{inlet}}} \quad \text{Eq. 2.36}$$

6.2 Cold gas efficiency (CGE)

To evaluate the efficiency of the system, cold gas efficiency (CGE) was frequently used as an important parameter. It is defined as:

$$\text{CGE} = (m_{\text{gas}} \text{LHV}_{\text{gas}}) / (m_{\text{biomass}} \text{LHV}_{\text{biomass}}) \quad \text{Eq. 2.37}$$

The values of mass and LHV for syngas and biomass were on a dry basis.

6.3 Exergetic efficiency (Ψ)

To evaluate the exergetic efficiency of the system, the following equation was used:

$$\Psi = \dot{E}_{x_i} / \sum \dot{E}_{x_{in}} \quad \text{Eq. 2.38}$$

Chapter 3 :

**THERMODYNAMIC ANALYSIS OF BIOMASS AND PSEUDO-
COMPONENTS PYROLYSIS IN A SEMI-CONTINUOUS
REACTOR.**

Introduction

The following chapter involves the thermodynamic analysis of the results obtained from the pyrolysis of biomass and pseudo components in a semi-continuous spoon reactor, obtained from the thesis by Mohabeer, 'Bio-oil production by pyrolysis of biomass coupled with a catalytic de-oxygenation treatment' [148]. Thermodynamic analysis consisted of calculating the energy balance and exergy evaluation and efficiency in order to determine process consumption and exergy destruction. The results of the pyrolysis of biomass principal components (cellulose, hemicellulose and lignin) and the biomasses (beech wood and flax shives) were evaluated, aiming to establish the thermodynamic results of biomass pyrolysis directly from investigation of the values from the pyrolysis of its principal components. Also included were energetic and exergetic investigation of the bio-oil upgrading process in order to evaluate its quality from a thermodynamic point of view.

This chapter focuses on adding important details that are usually missing in criticism and evaluation of the effectiveness of the thermochemical biomass process (pyrolysis). In addition, it comprises the novelty of thermodynamic analysis of the catalytic conversion of biomass with the catalysts HZSM-5 and Fe- HZSM-5, and the pyrolysis of biomass pseudo-components. The efficacy of these catalysts in the deoxygenation reaction of bio-oil was investigated in previously published articles [22], [27], [54]. The complete mass balance and discussion of the results obtained from the semi-continuous reactor are presented in **Appendix A1**.

The following results present a margin of error of approximately 2.7% due to the experimental uncertainty and deviations. The errors surrounding the experimental test are those found in deviation calculations after experiment repetitions, mass weighting, the rounding of values and equipment tolerance. The uncertainty of values is shown by error bars over the presented results. For convenience, gaseous products with more than one carbon molecule are presented as C₂₊ (including C₂H₂, C₂H₄ and C₂H₆) and C₃₊ (including C₃H₄, C₃H₆ and C₃H₈) in this work.

The results are presented in units of MJ/kg_i and MJ/kg_{Material} as this represents a better way to show the rates of energy/exergy per kg of individual phase (gas, liquids and biochar) and per kg of raw material. All experiments were repeated at least three times in order to assure repeatability.

In this work, the term anergy or heat waste is used to describe the difference between the energy and exergy values of a stream. In other words, it contains the non-profitable part of energy when a system was not fully reversible. Meanwhile, the exergy destruction (I) term was used to describe the difference between the inlet and outlet exergy of the conversion system.

Both energy and exergy destruction (I) terms are present due to entropy generation or the irreversibility of the process. **Table 3.1** and **3.2** summarize the energetic and exergetic values obtained from the thermodynamic evaluation of the experimental results, performing an energy balance and exergy evaluation as described in **chapter 2**.

1. Pyrolysis of beech wood and flax shives

As can be seen in **Figures 3.1** and **3.2**, the values of energy and exergy from pyrolysis products from both biomasses were very similar. The pyrolysis gases presented a difference between biomasses of 2.03 ± 0.06 MJ/kgGas for energy values and approximately 1.63 ± 0.04 MJ/kggas for exergy values,. Despite the biomasses having a similar elemental analysis, these differences could have come about because of the higher volatile matter values present in beech wood compared to flax shives. It also could be observed that pyrolysis gases and bio-oil total energy values were higher than exergy values. Thermodynamically, in an irreversible process, the difference between energy and exergy values is known as anergy and corresponds to the heat waste after a thermal reaction [149].

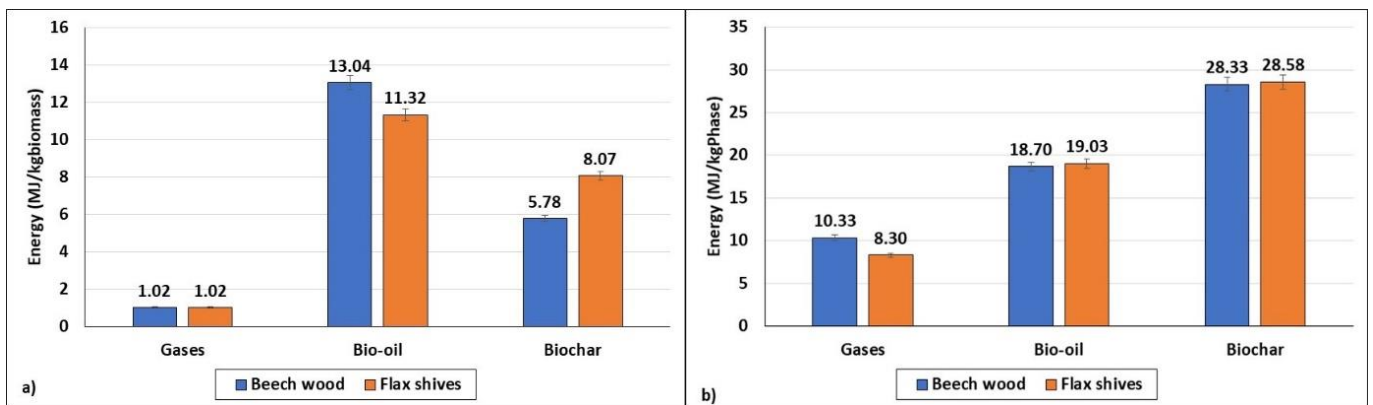


Figure 3.1. Energy distribution of products from biomasses at 500°C, a) MJ/kg_{biomass} b) MJ/kg_{phase}

Chapter 3

Table 3.1. Results of energy balance and exergy of biomasses pyrolysis.

Raw Material	Condition	LHV: MJ/kg	Exergy: MJ/kg	Mass Balance (yield %)			Energy Balance (MJ/kg _{Material})				Exergy (MJ/kg _{Material})				
				Gases	Bio-oil	Biochar	^a Gases	Bio-oil	Biochar	^b Q _{pyro}	^a Gases	Bio-oil	Biochar	Ex Heat	/
Beech wood	No-catalyst	17.87	19.90	9.87	69.73	20.40	1.02	13.04	5.78	1.97	0.86	12.89	6.03	1.97	2.10
	HZSM-5			28.48	49.67	21.85	3.40	12.13	6.19	3.85	3.20	12.11	6.46	3.85	1.99
	Fe-HZSM-5			19.80	57.76	22.44	3.69	15.20	6.36	7.38	3.45	15.18	6.63	7.38	2.03
Flax shives	No-catalyst	18.20	20.14	12.29	59.47	28.24	1.02	11.32	8.07	2.21	0.87	11.26	8.23	2.21	2.00
	HZSM-5			22.67	50.67	26.66	2.97	13.08	7.62	5.47	2.77	13.07	7.95	5.47	1.83
	Fe-HZSM-5			23.26	49.50	27.24	3.52	13.06	7.79	6.17	3.29	13.00	8.12	6.17	1.91

^a Gas carrier N₂, values were included.

^b Q_{Pyro} = EX_{Heat}.

Table 3.2. Results of energy balance and exergy of pseudo-components pyrolysis.

Raw Material	Condition	LHV: MJ/kg	Exergy: MJ/kg	Mass Balance (yield %)			Energy Balance (MJ/kg _{Material})				Exergy (MJ/kg _{Material})				
				Gases	Bio-oil	Biochar	^a Gases	Bio-oil	Biochar	^b Q _{pyro}	^a Gases	Bio-oil	Biochar	Ex Heat	/
Cellulose	No-catalyst	16.68	18.18	11.84	75.66	12.50	1.25	12.67	3.97	1.22	1.06	12.24	4.13	1.22	1.97
	HZSM-5			28.20	59.34	12.46	3.76	13.53	3.75	4.37	3.46	13.48	3.9	4.37	1.72
	Fe-HZSM-5			32.45	54.30	13.25	3.73	11.76	4.22	3.04	3.37	11.71	4.39	3.04	1.75
Hemicellulose	No-catalyst	17.06	18.62	8.58	78.54	12.87	0.77	14.22	3.50	1.43	0.62	14.16	3.66	1.43	1.62
	HZSM-5			29.37	60.73	9.90	3.83	13.48	2.64	2.89	3.56	13.44	2.76	2.89	1.75
	Fe-HZSM-5			39.02	47.21	13.77	4.51	10.78	3.77	2.00	4.19	10.68	3.94	2.00	1.81
Lignin	No-catalyst	21.79	21.96	10.60	32.78	56.62	0.93	7.86	13.85	0.86	0.78	7.77	13.76	0.86	0.51
	HZSM-5			10.30	32.56	57.14	0.90	8.03	13.90	1.05	0.75	7.96	13.81	1.05	0.50
	Fe-HZSM-5			13.25	28.48	58.28	1.08	7.72	13.94	0.96	0.94	7.65	13.84	0.96	0.49

^a Gas carrier N₂, values were included.

^b Q_{Pyro} = EX_{Heat}.

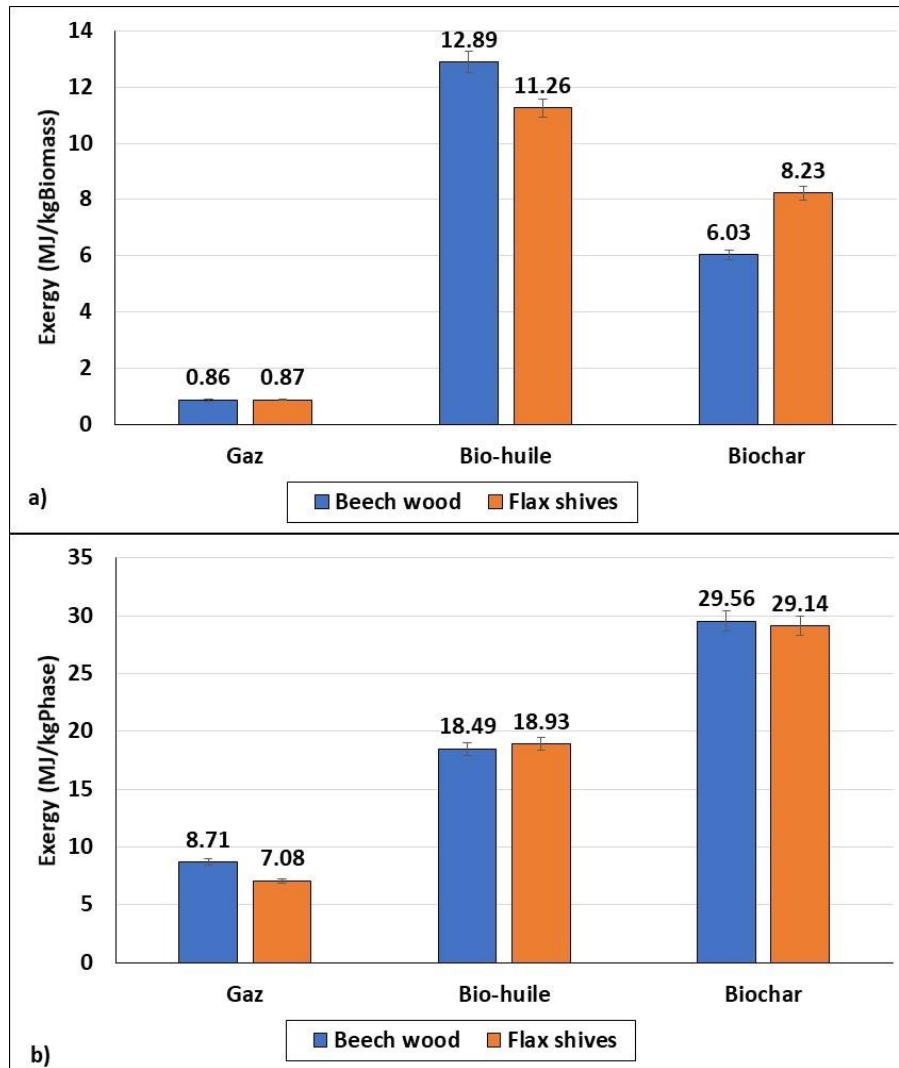


Figure 3.2. Exergy distribution of products from biomasses at 500°C, a) MJ/kg_{biomass} b) MJ/kg_{phase}.

1.1 Energetic and exergetic evaluation of biomass pyrolysis products

Biochar

Despite the energy statement following the energy principle of conservation, it is noted that calculations of biochar exergy showed higher values than energy. This statement had no physical meaning. An explanation was therefore found for this observed phenomenon: it was noted that the Szargut equation (Eq. 2.34) did not consider the possible entropy changes of non-conventional fuels. Since the pyrolysis reactions, especially biochar formation reactions, were not fully reversible, the irreversibilities of this reaction were not accounted for in the exergy calculation. Eboh and colleagues [150] also explained this statement in their work, evidencing the possibility of having higher chemical exergy values than energy values for non-conventional fuels because of missing information about entropy (irreversibility).

Comparing both biochar energy values, flax shives' biochar energy ($28.58 \pm 0.78 \text{ MJ/kg}_{\text{Biochar}}$) was slightly higher than that of beech wood biochar ($28.33 \pm 0.76 \text{ MJ/kg}_{\text{Biochar}}$), although the elemental analysis of beech wood biochar showed less oxygen and ash content and high fixed carbon values, which potentially could influence biochar energy calculation. Flax shives' mass balance showed a 28% yield for the obtained biochar: for this reason, it was found to be superior in energy value to beech wood. This can be observed when results are expressed in units of $\text{MJ/kg}_{\text{Biomass}}$, where $8.07 \pm 0.22 \text{ MJ/kg}_{\text{Biomass}}$ were obtained for flax shives and $5.78 \pm 0.16 \text{ MJ/kg}_{\text{Biomass}}$ for beech wood. The same applies to exergy values: for both obtained biochars, the difference between energy and exergy values was approximately $0.42 \pm 0.01 \text{ MJ/kg}_{\text{Biochar}}$ or $2.2 \pm 0.06 \text{ MJ/kg}_{\text{Biomass}}$. As mentioned before, this superior value of exergy over energy was attributed to the lack of calculation of entropy changes for biochar due to the heterogeneous reactions that took place in non-conventional fuels.

Gases

As can be seen, pyrolysis gases represent the lowest energy/exergy values distribution of products. The pyrolysis of biomass at 500°C favoured the production of bio-oil and biochar rather than gases, as observed in the mass balance yields in **Table 2.1**. In addition, pyrolysis gases were mainly constituted of CO_2 and CO compounds, and CO_2 energetic density was very low: for this reason, gas energy and exergy values were very low compared to other streams. The gases obtained from beech wood pyrolysis contained $10.33 \pm 0.28 \text{ MJ/kg}_{\text{Gas}}$, of which only $8.71 \pm 0.24 \text{ MJ/kg}_{\text{Gas}}$ could be profitable (exergy). On the other hand, for flax shives pyrolysis, $8.30 \pm 0.22 \text{ MJ/kg}_{\text{Gas}}$ could be obtained from the gases, of which exergy value was $7.08 \pm 0.19 \text{ MJ/kg}_{\text{Gas}}$.

The difference between the two biomasses' pyrolysis gases came principally from the high energy rate of CO ($4.14 \pm 0.11 \text{ MJ/kg}_{\text{Gas}}$) for beech wood compared to $3.02 \pm 0.08 \text{ MJ/kg}_{\text{Gas}}$ for flax shives. Also, C_2+ produced from pyrolysis of beech wood was higher than for flax shives. As can be observed in **Figure 3.3**, the energy value of this gas for beech wood was $1.26 \pm 0.03 \text{ MJ/kg}_{\text{Gas}}$ and $1.03 \pm 0.03 \text{ MJ/kg}_{\text{Gas}}$ for flax shives. It has been shown in the literature that the formation CO , CH_4 and C_2+ favours beech wood pyrolysis more than flax shives [22].

Bio-oil

In power generation endings, pyrolysis oil or bio-oil as it is known in the scientific community, represents the desirable product. The energy rate obtained after the pyrolysis of biomasses was slightly different for the two bio-oils, at $18.70 \pm 0.51 \text{ MJ/kg}_{\text{Bio-oil}}$ and $19.03 \pm 0.51 \text{ MJ/kg}_{\text{Bio-oil}}$ for beechwood and flax shives, respectively. The difference in energy was about $0.33 \pm 0.01 \text{ MJ/kg}_{\text{Bio-oil}}$ which could be considered insignificant compared to the obtained bio-oils values. Meanwhile, in terms of $\text{MJ/kg}_{\text{Biomass}}$, the energy rate of beech wood bio-oil (13.04 ± 0.35

MJ/kg_{Biomass}) was higher than for flax shives (11.32 ± 0.31 MJ/kg_{Biomass}) due to the difference in bio-oil yield.

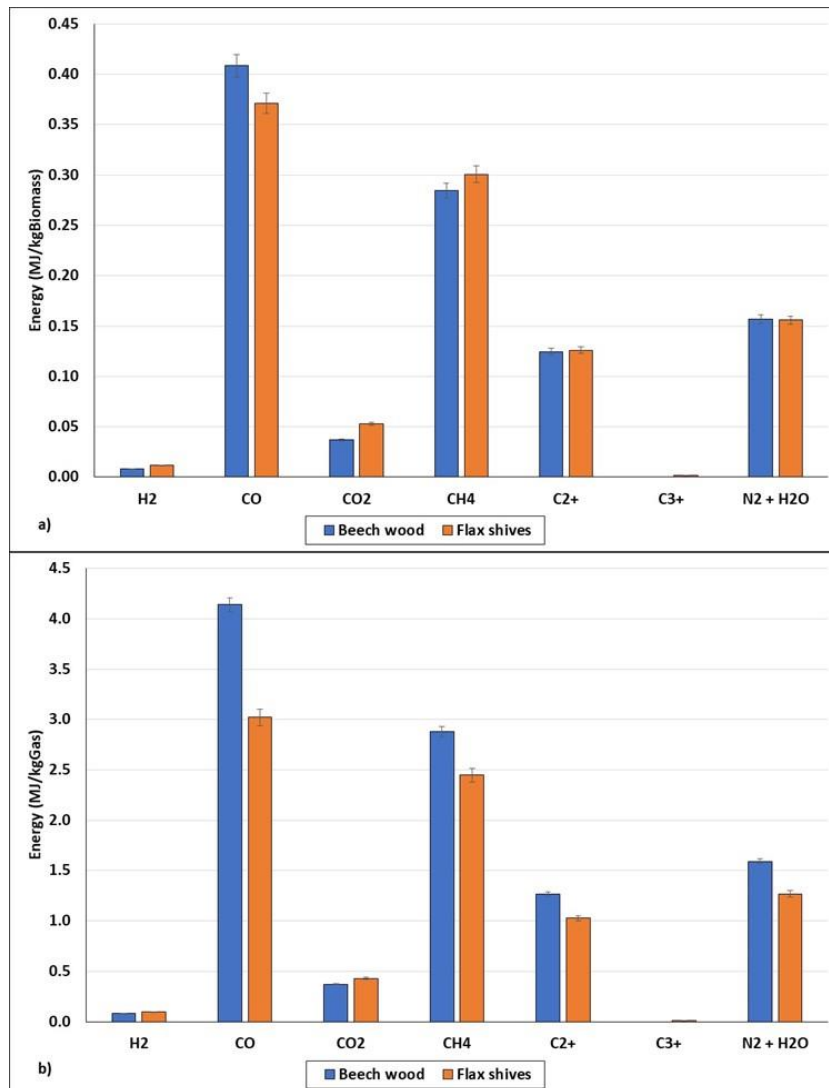


Figure 3.3. Energy distribution of gases from biomasses at 500°C, a) MJ/kg_{biomass} b) MJ/kg_{phase}.

The obtained bio-oils had similar oxygen content values, with 33.8% for beech wood oil and 34.76% for flax shives. This was one reason for the similarity of bio-oil values per kilogram of bio-oil. In addition, the energy and exergy distribution of bio-oil compounds followed a similar trend for the two biomasses. As observed in **Figure 3.4**, the behaviour of the energy and exergy values of the chemical families was identical.

Acids compounds represented the highest energy stream from bio-oil, at 4.32 ± 0.12 MJ/kg_{Bio-oil} for beech wood and 4.31 ± 0.12 MJ/kg_{Bio-oil} for flax shives, followed by amides, ketones and phenols. These results are evidenced in discussions in the literature [22], [27], [54] which saw acids as the most influential aliphatic compound at low-temperature pyrolysis, especially acetic

acid. Moreover, it can be seen that exergy values followed the same trend as energy values. As a difference of only $0.02 \pm 0.0005 \text{ MJ/kg}_{\text{Bio-oil}}$ was evidenced in bio-oil energy and exergy values, it can be said that almost all the bio-oil energy is converted into work.

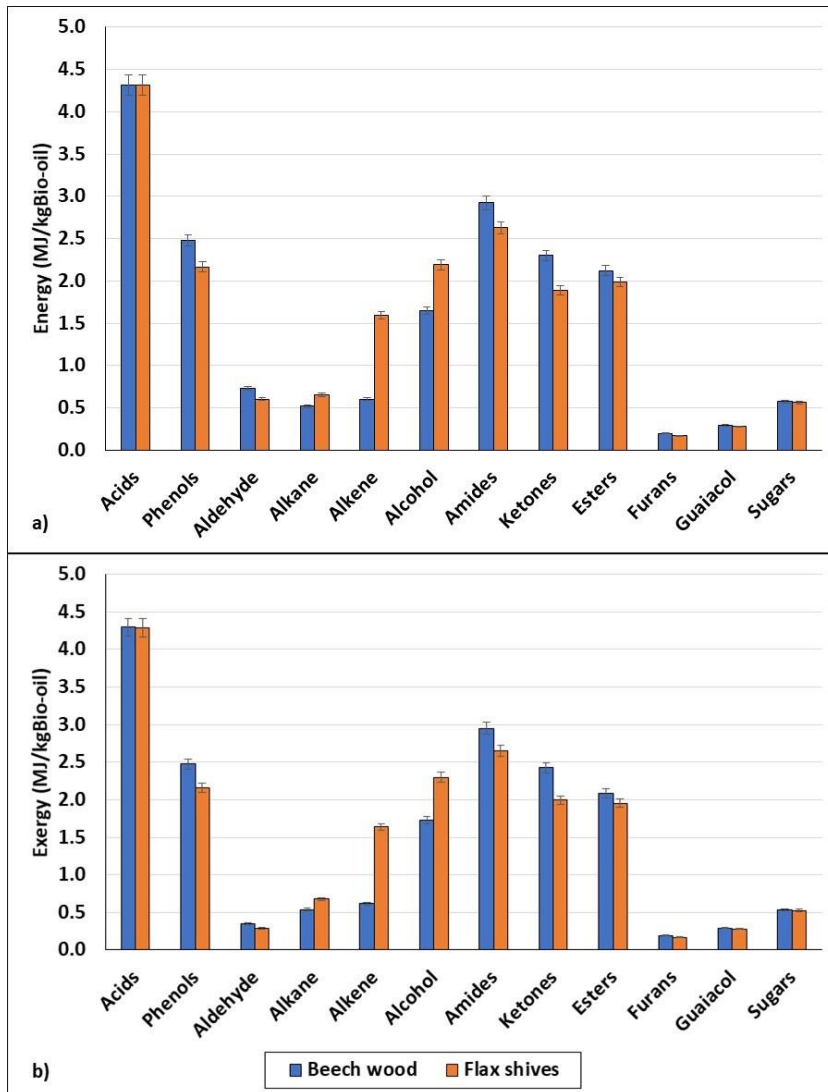


Figure 3.4. Energy and b) Exergy distribution of chemical families in bio-oil from beech wood and flax shives at 500°C.

1.2 Heat for pyrolysis and exergy destruction rate.

The calculation of heat for pyrolysis gives investigators a view of the process sustainability, showing how much heat is required to perform the pyrolysis reaction. Lignocellulosic biomasses tested in this study showed similar elemental and proximate analysis. Nevertheless, this does not mean that the heat input required is the same for both biomasses, due to variation in the principal compounds content of the biomass (cellulose, hemicellulose and lignin) [151], [152].

As can be seen in **Figure 3.5**, the pyrolysis of flax shives was more endothermic than beech wood pyrolysis, as the heat required for pyrolysis was higher. For pyrolysis of flax shives, 2.21 ± 0.06 MJ/kg_{Biomass} was needed to obtain the aforementioned products at a temperature of 500°C.; beech wood pyrolysis required 1.97 ± 0.05 MJ/kg_{Biomass}. The difference in heat for pyrolysis was 0.24 ± 0.006 MJ/kg_{Biomass}, with a deviation of approximately 11% from a biomass to the other. Technically, more heat was required for flax shives pyrolysis in the same conditions in order to break biomasses' structural bonds at a temperature of 500°C.

Another explanation of this difference in the heat for pyrolysis could be the thermal reaction type. The global energy balance of pyrolysis demonstrated that the reaction was endothermic, but this does not mean that all secondary reactions taking place inside the pyrolyzer were endothermic. There were exothermic reactions taking place alongside endothermic reactions [42], which helped make the pyrolysis process more self-sustainable. This could potentially have helped the beech wood pyrolysis be less endothermic than flax shives pyrolysis.

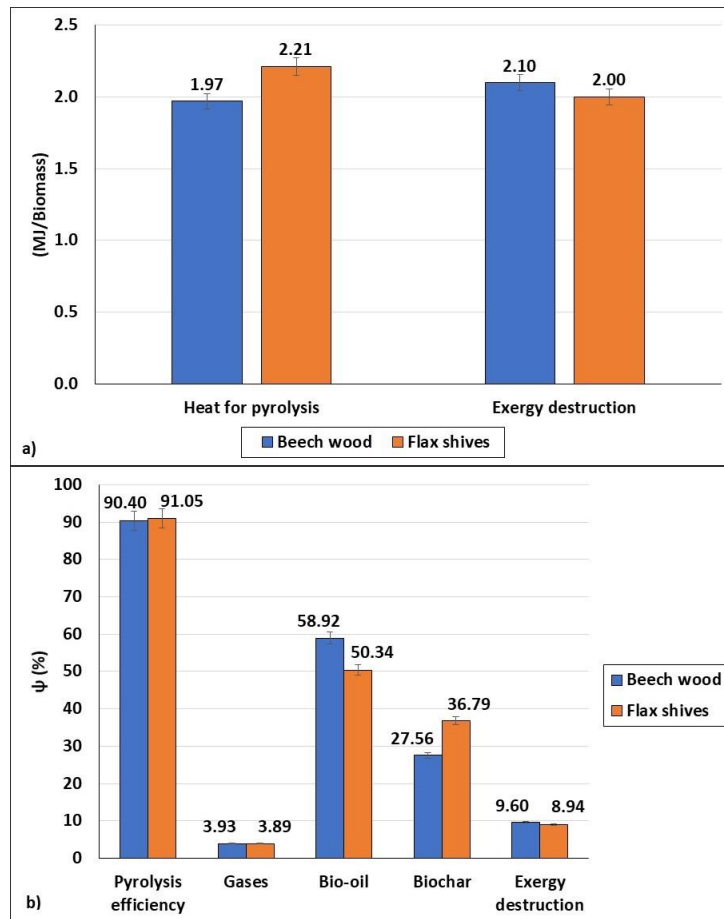


Figure 3.5. Heat for pyrolysis and exergy destruction b) exergetic efficiency of beech wood and flax shives pyrolysis at 500°C.

The total exergy value entering the pyrolyzer was different for each biomass, as the LHV of the biomass was not the same. Flax shives LHV was 18.20 ± 0.49 MJ/kg_{Biomass} and beech wood 17.87 ± 0.48 MJ/kg_{Biomass}. For flax shives a total of 22.36 ± 0.60 MJ/kg_{Biomass} was the available exergy value, meanwhile, for beech wood, it was 21.88 ± 0.59 MJ/kg_{Biomass}. In terms of exergy destruction, it was also observed that less exergy was destroyed when pyrolysis of flax shives took place. This meant that, exergetically, pyrolysis of flax shives was more efficient than beech wood, showing higher exergy values and less exergy destruction. In other words, flax shive products' exergy was less affected by entropy changes or irreversibilities. Although the exergy destruction difference between the two biomasses was only 0.10 ± 0.0027 MJ/kg_{Biomass}, it can be assumed that flax shive products showed higher energy/exergy quality.

Figure 3.5b shows the global pyrolysis exergetic efficiency, as for individual products. For the pyrolysis of flax shives, an exergy efficiency of 91.05% was obtained, as opposed to 90.40% for beech wood. The most influential product of pyrolysis was bio-oil, presenting an exergetic efficiency of 58.92% (12.89 ± 0.35 MJ/kg_{Biomass}) for beech wood and 50.34% (11.26 ± 0.30 MJ/kg_{Biomass}) for flax shives. This was followed by biochar; for flax shives, an efficiency of 37.79% (8.23 ± 0.22 MJ/kg_{Biomass}) was calculated, compared with 27.56% (6.03 ± 0.16 MJ/kg_{Biomass}) for beech wood. These values were a reflected trend in the mass balance yields observed for each pyrolysis experience.

2. Catalytic pyrolysis of beech wood and flax shives

In this section, the use of two catalysts for upgrading bio-oil is discussed. The main interest of the catalyst treatment in this study was to upgrade the bio-oil produced by pyrolysis by reducing the oxygen content in order to increase its energetic/exergetic quality. Two zeolite catalysts were tested: HZSM-5 and its iron modification, Fe-HZSM-5. **Figures 3.6** and **3.7** show the energy and exergy distribution of the products after catalyst treatment compared with the non-catalyzed pyrolysis results for beech wood in **Figure 3.8** and for flax shives in **Figure 3.9**.

As can be observed, use of the catalyst increases gas stream heating values and bio-oil. Both catalysts showed a positive effect on biomass products, though the iron modified zeolite Fe-HZSM-5 catalyst was more efficient than HZSM-5. The principle of the effectivity of these catalysts in pyrolysis products is discussed elsewhere in the literature [54], [153]. The catalysts were used to perform deoxygenation (DO) reactions by boosting the decarbonylation, decarboxylation and dehydration reactions of oxygenated molecules. This increased bio-oil's energetic and exergetic values and other thermochemical properties, at the same time increasing the gas stream values as more gas molecules were formed.

Chapter 3

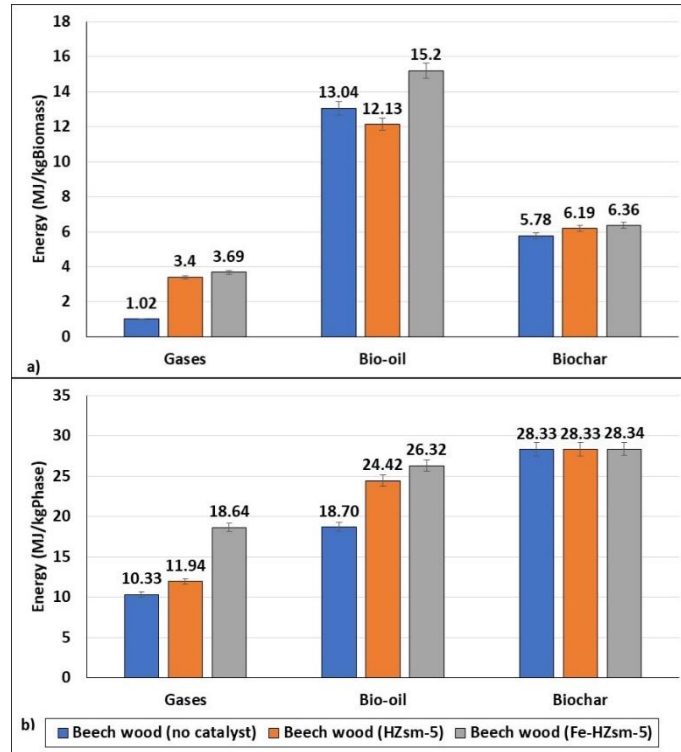


Figure 3.6. Energy product distribution for beech wood a) $MJ/kg_{Biomass}$, b) MJ/kg_{Phase} at $500^{\circ}C$.

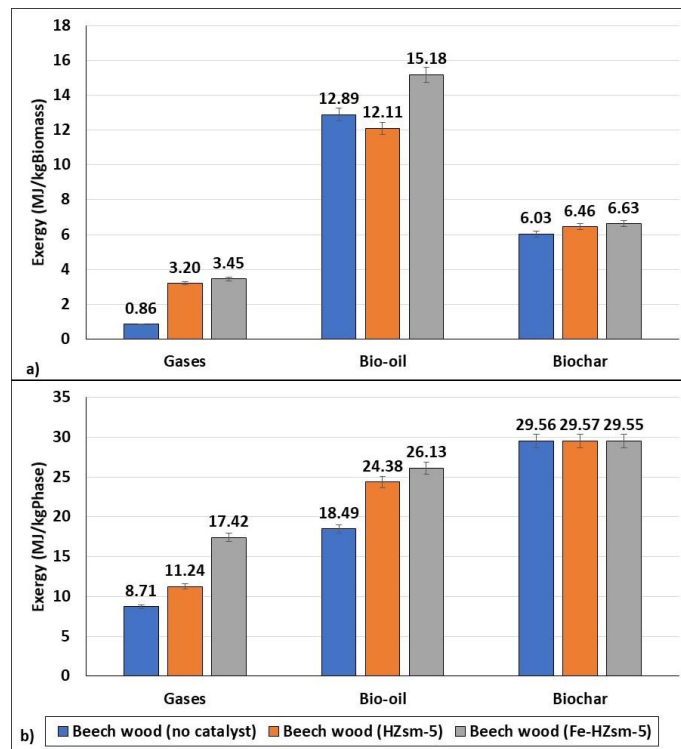


Figure 3.7. Exergy product distribution for beech wood a) $MJ/kg_{Biomass}$, b) MJ/kg_{Phase} at $500^{\circ}C$.

Chapter 3

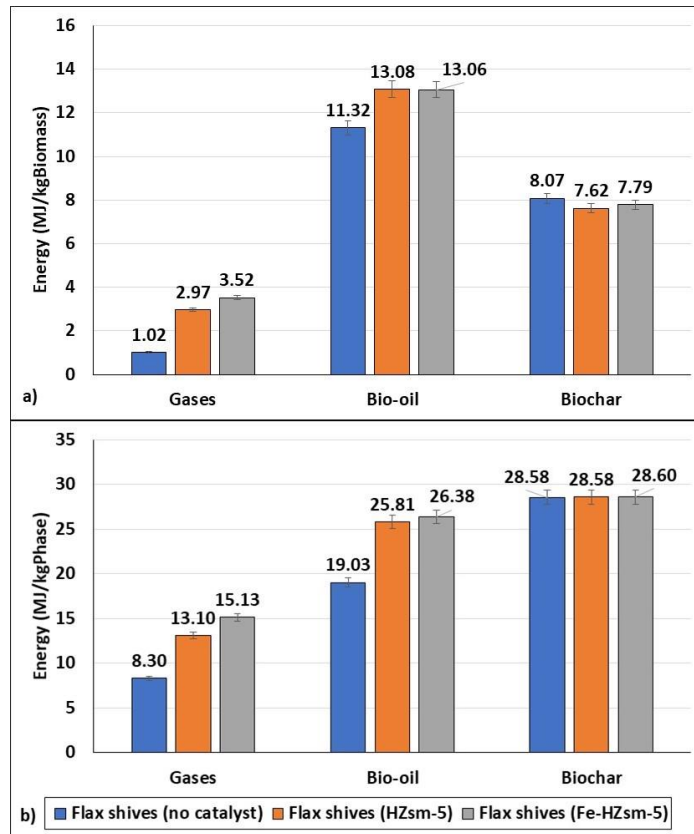


Figure 3.8. Energy product distribution for flax shives a) $MJ/kg_{Biomass}$, b) MJ/kg_{Phase} at $500^{\circ}C$.

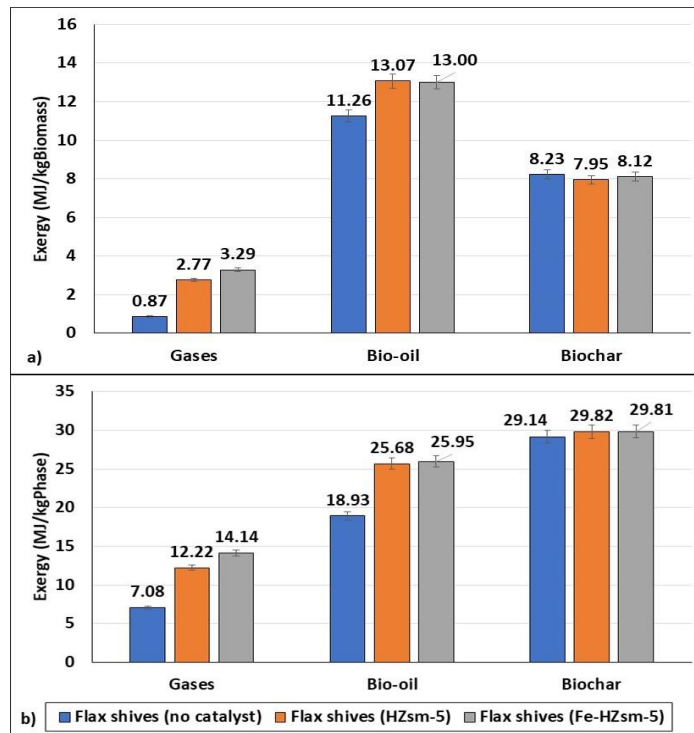


Figure 3.9. Exergy product distribution for flax shives a) $MJ/kg_{Biomass}$, b) MJ/kg_{Phase} at $500^{\circ}C$.

2.1 Energetic and exergetic evaluation of catalytic pyrolysis on products

Biochar

As was specified in **Section 2** the pyrolysis of all raw materials took place in the pyrolytic zone of the used setup. The catalyst was placed ex-situ in the destined catalytic zone of the reactor, where only volatile matters were in contact with it. For this reason, the obtained biochar was never in contact with the catalyst. Furthermore, no major biochar variation was seen, as the pyrolysis conditions were far from those required to affect biochar thermal stability, such as gasification.

Gases

The use of zeolite as a catalyst led to heterogeneous cracking reactions, which increased the formation of gaseous molecules. For this reason, an increase in the amount of energy in the gas content can be observed compared to the non-catalytic pyrolysis of biomasses. Pyrolysis of beech wood without catalytic treatment provided a gas energy value of 10.33 ± 0.28 MJ/kg_{Gas}, meanwhile, when HZSM-5 was used as catalyst, 11.94 ± 0.32 MJ/kg_{Gas} were obtained, an increase of 16% in its energy value. For the catalyst Fe-HZSM-5, 18.64 ± 0.50 MJ/kg_{Gas} was obtained, an incrementation of approximately 80%. These findings evidence the strong influence of the catalyst in energetic terms. For the flax shives, the trend was similar: Fe-HZSM-5 was the more efficient catalyst, increasing gas heating values by 82% (15.13 ± 0.41 MJ/kg_{Gas}) compared with the standard value obtained without catalyst treatment (8.3 ± 0.22 MJ/kg_{Gas}). For HZSM-5, it was increased by 58% (13.10 ± 0.35 MJ/kg_{Gas}).

The HZSM-5 catalyst favoured CO formation, which might come from the decarbonylation reaction of oxygenated molecules. Despite this, when HZSM-5 was used as a catalyst for beech wood pyrolysis, the CO energy was 1.20 ± 0.03 MJ/kg_{Biomass} compared to Fe-HZSM-5, where the CO value was 0.82 ± 0.02 MJ/kg_{Biomass}: as can be observed, there was a difference of 0.38 ± 0.01 MJ/kg_{Biomass}. For flax shives pyrolysis, this difference in CO values was slightly lower, at 0.12 ± 0.003 MJ/kg_{Biomass}.

The iron modification of the zeolite (Fe-HZSM-5) favoured all gaseous components' production. The most significant incrementation was observed for H₂ energy content. In pyrolysis of beech wood with Fe-HZSM-5 as the catalyst, 0.38 ± 0.01 MJ/kg_{Biomass} were obtained, compared to 0.02 ± 0.0005 MJ/kg_{Biomass} with the HZSM-5 catalyst. In flax shives, similar trends were obtained for H₂, with 0.34 ± 0.009 MJ/kg_{Biomass} using Fe-HZSM-5 and 0.02 ± 0.0005 MJ/kg_{Biomass} with HZSM-5. It was observed that the iron modification of the zeolite boosted H₂ production: this could be explained by the acid sites changing when the catalyst is loaded with iron, resulting in an increase of H₂, C₂₊ and C₃₊ yields and selectivity [154]. **Figure**

3.10 shows the energy values of gaseous components for catalytic pyrolysis of beech wood and flax shives. The values in units of MJ/kg_{Gas} can be found in **Appendix A2**.

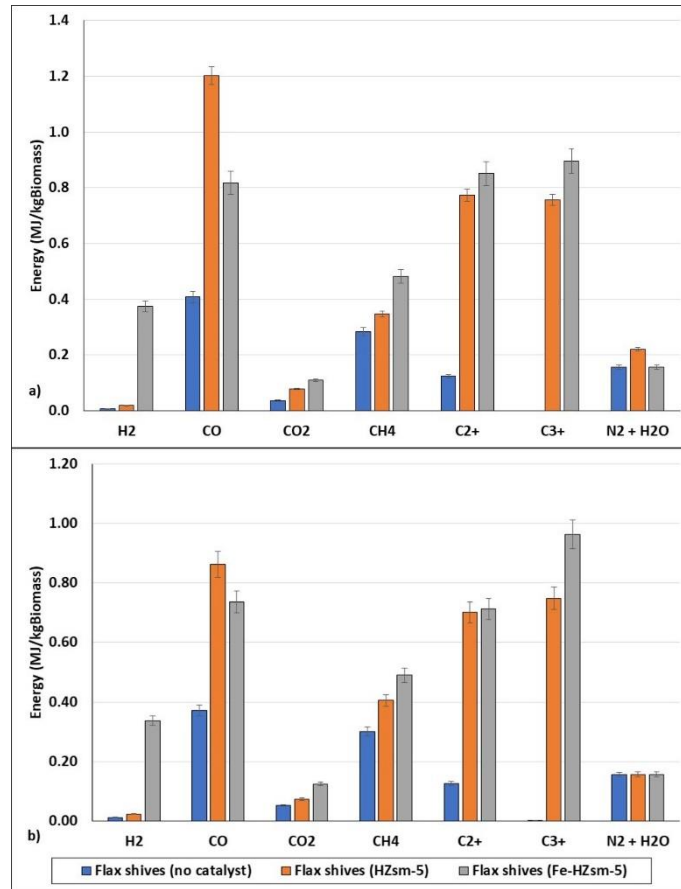


Figure 3.10. Energy product distribution of gases for a) beech wood and b) flax shives at 500°C.

Upgraded bio-oil

Bio-oil showed a significant increase in energy and exergy rates with the use of catalysts. The heating values of pyrolysis bio-oil from beech wood were increased by 30.6% (24.42 ± 0.66 MJ/kg_{Bio-oil}) when HZSM-5 was used, while with the iron modified catalyst Fe-HZSM-5 saw an increase of 40.72% (26.32 ± 0.71 MJ/kg_{Bio-oil}). For flax shives, the bio-oil heating value increased from 19.03 ± 0.51 to 25.81 ± 0.70 MJ/kg (increased 35.63%) with HZSM-5 and to 26.38 ± 0.71 MJ/kg_{Bio-oil} (38.62%) with Fe-HZSM-5. The iron modified catalyst showed better results in terms of increasing the bio-oil heating value. In addition, the bio-oil quality was increased through the reduction of oxygenated compounds' yield with the catalyst. Regardless of the presence of zeolites contributing to crack the heavy molecules in bio-oil into phenol compounds, the quality of the bio-oil was positively increased.

Figure 3.11 shows the energy distribution of the upgraded bio-oil. As can be observed for both biomasses, the phenol energy value increased drastically after the use of catalysts. For beech wood pyrolysis, after using the zeolite, phenols' energy values increased from 2.48 ± 0.7 MJ/kg_{Bio-oil} to 12.08 ± 0.33 MJ/kg_{Bio-oil} and 18.66 ± 0.50 MJ/kg_{Bio-oil} for HZSM-5 and Fe-HZSM-5, respectively. For flax shives pyrolysis, phenols' energy values increased from 2.16 ± 0.06 MJ/kg_{Bio-oil} to 16.87 ± 0.46 MJ/kg_{Bio-oil} and 16.58 ± 0.45 MJ/kg_{Bio-oil} for HZSM-5 and Fe-HZSM-5, respectively. Phenols represented the biggest major bio-oil energy value. Acids represented the highest oxygenated molecules and the highest energy and exergy values for pyrolysis of both biomasses without catalytic treatment the use of both catalysts significantly reduced this amount, providing an almost inexistent acid content in the bio-oil. It was therefore concluded that the bio-oil stream was upgraded chemically and thermodynamically with the use of zeolite-based catalysts.

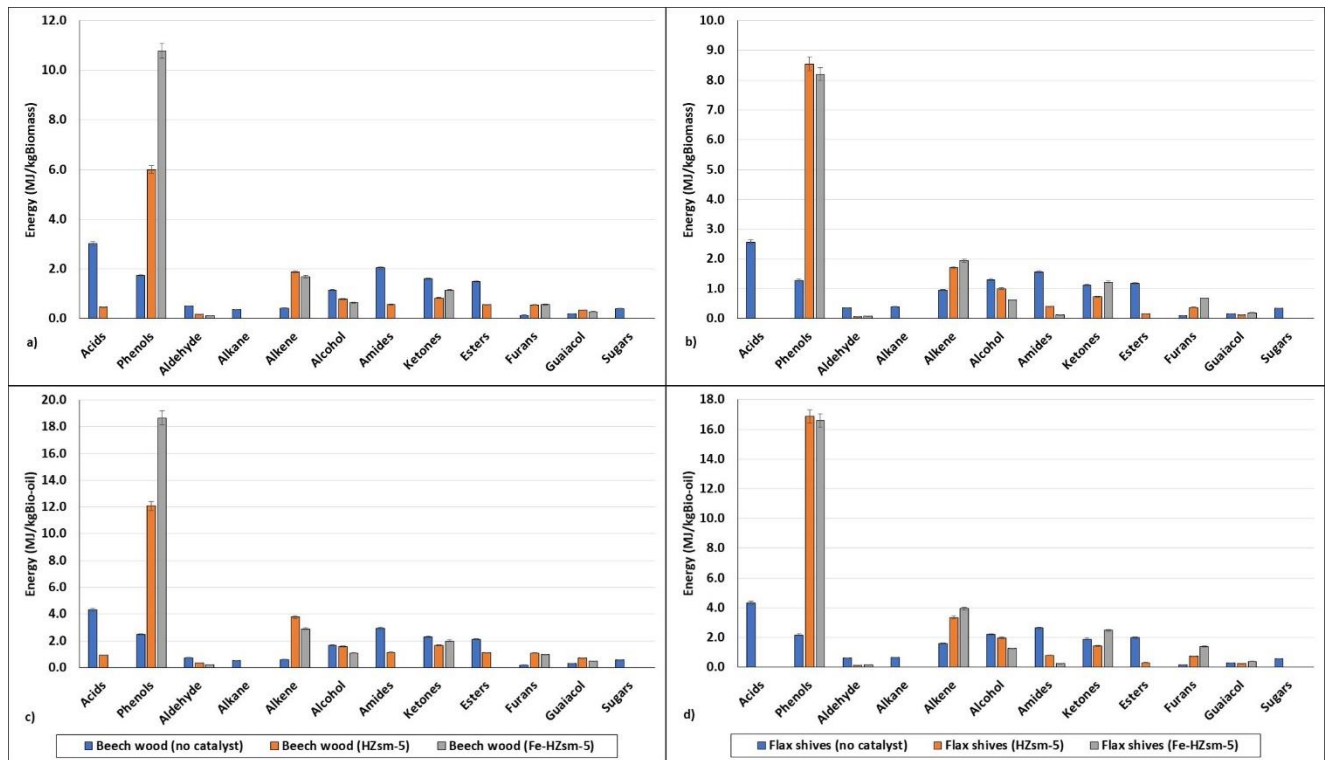


Figure 3.11. Energy product distribution of bio-oil families for a) beech wood (MJ/kg_{Biomass}), b) flax shives (MJ/kg_{Biomass}), c) beech wood (MJ/kg_{Bio-oil}) and d) flax shives (MJ/kg_{Bio-oil}) at 500°C.

2.2 Heat for pyrolysis and exergy destruction rate.

Figure 3. shows the heat required for pyrolysis when catalysts were used and the exergy destroyed. It can be seen that the heat for pyrolysis increased when a catalytic treatment was used. For beech wood, the required heat increased from 1.97 ± 0.05 MJ/kg_{Biomass} without a catalyst to 3.85 ± 0.10 MJ/kg_{Biomass} for the HZSM-5 catalyst and 7.38 ± 0.20 MJ/kg_{Biomass} for Fe-

HZSM-5 catalyst. For flax shives, it increased from $2.21 \pm 0.06 \text{ MJ/kg}_{\text{Biomass}}$ to $5.47 \pm 0.15 \text{ MJ/kg}_{\text{Biomass}}$ with HZSM-5 and to $6.17 \pm 0.17 \text{ MJ/kg}_{\text{Biomass}}$ with Fe-HZSM-5. This was due to the fact that deoxygenation (DO) reactions took place and it is known that DO is an endothermic reaction [155].

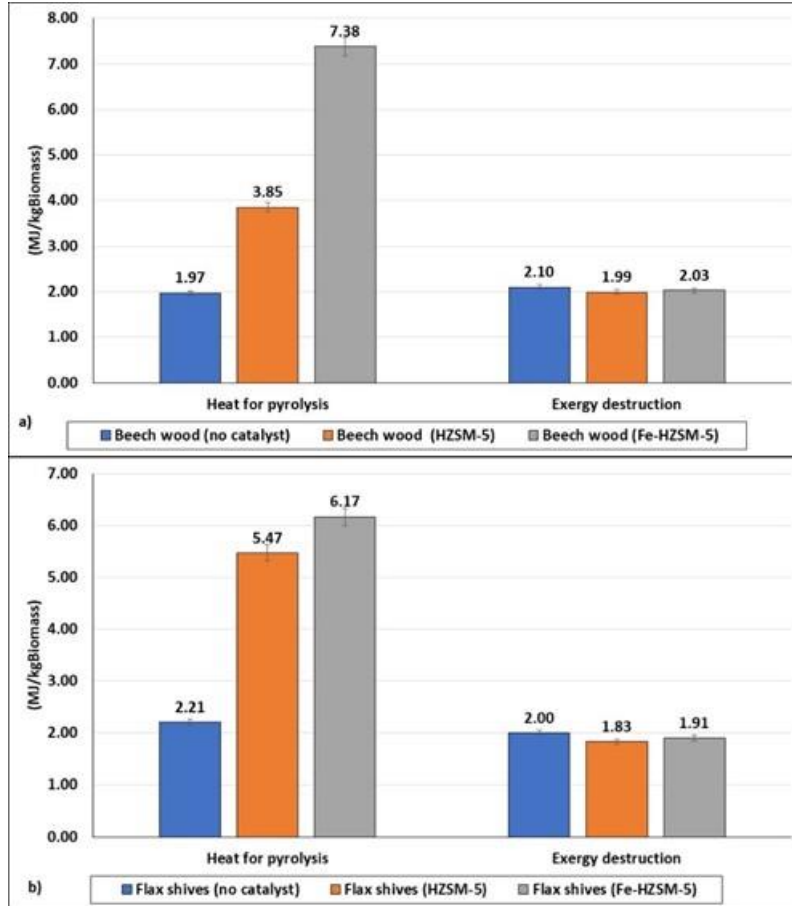


Figure 3.12. Energy Heat for pyrolysis and exergy destruction for a) beech wood and b) flax shives with and without catalyst treatment at 500°C.

Heat for pyrolysis results were not uniform in biomass for the different catalysts. Flax shives showed higher a heat requirement when the HZSM-5 catalyst was used compared to beech wood. Meanwhile, beech wood required heat increased by $1.21 \pm 0.03 \text{ MJ/kg}_{\text{Biomass}}$ when Fe-HZSM-5 was used.

The exergy destroyed varied slightly when catalysts were used compared to non-catalyst experiments for both biomasses. The same trend was observed for flax shives compared to beech wood after catalyst treatment: the exergy destroyed was inferior. Beech wood total exergy destroyed decreased from 2.1 ± 0.06 to $1.99 \pm 0.05 \text{ MJ/kg}_{\text{Biomass}}$, due to the use of catalyst, for a reduction of $0.11 \pm 0.003 \text{ MJ/kg}_{\text{Biomass}}$. For Flax shives the exergy destroyed was reduced from 2.00 ± 0.05 to $1.83 \pm 0.05 \text{ MJ/kg}_{\text{Biomass}}$ after catalyst treatment, reducing only

$0.17 \pm 0.005 \text{ MJ/kg}_{\text{Biomass}}$. The reduction of exergy destruction might be because of the diminution of process irreversibility due to the products upgrading with catalyst. As the produced compounds presented lower entropy changes when catalysts were used, the amount of exergy destroyed was slightly reduced.

3. Pyrolysis of biomass pseudo-components

Figure 3.13 and **Figure 3.14** show the energy and exergy distribution of products obtained after the pyrolysis of the three principal lignocellulosic biomass compounds. As can be observed, the gaseous stream represented the lowest energy/exergy value of the pyrolysis products. This is to be expected as pyrolysis promotes the formation of liquid products. Meanwhile, bio-oil and biochar production were one of the most attractive energetic process [46].

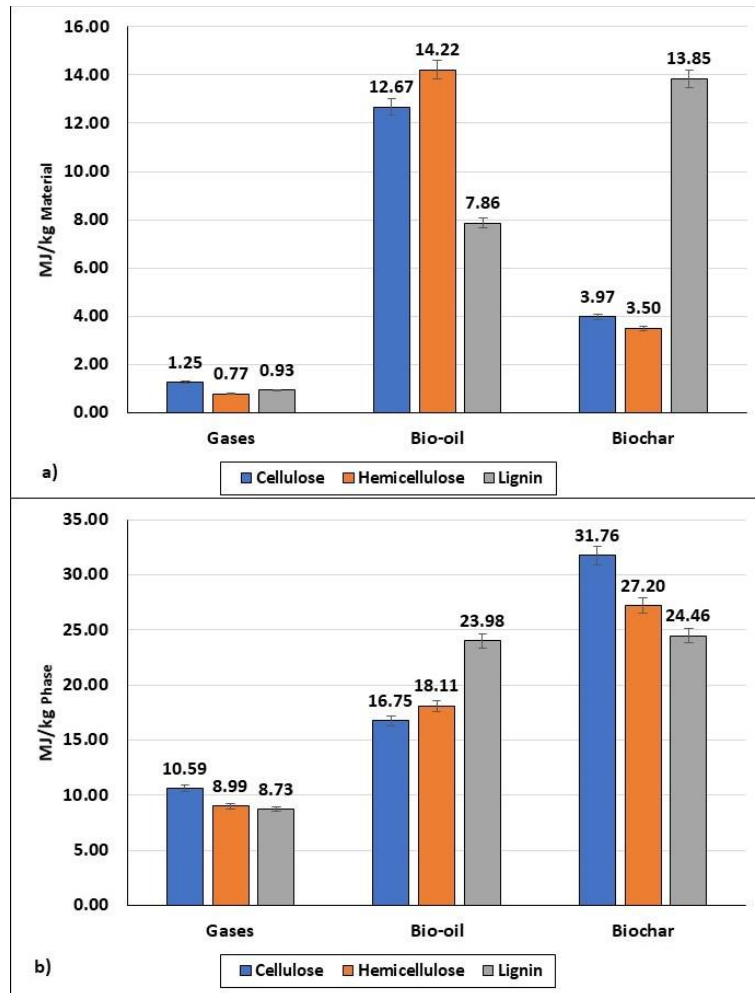


Figure 3.13. Energy distribution of pyrolysis products, for cellulose, hemicellulose and lignin at 500°C.

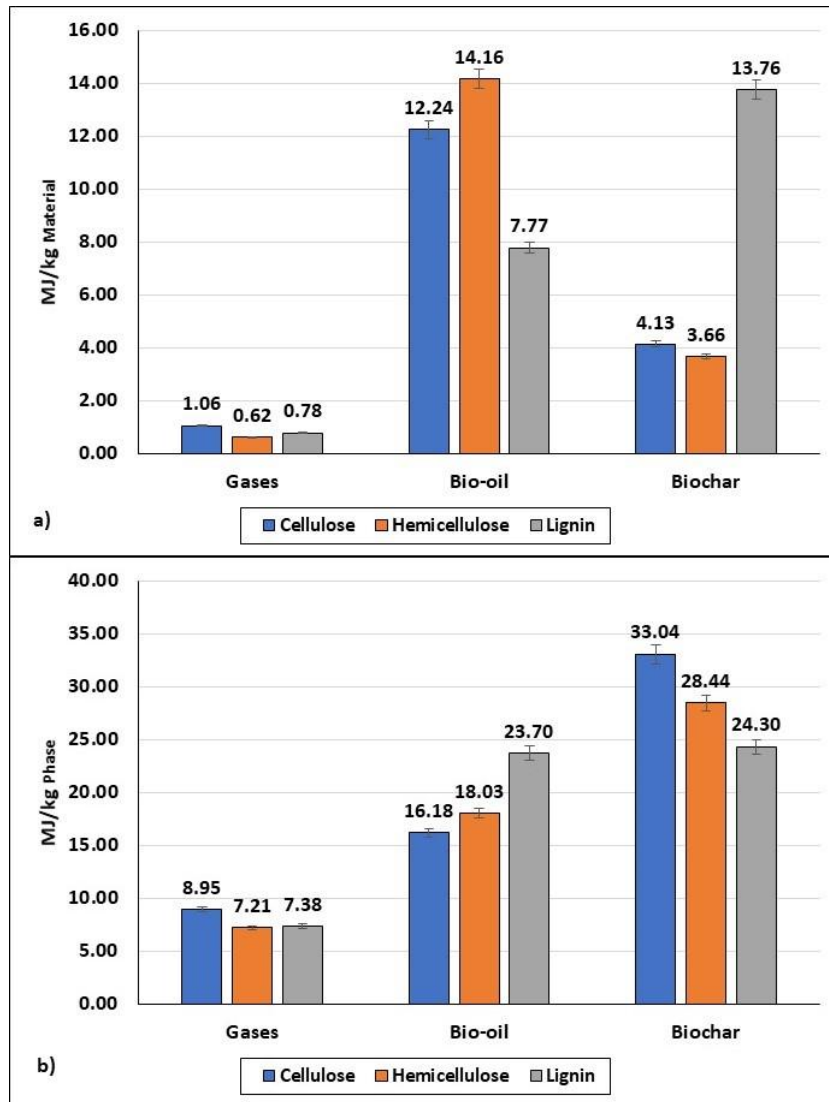


Figure 3.14. Exergy distribution of pyrolysis products, for cellulose, hemicellulose and lignin at 500°C.

Also, it was seen that the exergy values of gaseous and liquid products were lower than their respective energy values, evidencing the energy degradation or anergy. The opposite was observed for biochar. As was explained in **Section 1.1** of this chapter, there were constraints on calculating non-conventional fuels' entropy.

3.1 Energetic and exergetic evaluation of pseudo-components pyrolysis on products

Biochar

Biochar represented the highest energy and exergy values in terms of MJ/kg_{Phase} for each pyrolysis experience. Comparing the three pseudo components, cellulose biochar showed higher values of energy than hemicellulose and lignin. From cellulose, 31.76 ± 0.86 MJ/kg_{biochar} could be obtained, compared with, 27.20 ± 0.73 MJ/kg_{Biochar} from hemicellulose and $24.46 \pm$

0.66 MJ/kg_{Biochar} for lignin. An explanation for this can be found by looking at the elemental analysis of the biochar obtained after the pyrolysis reaction. Cellulose biochar has a higher carbon and hydrogen yield than hemicellulose and lignin char. Using the Dulong formula (**Eq. 2.19**) to calculate fuel energy, the higher the carbon and hydrogen yield in a fuel, the higher its heating value. In terms of oxygen content, cellulose biochar showed lower oxygen content (15.35%) than hemicellulose and lignin (25.61% and 39.3%, respectively). The low amount of oxygen was another reason for the higher energetic and exergetic quality of cellulose biochar, although the biochar yield of lignin was three times higher than that of cellulose and lignin. In terms of MJ/kg_{Material}, lignin biochar represented the highest energy value (13.85 ± 0.37 MJ/kg_{Material}), while the oxygen content was too elevated to provide better quality biochar.

In terms of energy/exergy, the values obtained from the pyrolysis of biomasses were close to those obtained from the pyrolysis of cellulose and hemicellulose. This observation was corroborated by the similarity of biomasses' biochar, with cellulose and hemicellulose char in their elemental analysis. It is established in this study that the energetic and exergetic evaluations of biomass biochar are highly influenced by cellulose and hemicellulose. The same was found in the literature in terms of elemental composition and biochar structures [156].

Gases

As observed in the last figure, cellulose permanent gases were energetically higher than for hemicellulose and lignin. To explain this observation, the detailed energy and exergy distribution of gases is shown in **Figure 3.15**. It can be seen that CO was the most relevant compound in terms of higher energy and exergy values. The amount of CO in cellulose produced gases was 5.07 ± 0.14 MJ/kg_{Gas} compared to hemicellulose with 4.18 ± 0.11 MJ/kg_{Gas} and lignin 0.90 ± 0.02 MJ/kg_{Gas}. Also, the energetic quantity of C₃+ gaseous compounds was approximately ten times higher from cellulose (1.45 ± 0.04 MJ/kg_{Gas}) compared to the other compounds (0.14 ± 0.004 MJ/kg_{Gas}). In addition, cellulose has a higher volatile matter (90.26%) compared to hemicellulose (74.99%) and lignin (61.41%).

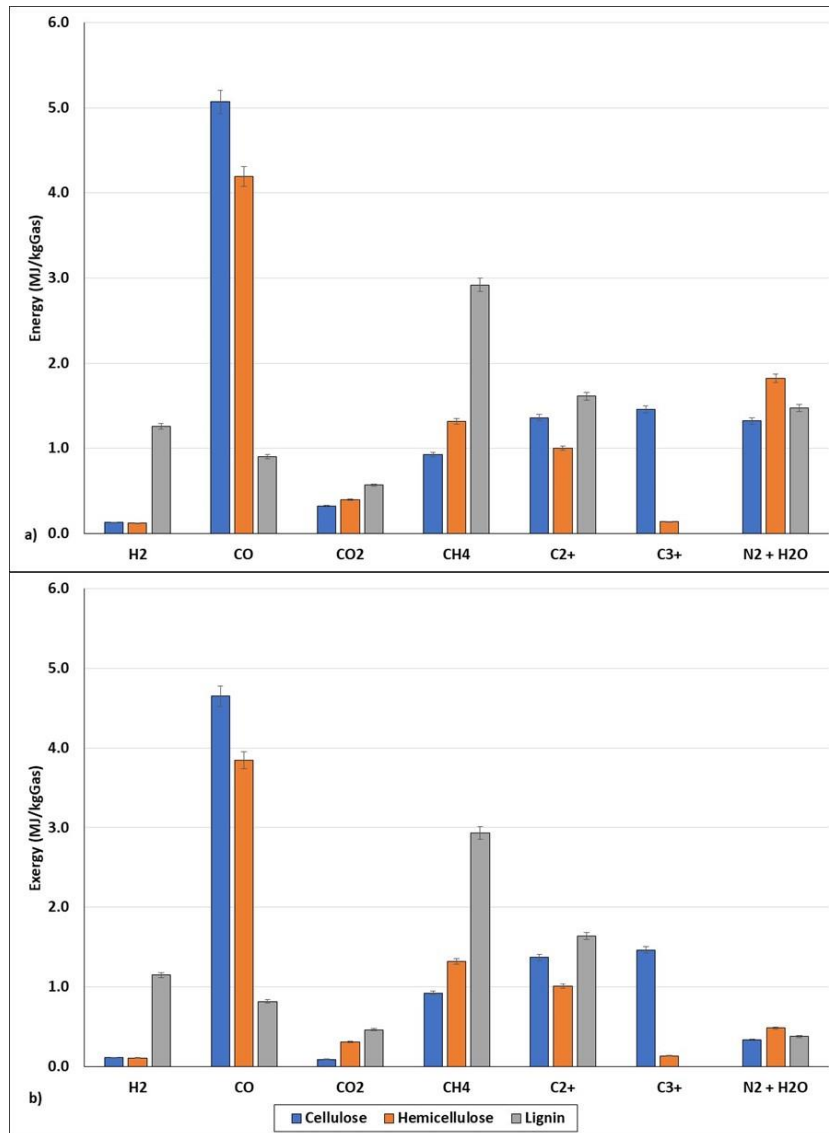


Figure 3.15. Exergy distribution of gaseous components, for cellulose, hemicellulose and lignin at 500°C.

For lignin pyrolysis, an important finding was observed concerning hydrogen production. It was seen in the mass balance that the hydrogen yield after lignin pyrolysis was 17.6% of the total molar flow of gases, translating to a hydrogen energy value of 1.26 ± 0.03 MJ/kg_{Gas}, which was approximately 10 or 11 times higher than the values obtained from the other pseudo components. Also, methane's energetic and exergetic values were very superior for lignin pyrolysis (2.92 ± 0.08 MJ/kg_{Gas}) compared to hemicellulose (1.32 ± 0.04 MJ/kg_{Gas}) and cellulose (0.92 ± 0.02 MJ/kg_{Gas}). It was observed that lignin had a higher moisture content than cellulose and hemicellulose, which could potentially favour hydrogen and methane production reactions [157], [158]. Despite these reactions perhaps having more influence at high

temperatures, this does not mean that they cannot take place at low temperatures such as 500°C.

Bio-oil

Study of the pyrolysis of biomass components gave researchers an idea of the potential influence of each component on the biomass bio-oil produced. Lignin bio-oil showed higher energy and exergy values than cellulose and hemicellulose bio-oils. To explain this, the oxygen content of the obtained bio-oils was considered. The oxygen content of the lignin bio-oil was lower (19.38%) than that from cellulose (33.82%) and hemicellulose (28.05%). This could be a reason why lignin bio-oil showed higher energy and exergy values. If the results are looked at in terms of MJ per kilogram of material ($\text{MJ}/\text{kg}_{\text{Material}}$), the energy/exergy rate of lignin bio-oil is inferior to the other compounds as the mass yield was lower.

In **Figure 3.16**, the energy and exergy distribution of the chemical families of bio-oils can be observed. Phenols, alkane and alkene molecules represent the most relevant molecules in lignin bio-oil in energetic terms. The energy provided from phenol represented 49.61% ($11.90 \pm 0.32 \text{ MJ}/\text{kg}_{\text{Bio-oil}}$) of the total lignin bio-oil energy, followed by alkane and alkenes, which represented 26.51% ($6.36 \pm 0.17 \text{ MJ}/\text{kg}_{\text{Bio-oil}}$). In cellulose bio-oil, the majority of the energy was represented by sugars, with values 14 times higher ($5.44 \pm 0.15 \text{ MJ}/\text{kg}_{\text{Bio-oil}}$) than hemicellulose ($0.37 \pm 0.01 \text{ MJ}/\text{kg}_{\text{Bio-oil}}$). Secondary ketones and phenolic compounds showed values of approximately $2.52 \pm 0.07 \text{ MJ}/\text{kg}_{\text{Bio-oil}}$. In hemicellulose bio-oil, energetic/exergetic values were constituted by alcohols, acids and ketones with values of 3.10 ± 0.08 , 2.63 ± 0.07 and $2.47 \pm 0.07 \text{ MJ}/\text{kg}_{\text{Bio-oil}}$ respectively. Due to this gap between lignin and the other compounds' bio-oil, it can be said that lignin provides better energy quality bio-oil. Meanwhile, in terms of quantity, cellulose and hemicellulose are favoured, as a lot of bio-oil was produced per kilogram of the individual material.

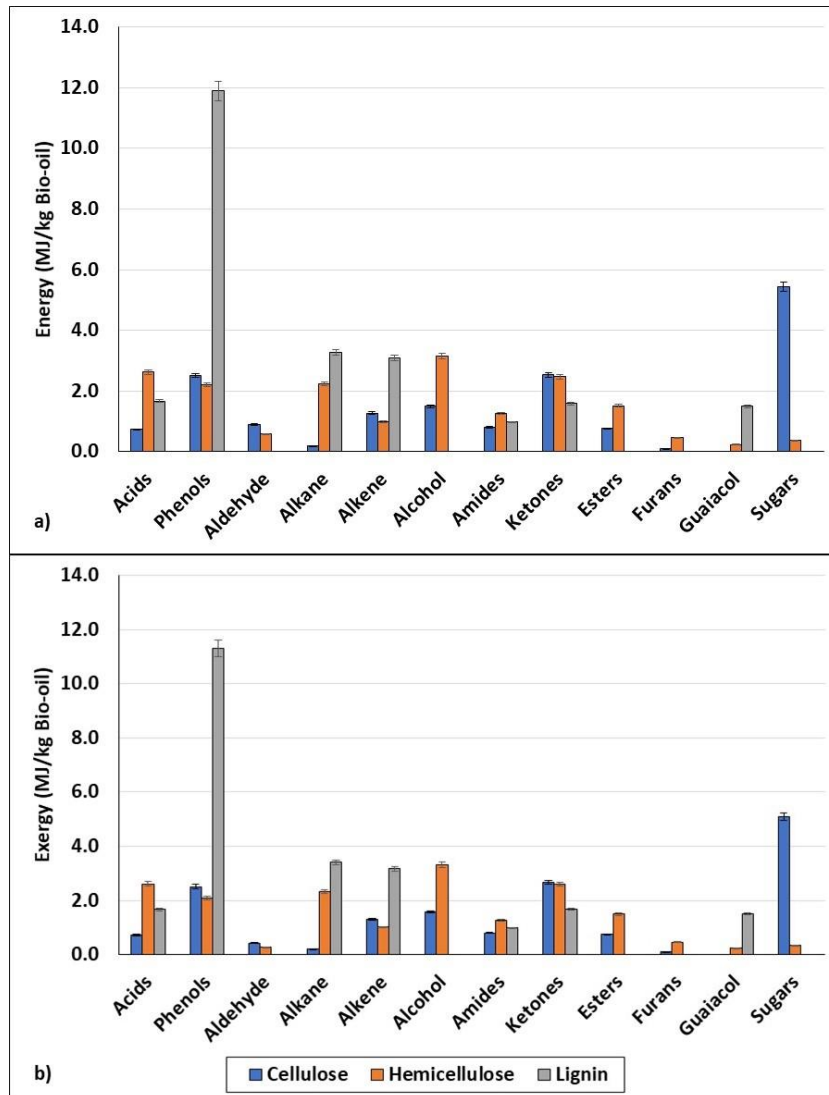


Figure 3.16. a) Energy and b) exergy distribution of chemical families in bio-oil, for cellulose, hemicellulose and lignin at 500°C.

Hemicellulose and cellulose bio-oils seem to have a closer energetic and exergetic distribution of chemical families with biomasses than lignin bio-oil. On the other hand, it can be seen that the pyrolysis of each individual compound would not give a strict identical thermodynamic behaviour that pyrolysis of biomasses. This could be due to the possible reaction competitiveness between the components inside the biomass [159]. Comparison of the energy and exergy values of bio-oils shows that there was low energy in the bio-oil stream, between approximately 0.08 ± 0.0002 and 0.57 ± 0.015 MJ/kg_{Bio-oil}. compared to gaseous streams, with values between 1.35 ± 0.04 to 1.78 ± 0.05 MJ/kg_{Gas}. It can be concluded that fewer irreversibilities were present in bio-oil streams, as less entropy change was calculated.

3.2 Heat for pyrolysis and exergy destruction.

Figure 3.17a shows the heat for pyrolysis and the exergy destroyed of the biomass components. Hemicellulose showed the highest heat requirement (1.43 ± 0.04 MJ/kg_{Material}) compared to cellulose (1.22 ± 0.03 MJ/kg_{Material}) and lignin (0.86 ± 0.02 MJ/kg_{Material}). The fact that the heat required for pyrolysis of lignin was lower than the other compounds can be explained, as it is found in the literature that biochar formation tends towards exothermicity as a function of the produced biochar. It was observed that the lignin biochar yield (56.6 %) was significant compared to the other compounds (12.50% and 12.87% for cellulose and hemicellulose, respectively). Meanwhile, the hemicellulose and cellulose biochar yields were very close, and this could potentially have an influence on their required heat. The number of heterogeneous and homogeneous reactions taking place in pyrolysis is large; therefore, the fact that only 0.22 ± 0.005 MJ/kg were additionally required for hemicellulose pyrolysis compared to cellulose could point to certain endothermic reactions.

Comparing biomasses required energy with the solo pseudo components, it can be seen that less heat was required when pyrolysis of individual components took place. This means that when these compounds were combined in a biomass, more heat was needed for pyrolysis than when the pyrolysis reaction was done for each one separately. The heat for pyrolysis from biomasses increased as a result of the competition of thermal reactions, potentially of cellulose, hemicellulose and lignin. Also, physical bonds between the three compounds in the biomass would strengthen in thermal conditions, resulting in an increase of required heat. Pyrolysis of lignin resulted in less exergy destroyed (0.51 ± 0.001 MJ/kg_{Material}) than the other compounds (1.62 ± 0.43 MJ/kg_{Material}) and 1.97 ± 0.05 MJ/kg_{Material} for hemicellulose and cellulose, respectively). Lignin pyrolysis showed an exergetic efficiency of approximately 97.74%, while cellulose and hemicellulose were at 91.95% and 89.82% respectively. Bio-oil exergetic efficiency was between 55.95% and 63.3% for cellulose and hemicellulose due to the high mass yields obtained. The opposite was showed by lignin, as the bio-oil yield was low compared to the other compounds. For lignin, the highest achieved efficiency was for the biochar produced, with 62.9% of the total exergy.

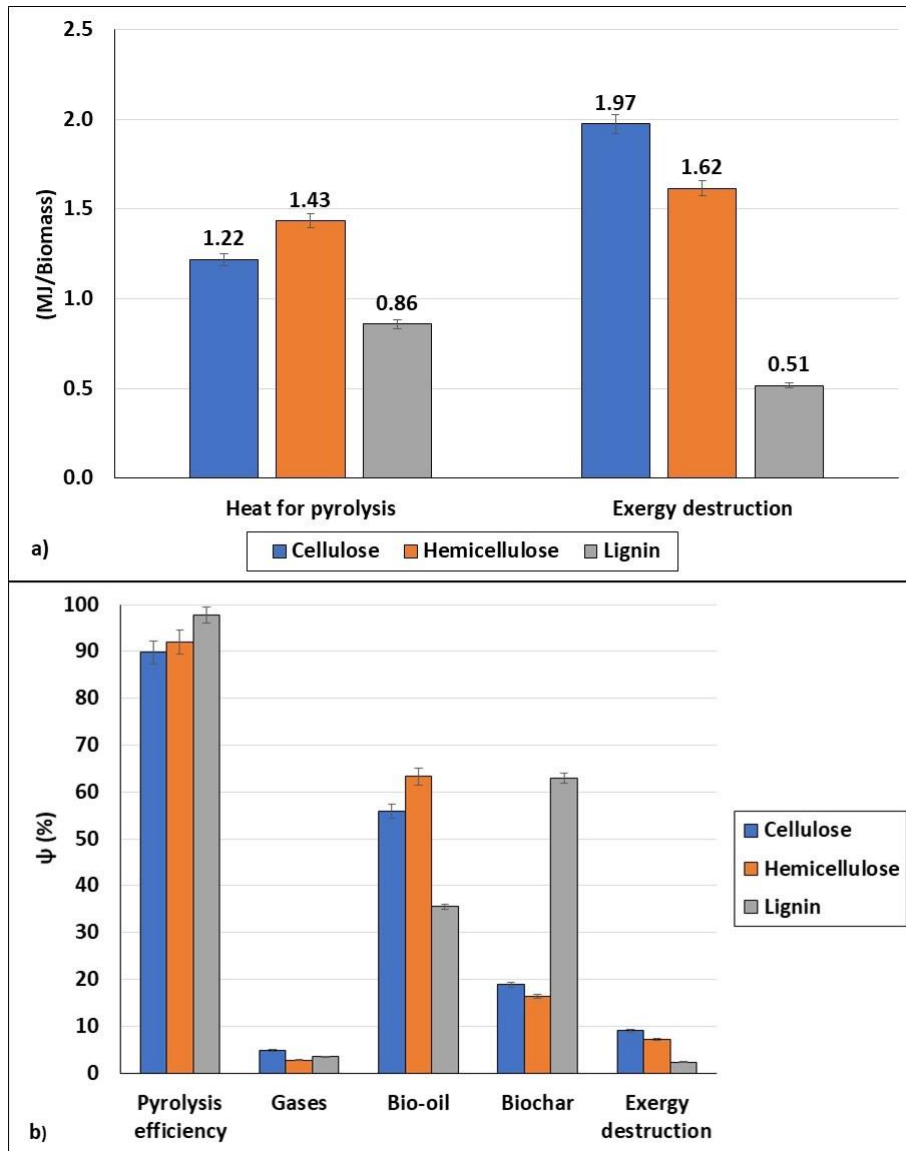


Figure 3.17. Heat for pyrolysis and exergy destruction, b) exergetic efficiency of biomass components at 500°C.

4. Catalytic pyrolysis of biomass pseudo-components

The catalytic pyrolysis of the three biomass pseudo-components was investigated from a thermodynamic point of view. The energy balance and exergy evaluation of the two best performing catalysts for bio-oil upgrading were proposed in order to study their similitude and behaviour compared with the catalytic pyrolysis of biomass previously reported in **section 2** of this chapter. In **Figures 3.18, 3.19 and 3.20** show the energy balance and exergy evaluation of products' distribution after catalytic treatment for cellulose, hemicellulose and lignin, respectively. In addition to the increase in the yield of gases and the reduction in the oxygen content in the mass balance, the use of catalysts influenced the energy/exergy evaluation of products.

Chapter 3

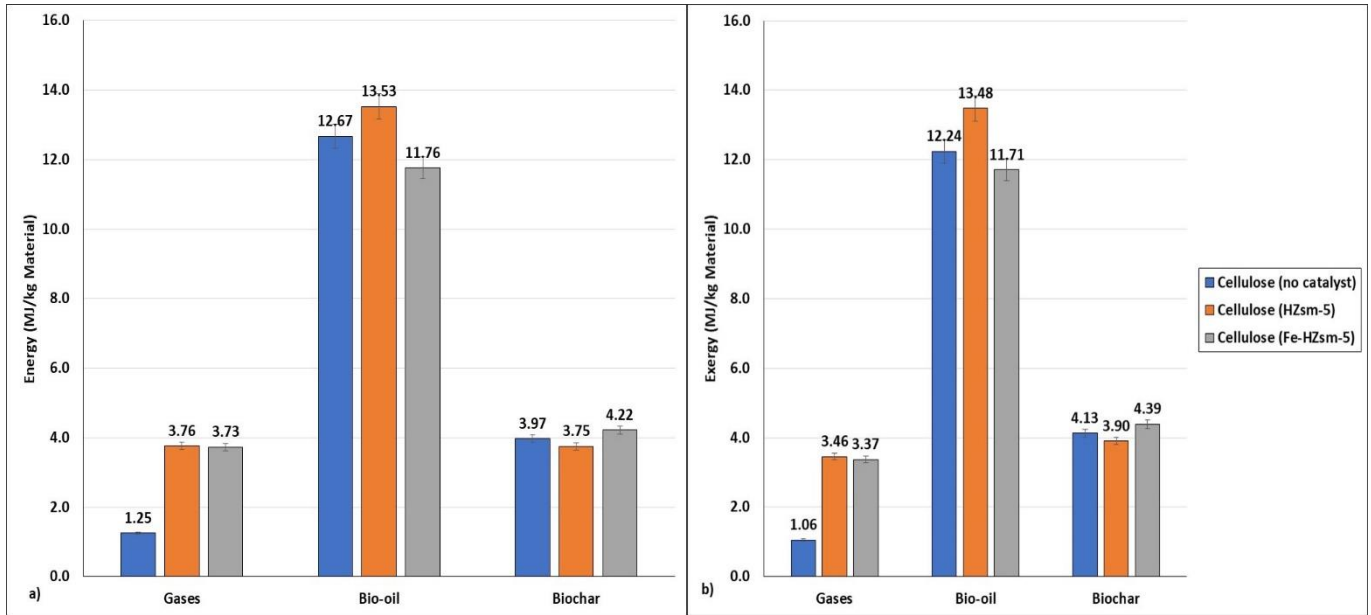


Figure 3.18. a) Energy balance, b) exergy evaluation for catalytic pyrolysis of cellulose at 500°C.

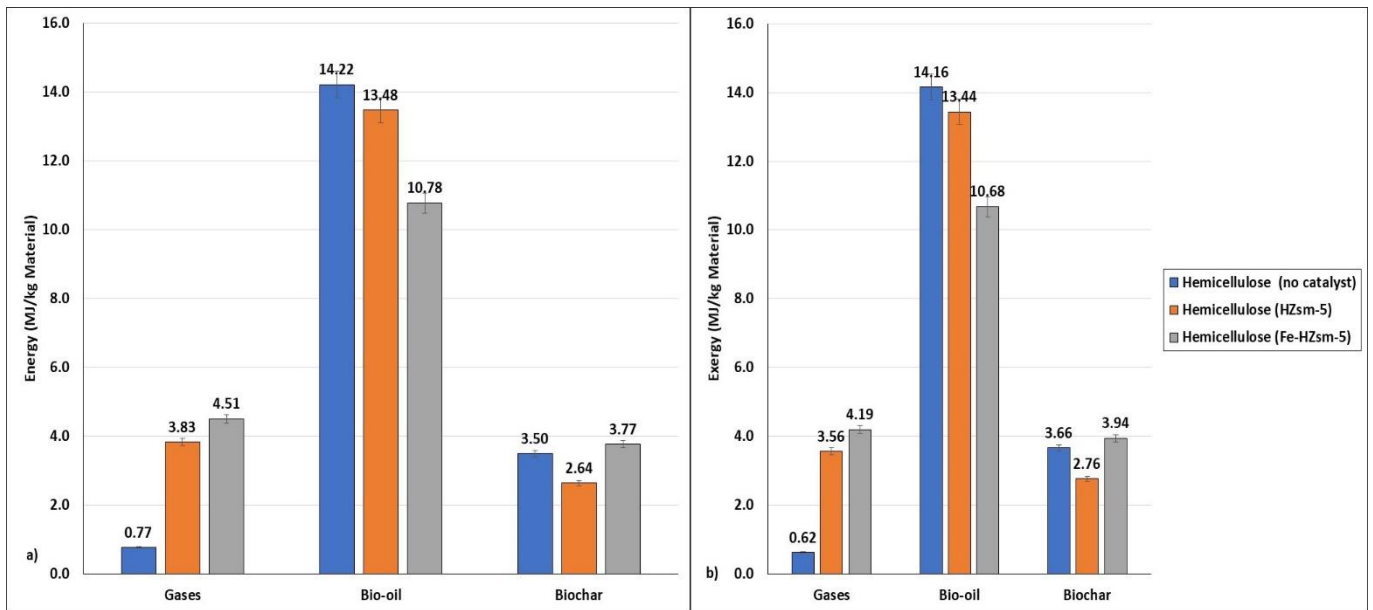


Figure 3.19. a) Energy balance, b) exergy evaluation for catalytic pyrolysis of hemicellulose at 500°C.

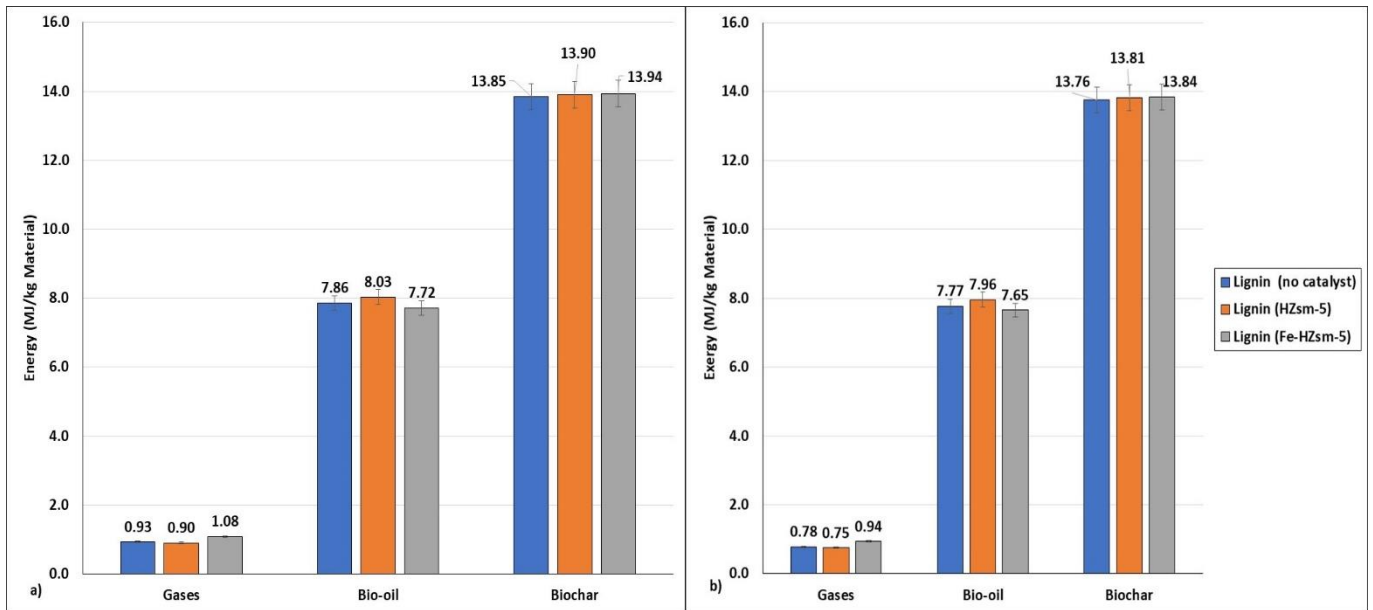


Figure 3.20. a) Energy balance, b) exergy evaluation for catalytic pyrolysis of lignin at 500°C.

4.1 Energetic and exergetic evaluation of catalytic pyrolysis of biomass pseudo-components

Biochar

As mentioned in **Section 2.1 of Chapter 2**, the catalyst was placed outside the pyrolysis zone so there was no contact of upgraded vapours and gases with the biochar produced once they exited the pyrolytic zone. Therefore, no variation was observed in biochar energetic/exergetic yield; moreover, the solid catalyst did not have an impact on biochar production or consumption.

Gases

It was observed for biomasses' catalytic pyrolysis that the use of these zeolites boosted the production of gaseous components. A similar trend for hemicellulose and cellulose was seen in this study. The energetic value was increased with the use of both catalysts. Meanwhile, for lignin, there was a very slight variation in the gas energy in terms of MJ per kilogram of lignin.

Figure 3.21 shows the evolution of gas components from lignin before and after catalytic treatment, showing that energetically there was not a substantial change for gaseous components. The energy rate of H_2 and C_{2+} was reduced with the use of catalysts, while CO , CO_2 and CH_4 increased very slightly. For cellulose and hemicellulose, the changes in the energy/exergy rate of gaseous compounds were significant. As the catalysts were very effective in heavy oil molecules' transformation, the energetic rate of compounds increased greatly. The individual energy rates of gaseous compounds can be seen in **Figure 3.22**.

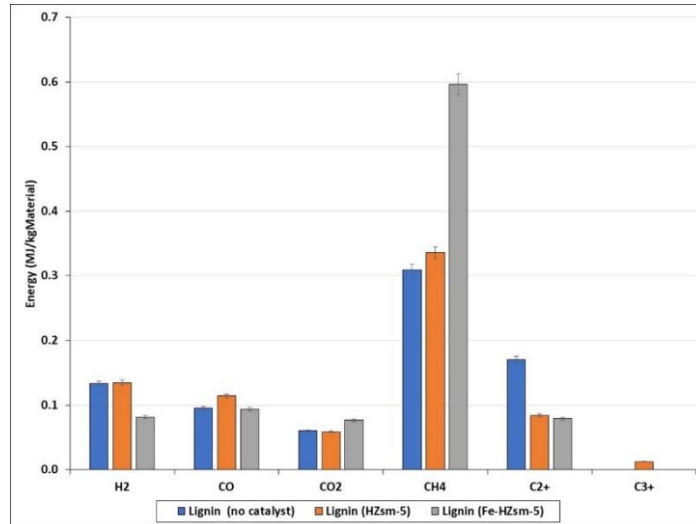


Figure 3.21. Energy distribution of gaseous components for catalytic pyrolysis of lignin at 500°C.

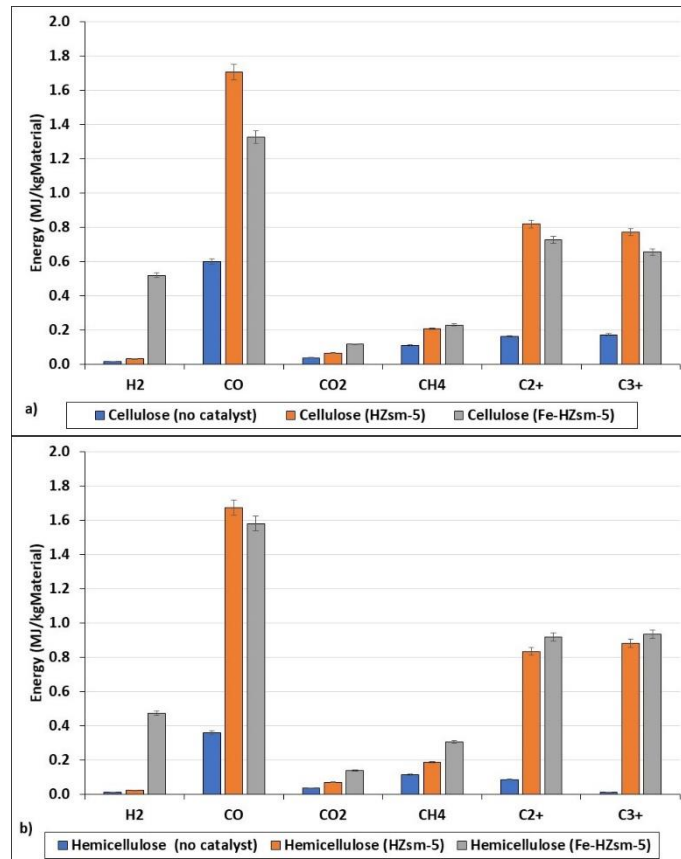


Figure 3.22. Energy distribution of gaseous components for catalytic pyrolysis of cellulose (up) and hemicellulose (down) at 500°C.

The most significant increase was observed in H₂ produced in Fe-HZSM-5 for both cellulose and hemicellulose. A slight increase in H₂ mass yield resulted in a high increase in the energy rate, because of the high energetic density of H₂. Hydrogen theoretical LHV is around 119.96

MJ/kg_{Gas}, while for other gases, such as CH₄ and CO, it was at 50.0 ± 1.35 MJ/kg_{Gas} and 10.11 ± 0.27 MJ/kg_{Gas}. Hence, a slight increase in hydrogen yield could potentially be more energetic than moderate yields of CH₄ and CO. In terms of MJ per kilogram of produced pyrolysis gases (MJ/kg_{Gas}), the used catalyst increased cellulose energy rate from 10.59 ± 0.29 MJ/kg_{Gas} to 11.5 ± 0.31 MJ/kg_{Gas} for Fe- HZSM-5 and to 13.35 ± 0.36 MJ/kg_{Gas} for HZSM-5. For hemicellulose, it was increased from 8.99 ± 0.24 MJ/kg_{Gas} to 11.55 ± 0.31 MJ/kg_{Gas} for Fe- HZSM-5 and 13.04 ± 0.35 MJ/kg_{Gas} for HZSM-5. Both catalysts were able to increase the gas stream energy rate, while HZSM-5 provided a richer CO gas stream with a higher energy rate than that produced with Fe-HZSM-5.

Comparing the results obtained from cellulose and hemicellulose with the catalytic pyrolysis of biomasses, it was observed that there was a difference in terms of the catalyst providing the highest energy rate. For biomasses, it was observed that Fe-HZSM-5 was able to increase the gas energy rate by approximately 80–82%, resulting in the most efficient catalyst in terms of increasing gas energy rate. Meanwhile, in the catalytic pyrolysis of the individual components (cellulose and hemicellulose), it was observed that HZSM-5 was most efficient in terms of increasing the gas energy rate from 26% to 45%, compared with Fe-HZSM-5 increasing the gas energy rate from 8.6% to 28.5%. As expressed in **Section 2.1** of this chapter, the catalyst HZSM-5 favoured CO production, showing higher yields of CO than Fe-HZSM-5, which was translated in the case of biomass components in the highest energy rate. In terms of gas energy rate, the catalytic pyrolysis of biomass components did not replicate the behaviour of biomass catalytic pyrolysis.

Upgraded bio-oil

In **Section 3.2.1** of this chapter, the results for upgraded bio-oil with the use of both catalysts for biomasses showed that Fe-HZSM-5 led to an increase in bio-oil energy of 40%, evidencing that in energetic terms this catalyst performed better than HZSM-5. For hemicellulose and lignin, the same behaviour as biomass was observed. In cellulose, the opposite was observed: HZSM-5 was able to increase the bio-oil energy rate by 36% compared to the initial bio-oil value, while Fe-HZSM-5 increased the bio-oil energy rate by 29%. This can be explained by the high energy yield of alkenes (BTX) and alcohols produced with HZSM-5 compared to Fe-HZSM-5. More details about the individual chemical families' energy rate in the upgraded bio-oil can be found in **Table 3.3**. The results were presented in terms of MJ/kg_{Bio-oil}.

Both catalysts favoured phenol production, hence phenol energy rate was the most significant in the upgraded bio-oil, followed by alkenes. It was observed that compounds that represented the highest energy/exergy yield in biomass catalytic pyrolysis were the same for cellulose and hemicellulose pyrolysis, despite there being differences in respect of the total energy rate with

Fe-HZSM-5 and HZSM-5. It can be added that even though the principal energy rates of the major compounds in cellulose and hemicellulose were very similar to the results for biomass catalytic pyrolysis in terms of which catalyst boosted the energy rate most, the results were diversified. From a thermodynamic point of view, the behaviour of biomass and separated components was not strictly the same because of the high yield of phenols present in bio-oil.

Table 3.3. Energy rates of chemical families with catalytic treatment (MJ/kg_{bio-oil}).

	Cellulose (no catalyst)	Cellulose (HZSM-5)	Cellulose (Fe-HZSM- 5)	Hemicellulo se (no catalyst)	Hemicellulo se (HZSM-5)	Hemicellulose (Fe- HZSM-5)	Lignin (no catalyst)	Lignin (HZSM-5)	Lignin (Fe- HZSM- 5)
Acids	0.73	0.00	0.22	2.63	0.24	0.00	1.67	0.00	0.00
Phenols	2.52	8.55	9.70	2.21	12.20	12.03	11.90	8.88	0.00
Aldehyde	0.90	0.20	0.29	0.58	0.34	0.13	0.00	0.00	0.00
Alkane	0.18	0.16	0.00	2.22	0.00	0.00	3.27	4.99	27.11
Alkene	1.27	7.42	6.13	0.99	4.41	4.24	3.10	0.00	0.00
Alcohol	1.50	4.15	1.78	3.16	1.24	1.53	0.00	0.00	0.00
Amides	0.80	0.30	0.22	1.25	0.16	0.27	0.97	2.54	0.00
Ketones	2.53	1.12	2.15	2.47	2.21	2.57	1.59	2.41	0.00
Esters	0.76	0.31	0.25	1.52	0.11	0.56	0.00	0.00	0.00
Furans	0.11	0.58	0.92	0.47	0.86	1.18	0.00	0.00	0.00
Guaiacol	0.00	0.00	0.00	0.24	0.42	0.31	1.49	5.84	0.00
Sugars	5.43	0.00	0.00	0.37	0.00	0.00	0.00	0.00	0.00
Total	16.74± 0.45	22.80± 0.62	21.66 ± 0.58	18.10 ± 0.49	22.19 ± 0.60	22.82± 0.61	23.99± 0.65	24.66± 0.67	27.11± 0.73

4.2 Heat for pyrolysis and exergy destruction rate

The results obtained for heat for pyrolysis for the catalytic treatment agreed with the results obtained for biomasses. **Figure 3.23** shows that the process became more energy-demanding when catalysts were used due to the increase in endothermic deoxygenation reactions. The use of both catalysts increased heat for pyrolysis two or three times compared to the heat required to perform pyrolysis without any catalyst for cellulose and hemicellulose. The same was observed with lignin, but with less impact due to the low variation in mass balance with use of a catalyst. It is worth noting that a difference was observed in the heat required for the pyrolysis of individual components and that compared for biomass. In the case of biomass with a catalyst, the highest energetic requirement came with the use of Fe-HZSM-5. In the case of the individual biomass components, the results were different, as HZSM-5 required more heat than the other catalyst. This was one of the main differences observed between biomass conversion and its components.

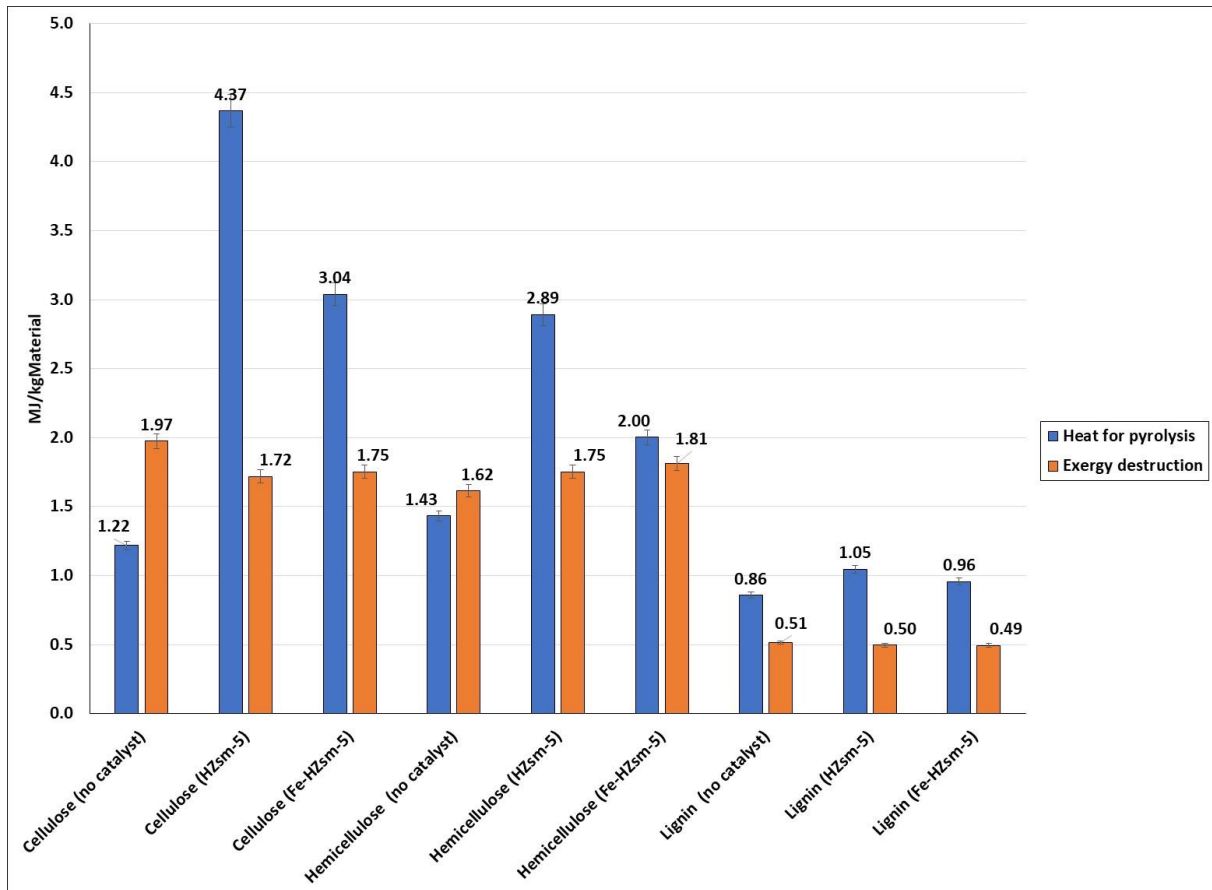


Figure 3.23. Heat for pyrolysis and exergy destruction with the catalytic treatment of biomass components at 500°C.

In terms of exergy destruction, the results obtained with cellulose showed a decrease with the use of catalytic treatment, as seen for biomasses, while for hemicellulose the opposite was observed. The process entropy increased with the use of the catalyst for hemicellulose. Despite this, the exergy destruction values were very similar for cellulose and hemicellulose, while for lignin it was almost constant, as low variations were observed in liquid and gaseous components, which were the phases presenting higher entropy variations in calculations. As can be seen, the average values for exergy destroyed for biomass components (cellulose and hemicellulose) were 1.7 ± 0.05 MJ/kg_{Material}, with the use of a catalyst. It was observed that the entropy variations (irreversibility) provoked by the use of both catalysts were very similar for both biomasses and the cellulose and hemicellulose, which are considered the major components of biomass.

4. Conclusions

From the results obtained for the thermodynamic study of beech wood and flax shive pyrolysis with and without catalyst treatment, and the pyrolysis of cellulose, hemicellulose and lignin with and without catalyst treatment, the main conclusions are summarized as follows.

Chapter 3

- Energy/exergy rates obtained from pyrolysis products of flax shives pyrolysis were higher than for beech wood due to the higher amount of volatile matter in flax shives.
- Permanent gases in the pyrolysis results represented the lowest energy/exergy rates of products, below biochar and bio-oil. The gaseous products were highly diluted in CO₂ and N₂, which had a low energy density compared to other combustible gases.
- Beech wood and flax shives' bio-oil energetic values were between 18.7 ± 0.50 and 19.03 ± 0.51 MJ/kg_{Bio-oil}, respectively, as the two bio-oils have similar thermodynamic behaviour and oxygen content.
- Flax shives required more heat to perform pyrolysis (2.21 ± 0.06 MJ/kg_{Biomass}) than beech wood (1.97 ± 0.05 MJ/kg_{Biomass}), with a difference of 11% between biomasses.
- The use of a catalyst increases energetic and exergetic rates by approximately 80% for gases and 40% for bio-oil.
- Heat for pyrolysis increases with the use of catalysts due to the triggering of deoxygenation reactions, while less entropy change is observed when a catalyst is used.
- Hemicellulose and cellulose bio-oils seem to have the closest energetic and exergetic distribution of chemical families when compared to biomasses than lignin bio-oil. On the other hand, the pyrolysis of individual compounds does not give a strictly identical thermodynamic behaviour to the pyrolysis of biomasses.
- Hemicellulose requires more heat for pyrolysis than cellulose and lignin; at the same time, the heat for pyrolysis was lower for individual components than for biomasses.
- The energy requirement for catalytic pyrolysis of pseudo components was not the same as that for biomasses' catalytic pyrolysis. Biomass required more heat with the use of the Fe-HZSM-5 catalyst, while pseudo-components were more energy-demanding with the HZSM-5 catalyst.

Chapter 4:

**THERMODYNAMIC ANALYSIS OF BIOMASS
GASIFICATION IN A FLUIDIZED BED REACTOR**

Introduction

The following chapter involves thermodynamic analysis of the results obtained from the gasification of beech wood pellets in a fluidized bed reactor in a bubbling fluidization regime. The investigation comprises study of the effect of temperature in the gasification of biomass, comparison of high-temperature pyrolysis with gasification, the effect of varying gasification agents, and the effect of changing inert bed material to a catalytic bed. This thermodynamic evaluation presents the innovation of comparing all parameters and processes with strict similar conditions using the same experimental setup. In addition, to our knowledge, very limited thermodynamic evaluation (principally exergy analysis) in the study of biomass gasification using biochar as a bed material is found in the literature.

This chapter focuses on adding important details that are usually missing in the criticism and evaluation of the effectiveness of the thermochemical biomass process (gasification and pyrolysis). The following results present an error of margin of approximately 1.7% due to the experimental uncertainty and deviations. The errors surrounding the experimental tests are those found in deviation calculations after experiment repetitions, mass weighting, the rounding of values and equipment tolerance. The uncertainty of values is shown by error bars over the presented results. For convenience, gaseous components with more than one carbon molecule are presented as C_{2+} (including C_2H_2 , C_2H_4 and C_2H_6) and C_{3+} (including C_3H_4 , C_3H_6 and C_3H_8) in this work.

In addition to this, the presented results are on a dry basis, N_2 and CO_2 free, and in this work only H_2 , CO , CH_4 , C_{2+} and C_{3+} were considered as syngas. As CO_2 and water formed part of the gasification agents, they were separated from the syngas stream in order to avoid calculation errors. Hence, gaseous components such as N_2 , CO_2 and H_2O were grouped in a stream called flue gas in order to lighten calculations. The flow rate of carrier gas or gasification agents was equal to 1.15 ml/min for a period of approximately 10.6 seconds, 2.5 times the minimum fluidization velocity. This fluidization condition in the reactor was considered a bubbling regime.

The results are presented in units $MJ/kg_{Biomass}$ as this represents a better way to show the rates of energy/exergy per kg of the raw material. All experiments were repeated at least three times to assure repeatability. In this work, the term anergy or heat waste is used to describe the difference between the energy and exergy values of a stream: in other words, it contains the non-profitable part of energy when a system was not fully reversible. Meanwhile, the exergy destruction (I) term was used to describe the difference between the inlet and outlet exergy of the conversion system. Both anergy and exergy destruction (I) terms are present due to the entropy generation or irreversibilities of the process.

The data used for the thermodynamic evaluation in the fluidized bed reactor are summarized in **Appendix A3**, including discussion of mass balances and product distribution. **Tables 4.1, 4.2 and 4.3** show the most relevant details of the mass, energy balance and exergy evaluation of the performed experimental runs.

1. Biomass gasification with carbon dioxide

The energy and exergy distribution values of various reaction temperatures are shown in **Figure 4.1**. Sand was used as a bed material in this case. Only the output products of energy distribution are shown. For inputs, including the biomass and the gasification agent, the sum of energy values varied from 16.7 ± 0.28 to 17.2 ± 0.29 MJ/kg_{Biomass}, while temperature increased from 600°C to 900°C and approximately 18.5 ± 0.31 MJ/kg_{Biomass} for exergy rate. As biomass quantity and CO₂ flow rate were kept constant, these variations were attributed to the change of sensible heat from the gasification agent. The total energy and exergy of the products increased as temperatures increased because of biochar conversion and tar cracking reactions.

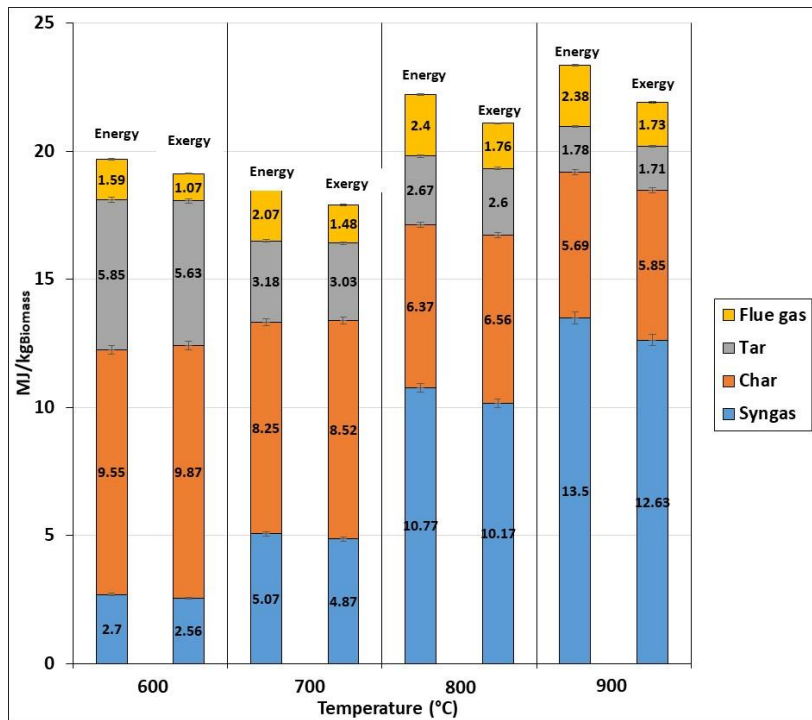


Figure 4.1. Effect of temperature on energy/exergy products distribution of gasification with CO₂.

Chapter 4

Table 4.1. Results of mass, energy balance and exergy evaluation of biomass gasification using fluidized bed reactor in this study.

Test	Bed material	Temperature °C	Mass balance (yield %)			^a Energy balance (MJ/kg _{biomass})					^b Exergy evaluation (MJ/kg _{biomass})							
			Gases	Tar	Char	Syngas	Char	Tar	Flue gas	Agent	Syngas	Char	Tar	Flue gas	Agent	Ex _{Heat}	^c <i>I</i>	
Gasification with CO ₂	Sand	600	45.61	29.63	24.75	2.70	9.55	5.85	1.59	1.16	2.56	9.87	5.63	1.07	1.00	4.15	1.94	
		700	61.78	25.46	12.77	5.07	8.25	3.18	2.07	1.33	4.87	8.52	3.03	1.48	1.11	3.04	2.46	
		800	73.23	19.52	7.26	10.77	6.37	2.67	2.40	1.51	10.17	6.56	2.60	1.76	1.24	6.67	2.90	
		900	78.05	17.31	4.64	13.50	5.69	1.78	2.38	1.69	12.63	5.85	1.71	1.73	1.37	7.80	3.20	
Pyrolysis		800	66.51	20.02	13.47	7.01	6.54	4.86	1.51	1.06	6.73	6.73	4.65	0.56	0.42	4.38	3.01	
		900	70.75	18.95	10.30	8.71	6.23	3.91	1.67	1.17	8.28	6.40	3.71	0.69	0.50	4.98	3.21	
Gasification with CO ₂		Biochar	600	49.99	21.83	28.17	3.53	9.08	5.05	1.98	1.67	3.39	9.39	4.89	1.40	1.43	4.10	2.34
			700	70.29	7.74	21.97	9.97	7.12	1.90	2.14	1.91	9.35	7.35	1.83	1.60	1.60	5.58	2.76
	800		79.67	5.46	14.87	12.53	4.85	1.90	2.45	2.17	11.69	5.00	1.84	1.85	1.78	6.20	3.14	
	900		92.61	1.91	5.48	17.18	1.80	0.69	2.93	2.42	15.89	1.85	0.66	2.23	1.97	7.06	3.75	
Steam gasification	600		55.44	21.36	23.20	3.60	7.47	5.20	0.74	0.45	3.41	7.73	5.08	0.26	0.13	1.47	2.31	
	700		70.52	12.84	16.64	8.25	5.40	4.11	0.86	0.58	7.79	5.57	4.02	0.36	0.19	3.09	2.67	
	800		80.80	5.92	13.28	13.90	4.34	2.11	0.99	0.59	13.23	4.47	2.07	0.47	0.22	5.80	2.87	
	900		87.13	4.39	8.48	16.55	2.79	1.82	1.26	0.65	15.76	2.87	1.79	0.70	0.26	6.89	3.07	

^aBiomass Energy 15.54 ± 0.26 MJ/kg.

^bBiomass Exergy 17.32 ± 0.29 MJ/kg.

^c*I* (exergy destruction rate) represented the difference between inlet and outlet exergy values.

Chapter 4

Table 4.2. Results of Energy balance and product composition of experimental runs of gasification.

Test	Temperature °C	Bed material	Syngas Components: MJ/kg _{biomass}					^a Tar: MJ/kg _{biomass}								Energy streams: MJ/kg _{biomass}					
			H ₂	CO	CH ₄	C ₂₊	C ₃₊	(a)	(b)	(c)	(d)	(e)	(f)	(g)	(h)	Syngas	Char	Tar	Flue gas	^b Agent	
Gasification with CO ₂	600	Sand	0.11	1.44	1.01	0.12	0.02	2.73	0.59	0.39	0.80	0.53	0.48	0.31	0.03	2.70	9.55	5.85	1.59	1.16	
	700		0.45	1.70	2.56	0.17	0.19	1.09	0.56	0.23	0.57	0.29	0.21	0.20	0.02	5.07	8.25	3.18	2.07	1.33	
	800		1.07	5.12	3.93	0.27	0.38	0.08	0.88	0.09	0.54	0.20	0.39	0.40	0.08	10.77	6.37	2.67	2.40	1.51	
	900		2.29	6.13	4.55	0.51	0.01	0.04	0.30	0.09	0.34	0.12	0.29	0.49	0.11	13.50	5.69	1.78	2.38	1.69	
Pyrolysis	800		0.59	2.44	1.89	1.28	0.81	0.16	1.55	0.35	1.01	0.32	0.70	0.64	0.13	7.01	6.54	4.86	1.51	1.06	
	900		1.35	2.82	2.18	1.72	0.63	0.06	0.70	0.29	0.99	0.17	0.53	0.98	0.18	8.71	6.23	3.91	1.67	1.17	
Gasification with CO ₂	600		Biochar	0.07	1.80	0.74	0.06	0.87	2.52	0.36	0.26	0.59	0.71	0.39	0.19	0.02	3.53	9.08	5.05	1.98	1.67
	700			0.38	6.58	1.83	0.23	0.95	0.83	0.32	0.10	0.26	0.17	0.11	0.10	0.01	9.97	7.12	1.90	2.14	1.91
	800	0.76		8.30	2.50	0.31	0.67	0.14	0.65	0.11	0.32	0.11	0.32	0.26	0.00	12.53	4.85	1.90	2.45	2.17	
	900	1.98		11.27	3.46	0.22	0.25	0.04	0.14	0.04	0.17	0.03	0.09	0.15	0.03	17.18	1.80	0.69	2.93	2.42	
Steam gasification	600	0.49		1.64	1.40	0.02	0.06	2.25	0.66	0.18	0.88	0.59	0.39	0.22	0.03	3.60	7.47	5.20	0.74	0.45	
	700	1.33		3.61	3.10	0.08	0.13	0.39	0.92	0.27	0.83	0.58	0.55	0.40	0.17	8.25	5.40	4.11	0.86	0.58	
	800	2.66		4.07	4.41	2.15	0.61	0.11	0.82	0.08	0.34	0.10	0.37	0.27	0.02	13.90	4.34	2.11	0.99	0.59	
	900	3.00		4.78	5.33	1.90	1.54	0.13	0.28	0.05	0.37	0.05	0.43	0.53	0.00	16.55	2.79	1.82	1.26	0.65	

^a a) Other aliphatic compounds, b) Phenols, c) Furans, d) Heterocyclic aromatic compounds, e) Aromatic compounds, f) Light poly-aromatic hydrocarbons, g) Naphthalenes, h) Heavy poly-aromatic hydrocarbons.

^bGasification agent.

Chapter 4

Table 4.3. Results of exergy and product composition of experimental runs of gasification.

Test	Temperature °C	Bed material	Syngas Components: MJ/kg _{biomass}					^a Tar: MJ/kg _{biomass}								Products exergy streams: MJ/kg _{biomass}				
			H ₂	CO	CH ₄	C ₂₊	C ₃₊	(a)	(b)	(c)	(d)	(e)	(f)	(g)	(h)	Syngas	Char	Tar	Flue gas	^b Agent
Gasification with CO ₂	600	Sand	0.09	1.31	1.01	0.12	0.02	2.70	0.59	0.19	0.79	0.52	0.51	0.30	0.03	2.56	9.87	5.63	1.07	1.00
	700		0.40	1.55	2.56	0.17	0.19	1.07	0.55	0.11	0.57	0.28	0.23	0.20	0.02	4.87	8.52	3.03	1.48	1.11
	800		0.96	4.65	3.91	0.27	0.39	0.08	0.87	0.05	0.56	0.19	0.41	0.39	0.07	10.17	6.56	2.60	1.76	1.24
	900		2.06	5.55	4.52	0.5	0.01	0.04	0.29	0.04	0.33	0.11	0.30	0.48	0.10	12.63	5.85	1.71	1.73	1.37
Pyrolysis	800		0.53	2.21	1.88	1.28	0.82	0.15	1.53	0.17	0.99	0.31	0.74	0.63	0.12	6.73	6.73	4.65	0.56	0.42
	900		1.22	2.55	2.17	1.71	0.64	0.06	0.69	0.14	0.97	0.17	0.56	0.95	0.16	8.28	6.40	3.71	0.69	0.50
Gasification with CO ₂	600	Biochar	0.06	1.64	0.74	0.06	0.89	2.50	0.36	0.12	0.59	0.70	0.41	0.19	0.02	3.39	9.39	4.89	1.40	1.43
	700		0.34	6.00	1.82	0.22	0.97	0.82	0.32	0.05	0.25	0.16	0.12	0.10	0.01	9.35	7.35	1.83	1.60	1.60
	800		0.67	7.54	2.49	0.30	0.68	0.13	0.64	0.05	0.32	0.11	0.33	0.25	0.00	11.69	5.00	1.84	1.85	1.78
	900		1.77	10.22	3.43	0.22	0.25	0.04	0.13	0.02	0.17	0.03	0.10	0.15	0.02	15.89	1.85	0.66	2.23	1.97
Steam gasification	600		0.44	1.49	1.40	0.02	0.06	2.23	0.65	0.09	0.87	0.58	0.42	0.21	0.02	3.41	7.73	5.08	0.26	0.13
	700		1.20	3.28	3.10	0.08	0.13	0.40	0.93	0.13	0.84	0.58	0.59	0.39	0.15	7.79	5.57	4.02	0.36	0.19
	800		2.4	3.68	4.39	2.14	0.62	0.11	0.81	0.04	0.33	0.10	0.39	0.26	0.02	13.23	4.47	2.07	0.47	0.22
	900		2.70	4.32	5.29	1.88	1.57	0.12	0.27	0.02	0.36	0.05	0.46	0.51	0.00	15.76	2.87	1.79	0.70	0.26

^a a) Other aliphatic compounds, b) Phenols, c) Furans, d) Heterocyclic aromatic compounds, e) Aromatic compounds, f) Light poly-aromatic hydrocarbons, g) Naphthalenes, h) Heavy poly-aromatic hydrocarbons.

^bGasification agent.

It was observed that the total energy values were higher than the total exergy values for all temperatures tested. This was due to the fact that not all the energy could be exploited due to irreversibilities. In other words, anergy and exergy destruction evidenced the non-profitable part of energy when a system was not fully reversible. This waste increased as temperature increased: for the case of products, it was observed that at 900°C the difference reached the highest value ($1.43 \pm 0.02 \text{ MJ/kg}_{\text{Biomass}}$).

Figure 4.2 shows the values of products' chemical and physical exergy. The chemical exergy was around 12–18 times higher than the physical exergy for products such as tar, biochar and syngas; these results were in agreement with the literature [160]. This was not the case for the flue gas stream, due to the fact that the molar flow rate of CO_2 in this stream was around 32 mol/min. This value caused the enthalpy difference to be more significant than its chemical exergy.

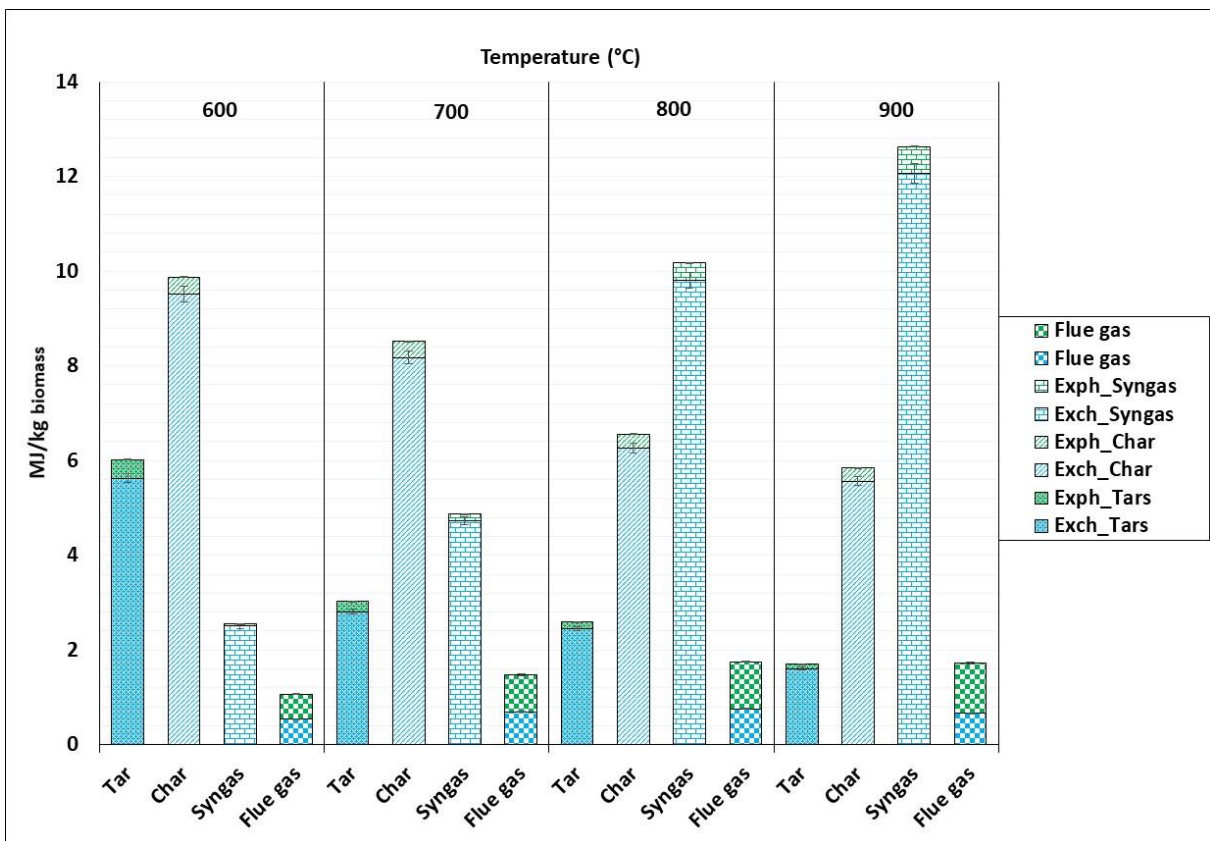


Figure 4.2. Chemical and physical exergy products distribution of gasification with CO_2 .

The total exergy destruction of the system was calculated taking into consideration the exergy inputs stream. As the biomass was the principal source of energy, its exergy value must be calculated. As was explained in **Section 1.1 of Chapter 3**, for non-conventional solid fuels, exergy calculations are complex because devolatilization takes place and entropy evaluation

is quite complicated. In thermodynamics, exergy studies are mostly done to find the quantity of useful energy and to find process irreversibility [161], which is linked to the increase of entropy when a process is not fully reversible. In this study, the term irreversibility refers to the energy of a stream and the exergy destruction due to entropy generation, which for non-conventional fuels was difficult to estimate. Consequently, the exergy values were higher than the energy values.

Figure 4.3 shows the obtained results for energy and exergy values for non-conventional fuels (biomass and biochar). A difference can be observed between energy and exergy values, corresponding to the irreversibilities or entropy changes of the stream.

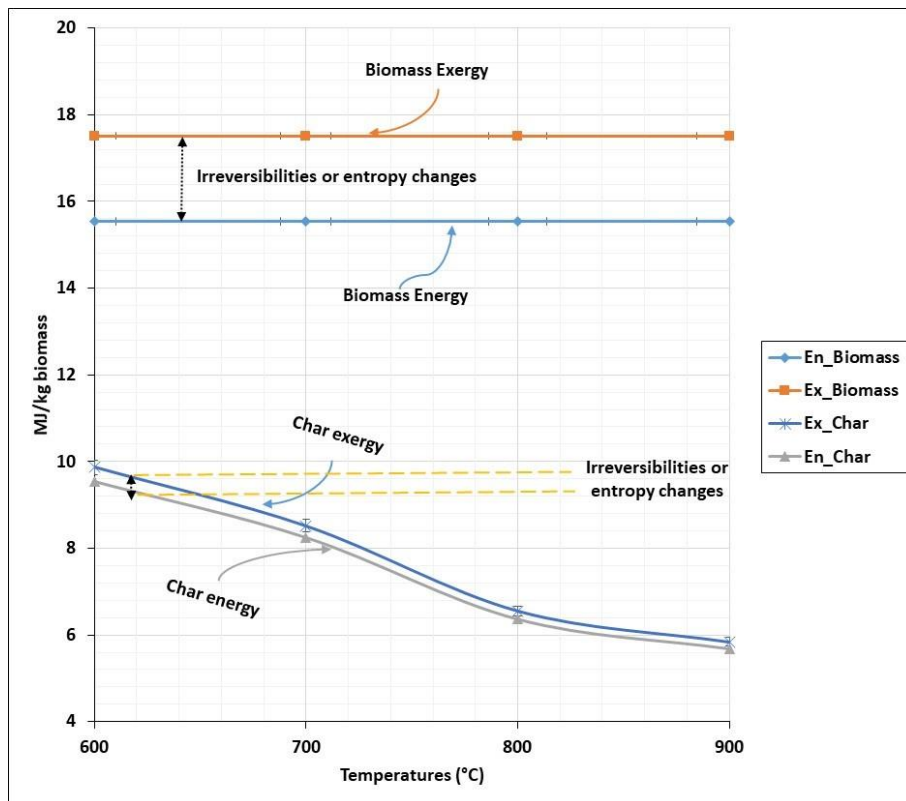


Figure 4.3. Energy and exergy difference for biochar and biomass, gasification with CO₂.

1.1 Effect of gasification temperature on energy and exergy rate of products

Biochar

For unconverted biochar, the energy and exergy rate trends decreased as temperature increased. Due to the presence of a gasification agent and the increase of temperature, Boudouard reaction and biochar conversion were clearly favoured. Thus, biochar energy was transferred to syngas. At 600°C and 700°C, biochar still represented 48% and 44% ($9.55 \pm$

0.16 and 8.25 ± 0.14 MJ/kg_{Biomass}) of the output energy of the system, respectively. This observation shows that less biochar was converted at low temperatures.

At 800°C and 900°C, temperatures that in gasification terms are considered high, the biochar energy percentage changed to 29% and 24% (6.37 ± 0.11 and 5.69 ± 0.10 MJ/kg_{Biomass}), respectively, as syngas represented the highest percentages—48% and 58% (10.77 ± 0.18 and 13.50 ± 0.23 MJ/kg_{Biomass}) of the total produced energy, respectively. For the highest temperature of 900°C, the biochar energy value was 5.7 ± 0 MJ/kg_{Biomass}. In addition, biochar exergy decreased from 9.87 ± 0.17 MJ/kg_{Biomass} to 5.87 ± 0.1 MJ/kg_{Biomass} when temperature passed from 600°C to 900°C. This reduction in biochar energy and exergy can also be explained by the fact that biochar conversion and reactivity increased with temperature. These biochar energy values still represent a high amount of energy to be conceded to syngas if higher biochar conversion is achieved [162].

Tar

As mentioned for biochar, the tar energy and exergy were reduced as the temperature increased. At 600°C, the amount of tar was significant, leading to high energetic and exergetic values. At this temperature, the energy available from tar represented 30% (5.85 ± 0.10 MJ/kg_{Biomass}) of the total energy of the products, while at 900°C it represented only 8% of the total distribution (1.78 ± 0.03 MJ/kg_{Biomass}). Exergy was reduced from 5.63 ± 0.09 MJ/kg_{Biomass} (30.9% of the total exergy of products) to 1.71 ± 0.03 MJ/kg_{Biomass} (7.8% of the total exergy of products) from 600°C to 900°C, respectively. Tar exergy was observed to be lower than its energy values: at 900°C, a reduction of 0.07 MJ/kg_{Biomass} was observed, this value mainly deriving from irreversibilities and tar compounds, especially from naphthalene, whose quantity and entropy values were the highest. This reduction in tar energy and exergy can be explained by thermal cracking reactions. Tar energy was transferred to the syngas stream as new gas molecules were formed.

Gases

The syngas energy increased with temperature: 13.5 ± 0.23 MJ/kg_{Biomass} was obtained at 900°C, proving the high energetic value of syngas produced from gasification. As temperature favoured biochar conversion and tar cracking, the syngas energy increased directly, as biochar conversion led to syngas formation and tar cracking led to the formation of smaller molecules, including syngas. A similar tendency was observed for the flue gas exiting the system, noting that, in this study, the water produced, N₂ and CO₂ were considered flue gas. For each experiment at different temperatures, CO₂ was also produced through the devolatilization process. Hence, flue gas molar flow rates increased slightly as temperatures went up. As the

temperature of gasification was increased, the energy was more significant, as can be observed in **Figure 4.4**. At 600°C, only 0.14 ± 0.002 MJ/kg_{Biomass} represented the energy from syngas, while at 900°C, the energy values were around 0.86 ± 0.01 MJ/kg_{Biomass}. It can be noted that temperature influenced the increase of energy as gas entropy increased with temperature.

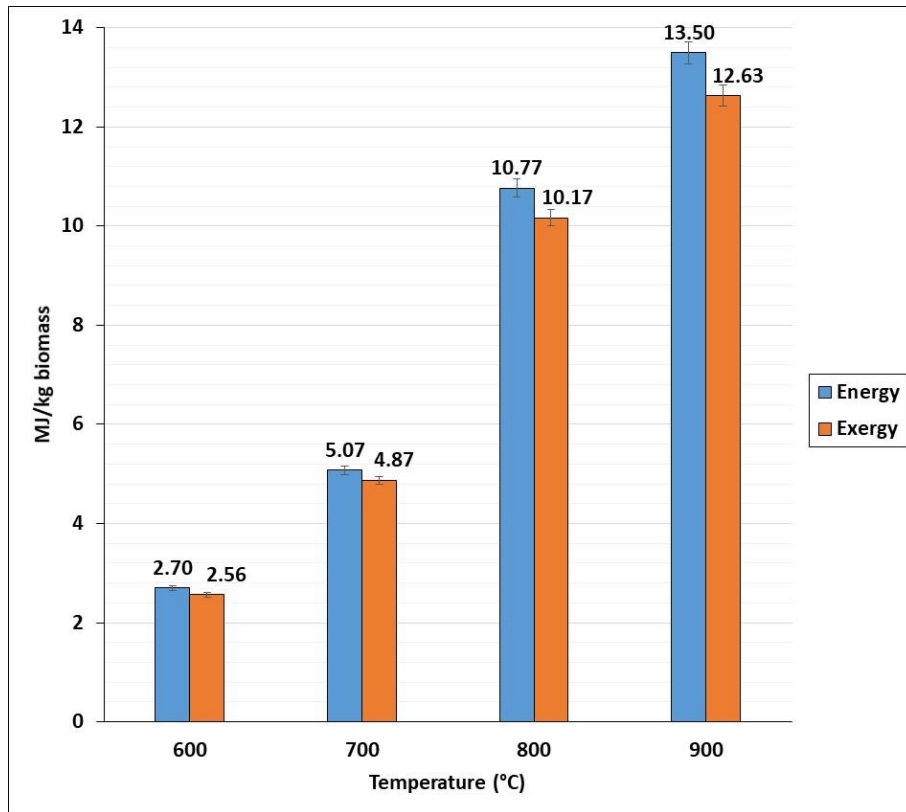


Figure 4.4. Syngas energy and exergy value evolution with temperature, gasification with CO₂.

Figure 4.5 shows the energy and exergy distribution for the principal compounds in the syngas as a function of temperature. It can be seen that H₂, CH₄ and CO represent the highest values at all temperatures. H₂ energy and exergy increased significantly as temperature increased, but lower values than the ones for CH₄ were obtained due to the higher energy density values of CH₄. At high temperatures, CO represented the highest energy and exergy values because of high molar flow rates in the syngas. Comparing CO and CH₄, as the principal syngas compounds obtained from experiments at the highest temperature of 900°C, the energy was more significant for CO (0.58 ± 0.01 MJ/kg_{Biomass}) than for CH₄ (0.03 ± 0.0005 MJ/kg_{Biomass}). This remarkable difference was due to the fact that CO content was around nine times higher than CH₄. Other gas species, such as C₂₊ and C₃₊, increased at higher temperatures, except at 900°C, where the amount of C₃₊ decreased because of its decomposition to smaller molecules.

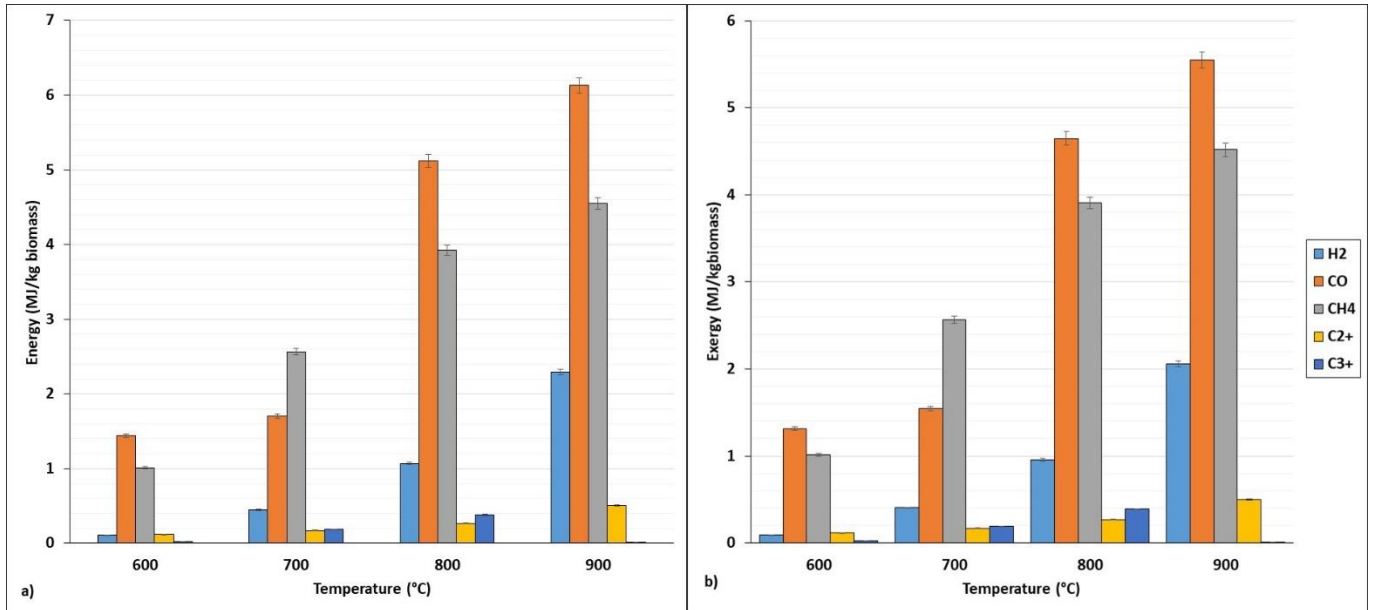


Figure 4.5. Effect of temperature on a) energy, b) exergy distribution of syngas components, gasification with CO₂.

1.2 Heat requirement

The specific heat input needed to perform gasification was calculated without taking into consideration the energy of the gasification agent stream. This was done in order to normalize the obtained results and compare them with the literature [107], [160], [163]. As the CO₂/C molar ratio significantly influences the specific heat of gasification [68], it was recommended to normalize the energy input before comparing it with other results. The higher the molar flow rate of the gasification agent, the higher the sensible heat, and vice versa. This occurrence was frequently taken into consideration for these calculations.

Figure 4.6 shows the input heat of gasification as a function of the reaction temperature compared with the amount of energy obtained from the syngas. Globally, from 600°C to 900°C, the heat of gasification increased from 4.15 ± 0.07 to 7.80 ± 0.13 MJ/kg_{Biomass}. Between 600°C and 700°C, there was a decrease in the input heat for gasification. This phenomenon was also observed by Renganathan et al. [107], who argued that a minimum occurred in the curve of heat input vs. temperature using pure CO₂ as a gasification agent for various carbonaceous feedstock. For different CO₂/C ratios vs. temperature, a minimum of heat input can be found at temperatures between 600°C and 800°C. The author explained that for a given condition of feedstock and gasifying agent, the heat input required could vary because of the flow rate of CO₂ used and the temperature region. In the low-temperature region, with an increase in temperature, the quantity of CO₂ required decreases radically, reducing the heat input needed

steeply. An incrementation in exothermic reactions was seen, providing sustainability to the gasification reaction and reducing the endothermicity, as less heat input was required.

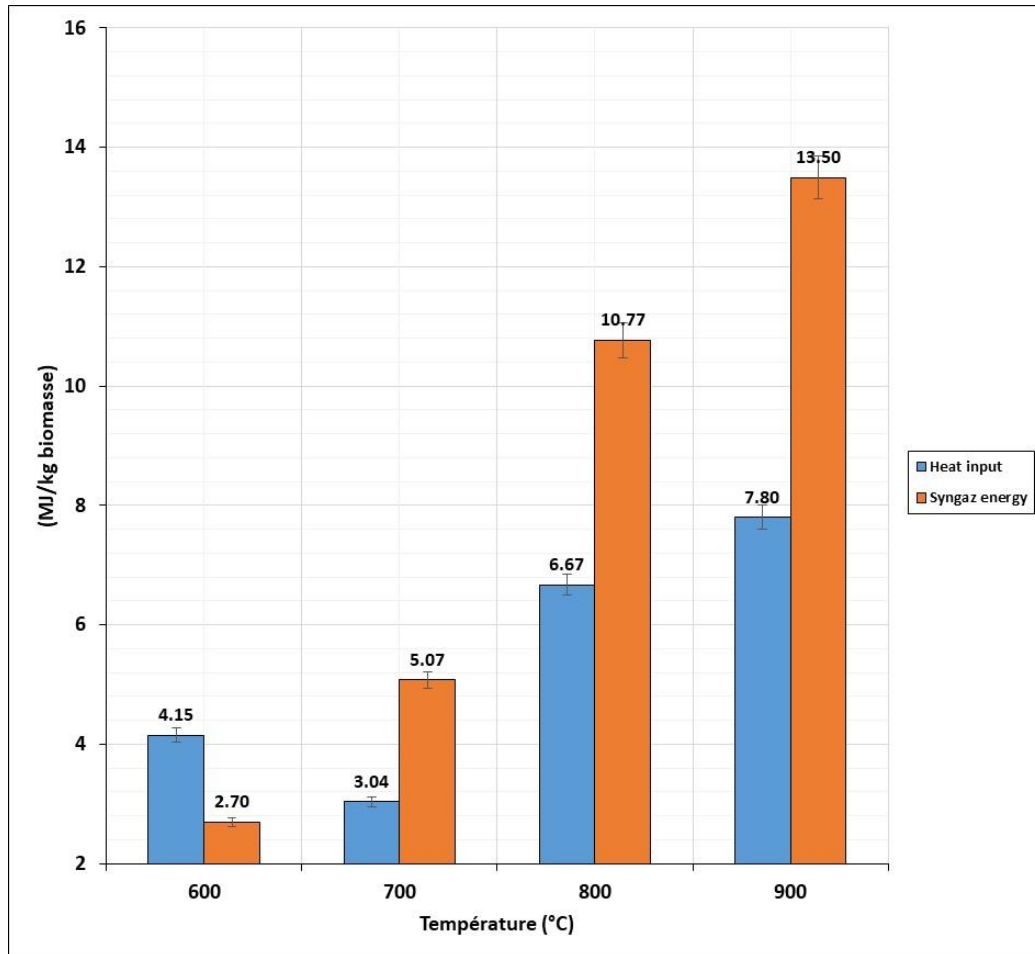


Figure 4.6. Effect of temperature in the heat input for CO₂ gasification.

In this section, high-temperature pyrolysis is compared with gasification using CO₂ with sand as the bed material at 800°C and 900°C. **Figure 4.7** shows the results of the energy and exergy distribution of products at 800°C and 900°C for pyrolysis compared with gasification with CO₂. For pyrolysis, the total energy of the products increased very slightly from 800°C to 900°C (19.9 ± 0.34 to 20.5 ± 0.35 MJ/kg_{Biomass}). For gasification cases, from 800°C to 900°C, the total energy varied between 22.2 ± 0.38 and 23.3 ± 0.40 MJ/kg_{Biomass}. It was seen that gasification provided higher energy values to products than pyrolysis. The impact on the energy balance of the gasification agent is clearly observed when CO₂ is used in gasification.

The difference in total exergy of products in pyrolysis from one temperature to other was very small (0.41 ± 0.007 MJ/kg_{Biomass}); for gasification, the value was 0.83 ± 0.014 MJ/kg_{Biomass}. This was due to the fact that the energy values of products were higher when CO₂ was used as a gasification agent: consequently, the exergy value would be higher. For both test pyrolysis and

gasification, the exergy destruction rate increased as temperature increased. Comparing both setups, more exergy was destroyed when pyrolysis took place than with gasification. The values were close from one experiment to the other. At 800°C, 3.01 ± 0.05 MJ/kg_{Biomass} was destroyed for pyrolysis, while for gasification it was 2.90 ± 0.05 MJ/kg_{Biomass}. At 900°C for pyrolysis, 3.21 ± 0.05 MJ/kg_{Biomass} was destroyed, and for gasification 3.20 ± 0.05 MJ/kg_{Biomass}: the difference interval was very close at this temperature. This showed that as temperature increased, the exergy destruction rate of gasification increased faster than pyrolysis, while pyrolysis products showed higher irreversibilities than gasification.

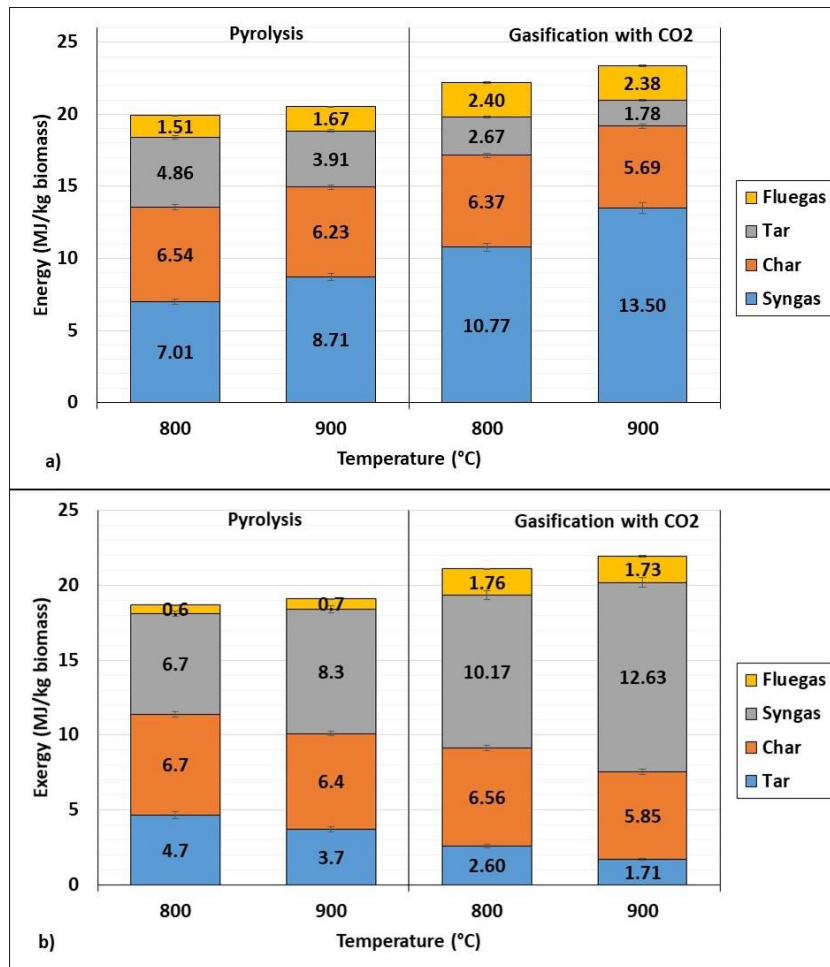


Figure 4.7. Energy a) and exergy b) products distribution for pyrolysis and gasification with CO₂ at 800°C and 900°C.

2.1 Comparison of pyrolysis and gasification with CO₂ of biomass in terms of energy and exergy rate of products

Biochar

As the conversion of biochar was influenced by the presence of the gasification agent, higher energy values of biochar were observed for pyrolysis. This was due to its inferior conversion

in pyrolysis than gasification. At 800°C and 900°C, values were 6.54 ± 0.11 and 6.22 ± 0.10 MJ/kg_{Biomass} for the pyrolysis case and 6.37 ± 0.11 and 5.69 ± 0.10 MJ/kg_{Biomass} for gasification for the respective temperatures. Generally, as temperature increased, the energy value of the output biochar stream decreased. In pyrolysis, for a reduction in the mass balance of biochar yield of 1.1% from 800°C to 900°C, its energy was reduced by 0.32 ± 0.005 MJ/kg_{Biomass}. Comparing this value with gasification, which yielded a reduction of 2.2% for the respective temperatures, biochar energy was reduced by 0.68 ± 0.01 MJ/kg_{Biomass}. This evidences the high energetic value that non-conventional solid fuels represent.

The biochar exergy was reduced significantly when CO₂ was used as an agent, as CO₂ favours CO formation when the Boudouard reaction takes place. From 800°C to 900°C, the observed reduction for gasification was 0.71 ± 0.012 MJ/kg_{Biomass}, whilst for pyrolysis it was 0.33 ± 0.005 MJ/kg_{Biomass}. Despite this decrease in biochar exergy, it still represents between 33.51% and 36.0% (6.39 ± 0.11 to 6.73 ± 0.11 MJ/kg_{Biomass}) of the total product exergy for pyrolysis and 26.7% to 31.1% (5.85 ± 0.10 to 6.56 ± 0.11 MJ/kg_{Biomass}) for gasification.

Tar

As observed for biochar, tar energy and exergy values decreased with a temperature increase. This was clearly influenced by tar thermal cracking reactions. For pyrolysis, at the respective temperatures of 800°C and 900°C, tar energy decreased from 4.9 ± 0.08 to 3.9 ± 0.07 MJ/kg_{Biomass}, and from 2.7 ± 0.05 to 1.8 ± 0.03 MJ/kg_{Biomass} for gasification. The values of tar energy for pyrolysis represent between 19.4% and 24.4% of the total energy distribution of the products. These values are considered a negative point for the thermal conversion process, where syngas is needed as the principal energy stream. On the other hand, in gasification, tar only represented from 12.0% to 7.6% of the total energy of products. Generally, a lower tar energy rate was obtained from CO₂ gasification than from pyrolysis because of dry reforming reactions between tar compounds and CO₂, potentially leading heavy molecules of tars to be decomposed into light hydrocarbons, as was expressed in literature [164], [165]. The authors described the increase in the tar decomposition reaction rate as CO₂ was used as a reformer, testing tar model molecules such as benzene and toluene. The results showed that these molecules with CO₂ lead to the formation of CO and H₂, evidencing the influence of CO₂ in tar cracking.

For pyrolysis, at 900°C, tar energy was 3.91 ± 0.07 MJ/kg_{Biomass} and its exergy value was 3.71 ± 0.06 MJ/kg_{Biomass} for an energy value of 0.2 ± 0.00034 MJ/kg_{Biomass}. For gasification, the energy value for this stream was approximately 0.07 ± 0.001 MJ/kg_{Biomass}. This difference was due to the high content of tar present in pyrolysis compared to gasification. As a higher molar

content of compounds was present in a stream, higher entropy change was achieved for a given temperature, and so more irreversibilities were present.

Gases

In pyrolysis, it was observed at 800°C that 7.0 ± 0.12 MJ/kg_{Biomass} were contributed by the syngas produced, while at 900°C, 8.7 ± 0.15 MJ/kg_{Biomass} were contributed. In the case of gasification with CO₂, 10.7 ± 0.18 to 13.5 ± 0.23 MJ/kg_{Biomass} were noted for 800°C and 900°C, respectively. For power generation purposes, the syngas obtained from gasification with CO₂ gives higher energetic values than that obtained from pyrolysis. Generally, both temperatures for pyrolysis showed lower energetic values when compared with gasification, which can be explained by the fact that the use of CO₂ as an agent favoured tar and biochar conversion, which consequently increased the syngas energy value.

The energy and exergy distribution of the gas obtained from pyrolysis are presented in **Figure 4.8** and **Figure 4.9**, respectively. As was the case for gasification, CO and CH₄ present the highest energetic values for the gaseous components. Both energetic values increased as temperature increased. The energetic values of the C₂₊ and C₃₊ gases were very remarkable in the case of pyrolysis, where the values were all higher than the H₂ values, except for C₃₊ at 900°C. In comparison with gasification, only C₂₊ and C₃₊ values were higher for pyrolysis. All the other gases displayed higher values for gasification. The fact that C₂₊ and C₃₊ values were higher for pyrolysis showed that gasification was able to crack heavier molecules into lighter compounds [166], [167].

At 900°C, syngas from pyrolysis showed an anergy of 0.43 ± 0.007 MJ/kg_{Biomass}, while for gasification the anergy was 0.86 ± 0.01 MJ/kg_{Biomass}. This variance was due to the CO content difference for both setups: for gasification, it represented 67.4% of the total anergy of the stream (0.58 ± 0.01 MJ/kg_{Biomass}). The energy content of CO represents the major energy difference between both systems of syngas, knowing that the Boudouard reaction might increase the CO formation.

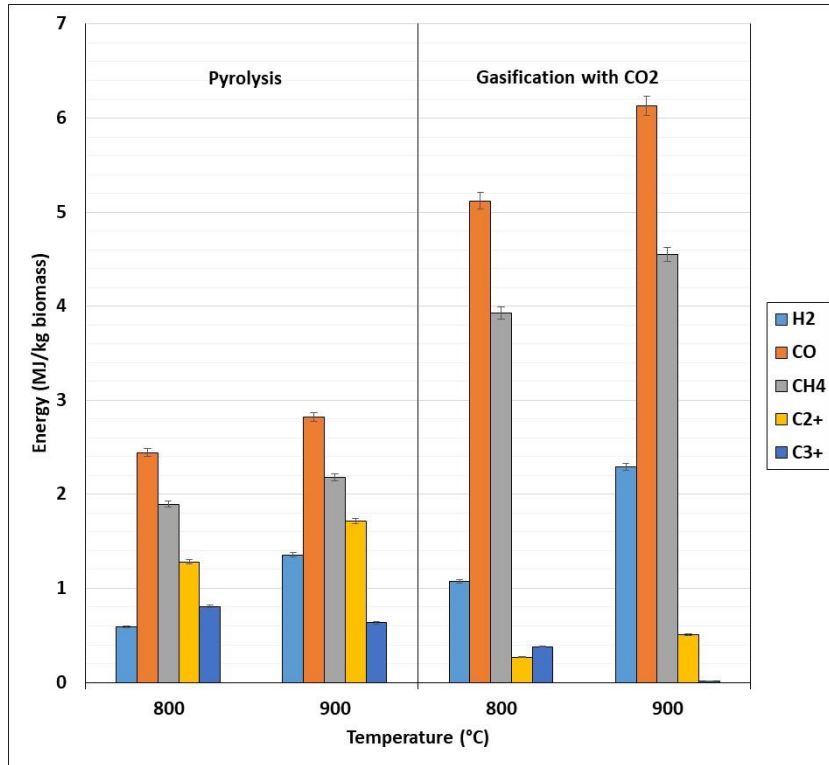


Figure 4.8. Energy distribution of syngas components for pyrolysis and gasification with CO₂ at 800°C and 900°C.

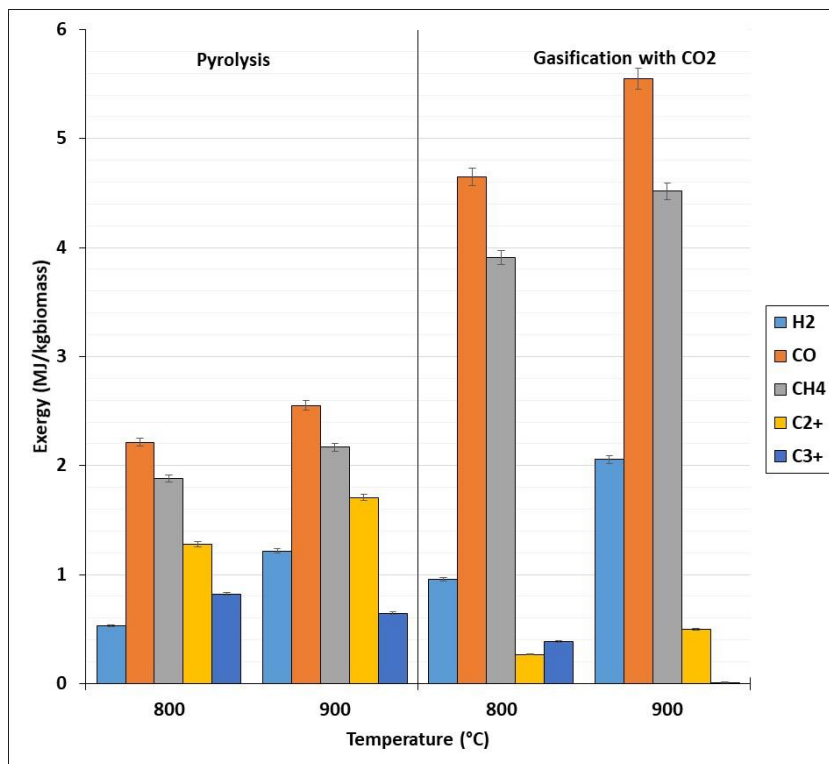


Figure 4.9. Exergy distribution of syngas components for pyrolysis and gasification with CO₂ at 800°C and 900°C.

2.2 Heat requirement

Figure 4.10 10 shows the values of the heat input for both setups compared with the amount of energy obtained from the syngas. The heat input needed for pyrolysis was lower than that needed for gasification for both temperatures. This is due to the fact that biochar conversion reactions are highly endothermic, and a higher amount of biochar was converted when using CO₂. The input heat for pyrolysis increased when temperature increased from 4.38 ± 0.07 to 4.98 ± 0.35 MJ/kg_{Biomass}; the same is true for gasification, but with higher impact, from 6.67 ± 0.11 to 7.80 ± 0.13 MJ/kg_{Biomass}. Atsonios et al. [35] reported that these values could be $\pm 15.5\%$ different from one process to another due to calculation uncertainty while calculating heating values for solid fuels. These results show that energetically, pyrolysis is more sustainable than gasification in terms of the required heat input, considering that exothermic and endothermic reactions took place in both processes. As gasification was an intermediate between pyrolysis and combustion, as was discussed before, the heat required for gasification can be considered as the accounted energy required for pyrolysis plus energy required for biochar conversion, which is considered highly endothermic.

The difference in heat input between pyrolysis and gasification was about 2.3 ± 0.04 MJ/kg_{Biomass} at 800°C and 2.8 ± 0.05 MJ/kg_{Biomass}, respectively, at 900°C. For gasification at 900°C, only 2.8 ± 0.05 MJ/kg_{Biomass} of heat input was needed to obtain a difference of 4.8 ± 0.08 MJ/kg_{Biomass} in syngas energy compared with pyrolysis. It can be deduced that gasification is indeed a better option than pyrolysis in energetic terms.

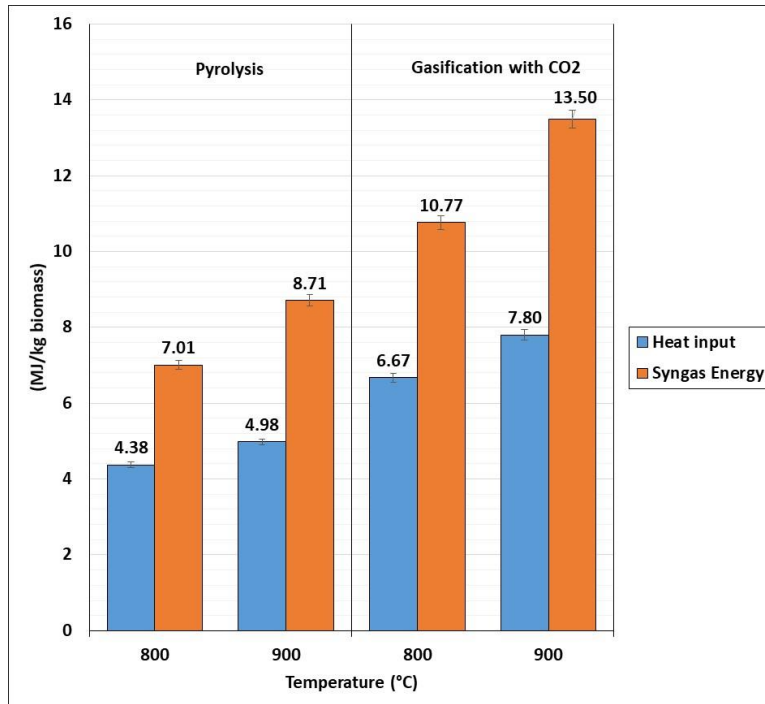


Figure 4.10. Heat for pyrolysis vs heat for gasification with CO₂ at 800°C and 900°C.

3. Steam and CO₂ gasification of biomass with biochar as a bed material

Biochar is frequently used as a bed material in order to catalytically crack the undesirable products of gasification. In this section, the energy balance and exergy evaluation of two gasification setups are analysed using CO₂ and steam as gasifying agents in a temperature range of 600°C to 900°C. The energy results obtained when CO₂ and steam were used are detailed in **Figure 4.11**. It must be noted that for all calculations of heat input, the energy of the gasification agent was not taken into consideration in order to normalize results and be able to compare them. The energy rate from the biomass was constant for all experiments. Comparing the tests, it may be observed that more energy was available in the products when using CO₂ than when using steam. At high temperatures, the energy difference became smaller because of similar energy values of the product streams.

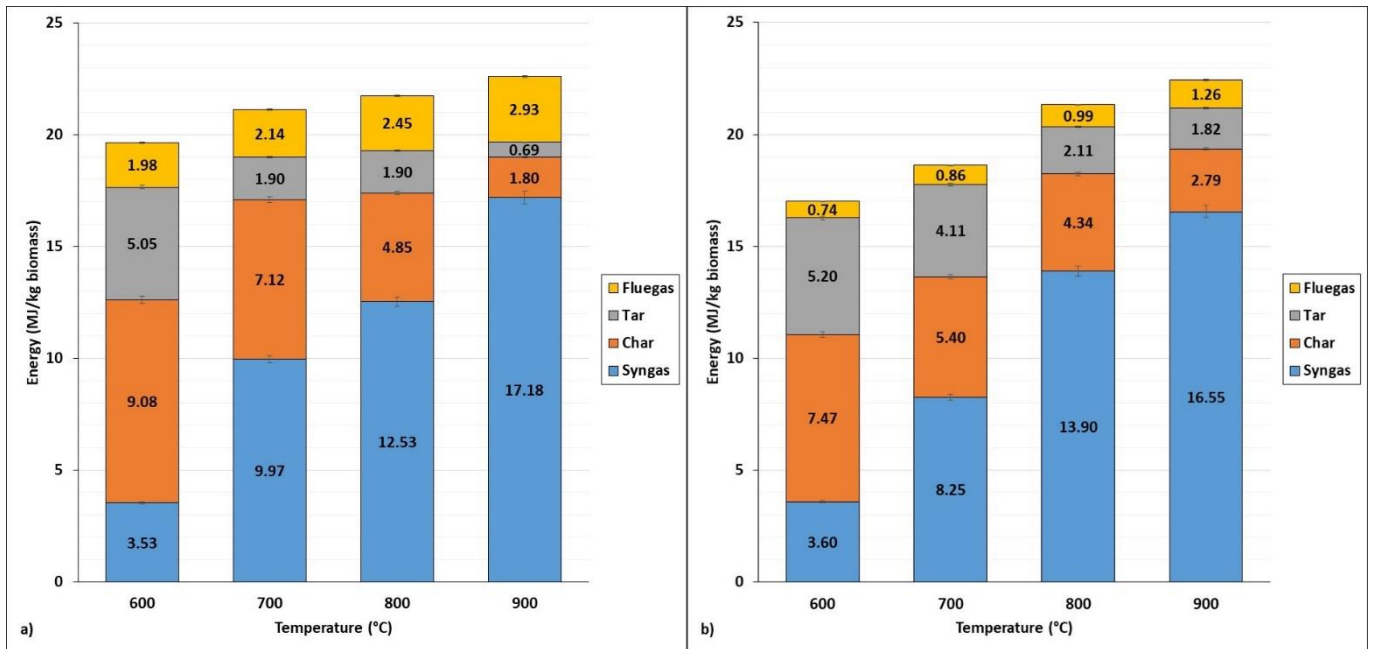


Figure 4.11. Energy distribution of products for a) CO₂ and b) Steam gasification with biochar bed.

Figure 4.12 illustrates the exergy results obtained for both gasification conditions. The exergy values were divided into chemical and physical exergy. The chemical exergy of products was between 10 and 22 times higher than its physical exergy, showing the potential of gasification products in engines for power generation. It can also be observed that from 700°C to 900°C, syngas represented the highest exergy of products.

Chapter 4

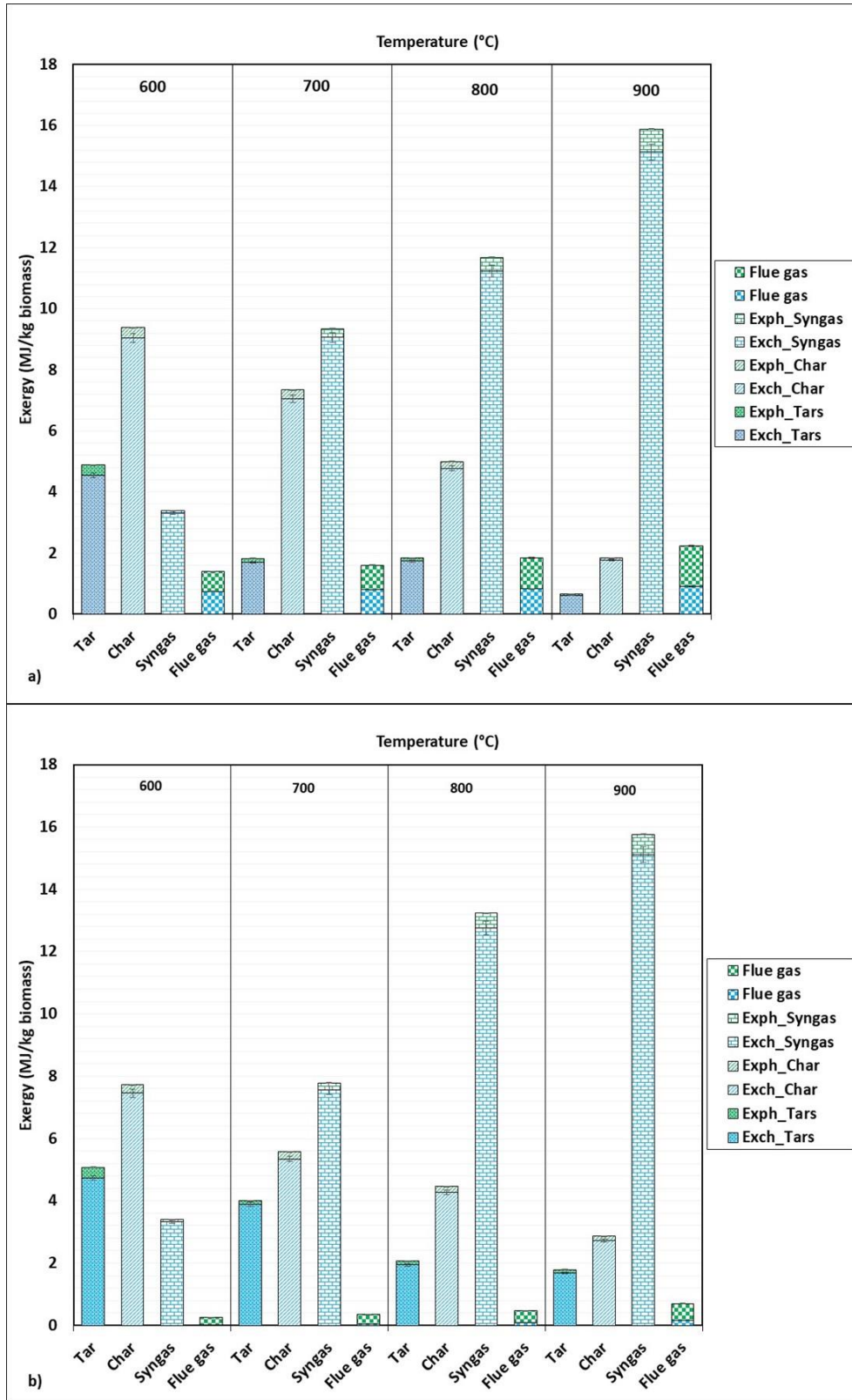


Figure 4.12. Chemical and physical exergy distribution of products for a) steam and b) CO₂ gasification with biochar bed.

Steam gasification showed lower exergy values of products (16.48 ± 0.28 to 20.24 ± 0.34 MJ/kg_{Biomass}) than CO₂ gasification (19.06 ± 0.32 to 20.37 ± 0.35 MJ/kg_{Biomass}). Despite these results, exergy destruction was higher for CO₂ gasification than for steam gasification (**Figure 4.13**). The exergy destruction rate increased as the temperature increased for both gasification agents. At 900°C, in CO₂ gasification, 3.75 ± 0.06 MJ/kg_{Biomass} were destroyed, while for steam gasification, this figure was only 3.08 ± 0.05 MJ/kg_{Biomass}: these values represent 15.38% and 12.71% respectively of the total inlet exergy to the process.

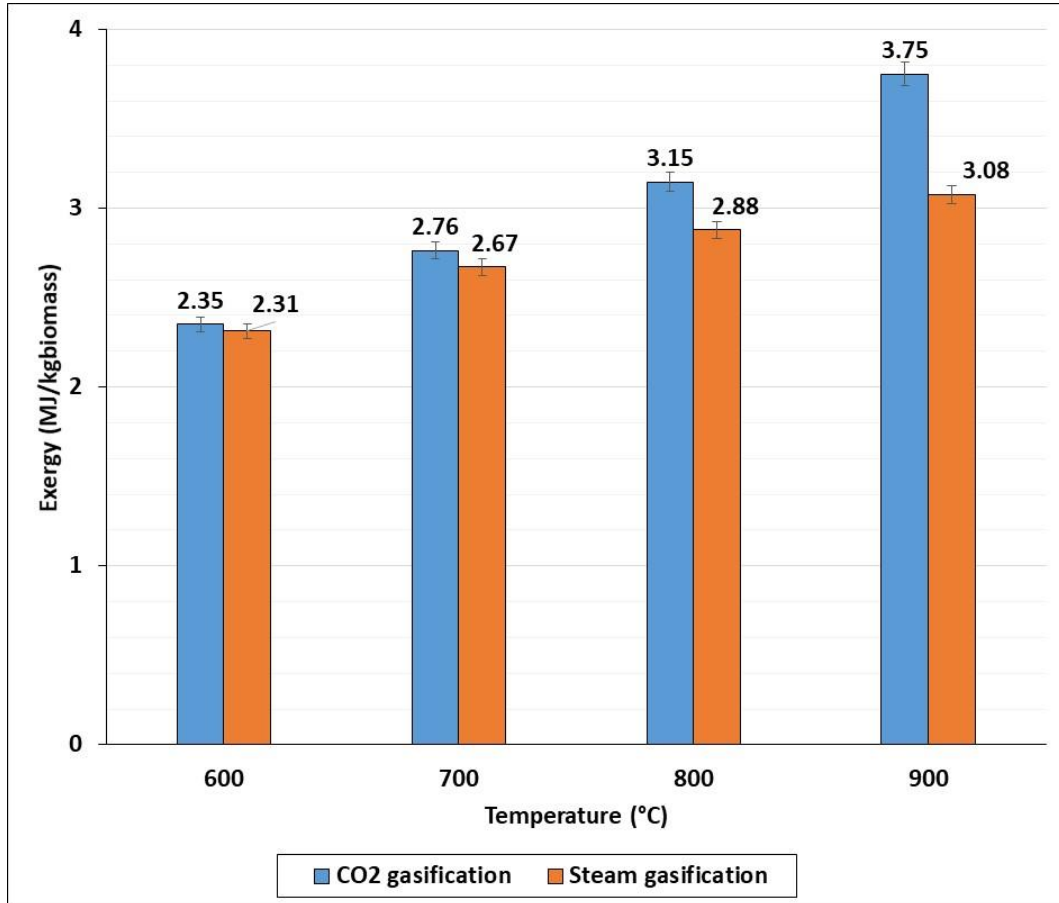


Figure 4.13. Exergy destruction for steam and CO₂ gasification with biochar bed.

3.1 Effect of varying gasification agent in terms of energy and exergy rate of products

Biochar

As illustrated in **Section 1** of this chapter, for gasification with CO₂ and steam, the energy and exergy of biochar were reduced as temperature increased as mentioned before **1** of this chapter. At 600 °C, the energy difference between both set-ups came mainly from the unconverted biochar, which represented around 9.1 ± 0.15 MJ/kg_{biomass} for CO₂ gasification and 7.5 ± 0.12 MJ/kg_{biomass} for steam gasification. As the temperature increased, steam gasification showed lower energy values of biochar, due to higher conversion that was

achieved using this agent. Only at 900°C, the conversion was lower for steam than for CO₂ gasification, by the fact, less biochar was converted with steam. Therefore, at temperatures between 600 and 800°C biochar energy with steam was 2.6 times higher, equivalent to 1.8 ± 0.03 MJ/kg_{biomass}.

The reactivity of biochar with steam was faster than with CO₂, and this could explain the fact that lower conversion was achieved with CO₂ compared to steam gasification [168], [169]. The reactivity of biochar depends on many factors such as temperature, porosity, presence of inhibitors, heating rate and others. Higher temperature increased reactivity for both steam and CO₂ gasification, while as the temperature increased, the difference in reactivity of the two gasification agents narrowed. At 900°C, there was strong production of H₂ in steam gasification: as hydrogen is known to be an inhibitor of biochar steam reforming gasification, it could be one reason for the lower conversion at 900°C compared to CO₂. Tar and hydrogen both provoke inhibition of steam gasification of char [170].

Tar

Steam and CO₂, besides their efficacy in biochar gasification, played an important role in biochar catalytic activity through cracking tar molecules. As the tar molecules' content was different for the cracking of tar over char with steam and CO₂, different tar energy and exergy values were provided. As could be observed for CO₂ gasification, the tar exergy varied from 4.89 ± 0.08 to 0.66 ± 0.01 MJ/kg_{biomass}, while for steam, it varied from 5.08 ± 0.09 to 1.79 ± 0.03 MJ/kg_{biomass} as temperature increased. For all temperatures, tar from steam gasification showed higher values than from CO₂ gasification. An explanation of this can be found by looking at the tar yield. The yield of tar was generally higher when steam was used as a gasification agent, despite tar concentration in some cases being lower in syngas with steam than with CO₂ gasification.

Gases

In the case of the flue gas stream, significant energy values were obtained (CO₂, H₂O and N₂); at 600°C, the energy rate was 2.1 ± 0.04 and 0.7 ± 0.01 MJ/kg_{biomass} for CO₂ and steam gasification, respectively. For all temperatures, the quantity of flue gas was higher when CO₂ was used as the gasification agent. The same was observed for the exergy values. The reason for this was the elevated CO₂ flow rate at the exit of the process, where physical exergy provided higher values than steam gasification.

For the syngas, at 600°C and 800°C, the exergy values from steam gasification were slightly higher than from CO₂ gasification. The opposite was noted at 700°C and 900°C: the exergy of the syngas with CO₂ was higher than with steam gasification. Parvez and colleagues [171]

also observed higher values of syngas coming from CO₂ gasification compared to conventional gasification (e.g. with steam) at high temperatures, but no clear explanation was given. As there was a strong conversion of tar molecules to light molecules (syngas) at 700°C, which significantly increased the syngas values, this could be the reason for the difference observed in the trend values.

The energy distribution of the gases in the syngas is shown in **Figure 4.14**. The syngas energy for gasification with CO₂ is mainly distributed in gas CO, which represents between 50% and 66% (1.80 ± 0.03 and 11.27 ± 0.19 MJ/kg_{Biomass}) of the total energy of the syngas. For steam gasification, it represented between 28% and 45% (4.78 ± 0.08 and 1.40 ± 0.02 MJ/kg_{Biomass}) and decreased as temperature increased. For steam gasification, gas product distribution was more variable: H₂ varied from 13.5% to 19.1% (0.49 ± 0.008 to 3.00 ± 0.051 MJ/kg_{Biomass}) and CH₄ from 32% to 39% (5.33 ± 0.09 to 1.40 ± 0.02 MJ/kg_{Biomass}) of the total energy value. For gasification with CO₂, the H₂ and CH₄ varied from 2.0% to 11.5% (0.07 ± 0.001 to 1.98 ± 0.03 MJ/kg_{Biomass}) and from 18.3% to 20.1% (1.83 ± 0.03 to 0.74 ± 0.01 MJ/kg_{Biomass}) of the total energy of the syngas. Comparing both gases' distribution, CO₂ gasification provided a mono-energetic product, in which the majority of the energy came from a single compound, CO. In the case of steam, a poly-energetic product was obtained, where no one component contained the majority of the energy.

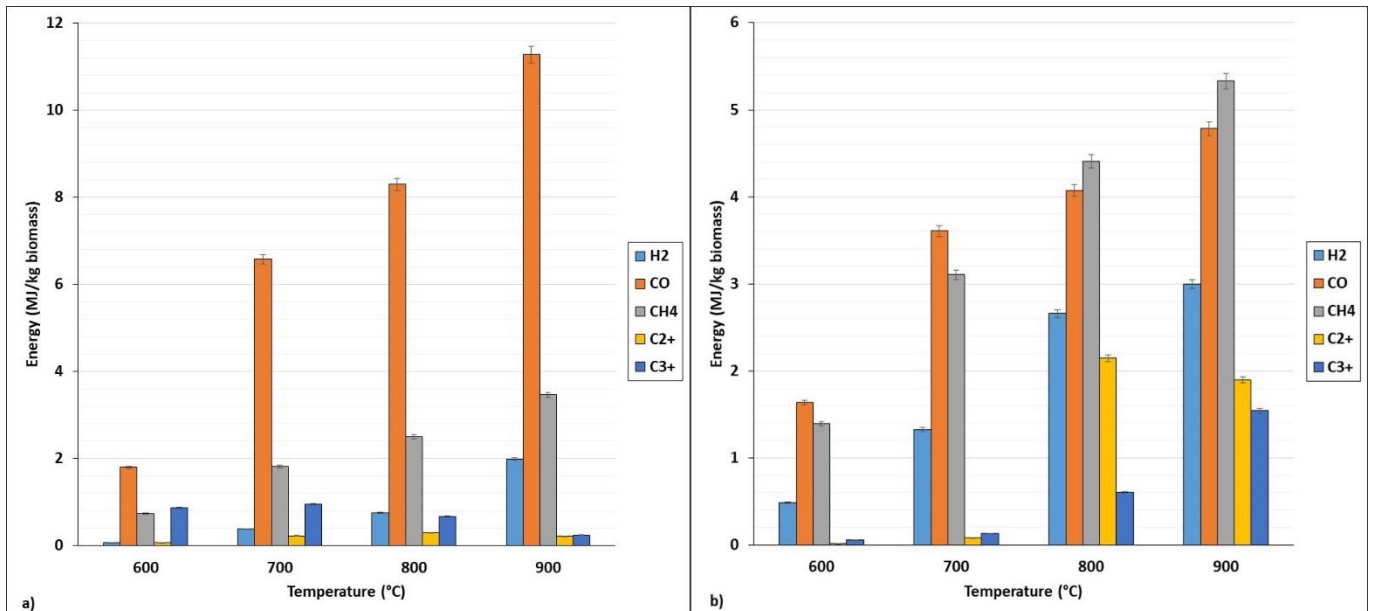


Figure 4.14. Syngas components energy distribution for a) CO₂ and b) Steam gasification with biochar bed.

Figure 4.15 illustrates the exergy distribution of the individual gas components of the syngas. It is observed that CO₂ gasification was primarily represented by CO exergy, while steam

gasification was represented by a mixture of H₂, CH₄ and CO. The exergy amount of CO obtained from CO₂ gasification (e.g. at 900°C, 10.22 ± 0.17 MJ/kg_{Biomass}) was between 1.1 and 2.4 times higher than the amount obtained from steam gasification (e.g. at 900°C, 5.29 ± 0.09 MJ/kg_{Biomass}). Meanwhile, H₂ with steam gasification was between 1.5 and 7.1 times higher than that from CO₂ gasification, proving the exergetic advantage of steam gasification in H₂ production. For the case of CH₄, looking at the exergetic average between steam and CO₂ gasification, it was about 1.7 times higher in the case of steam gasification, which might be due to the effect of methane formation reactions.

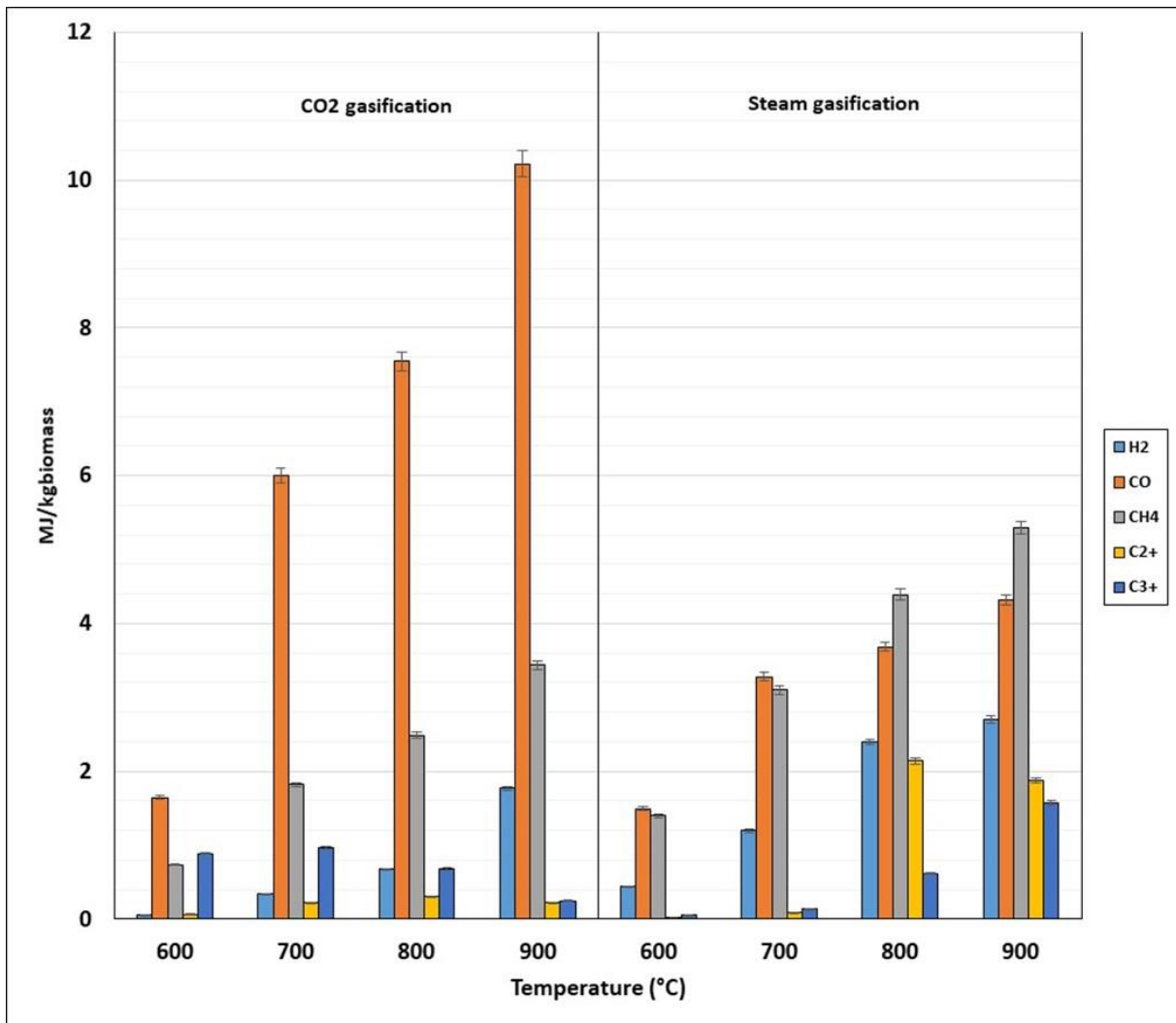


Figure 4.15. Syngas components exergy distribution for a) Steam and b) CO₂ gasification with biochar bed.

3.2 Heat requirement

Figure 4.16 shows the heat inputs for each setup. It can be seen that the heat input needed for gasification was higher when CO₂ was used as a gasification agent. For both cases, as temperature increased, the heat input also increased. At low temperatures, the difference was

larger between each setup. At 600°C, the difference was about 2.6 ± 0.04 MJ/kg_{Biomass}, while at 700°C, it was 2.5 ± 0.04 MJ/kg_{Biomass}. At 800°C and 900°C, the gap was closer: 0.4 ± 0.007 and 0.17 ± 0.003 MJ/kg_{Biomass}, respectively.

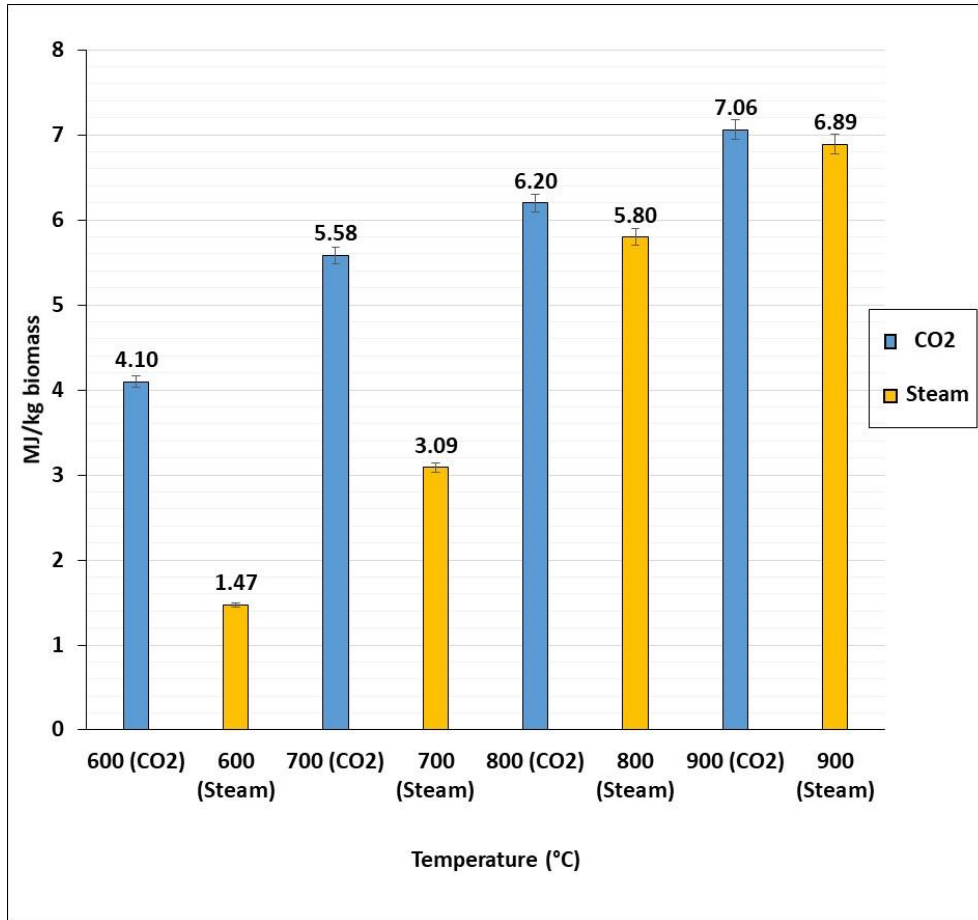


Figure 4.16. Heat input for steam and CO₂ gasification with biochar bed.

These results demonstrate that in catalytic cracking of tars at high temperatures, especially 900°C, with biochar as the bed material and CO₂ as the gasification agent, less tar will exit with the syngas. The latter will have a higher energetic value than the syngas produced with steam as the gasification agent. The additional heat input difference in these conditions will only be around 0.17 ± 0.003 MJ/kg_{Biomass}. Therefore, it is only at low temperatures, especially 600°C–700°C, that steam gasification is energetically favourable.

These differences in heat input can be explained by the fact that more exothermic reactions take place when steam is used as a gasification agent. There was a significant increase in methane formation and hydrogen. Both reactions—methane formation and water gas shift reactions—are known to be highly exothermic, and so a compensation of energy was provided from these reactions.

4. Thermodynamic efficiency

4.1 Cold gas efficiency- CGE

The results obtained for cold gas efficiency (CGE) using **Eq. 2.37**, for each studied configuration are shown in **Table 4.4** CGE was calculated taking only the biomass stream as the energy inlet [106]. This consideration showed the efficacy of the syngas as a function of the supplied biomass energy. As illustrated, CGE increased as temperature increased for all experiments, and similar trends have been obtained in literature for steam and CO₂ gasification [98], [101], [107], [171], [172]. For CO₂ gasification using sand as a bed material, the highest values of CGE, 0.63 and 0.78, corresponded to 800°C and 900°C, respectively. The CGE values obtained for pyrolysis were lower than those obtained for gasification when sand was used as the bed material. This means that when gasification was performed, the energetic contribution of the syngas provided better energy yields than pyrolysis.

Where biochar was used as the bed material, in order to catalytically crack tar, the CGE values were quite similar for the two configurations (CO₂ and steam gasification). At 600°C, the values were superposed at 0.21. At a temperature of 700°C, CO₂ gasification was superior, with 0.59, and at 800°C, steam gasification was superior, with 0.82. For the highest temperature, 900°C, the two values were close, although CO₂ presented a higher result of 0.99 and steam 0.97. CGE values closest to unity did not mean that all the energy available in the biomass was transformed into syngas. These values were obtained as the heat input was not considered in the calculations. It was for this reason that it was possible to have values close to unity or even higher, as reported by Renganathan et al. [107].

Table 4.4. LHV, cold gas efficiency (CGE), and exergetic efficiency ψ of syngas.

Experiment	Temperature (°C)	Bed material	LHV_{syngas} (MJ/kg _{Biomass})	CGE (ratio)	ψ (%)
Gasification with CO ₂	600	Sand	2.5 ± 0.04	0.16	11.9
	700		4.7 ± 0.08	0.30	23.9
	800		9.8 ± 0.17	0.63	42.4
	900		12.2 ± 0.21	0.78	50.3
Pyrolysis	800	Sand	6.5 ± 0.11	0.42	31.0
	900		7.9 ± 0.13	0.51	37.2
Gasification with CO ₂	600	Biochar	3.3 ± 0.06	0.21	15.8
	700		9.2 ± 0.16	0.59	40.8
	800		11.4 ± 0.19	0.73	49.7
	900		15.4 ± 0.26	0.99	65.2
Gasification with steam	600	Biochar	3.3 ± 0.06	0.22	18.1
	700		7.6 ± 0.13	0.49	38.2
	800		12.8 ± 0.22	0.82	57.2
	900		15.1 ± 0.26	0.97	65.1

4.2 Exergetic efficiency

Considering the useful part of the energy, the exergy efficiency was calculated for each experiment (**Table 4.4**). The exergy efficiency increased with temperature increase for all setups. For the test of gasification with CO₂ using sand as the bed material, an increase from 11.9% to 50.3% of syngas exergy efficiency was observed. This increase was principally due to the reduction of tar and biochar yielding to the formation of new gas molecules. As tar and biochar underwent cracking and gasification reactions, energy and exergy amounts were transferred to the syngas stream. Syngas LHV increased as a function of the temperature: at 900°C, a value of 12.2 ± 0.21 MJ/kg_{Biomass} was achieved, an increase of approximately 4.9 times the amount obtained at 600°C (2.5 ± 0.04 MJ/kg_{Biomass}).

Comparing gasification with CO₂ and pyrolysis when sand was used as the bed material, CO₂ gasification was more exergetically efficient than pyrolysis syngas. At the highest temperature of 900°C, 37.2% of the system exergetic efficiency came from syngas, which increased to 50.3% due to the presence of the CO₂ agent favouring biochar gasification and potentially tar dry reforming. As both tests were done under the same operating conditions with the variation of only the gasification agent, it can be said that pyrolysis or the devolatilization reaction increased the exergy efficiency by 13.1% if CO₂ was used as the agent. This increase of 13.1% of the total exergy efficiency of syngas came from the increase of CO and H₂ content, which represented approximately 60% of this variation.

The difference in the LHV obtained from pyrolysis compared to CO₂ gasification showed the advantage of the latter in energy terms. At 900°C, CO₂ gasification showed syngas LHV 54% higher than in pyrolysis, a difference of 4.3 ± 0.07 MJ/kg_{Biomass}. In addition, the exergy destruction was slightly lower for gasification than for pyrolysis. This shows without doubt the energetic advantage of gasification with CO₂ over pyrolysis, at the same time showing less exergy degradation in the global process. This can be attributed to the low variation of tar and biochar conversion with an inert atmosphere (N₂), contrary to the reactive atmosphere caused by the presence of CO₂.

In cases where biochar was used as the bed material, steam gasification showed higher syngas efficiency at 600°C and 800°C, while at 700°C, the efficiency of CO₂ gasification was higher. The latter was due to the fact that at 700°C there was a strong conversion of tar molecules to light molecules (syngas), which significantly increased the syngas values. At 900°C, the values were identical: 64% of the total exergy entering the system was recovered as syngas, proving that exergetically the processes were similar at this temperature.

The values of syngas exergy efficiency obtained were in the interval of the maximum exergetic values obtained for a gasification process of lignocellulosic biomass (71%) in the literature [110]. The lower heating value of syngas was also studied: as can be seen, LHV increased as the temperature was increased for each experiment with CO₂ and steam gasification. This was because the concentration of combustible gases (e.g. CO, H₂ and CH₄) increased significantly as thermal and cracking reactions took place. The highest value of LHV of syngas obtained came from CO₂ gasification at 900°C, with a value of 15.4 ± 0.26 MJ/kg_{Biomass}.

In steam gasification, more exergy was conserved at all temperatures, which indicates that steam gasification was exergetically more efficient at low gasification temperatures. As less exergy was destroyed with steam gasification, fewer irreversibilities were present in this configuration. Wang and colleagues [111], also detailed in their work the effect of temperature on irreversibilities, corroborating the behaviour found in this study.

Comparing steam and CO₂ gasification, no major differences were found in the LHV of gases: values were close from one experiment to the other. The potential use of the syngas provided could be a subject of interest to address the difference in LHV, as steam syngas was mainly formed by H₂ and CH₄, while CO₂ syngas was strongly influenced by CO. Increased LHV and the exergetic efficiency of syngas with the introduction of biochar as the bed material were also seen compared with sand as the bed material. This was due to the cracking reactions of heavy molecules such as naphthalene, toluene, indene, heavy poly-aromatics and other aromatic compounds that were reduced into lighter molecules.

The gasification experiments with biochar as the bed material showed an increase from 15.8% to 65.2% in exergetic efficiency. Comparing this to experiments where sand (11.9% to 50.3%) was used, a clear increase in syngas exergy efficacy can be observed. The use of biochar not only upgrades syngas quality by reducing its tar concentration rate to 5.73 g/Nm³, but also increases its exergetic value. This shows biochar's potential in exergy analyses, as evidenced by a significative positive change in energy and exergy values.

5. Conclusion

The following conclusions are established from the results obtained from the thermodynamic study of biomass gasification in a pilot lab-scale fluidized bed reactor with variation of the operating temperature, gasification agent and bed material.

- An increase in temperature increased the syngas energetic value. For CO₂ gasification, syngas energy increased from 2.7 ± 0.05 to 13.5 ± 0.23 MJ/kg_{Biomass} when temperature varied from 600°C to 900°C.
- The syngas energy increase was due to the conversion reactions of biochar and tar. As biochar and tar yield were reduced due to gasification and cracking reactions, their energy was transferred to the syngas.
- Gasification with CO₂ using sand as the bed material showed that total product exergy increased with the increase of temperature. The exergy destruction increased as temperature increased, from 1.94 ± 0.03 MJ/kg_{Biomass} at 600°C to 3.20 ± 0.05 MJ/kg_{Biomass} at 900°C. This exergy destruction is referred to as irreversibilities.
- Syngas from gasification with CO₂ provided better energetic values than high-temperature pyrolysis. The syngas obtained from pyrolysis at 800°C and 900°C had energetic values of 7.01 ± 0.12 and 8.01 ± 0.14 MJ/kg_{Biomass}, respectively, compared to the syngas obtained from gasification with CO₂, where the values were 10.77 ± 0.18 and 13.50 ± 0.23 MJ/kg_{Biomass}, respectively, at the same temperatures.
- CGE values increased with temperature. Gasification with CO₂ showed better CGE values (0.63–0.78) than pyrolysis (0.42–0.51) at temperatures from 800°C to 900°C. Despite this, the heat input required to perform the thermochemical conversion was lower for pyrolysis (4.38 ± 0.07 to 4.98 ± 0.08 MJ/kg_{Biomass}) than for gasification (6.67 ± 0.11 to 7.80 ± 0.13 MJ/kg_{Biomass}). This was attributed to the Boudouard reaction which took place due to the use of CO₂ as a gasification agent.
- Exergy destruction was higher for pyrolysis than for CO₂ gasification. For example, at 800°C, the exergy destroyed was 3.01 ± 0.05 MJ/kg_{Biomass} for pyrolysis and 2.90 ± 0.05 MJ/kg_{Biomass} for gasification with CO₂. This means more irreversibilities were found in pyrolysis than in gasification.
- The change of bed material from sand to biochar boosted the syngas energy content for CO₂ gasification from 3.53 to 17.18 MJ/kg_{Biomass}, and for steam gasification from 3.6 ± 0.06 to 16.55 ± 0.28 MJ/kg_{Biomass}. This improvement was due to the more relevant cracking reactions of tar and biochar conversion.
- The presence of biochar as the bed material also increased the heat input required for gasification from 4.10 ± 0.07 to 7.06 ± 0.12 MJ/kg_{Biomass} for CO₂ gasification and from

1.47 ± 0.02 to 6.89 ± 0.12 MJ/kg_{Biomass} for steam. Also, less heat for gasification was required for steam gasification than for CO₂ gasification. This is explained by the energy contribution of exothermic reactions present in steam gasification, reducing the energy required.

- The CGE value ranges from 600°C to 900°C for CO₂ and steam gasification were very similar: the CO₂ gasification range was from 0.21 to 0.99, while steam gasification ranged from 0.22 to 0.97.
- The syngas exergetic efficiency of CO₂ gasification increased with the use of biochar as the bed material compared to the sand bed. At 900°C, it increased from 50.3% to 65.2% due to an increase in cracking reactions because of biochar presence.
- More exergy was destroyed when CO₂ was used as the agent compared to steam. Values of up to 15.4% of the total exergy entering the system were destroyed in the case of CO₂ gasification and around 12.7% for steam gasification.

After the thermodynamic evaluation of two of the most employed methods for thermochemical biomass conversion (pyrolysis and gasification), the advantageous influence of a biochar bed was observed in the gasification of biomass with CO₂, which resulted in one of the most efficient conversion processes thermodynamically. Hence, the following chapter focuses on performing a deeper investigation of the biochar and CO₂ gasification in a fluidized bed reactor with the aim of conducting parametric and kinetic modelling of this reaction.

Chapter 5:

**DEVELOPMENT OF A KINETIC MODEL OF BIOCHAR
GASIFICATION WITH CO₂**

Introduction

This chapter focuses on the development of a kinetic model for the gasification reaction of biochar with carbon dioxide. This model was developed with the objective to be integrated into the simulation process of biochar gasification to perform the energetic and exergetic evaluation of the overall gasification of biomass using a simulator, such as Aspen Plus. From the previous investigation into energy balance and exergy evaluation in **chapter 4**, it was observed that the use of CO₂ as a gasification agent showed a high energetic and exergetic density CO molecule which represented the majority of the syngas produced. In addition, the energetic and exergetic efficiency of CO₂ gasification was superior to high-temperature pyrolysis and very similar to the one obtained from steam gasification. These were some of the principal reasons for the selection of the reaction biochar-CO₂ to perform the kinetic model development. Also, the fact that the use of alternative ways to value CO₂ is highly encouraged in the scientific community in order to find a potential usage of this greenhouse gas.

Two investigations were undertaken in parallel: the development of a kinetic model in a Thermogravimetric analyser (TGA) and a fluidized bed reactor. The latter was carried out to investigate the potential differences that can be found in thermogravimetric set-up compared to a fluidized bed reactor when modelling biochar gasification. The kinetic study involved the variation of the CO₂ partial pressure (0.33 to 1 atm), temperature (800°C to 1000°C), and finally CO₂/C ratio (3.5 to 10.5). Three structural models were tested: shrinking core, volumetric and power-law.

The following results presented an error margin of approximately 3.3 % due to the experimental uncertainty and deviations. The errors surrounding the experimental tests were those found in deviation calculations after experiment repetitions, mass weighting, value rounding and equipment tolerance.

1. Effects of gasification temperature on biochar consumption

Temperature plays an important role in the Boudouard reaction and the formation of carbon monoxide. In this case, the Boudouard reaction is endothermic (**Table 1.2**) and is favoured by an increase in temperature [173], as the reaction equilibrium is varied due to the Van 't Hoff and le Chatelier laws. This principle claims that an increase in temperature partially moves the reaction equilibrium in the other direction, which increases its heat requirement. Following this principle, the reaction becomes more exergonic, meaning that the Gibbs free energy becomes more negative [174].

Figure 5.1 illustrates the gasification of biochar for both set-ups (TGA and FBR) from 800°C to 1000°C, with a partial pressure of 0.67 atm. For the TG analyzer, it can be observed that

as temperature increased the required biochar conversion time decreased. At 800°C and for a reaction time of 120 min, only 56% of the total biochar sample was able to be converted into CO molecules, evidencing the high heat requirements of the Boudouard reaction. Meanwhile, as temperature increased, the total conversion of biochar was reached at 32.9 min at 900°C, and 10.7 min at 1000°C. The same phenomena were observed in literature corroborating these findings [175], [176]; Therefore, the increase of temperature resulted in a shift of the reaction equilibrium, promoting the conversion of biochar samples. This statement was also proposed by Khuma et al. [177] who concluded that in gasification as described by the Arrhenius equation, temperature increase favored faster reaction kinetics.

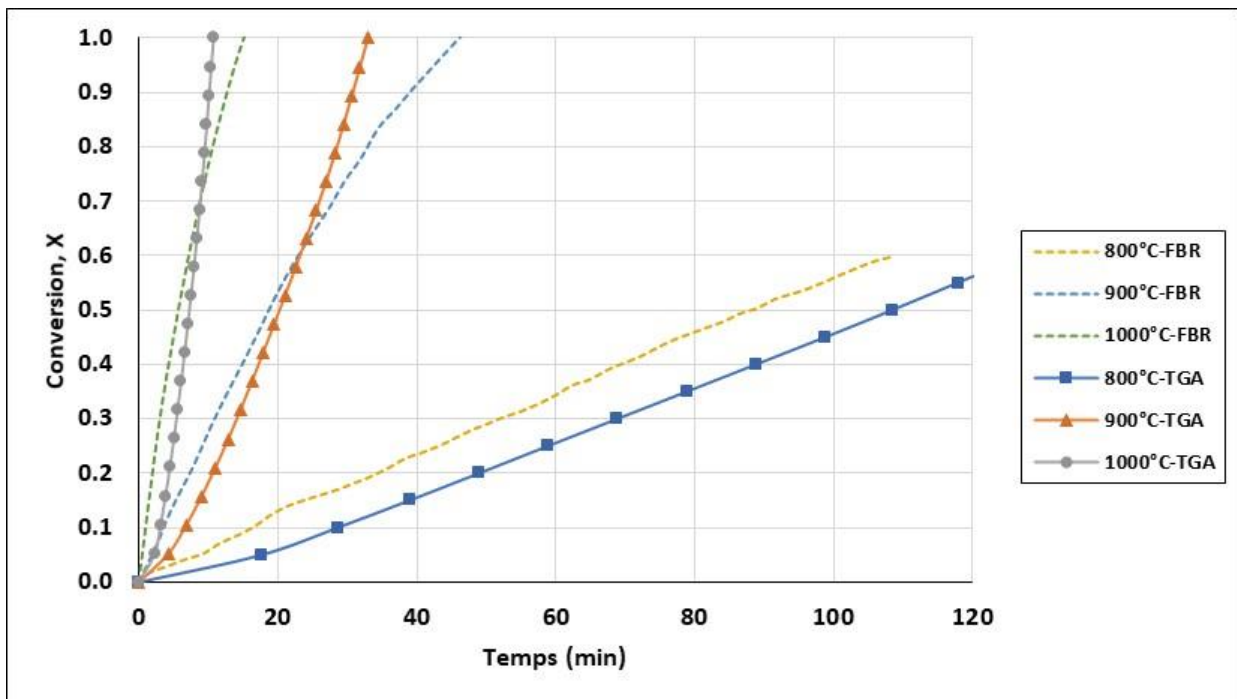


Figure 5.1. Comparison between TGA and FBR results. Effect of reaction temperature on biochar conversion: pressure 0.67 atm and CO₂/C ratio 7.05.

For the case of the fluidised bed gasifier, as it was illustrated for the TG analyzer, temperature favored the biochar conversion when it was increased. At 800°C, a conversion of 60% was achieved for a reaction time of approximately 110 min. Whereas for 900°C and 1000°C, the time required for total conversion decreased to 46.5 and 17.1 min, respectively.

Comparing both set-ups, it was seen that at 800°C, the fluidised bed reactor showed a more rapid conversion curve than the one obtained from the TGA reactor. Fluidised bed reactors have better mixing conditions than TG analyser (which might be considered to be a fixed bed reactor), and hence, external heat and mass transfer limitations could, potentially, be less affected in FBR than in the TG analyser. Meanwhile, at 900°C and 1000°C, it can be seen that for the conversion of approximately 65-75% of biochar, the consumption curve of the FB

reactor of biochar intercepted the one obtained from the TG analyser, meaning that, over this conversion point, the conversion was faster in the TGA than in the FB reactor. This translated into a reduction of the biochar reaction rate in the FB reactor compared with the TG analyser. As in the fluidised bed reactor, a higher formation of CO was achieved in the first 5 and 20 min for 900°C and 1000°C, respectively, and this could have sequentially inhibited the reaction in the FBR than in the TGA. It is known that the presence of CO can inhibit the Boudouard reaction [178] according to the Langmuir–Hinshelwood mechanism.

In addition to this, Mueller et al. [134] compared the gasification rates for TGA and FBR using the same conditions for wood biochar as in this study. The authors also observed an interception of the FBR and TGA conversion curves at higher conversion values (between approximately 75 and 90%), claiming that the mixing advantages of FBR became less significant with the increase of conversion. Moreover, it was also expressed that the gasification rate maximum was achieved faster with the FB reactor than with TG analyser, as was observed in our work. Zeng et al. [179] also claimed that the maximum gasification reactivity was achieved quicker with a fluidised bed gasifier than with a thermogravimetric analyser. The fact that, for this study, the interception of both curves was achieved at lower conversion rates could be due to the delay in gas-chromatography detection time. For this study, each FBR result was calculated every 2-3 minutes, contrary to other studies where more accurate equipment was used, such as FTIR (Fourier transform infrared) and real time-gas plot chromatography.

Another factor that could have influenced the consumption of biochar in the fluidized bed reactor is the agglomeration phenomena. This type of segregation phenomenon is generally present at high temperatures when alkali metals are present in biochar ash can fuse with sand to form agglomerates that can evoke defluidization and mass and heat transfer limitations [180]. Lardier et al. [181] observed that for lignocellulosic biochar the formation of silicates is generally reached at conditions below the temperature process, between 800°C and 1000°C [182]. This provokes an increase of the external mass transfer characteristic time for gasification, as the gas takes more time to interpenetrate the particle.

Figure 5.2 illustrates the gasification rate at a conversion of 50% for TGA and FBR for each tested temperature. It can be observed that as temperature increases the gasification rate increased for both set-ups as expected. By comparing TGA and FBR, it can be seen that at temperatures of 800 and 900°C, the difference between each set-up was slightly superior for FBR, compared to TGA. At 1000°C, the difference was more significant, as a gap of $19.7 \times 10^{-3} \text{ min}^{-1}$ (23%) was calculated between both set-ups. This evidenced the rapidity of biochar

conversion achieved with the mixing conditions of fluidised bed gasifiers compared to the TG analyser which emulated fixed bed gasifiers at a low scale.

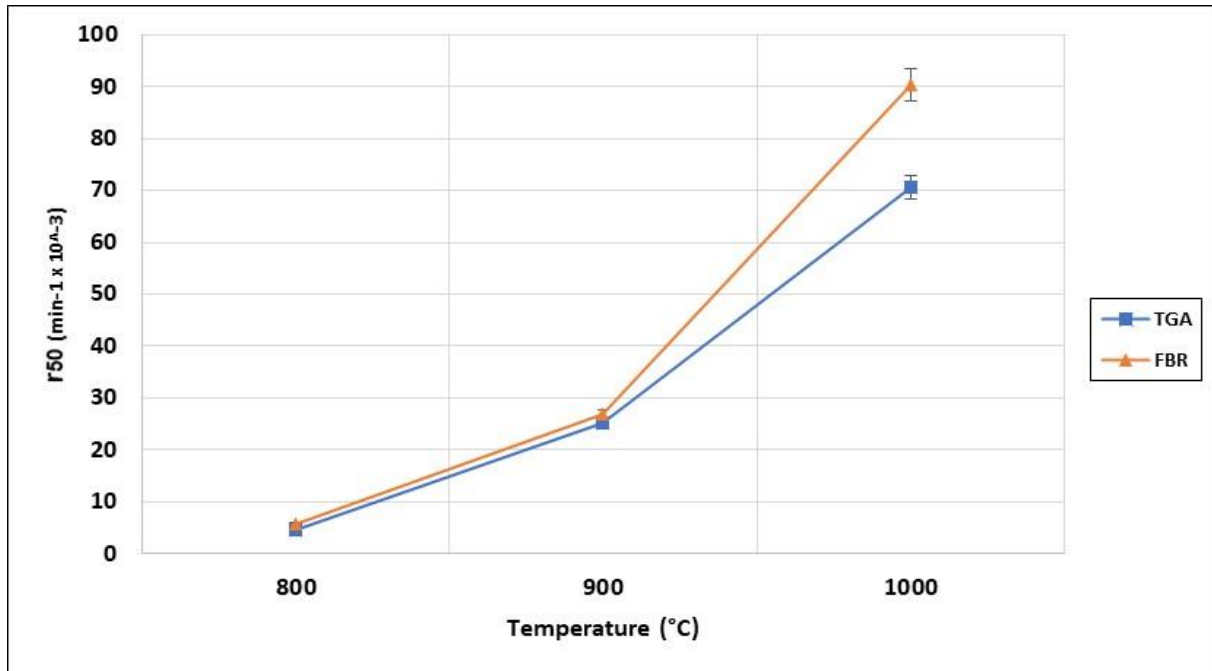


Figure 5.2. Effect of temperature on r_{50} for TGA and FBR: pressure 0.67 atm and CO_2/C ratio: 7.05.

2. Effect of partial pressure on biochar consumption

The effect of the partial pressure of CO_2 on biochar conversion was investigated for both set-ups. The CO_2 pressure was varied from 0.33 atm to 1 atm, in order to evaluate its influence on biochar consumption. **Figure 5.3** shows the effect of CO_2 partial pressure on the gasification rate of biochar. It can be seen that the variation of CO_2 pressure altered the reaction rate of the gasification of biochar. As the partial pressure of CO_2 was increased for both set-ups, the time required for the total conversion of biochar was reduced, resulting in a faster transformation of the biochar.

For the TGA, increasing the pressure from 0.33 atm to 1 atm reduced the total conversion time from 13.21 min to 8.21 min. Meanwhile, for the fluidised bed gasifier, conversion time was reduced from 23.71 min to 9.02 min. The increase of partial pressure favoured the conversion of biochar into CO , as the reaction velocity is increased. In the case of the Boudouard reaction, it would favour the formation of CO . Another explanation could be the fact that increasing CO_2 pressure, provokes a higher concentration gradient, which forces the agent to enter the biochar pores faster and favoring the heterogenous reaction, Sajjadi et al. [183] compared this phenomenon to the bulk diffusion.

Comparing the results for the TG analyser and FBR reaction, it can be observed that the same behaviour that was commented on **Section 1** of this chapter was also observed here. The results obtained from the FBR showed a faster gasification rate than TGA, under conversion values of approximately 70% to 95%. The maximum of the gasification rate in the FBR could have been achieved faster than TGA (also due to the high production of CO) and, consequently, a potential reaction inhibition could have been taking place, which resulted in the reduction of the reaction rate in the FBR. Also, the presence of agglomerations in FBR could have favored the increase of diffusional limitations.

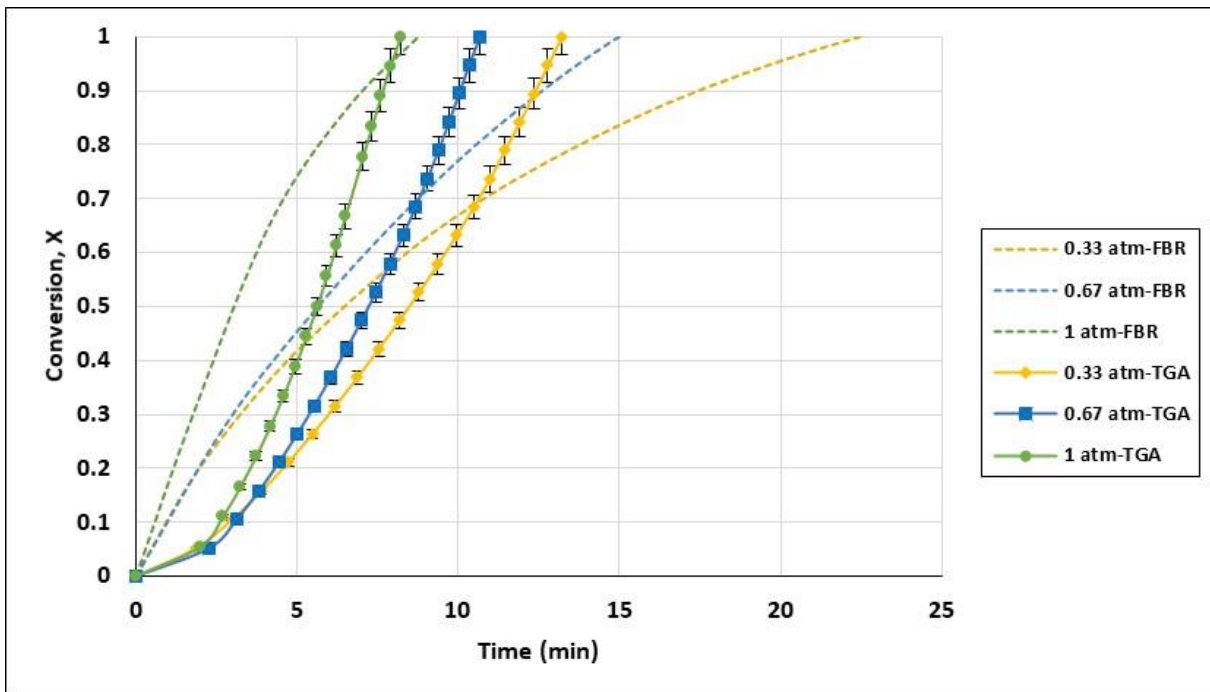


Figure 5.3. Comparison between TGA and FBR. Effect of CO₂ partial pressure on biochar conversion: Temperature 1000°C and CO₂/C ratio 7.05.

The reaction rate was also evaluated for both set-ups, at a biochar conversion of 50%. **Figure 5.4** shows the evaluation of increasing the partial pressure of CO₂. As can be observed, both for TGA and FBR, the gasification rate was increased with an increase in the partial pressure of CO₂ in the volumetric flow entering the reactor. For the TGA, it was increased from 60.0 to 89.0 x 10⁻³ min⁻¹, varying gasification agent pressure from 0.33 atm to 1 atm. For the case of the FB reactor for the same interval, it varied from 76.3 to 157.4 x 10⁻³ min⁻¹. As can be seen, at this point, the fluidised bed gasifier showed a higher reaction rate than the TG analyzer due to better heat and mass transfer conditions.

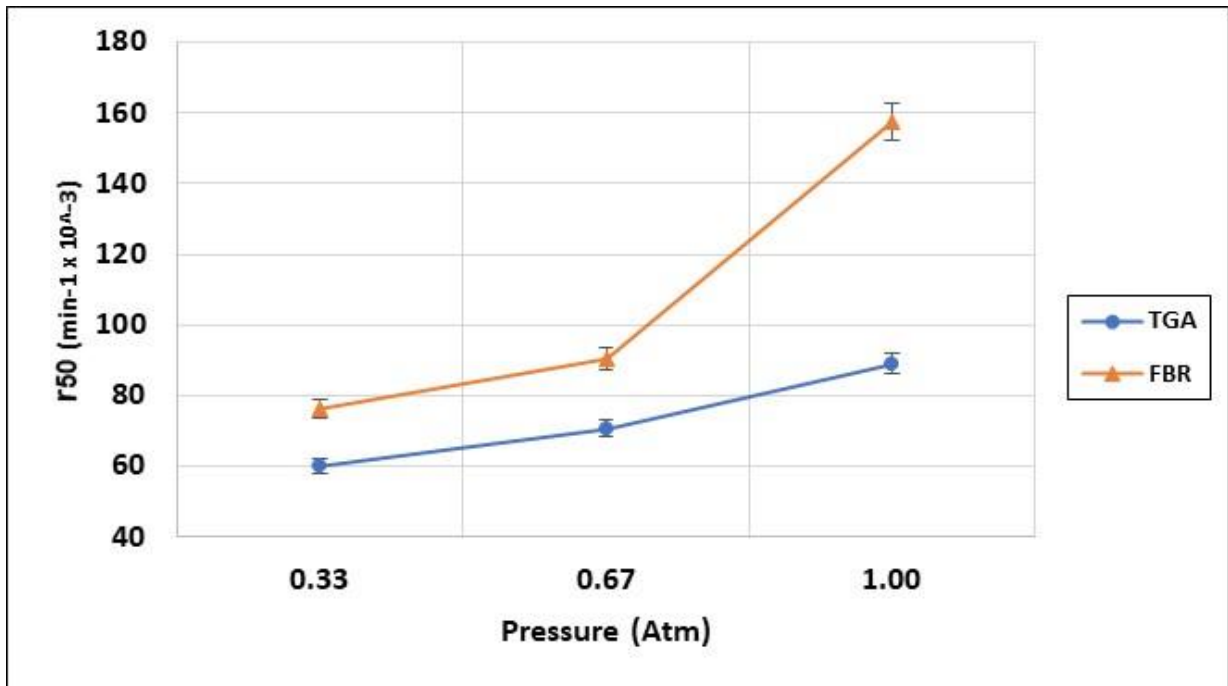


Figure 5.4. Effect of the partial pressure of CO₂ on r_{50} for TGA and FBR: Temperature 1000°C and CO₂/C ratio 7.05.

3. Effect of CO₂/C ratio on biochar consumption

The effect of the molar ratio of carbon dioxide to char is evaluated in the following section. Three ratios were selected for this study (3.50, 7.01 and 10.50), representing the common CO₂/C ratios used in char gasification in TG analysers. The CO₂/C ratio was calculated by fixing the amount of char, 7 mg for TGA and 100 mg for FBR and varying the gasification agent flow rate from 50 to 150 mL/min for TGA and from 713 to 2142 mL/min for the FBR, at a temperature of 1000°C. It is worth noting that this study was only focused on evaluating the effect of the volumetric flow of CO₂ over biochar conversion in the TG analyzer and to compare the results with the fluidized bed reactor with the same ratio and conditions.

Figure 5.5 shows the effect of CO₂/C in the TGA at 1000°C. It can be seen that by increasing the CO₂/C ratio, which meant an increase in the CO₂ flow rate, speeded up the total conversion of biochar. For a CO₂/C ratio of 3.5, the required time to convert all biochar into syngas was 15.15 min, by increasing this molar ratio to 10.5 the required time was reduced to 9.1 min. As can be observed, increasing the gasification ratios favoured the conversion of biochar into CO. Higher CO₂ rates increased the removal of products from the reaction zone and carried the reaction forward, favouring CO formation [184]. Due to the fast removal of CO in the reaction, less inhibition of the Boudouard reaction took place, and it boosted the formation of new CO molecules, hence biochar conversion rates increased. The same behaviour was observed in the FBR, corroborating the TGA results.

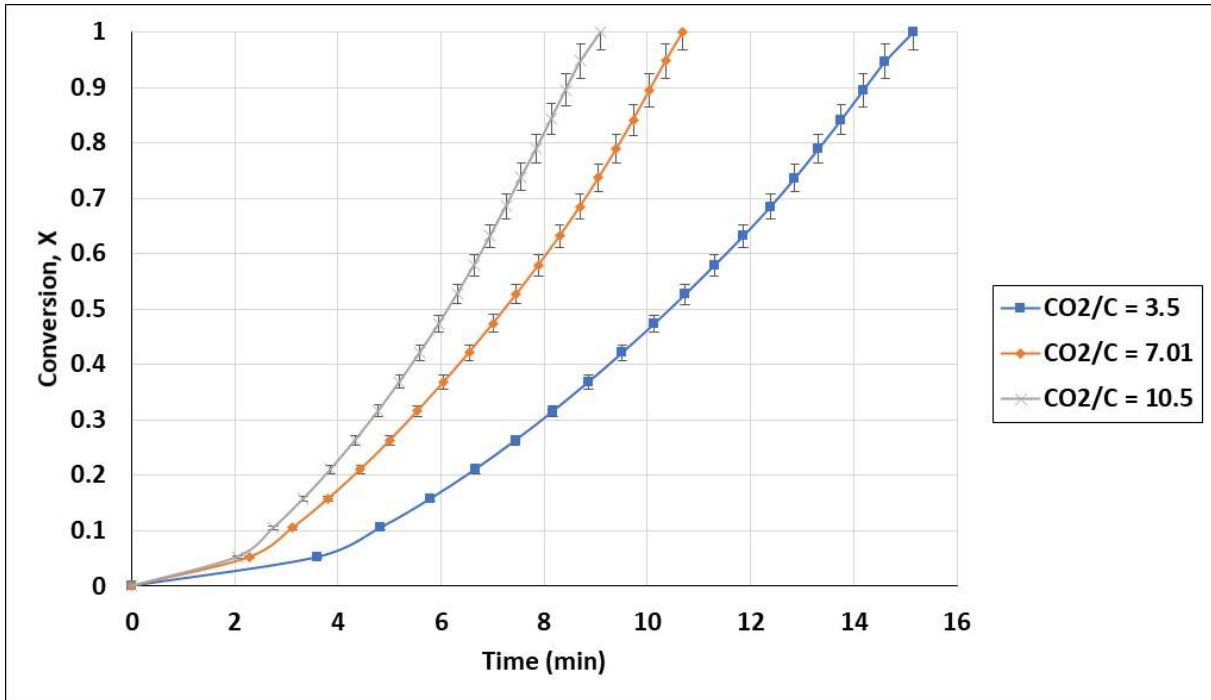


Figure 5.5. Effect of CO₂/C ratio on biochar conversion for TGA: Temperature 1000°C and pressure of CO₂ 0.67 atm.

4. Development and selection of the kinetic model.

The kinetic study of the heterogeneous reaction between biochar particles and CO₂ is generally based on the single-step equation, where the reaction rate of gasification or the variation of biochar conversion with time, is expressed as:

$$r = dX/dt = k(T)P_{CO_2}^n f(X) \quad \text{Eq. 5.1}$$

Where $k(T)$, P_{CO_2} , and n are the apparent reaction rate constant (which is temperature-dependent), CO₂ partial pressure and reaction order, respectively. The variable $f(X)$ represents a function that is dependent on the biochar conversion mechanism, which describes the evolution in chemical or physical profiles throughout the heterogeneous reaction.

The reaction rate constant $k(T)$ is evidenced in the literature [185] as being temperature dependent on the reaction, hence it can be replaced in the Arrhenius equation, as follows:

$$k(T) = A_0 \exp(-E_a/RT) \quad \text{Eq. 5.2}$$

Where A_0 , E_a , R and T are the pre-exponential factor, activation energy, the universal gas constant and the reaction temperature, respectively.

Substituting **Equation 5.2** into **Equation 5.1**, turns the final equation into,

$$r = dX/dt = A_0 \exp(-E_a/RT) P_{CO_2}^n f(X) \quad \text{Eq. 5.3}$$

The resultant equation represents the gasification reaction rate as a function of the biochar conversion. The dependent conversion function $f(X)$ can be represented by different mathematical models. The selection of $f(X)$, is to a certain degree arbitrary and convoluted, as the evolution of biochar conversion depends on many factors, such as structure, porosity, physical and chemical properties, gasification agent and others. For this study, various models were tested in which three types were selected, according to the best fitting results obtained. The models used were: the volumetric model (VM), the shrinking core model (SCM) and the power law model (PLM).

4.1 Kinetic models studied

4.1.1 Volumetric Model (VM)

The volumetric model is based on the hypothesis that there is a quasi-homogeneous reaction throughout the char particles, in which the solid particle does not suffer any structural change during gasification. Hence **Equation 5.3** can be modified as:

$$r = dX/dt = A_0 \exp(-E_a/RT) P_{CO_2}^n (1-X) \quad \text{Eq. 5.4}$$

4.1.2 Shrinking Core Model (SCM)

This model assumes that the heterogeneous reaction is taking place on the surface of the particle, which is considered spherical and moves progressively to the centre of the solid [125]. At the end of the reaction, an ash layer is left in the reactor, evidencing the complete consumption of the carbonaceous matter. By substituting the kinetic SCM into the gasification rate equation, it can be now expressed as:

$$r = dX/dt = A_0 \exp(-E_a/RT) P_{CO_2}^n (1-X)^{2/3} \quad \text{Eq. 5.5}$$

4.1.3 Power-law Model (PLM)

The power-law models are purely empirical mathematical correlations that have a non-defined physical meaning. These models are generally used in order to account for the biochar conversion profiles that conventional models such as (volumetric, shrinking core, random pore and other models) are not able to describe. Hence, power-law models provide an adapted reactivity evolution of heterogeneous reactions [186]. The function $f(X)$ for power-law models can be expressed as:

$$f(X) = aX^b \quad \text{Eq. 5.6}$$

Where a and b represent the coefficient and exponential order of the power-law model that can be found empirically.

Substituting **Equation 5.6** into **Equation 5.3**,

$$r = dX/dt = A_0 \exp(-E_a/RT) P_{CO_2}^n aX^b \quad \text{Eq. 5.7}$$

Volumetric and shrinking core models are known as decelerator models, which represent a decrease in the reaction rate with the conversion. Meanwhile, power-law models do not have defined paths, they can be decelerator as well as very rapid models determined by mathematical fitting with the gasification rate.

A common practice for the selection of kinetic models for heterogeneous reactions between solid particles and gaseous components is the mathematical evaluation of the experimental reaction rate curve. **Figure 5.6** shows an adaptation of the reaction models for solids in isothermal conditions presented by Vyazovkin et al. [136]. It can be observed that each kinetic model represents a different curve form. Hence, by associating the gasification rate curve of experiments with the proposed mathematical models can facilitate the selection and definition of kinetic models for solid decomposition.

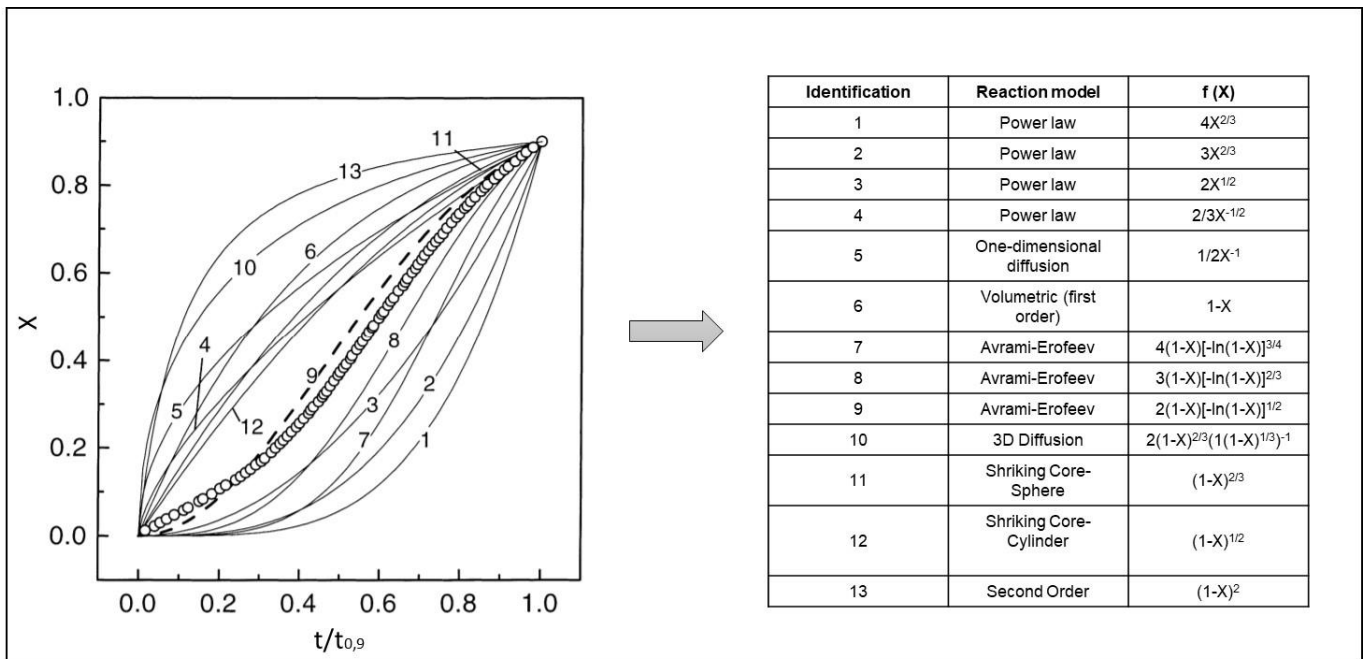


Figure 5.6. Reaction models data plots in reduced times for isothermal solid conversion (adapted from Vyazovkin et al. [16]).

4.2 Kinetic model for TG analysis.

As previously mentioned, three functions f(X) were tested for the development of the most adapted kinetic model for TGA. The volumetric model $(1-X)$, the shrinking core model $(1-X)^{2/3}$, and finally, the power-law model $(5/3X^{-2/3})$. For the purpose of determining the order of the reaction, the natural logarithm was applied to **Equation 5.1**.

$$\ln r = \ln k (T) + \ln f (X) + n \ln P_{CO_2} \quad \text{Eq. 5.8}$$

The plot of $\ln r$ against $\ln P_{CO_2}$, fits to a line with $\ln k(T) + \ln f(X)$ and the reaction order n , obtained from the intercept and the slope, respectively. **Figure 62** shows the relation between $\ln r$ and partial pressure. As can be observed the coefficient of determination (R^2) averaged values of 0.98, showing that the obtained results were well predicted. Meanwhile, the reaction order varied slightly with conversion, between 0.38 and 0.41, hence an average value of 0.4 was selected. The selected order was in good agreement with the literature for char gasification in TG analysers [132], [187], [188]. The selection of only three points to determinate the tendency equation is a common practice employed in literature to develop kinetic models in gasification.

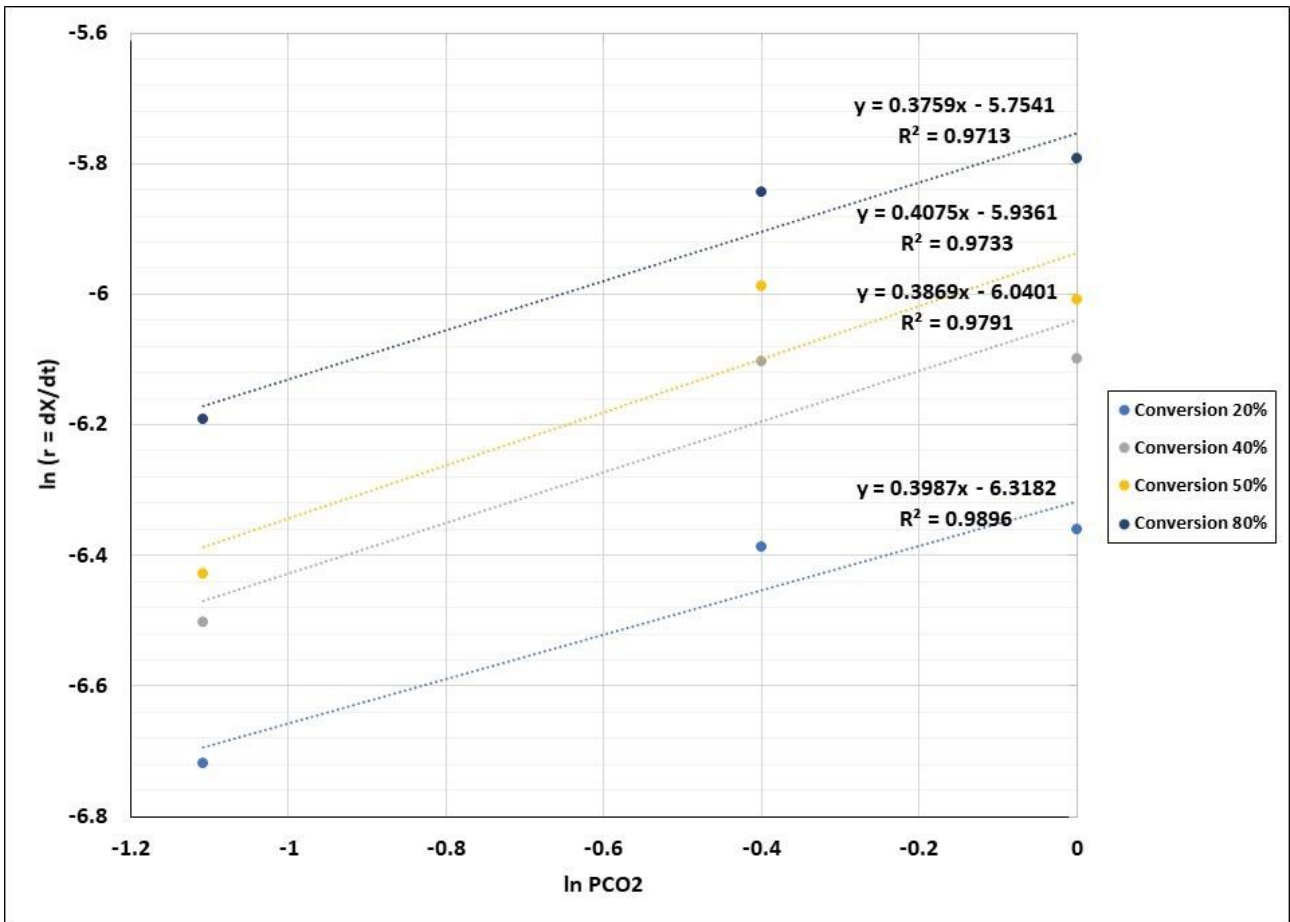


Figure 5.7. Fitting results between $\ln r$ and $\ln P_{CO_2}$, reaction order determination. Temperature 1000°C and CO_2/C 7.01.

Once the kinetic mechanism function of the biochar conversion $f(X)$ was defined, it was now the necessary to calculate the kinetic parameters of the model. In order to do this, the integral form of Equation 5.1 was employed to determine the kinetic parameter $k(T)$.

For the volumetric model:

$$-\ln(1-X) / t P_{CO_2}^n = k(T) \quad \text{Eq. 5.9}$$

For the shrinking core model:

$$1 - \ln(1-X)^{1/3} / t P_{CO_2}^n = k(T) \quad \text{Eq. 5.10}$$

and for the power law model:

$$X^{3/5} / t P_{CO_2}^n = k(T) \quad \text{Eq. 5.11}$$

Using the Arrhenius equation and applying natural logarithm at both sides of **Equation 5.2** gives:

$$\ln k(T) = \ln A_0 - E_a/R * 1/T \quad \text{Eq. 5.12}$$

The plot of $\ln k(T)$ against $1/T$, fits to a line where $\ln A_0$ and E_a/R were obtained from the intercept and the slope, respectively. **Figure 5.8** shows the plot of $\ln k(T)$ against $1/T$, for the power-law model. As can be observed, the values of E_a/R increased with the conversion; this phenomenon shows that the gasification rate decreased progressively, as discussed by Sun et al. [189]. It was explained that the slight increase of activation energy can be observed when char reactivity is gradually reduced, due to the fact that reactive sites decrease with the conversion.

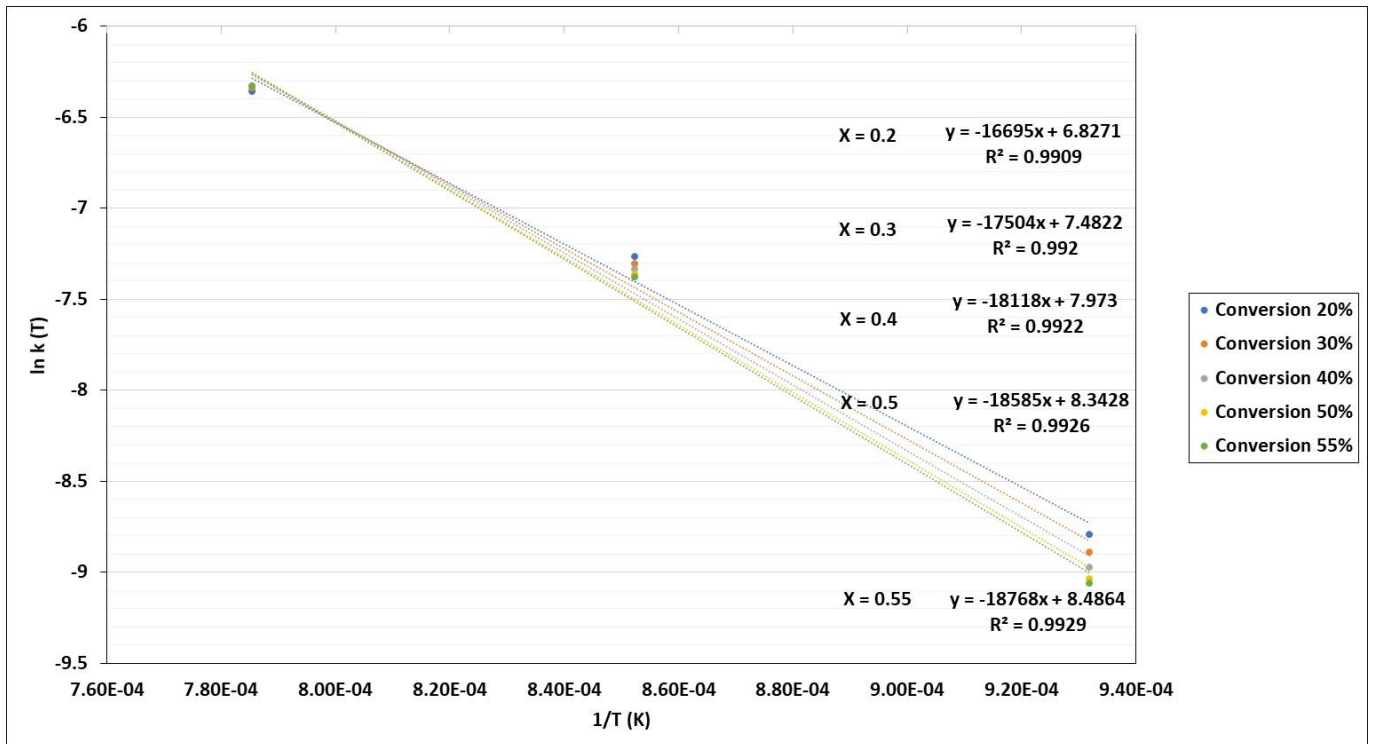


Figure 5.8. Fitting results between $\ln k(T)$ as a function of $1/T$: kinetic parameter determination for TGA. CO_2 pressure 0.67 atm and CO_2/C 7.01.

Table 5.1 shows the average values of the pre-exponential factor, activation energy and coefficient of determination obtained using the three kinetic models. As observed in the table, the values of the activation energy for the three selected models were almost the same, this was evidence that the performed calculations were correct. For all models, the amount of energy required to activate the reaction was invariable as this parameter is known to be independent of the kinetic model. On the other hand, the coefficient of determination (R^2) for VM and SCM was lower than the one obtained for PLM. This means that PLM model could potentially have better fitting results with the experimental results from the other models.

Table 5.1. Kinetic parameters obtained for each gasification model.

Kinetic Model	E_a (MJ/kmol)	A ($\text{atm}^{-n} \text{s}^{-1}$)	R^2
VM	157.12	5941.4	0.9237
SCM	156.61	4269.3	0.9301
PLM	155.74	4992.0	0.9930

Figure 5.9 shows the comparison conversion curves at temperatures from 800°C to 1000°C of biochar at a partial pressure of 0.67 atm, for all three tested models. As illustrated, the volumetric and shrinking core models were less accurate than the power-law model. The volumetric and shrinking models predicted that the biochar gasification rate decreased gradually between conversions of 40 and 60%. Meanwhile, when looking at the model curve, it can be observed that the model did not follow the predicted path of the results. For temperatures from 800°C to 1000°C, PLM was able to predict a very accurate path, very similar to the experimental results. The standard deviation of the PLM was between 8 and 9%, compared to the experimental values for the test evaluating the effect of temperature over biochar samples. For the case of varying the partial pressure variation at 1000°C, the PLM was able to predict the results with a standard deviation of between, approximately, 2.6 and 6.6%. More validation results of the PLM can be found in **Appendix A4**. The observed variations between the kinetic model and the experimental values might be due to the fact that the power-law model does not predict the structural degradation of biochar particles.

The final kinetic model for the thermogravimetric analyser according to PLM model can be illustrated by the following expression:

$$r \text{ (s}^{-1}\text{)} = dX/dt = 4992.0 \exp(-155.74/RT) P_{\text{CO}_2}^{0.4} (5/3X^{-2/3}) \quad \text{Eq. 5.13}$$

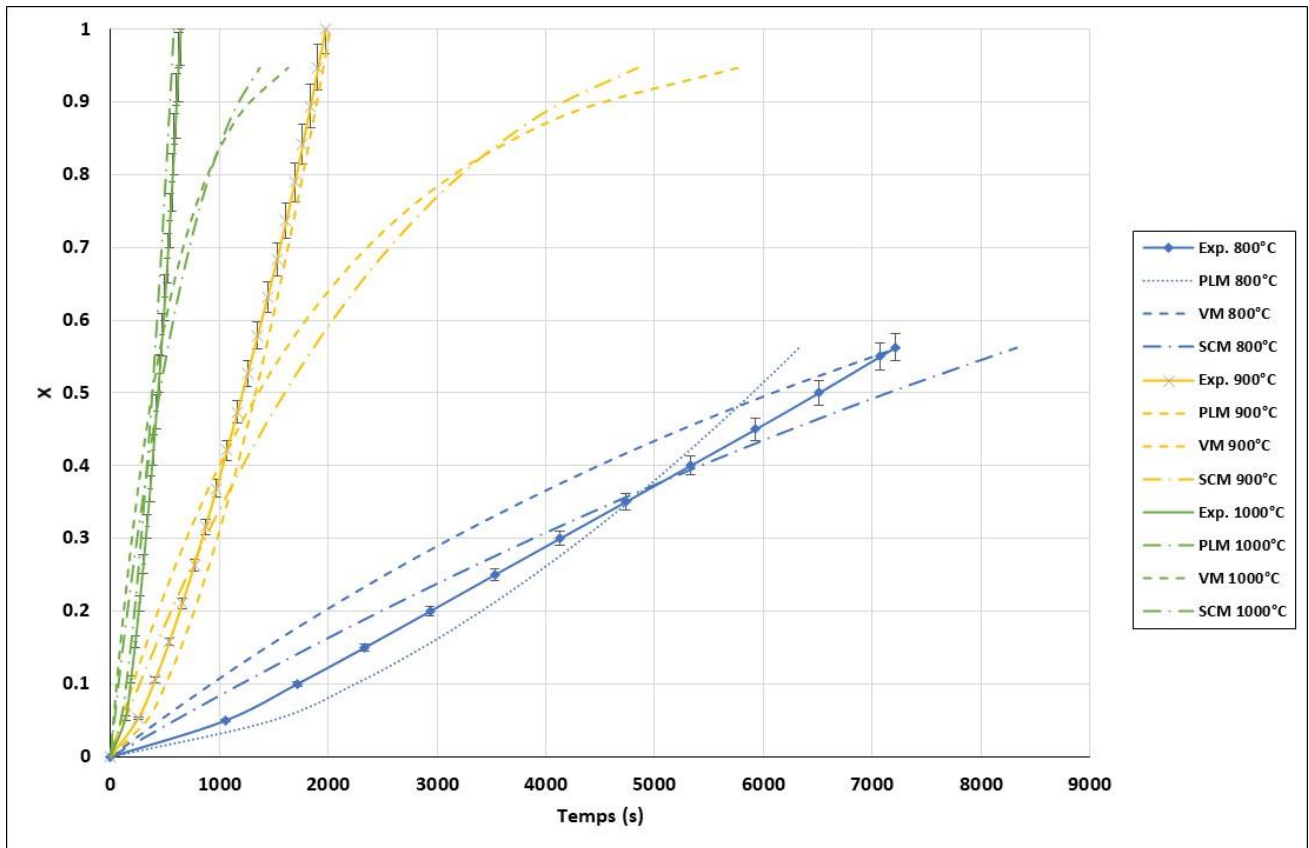


Figure 5.9. Conversion curves for biochar gasification and calculated conversion with the selected models for TGA: CO_2 pressure 0.67 atm and CO_2/C 7.01.

4.3 Kinetic model in fluidised bed reactor

For the case of FBR, the same procedure described in **Section 4.2** of this chapter (for the TGA) was employed to determine the kinetic parameters and the most suitable model to validate the experimental results. **Figure 5.10** shows the plot of $\ln r$ against \ln of the partial pressure, in order to determine the reaction order. As can be seen, the coefficient of determination (R^2) was approximately 0.99 in the linear equation of the conversion curve at 50%, meaning that the reaction order might be very close to the value of 0.4858 obtained at this conversion. The obtained values for reaction order oscillated from 0.47 to 0.51, hence an average value of 0.49 was selected.

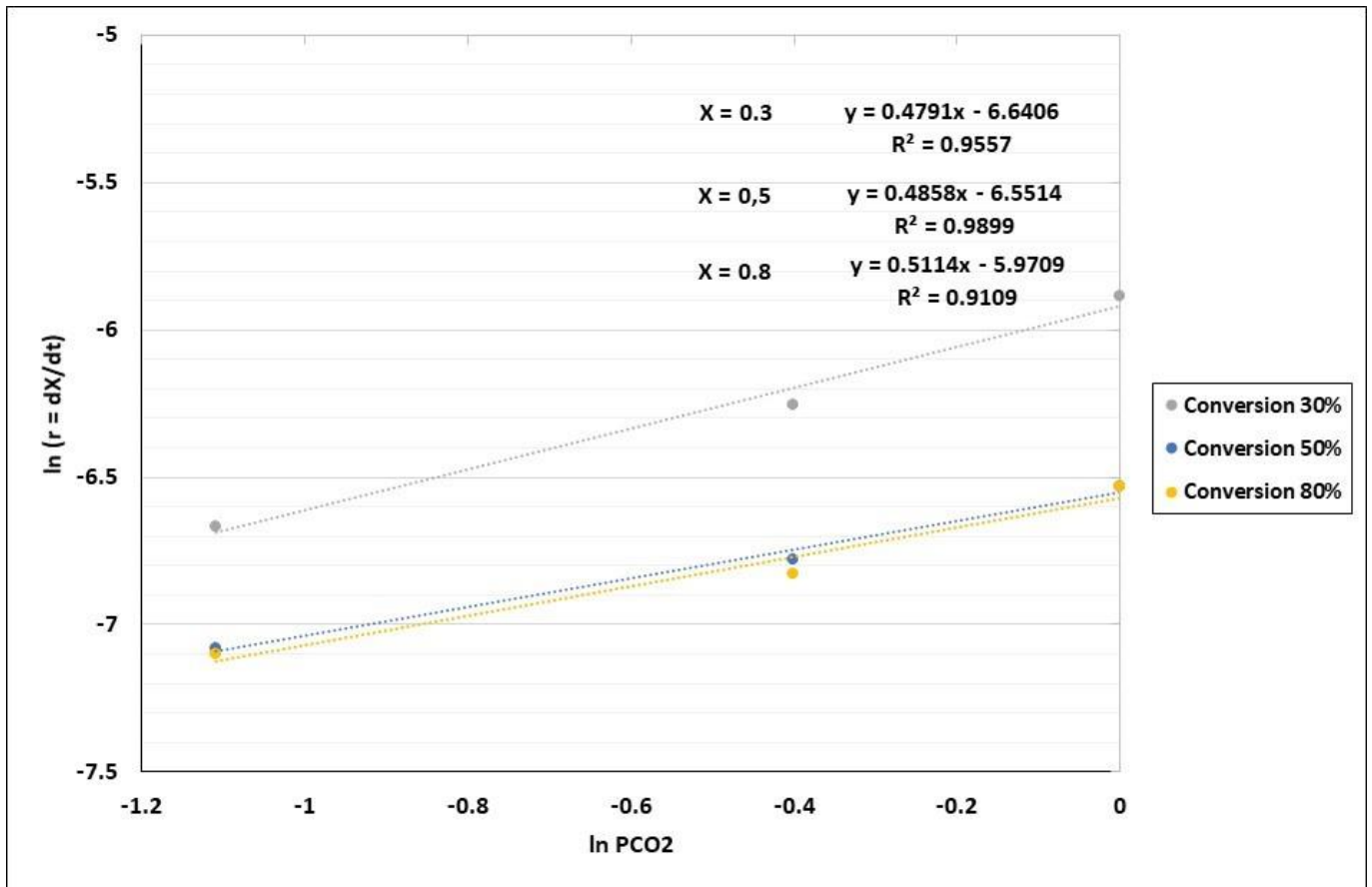


Figure 5.10. Fitting results between $\ln r$ and $\ln P_{CO_2}$, reaction order determination for FBR. Temperature: 1000°C and $CO_2/C/ 7.01$.

The activation energy and pre-exponential factors were determined by the same method as the TGA, by plotting $\ln k(T)$ against the reciprocal value of operation temperature ($1/T$). **Figure 5.11** shows the plot for the FBR. The same phenomenon was observed as for the TGA, in terms of the determination of the activation energy; the values varied with the conversion. Meanwhile, unlike the TGA results, the FBR values varied slightly from 157.1 to 162.5 MJ/kmol, therefore the activation energy value selected in this section was $159.8 \text{ MJ/kmol} \pm 2.7 \text{ MJ/kmol}$ and the pre-exponential factor was $2095.8 \text{ atm}^{-1} \text{ s}^{-1} \pm 36 \text{ atm}^{-1} \text{ s}^{-1}$. A slight increase in activation energy can be observed when char is gradually reduced, due to the fact that reactive sites decrease with the conversion. In addition to this, biochar was not completely composed of carbon, consequently, it may be possible to have additional reactions in the reactor. The latest could potentially alter the values of the activation energy.

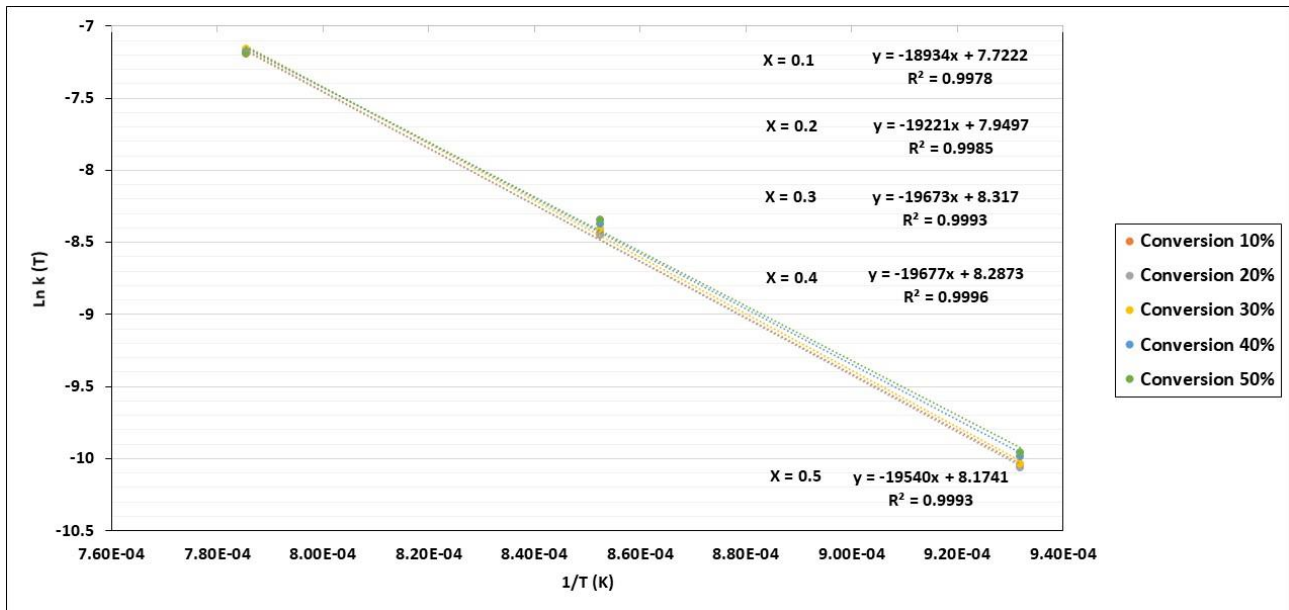


Figure 5.11. Fitting results of $\ln k (T)$ as a function of $1/T$, kinetic parameters determination for FBR. CO_2 pressure: 0.67 atm and CO_2/C : 7.01.

The kinetics models were compared with the experimental results, in which SCM was found to be the most adequate model for FBR. **Figure 5.12** shows the obtained results for VM and SCM, compared with experimental data. It can be observed that volumetric model curves were over shrinking core curves, this meant that the prediction of VM indicated a faster reaction rate than SCM. Contrary to this, SCM curves were in good agreement with experimental data. It can be observed that models presented a slight variation from the experimental data, principally after biochar conversion reached approximately 80%. This was due to the fact that the kinetic model predicted a high motion reduction of the gasification rate of biochar, which was not truly the case. Also, these models do not take into account diffusional limitations as the segregation phenomena of biochar and sand agglomerations.

The comparison of the SCM curves with the experimental data resulted in a standard deviation of approximately 1.5%. In **Figure 5.13**, the accuracy of this model can be clearly seen. Following the definition of this model, it indicated that biochar gasification rate in the FBR decreased gradually after reactivity reached its maximum value. In addition, the reaction was taking place on the surface of the particle and moves progressively to the centre of the solid, in other words, it started in the out-layer through the inner layer of the particle.

The final kinetic model for the fluidised bed reactor according to SCM model can be defined by the following expression:

$$r (\text{s}^{-1}) = dX/dt = 2095.8 \exp(-159.8/RT) P_{\text{CO}_2}^{0.49} (1-X)^{2/3} \quad \text{Eq. 5.14}$$

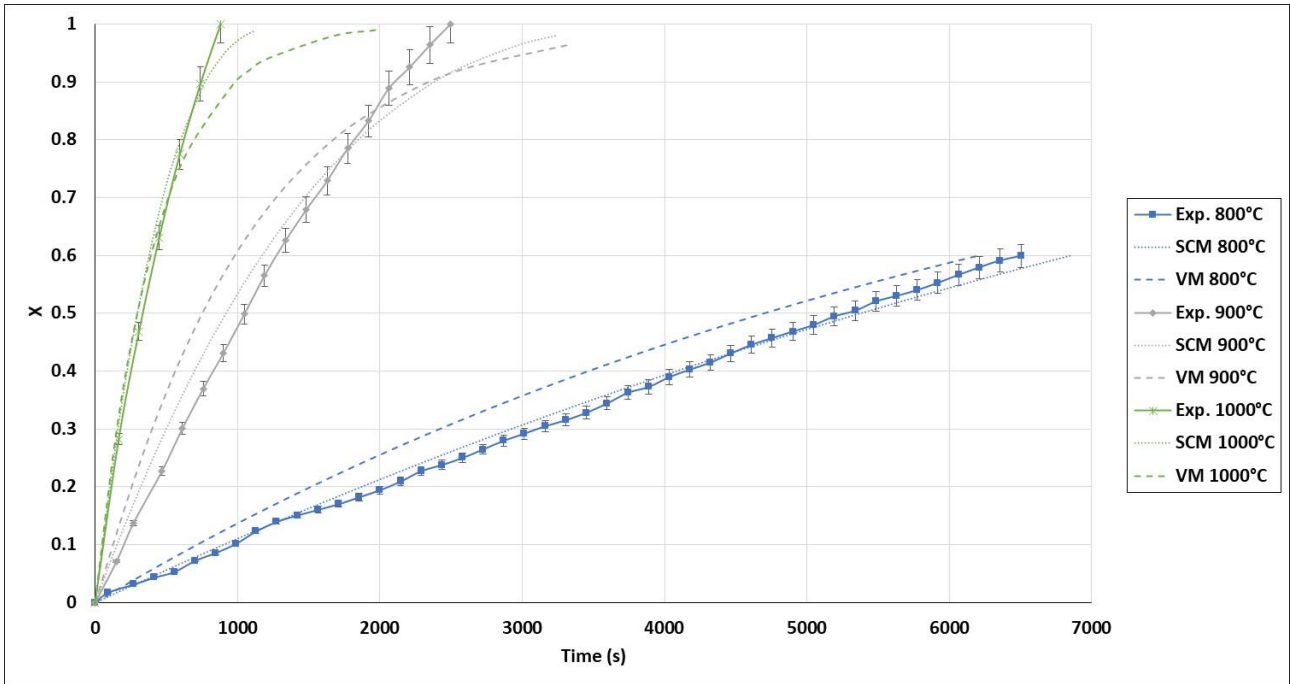


Figure 5.12. Conversion curves for biochar gasification and calculated conversion with selected model for FBR. CO_2 pressure: 0.67 and CO_2/C : 7.01.

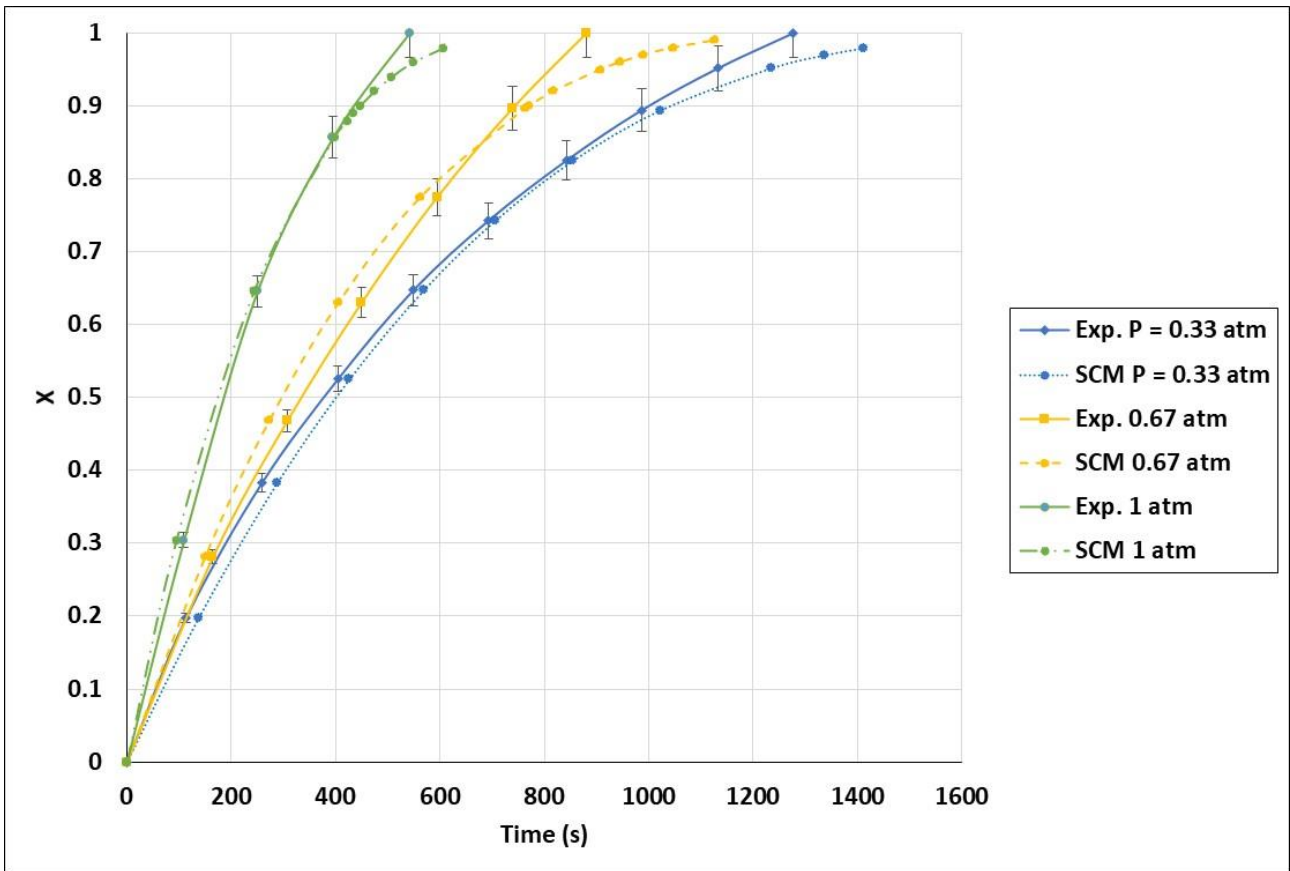


Figure 5.13. Validation of conversion curves of experimental test and shrinking core model (SCM), partial pressure effect. Temperature: 1000°C and CO_2/C : 7.01.

The power-law model was not used for the development of the kinetic model in the fluidized bed reactor due to the fact, that it was not found a Power Law mathematical equation adapted to predict the FBR results. Hence when using PLM, the consumption mechanism of this model for biochar did not agree with the FBR results.

4.4 Further discussion

The previously obtained results provided evidence that, for this study, the kinetic model developed in the TGA study cannot be directly extrapolated to the FB reactor. This is due to the fact that the localised behaviour in the TG analyser was represented by a different phenomenological model (Power Law) which showed a distinct char consumption mechanism from the FB reactor. The gasification rate in the FBR was faster than TGA, as fluidised bed gasifiers showed better heat and mass transfer conditions, meanwhile, the gasification rate in FBR decreased as conversion increased in a faster way than TGA, the fusion of biochar ash forming silicates segregation phenomena knowns as agglomeration could be the reason of this. The agglomeration phenomena are strongly present at high temperatures, especially at 900°C where alkali metals compounds in ash start melting. For the fluidised bed results, the shrinking core model was able to predict experimental results with very low deviations; this model describes biochar conversion as a layer-by-layer consumption, for which the gasification rate becomes very slow, at higher conversion values. For the TGA, the selected model did not follow any path described in the literature and it was described by a mathematic function. This function evidenced a decrease in the rapidity of biochar gasification rate, but with less impact than FBR results.

Figure 5.14 describes the biochar consumption mechanism that this study supposes to take place for TGA and FBR. In the Thermogravimetric analyser, CO₂ molecules enter the reacting zone, react with the biochar, and principally form CO molecules. Due to the set-up conditions in the TGA, the formed CO exits the reactor in an organised way and on a slower pathway than FBR. It is considered that the rapidity with which CO molecules leave the reacting zone potentially limits the new CO₂ molecules to penetrate and react with the biochar structure. As the amount of biochar is reduced, this limitation becomes more significant probably reduces the gasification rate. In addition to this, the TGA set-up is similar to fixed bed reactors, in which CO₂ molecules are not in full contact with all of the samples. First of all, they react with the upper layer of the sample and, once this layer is consumed, they then pass to another layer successively until the reaction is finished.

On the other hand, for the fluidised bed gasifier, the advantageous mixing conditions make new CO₂ molecules react with all of the biochar samples simultaneously, because of the fluidisation conditions. A high formation of CO molecules is achieved, but, at a certain point

(conversion value), the coexistence of CO molecules in the reaction zone inhibits the CO₂ molecules from reacting with biochar, significantly reducing the biochar gasification rate. The presence of CO affects the reaction equilibrium, provoking a stagnation of the biochar consumption [190], [191]. For these reasons in this study considered that biochar consumption was faster in FBR compared to TGA, but, at a certain conversion point, CO inhibition significantly reduced the biochar gasification rate for FBR in a higher magnitude than for TGA.

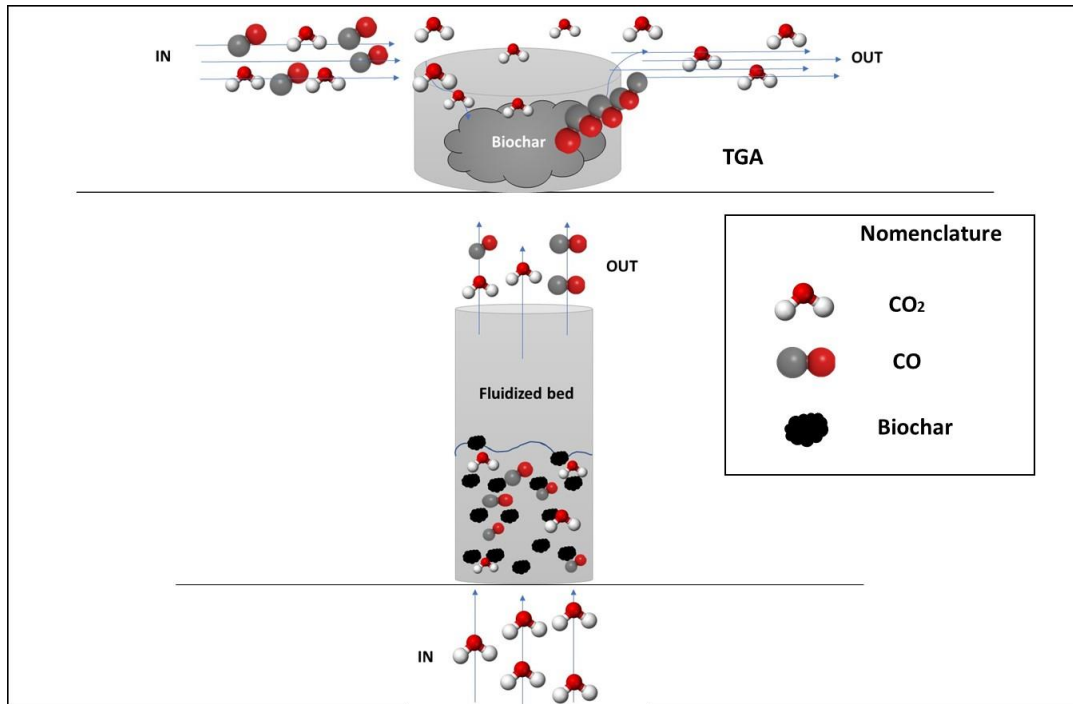


Figure 5.14. Hypothetical mechanism of biochar gasification in TGA (up) and FBR (down).

In order to compare the results obtained by this study with the literature, the developed models for TGA and fluidised bed were evaluated with kinetic models that were previously published in the research community, using the same operating conditions and biochar type. **Figure 5.15** shows a comparison of the kinetic models in the literature with the kinetic model obtained in this work (PLM model). The comparison was carried out by bringing the literature models to the same operational conditions of 1000°C and CO₂ partial pressure of 1 atm. Despite the models were presented in the same conditions, the comparison is limited due to the lack of information about the different mass and heat transfer limitations of each condition. The used biochar for all models was from a wood origin. As can be observed, there was a diversification of the conversion curves. As an example, the models proposed by Diedhiou et al. [192] and De Groot et al. [193] showed that the biochar gasification rate in the TGA results decreased significantly with the conversion proposing $f(X)$ to be modelled with the shrinking core and volumetric model. Despite the change of the biochar structure being different in the gasification

for these investigations, it can be observed that the required time for the total conversion of biochar was very similar to our investigation. On the other hand, the results obtained by Gomez-Barea et al. [132] and Van de Steene et al. [194] showed a very similar conversion curve to our work. Both authors used power-law models developed mathematically in order to express the biochar consumption mechanism, because the conventional models did not show accordance with the obtained results. The latest results corroborated the behaviour found in this study. The kinetic models of the previously presented literature can be found in **Appendix A4**.

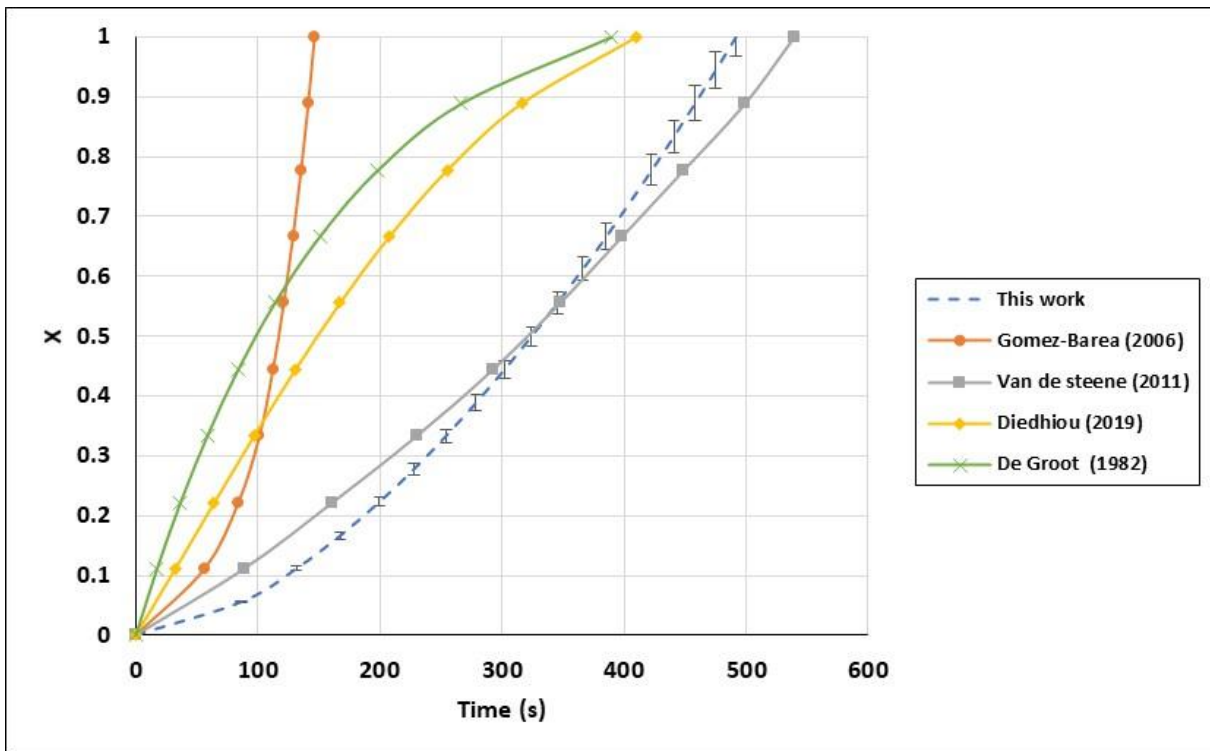


Figure 5.15. Biochar gasification kinetic model comparison with the literature at fixed conditions, for TGA. Temperature: 1000°C and CO₂ pressure: 1 atm.

As was discussed for the TGA kinetic models, in the case of the FBR the predicted values of this work (SCM model) at 1000°C and a CO₂ partial pressure of 1 atm, were shown to be in the same range of values from other predictions from the kinetic models in the literature for FBR (**Figure 5.16**). Some of the variations in conversion time were attributed to the difference in particle size, which is known to be a boundary parameter in gasification. The kinetic model proposed by Mueller et al. [134] and Matsui et al. [195] for gasification of woody biochar with CO₂, showed very good agreement with the results presented in this study. In addition to this, the selected conversion function for these investigations was the volumetric and shrinking core models, which were also the models that better adapted to the results of our work.

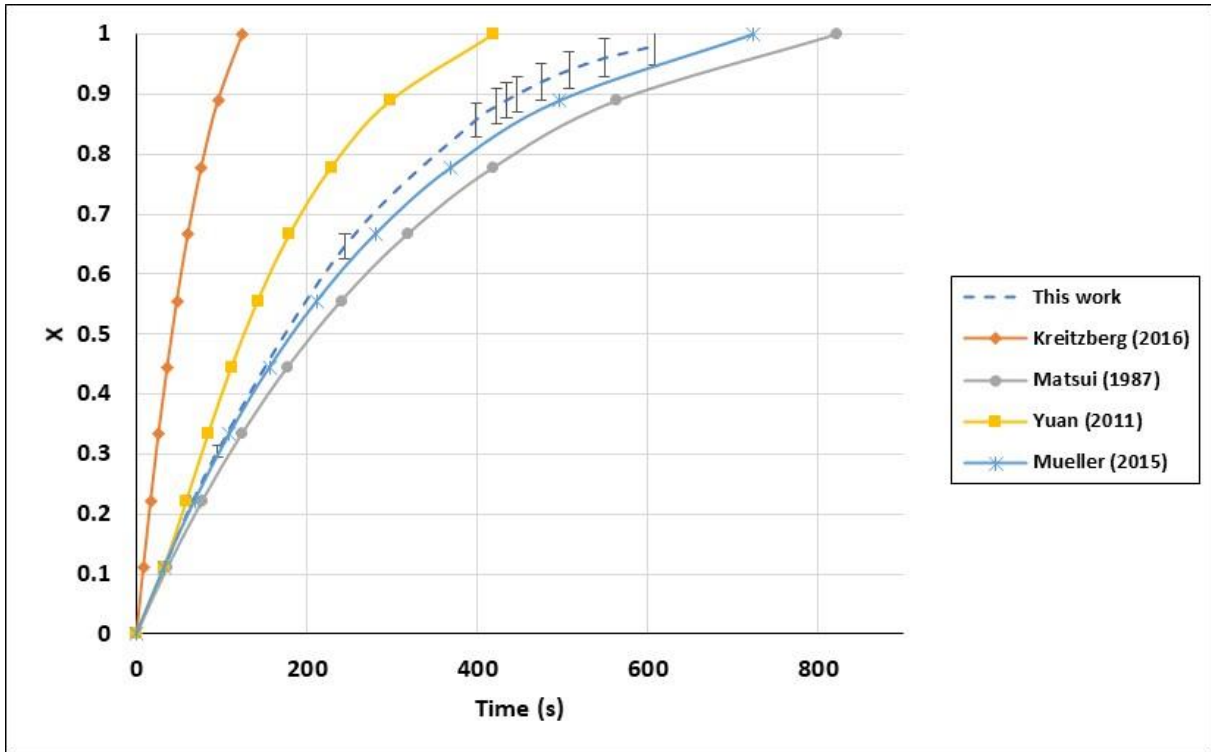


Figure 5.16. Biochar gasification kinetic model comparison with the literature at fixed conditions, for FBR. Temperature: 1000°C and CO₂ pressure: 1 atm.

5. Conclusion

From the development of the kinetic model for biochar gasification in a thermogravimetric analyser and a fluidised bed reactor, we can conclude as follows:

- The increase in temperature, partial pressure and CO_2/C ratio increased biochar gasification rate by reducing the required time for biochar total conversion.
- The comparison of the results obtained for TGA and FBR showed that the gasification rate was faster in FBR than in TGA, due to the better mixing conditions favouring heat and mass transfer. Meanwhile, at conversion rates between 65 and 75%, for FBR the biochar gasification rate decreased to lower values than in TGA, as the reaction was affected by CO inhibition.
- The gasification rate r_{50} was slightly superior for FBR compared with TGA, while, at high temperatures (1000°C) it was seen to increase significantly and presenting a higher gap ($19.7 \times 10^{-3} \text{ min}^{-1}$, 23%).
- The kinetic parameters obtained from both reactors showed similar values of activation energy for both set-ups, between 156 MJ/kmol and 159 MJ/kmol and a reaction order of 0.4 to 0.49 for TGA and FBR, respectively.
- For the TGA, the power-law model (PLM) showed the most adapted results in terms of validating the experimental results, with standard deviations of 2.6% to 9%. For FBR, the shrinking core model (SCM) represented the most adapted model, with an average standard deviation of approximately 1.5% from the experimental results.
- For the fluidised bed results, the shrinking core model was able to predict experimental results with very low deviations; this model describes biochar conversion as a layer by layer consumption at which, at high conversion values, the gasification rate becomes very slow.
- For the TG analyser, the selected model (PLM) did not follow any path described in the literature and it was described by a mathematic function. This function showed a decrease in biochar gasification rate, but with less impact than the FBR results.
- It was observed that the kinetic model developed for the TGA analyser cannot be extrapolated in the FBR, due to the different localised behaviour in TGA, which was represented by PLM. The difference in the kinetic model provided evidence of a distinct char consumption mechanism in both reactors.

General conclusions and perspectives

Conclusions

The objective of the thesis was to evaluate the energetic performance of two types of thermochemical conversion of woody biomass: pyrolysis in a semi-continuous reactor and gasification in a fluidized bed reactor. The aim of the study was to compare the energy balance and exergy evaluation of the processes after both were exposed to operating conditions variations, such as the use of catalyst in-situ or ex-situ, and temperature and gas carrier variation.

Firstly, the energetic and exergetic evaluations were evaluated for the pyrolysis of two biomasses (beech wood and flax shives) and pseudo-components (cellulose, hemicellulose and lignin) with and without the use of a catalyst to upgrade the bio-oil obtained. The problematic involved how thermodynamically advantageous the variation of operating conditions for product upgrading was for pyrolysis.

- The heat for pyrolysis for both biomasses was slightly higher than the values required for the pyrolysis of individual biomass pseudo-components. This can result from the potential competition between the thermal reactions of cellulose, hemicellulose and lignin in the biomass. Also, structural interactions between the three compounds in the biomass will strengthen thermal conditions, resulting in an increase in the required heat.
- The exergy destruction rate of the pyrolysis of biomass pseudo-components was lower than for the biomasses, evidencing fewer irreversibilities in the conversion process due to the strengthening of thermal conditions in biomass.
- The use of a catalyst increases gas and bio-oil energetic and exergetic rates by approximately 80% for gases and 40% for bio-oil.
- The exergy destruction rate decreased when a catalyst was used compared with the non-catalyst test.
- The heat needed for pyrolysis increased with the use of catalysts due to the increase in deoxygenation reactions.

The second step of this work was the evaluation of the same parameters for the gasification of beech wood in a continuous setup (fluidized bed reactor) as functions of operating conditions such as reaction temperature, gasification agent and bed material. The study of the energy, exergy and thermodynamic efficiency of the process showed that:

- An increase in temperature increased the syngas energetic value, the total product exergy and the exergy destruction rate.
- From the comparison of high-temperature pyrolysis and gasification, it was seen that the heat input required to perform the thermochemical conversion was lower for

Conclusion and perspectives

pyrolysis than for gasification. This was attributed to the Boudouard reaction which took place due to the use of CO₂ as a gasification agent. Meanwhile, the exergy destruction rate was higher for pyrolysis, meaning that more irreversibility was found in pyrolysis than in gasification.

- Less heat was required for steam gasification than for CO₂ gasification. This is explained by the energy contribution of exothermic reactions present in steam gasification able to reduce the required energy.
- More exergy was globally destroyed when CO₂ was used as the agent compared to steam, evidencing steam gasification in a more thermodynamically efficient process than CO₂ gasification.

The last part of the investigation was the development of a kinetic model of the CO₂-biochar gasification reaction. This reaction proved to be very advantageous in energetic and exergetic terms as the main product (CO) represented the most energetic product. The CO₂ gasification of biochar in a fluidized bed reactor and TGA were analysed, followed by development of a kinetic model. The results obtained from this study were the following.

- The increase in temperature, partial pressure and CO₂/C ratio increased the biochar gasification rate by reducing the time required for biochar total conversion.
- Comparison of the results obtained for TGA and FBR showed that the gasification rate was faster in FBR than in TGA due to the better mixing conditions, favouring heat and mass transfer. Meanwhile, at conversion rates between 65% and 75%, the biochar gasification rate for FBR decreased to lower values than in TGA as the reaction was affected by CO inhibition.
- For TGA, the power-law model showed the most adapted results in terms of validating the experimental results, while for FBR, the shrinking core model represented the most adapted model.
- The kinetic model developed based on TGA cannot be extrapolated to FBR due to the different localized mass and heat transfer behaviour in TGA. The difference in the kinetic model provided evidence of a distinct char consumption mechanism in both reactors.

Perspectives

In addition to the results presented in this work, the following section proposes some directions to continue with the investigation path.

Regarding the thermodynamic analysis and kinetic modelling of this work, two studies are proposed for future investigation.

- A thermodynamic study of the overall gasification process using the Aspen Plus simulator.

The results presented in this thesis mainly involved comparison of the thermodynamic results of the reactors without taking into consideration other operating units. Future work might include the development and simulation of the overall gasification process, including biomass pre-treatment, solids separation, gas cleaning, solids and syngas valorization, CO₂ capture and, as a final objective, electricity production. A simulator such as Aspen Plus can be used to model the previously obtained results and to study the energy balance and exergy evaluation of the overall process. This perspective is focused on the investigation procedure presented in the work of Francois et al. [196] using Aspen Plus to simulate the overall process for the electricity production of wood combustion/gasification. The proposed investigation would provide results such as which operation units are more energy demanding, show more irreversibilities, and have the lowest and highest exergy efficiency of the overall gasification installation. **Figure ii** shows a proposed scheme of this recommended investigation after a literature review.

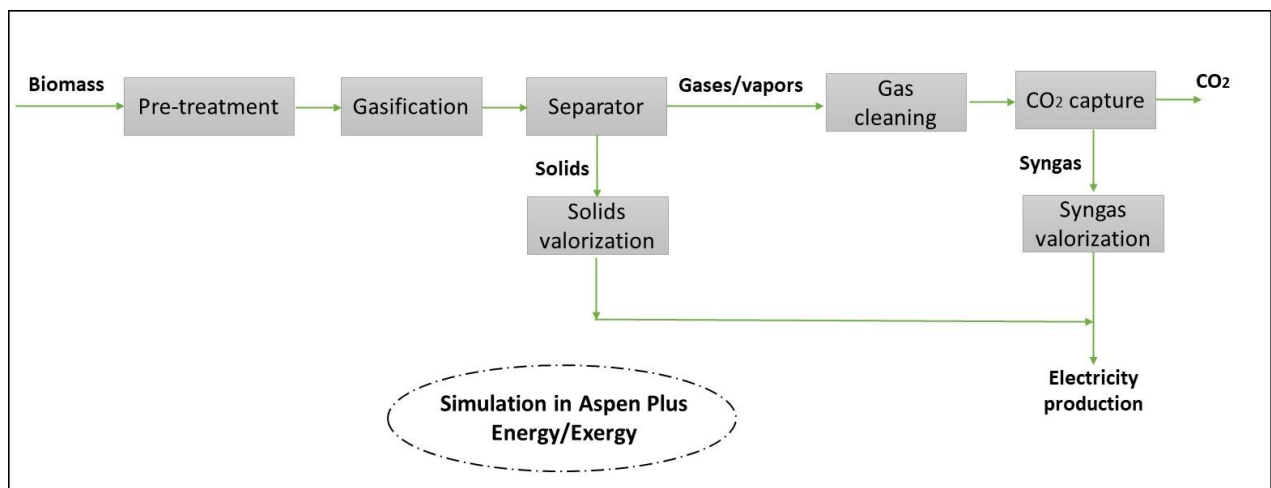


Figure ii. Proposed scheme for simulation in Aspen plus, determination of the overall energy and exergy of the process.

Conclusion and perspectives

- A computational fluid dynamics (CFD) modelling of the gasification kinetics in the fluidized bed reactor.

The kinetic model developed for the gasification of biochar in the fluidized bed gasifier can be integrated into mass, heat and momentum equations in order to study the behaviour in the fluid and solid phases inside the reactor. Study of the reactor dynamic by varying the operation conditions and using a validated kinetic model of the fluidized bed reactor could be a very interesting continuation of this investigation. The study would show very accurate heat and mass profiles inside the reactor, which can later be used for process design. For this investigation, we have conducted some work on CFD modelling of the gasification reaction in the fluidized bed using the open-source software OpenFOAM. The reactor geometry has been developed and non-reactive tests of the solid and gas phase iterations have been performed. Introduction of the kinetic model of gasification in the conservation equations could be further investigated and a complete kinetic and computational model proposed.

REFERENCES

References

- [1] B. Looney, « BP: Statistical Review of World Energy 2020 », *Economic Policy*, vol. 1, n° 69, p. 1-69, 2020.
- [2] N. Scarlat, J.-F. Dallemand, N. Taylor, et M. Banja, « Brief on biomass for energy in the European Union », Publications Office of the European Union, 2019.
- [3] M. Juraščík, A. Sues, et K. J. Ptasiński, « Exergy analysis of synthetic natural gas production method from biomass », *Energy*, vol. 35, n° 2, p. 880-888, févr. 2010, doi: 10.1016/j.energy.2009.07.031.
- [4] I. Dincer et M. A. Rosen, « Chapter 2 - EXERGY AND ENERGY ANALYSES », in *EXERGY*, I. Dincer et M. A. Rosen, Éd. Amsterdam: Elsevier, 2007, p. 23-35.
- [5] R. A. Houghton, « Biomass », in *Encyclopedia of Ecology*, S. E. Jørgensen et B. D. Fath, Éd. Oxford: Academic Press, 2008, p. 448-453.
- [6] N. Edomah, « Economics of Energy Supply☆ », in *Reference Module in Earth Systems and Environmental Sciences*, Elsevier, 2018.
- [7] K. B. Hicks, J. Montanti, et N. P. Nghiem, « Chapter 11 - Use of Barley Grain and Straw for Biofuels and Other Industrial Uses », in *Barley (Second Edition)*, P. R. Shewry et S. E. Ullrich, Éd. AACCC International Press, 2014, p. 269-291.
- [8] B. M. Fekete, « 3.05 - Biomass », in *Climate Vulnerability*, R. A. Pielke, Éd. Oxford: Academic Press, 2013, p. 83-87.
- [9] A. Tursi, « A review on biomass: importance, chemistry, classification, and conversion », *Biofuel Research Journal*, vol. 6, n° 2, p. 962-979, juin 2019, doi: 10.18331/BRJ2019.6.2.3.
- [10] S. V. Vassilev, D. Baxter, L. K. Andersen, C. G. Vassileva, et T. J. Morgan, « An overview of the organic and inorganic phase composition of biomass », *Fuel*, vol. 94, p. 1-33, avr. 2012, doi: 10.1016/j.fuel.2011.09.030.
- [11] X. Ge *et al.*, « Chapter Five - Conversion of Lignocellulosic Biomass Into Platform Chemicals for Biobased Polyurethane Application », in *Advances in Bioenergy*, vol. 3, Y. Li et X. Ge, Éd. Elsevier, 2018, p. 161-213.
- [12] E. W. Qian, « Chapter 7 - Pretreatment and Saccharification of Lignocellulosic Biomass », in *Research Approaches to Sustainable Biomass Systems*, S. Tojo et T. Hirasawa, Éd. Boston: Academic Press, 2014, p. 181-204.
- [13] A. J. A. van Maris *et al.*, « Alcoholic fermentation of carbon sources in biomass hydrolysates by *Saccharomyces cerevisiae*: current status », *Antonie Van Leeuwenhoek*, vol. 90, n° 4, p. 391-418, nov. 2006, doi: 10.1007/s10482-006-9085-7.
- [14] D. Shen, R. Xiao, S. Gu, et H. Zhang, « The Overview of Thermal Decomposition of Cellulose in Lignocellulosic Biomass », *Cellulose - Biomass Conversion*, août 2013, doi: 10.5772/51883.

- [15]X. Yuan et G. Cheng, « From cellulose fibrils to single chains: understanding cellulose dissolution in ionic liquids », *Phys. Chem. Chem. Phys.*, vol. 17, n° 47, p. 31592-31607, nov. 2015, doi: 10.1039/C5CP05744B.
- [16]P. Bajpai, « Chapter 2 - Wood and Fiber Fundamentals », in *Biermann's Handbook of Pulp and Paper (Third Edition)*, P. Bajpai, Éd. Elsevier, 2018, p. 19-74.
- [17]R. C. Kuhad et A. Singh, « Lignocellulose Biotechnology: Current and Future Prospects », *Critical Reviews in Biotechnology*, vol. 13, n° 2, p. 151-172, janv. 1993, doi: 10.3109/07388559309040630.
- [18]M. Balat, « Experimental Study on Pyrolysis of Black Alder Wood », *Energy Exploration & Exploitation*, vol. 26, n° 4, p. 209-220, août 2008, doi: 10.1260/014459808787548714.
- [19]C. Z. Zaman *et al.*, « Pyrolysis: A Sustainable Way to Generate Energy from Waste », *Pyrolysis*, juill. 2017, doi: 10.5772/intechopen.69036.
- [20]F.-X. Collard et J. Blin, « A review on pyrolysis of biomass constituents: Mechanisms and composition of the products obtained from the conversion of cellulose, hemicelluloses and lignin », *Renewable and Sustainable Energy Reviews*, vol. 38, p. 594-608, oct. 2014, doi: 10.1016/j.rser.2014.06.013.
- [21]K. B. Ansari, J. S. Arora, J. W. Chew, P. J. Dauenhauer, et S. H. Mushrif, « Fast Pyrolysis of Cellulose, Hemicellulose, and Lignin: Effect of Operating Temperature on Bio-oil Yield and Composition and Insights into the Intrinsic Pyrolysis Chemistry », *Ind. Eng. Chem. Res.*, vol. 58, n° 35, p. 15838-15852, sept. 2019, doi: 10.1021/acs.iecr.9b00920.
- [22]C. Mohabeer, L. Abdelouahed, S. Marcotte, et B. Taouk, « Comparative analysis of pyrolytic liquid products of beech wood, flax shives and woody biomass components », *Journal of Analytical and Applied Pyrolysis*, vol. 127, p. 269-277, sept. 2017, doi: 10.1016/j.jaap.2017.07.025.
- [23]S. Wang, Z. Guo, Q. Cai, et L. Guo, « Catalytic conversion of carboxylic acids in bio-oil for liquid hydrocarbons production », *Biomass and Bioenergy*, vol. 45, p. 138-143, oct. 2012, doi: 10.1016/j.biombioe.2012.05.023.
- [24]A. Bridgwater, « 7 - Fast pyrolysis of biomass for the production of liquids », in *Biomass Combustion Science, Technology and Engineering*, L. Rosendahl, Éd. Woodhead Publishing, 2013, p. 130-171.
- [25]T. Suzuki, H. Nakajima, N. Ikenaga, H. Oda, et T. Miyake, « Effect of mineral matters in biomass on the gasification rate of their chars », *Biomass Conv. Bioref.*, vol. 1, n° 1, p. 17-28, mars 2011, doi: 10.1007/s13399-011-0006-2.
- [26]C. Hognon, C. Dupont, M. Gâteau, et F. Delrue, « Comparison of steam gasification reactivity of algal and lignocellulosic biomass: Influence of inorganic elements »,

- Bioresource Technology*, vol. 164, p. 347-353, juill. 2014, doi: 10.1016/j.biortech.2014.04.111.
- [27] C. Mohabeer, L. Reyes, L. Abdelouahed, S. Marcotte, et B. Taouk, « Investigating catalytic de-oxygenation of cellulose, xylan and lignin bio-oils using HZSM-5 and Fe-HZSM-5 », *Journal of Analytical and Applied Pyrolysis*, vol. 137, p. 118-127, janv. 2019, doi: 10.1016/j.jaap.2018.11.016.
- [28] T. Qu, W. Guo, L. Shen, J. Xiao, et K. Zhao, « Experimental Study of Biomass Pyrolysis Based on Three Major Components: Hemicellulose, Cellulose, and Lignin », *Ind. Eng. Chem. Res.*, vol. 50, n° 18, p. 10424-10433, sept. 2011, doi: 10.1021/ie1025453.
- [29] C. Zhao, E. Jiang, et A. Chen, « Volatile production from pyrolysis of cellulose, hemicellulose and lignin », *Journal of the Energy Institute*, vol. 90, n° 6, p. 902-913, déc. 2017, doi: 10.1016/j.joei.2016.08.004.
- [30] M. Van de Velden, J. Baeyens, A. Brems, B. Janssens, et R. Dewil, « Fundamentals, kinetics and endothermicity of the biomass pyrolysis reaction », *Renewable Energy*, vol. 35, n° 1, p. 232-242, janv. 2010, doi: 10.1016/j.renene.2009.04.019.
- [31] D. Vamvuka, « Bio-oil, solid and gaseous biofuels from biomass pyrolysis processes—An overview », *International Journal of Energy Research*, vol. 35, n° 10, p. 835-862, 2011, doi: 10.1002/er.1804.
- [32] J.-P. Lange, « Lignocellulose conversion: an introduction to chemistry, process and economics », *Biofuels, Bioproducts and Biorefining*, vol. 1, n° 1, p. 39-48, 2007, doi: 10.1002/bbb.7.
- [33] A. Dufour, « Bioenergy Chain and Process Scales », in *Thermochemical Conversion of Biomass for the Production of Energy and Chemicals*, John Wiley & Sons, Ltd, 2016, p. 1-28.
- [34] C. Di Blasi, C. Branca, F. Masotta, et E. De Biase, « Experimental Analysis of Reaction Heat Effects during Beech Wood Pyrolysis », *Energy Fuels*, vol. 27, n° 5, p. 2665-2674, mai 2013, doi: 10.1021/ef4001709.
- [35] K. Atsonios, K. D. Panopoulos, A. V. Bridgwater, et E. Kakaras, « Biomass fast pyrolysis energy balance of a 1kg/h test rig », *International Journal of Thermodynamics*, vol. 18, n° 4, p. 267-275, déc. 2015, doi: 10.5541/ijot.5000147483.
- [36] T. B. Reed et C. D. Cowdery, « Heat flux requirements for fast pyrolysis and a new method for generating biomass vapor », *Prepr. Pap., Am. Chem. Soc., Div. Fuel Chem.; (United States)*, vol. 32:2, Art. n° CONF-870410-, avr. 1987.
- [37] D. E. Dugaard et R. C. Brown, « Enthalpy for Pyrolysis for Several Types of Biomass », *Energy Fuels*, vol. 17, n° 4, p. 934-939, juill. 2003, doi: 10.1021/ef020260x.

- [38]Y. Haseli, J. A. van Oijen, et L. P. H. de Goeij, « Modeling biomass particle pyrolysis with temperature-dependent heat of reactions », *Journal of Analytical and Applied Pyrolysis*, vol. 90, n° 2, p. 140-154, mars 2011, doi: 10.1016/j.jaap.2010.11.006.
- [39]I. Ph. Boukis, P. Grammelis, S. Bezergianni, et A. V. Bridgwater, « CFB air-blown flash pyrolysis. Part I: Engineering design and cold model performance », *Fuel*, vol. 86, n° 10, p. 1372-1386, juill. 2007, doi: 10.1016/j.fuel.2006.11.002.
- [40]I. Milosavljevic, V. Oja, et E. M. Suuberg, « Thermal Effects in Cellulose Pyrolysis: Relationship to Char Formation Processes », *Ind. Eng. Chem. Res.*, vol. 35, n° 3, p. 653-662, janv. 1996, doi: 10.1021/ie950438l.
- [41]H.-C. Kung, « A mathematical model of wood pyrolysis », *Combustion and Flame*, vol. 18, n° 2, p. 185-195, avr. 1972, doi: 10.1016/S0010-2180(72)80134-2.
- [42]A. F. Roberts, « The heat of reaction during the pyrolysis of wood », *Combustion and Flame*, vol. 17, n° 1, p. 79-86, août 1971, doi: 10.1016/S0010-2180(71)80141-4.
- [43]D. J. Holve et A. M. Kanury, « A Numerical Study of the Response of Building Components to Heating in a Fire », *J. Heat Transfer*, vol. 104, n° 2, p. 344-350, mai 1982, doi: 10.1115/1.3245094.
- [44]M. Franck, E.-U. Hertge, S. Heinrich, B. Lorenz, et J. Werther, « Energetic Optimization of the Lignin Pyrolysis for the Production of Aromatic Hydrocarbons », *10th International Conference on Circulating Fluidized Beds and Fluidization Technology - CFB-10*, mai 2011.
- [45]J. I. M. Arbeláez, F. C. Janna, et M. Garcia-Pérez, « Fast pyrolysis of biomass: A review of relevant aspects. Part I: Parametric study », *DYNA*, vol. 82, n° 192, Art. n° 192, juill. 2015, doi: 10.15446/dyna.v82n192.44701.
- [46]P. Basu, « Chapter 5 - Pyrolysis », in *Biomass Gasification, Pyrolysis and Torrefaction (Third Edition)*, P. Basu, Éd. Academic Press, 2018, p. 155-187.
- [47]I. Dincer et M. A. Rosen, *EXERGY: Energy, Environment and Sustainable Development*. Elsevier, 2007.
- [48]J. Keedy *et al.*, « Exergy Based Assessment of the Production and Conversion of Switchgrass, Equine Waste, and Forest Residue to Bio-Oil Using Fast Pyrolysis », *Ind. Eng. Chem. Res.*, vol. 54, n° 1, p. 529-539, janv. 2015, doi: 10.1021/ie5035682.
- [49]J. F. Peters, F. Petrakopoulou, et J. Dufour, « Exergetic analysis of a fast pyrolysis process for bio-oil production », *Fuel Processing Technology*, vol. 119, p. 245-255, mars 2014, doi: 10.1016/j.fuproc.2013.11.007.
- [50]J. F. Peters, F. Petrakopoulou, et J. Dufour, « Exergy analysis of synthetic biofuel production via fast pyrolysis and hydrougrading », *Energy*, vol. 79, p. 325-336, janv. 2015, doi: 10.1016/j.energy.2014.11.019.

- [51] A. A. Boateng, C. A. Mullen, L. Osgood-Jacobs, P. Carlson, et N. Macken, « Mass Balance, Energy, and Exergy Analysis of Bio-Oil Production by Fast Pyrolysis », *TRANSACTIONS-AMERICAN SOCIETY OF MECHANICAL ENGINEERS JOURNAL OF ENERGY RESOURCES TECHNOLOGY*, vol. 134, n° 4, p. 042001, 2012.
- [52] Q. Lv, H. Yue, Q. Xu, C. Zhang, et R. Zhang, « Quantifying the exergetic performance of bio-fuel production process including fast pyrolysis and bio-oil hydrodeoxygenation », *Journal of Renewable and Sustainable Energy*, vol. 10, n° 4, p. 043107, juill. 2018, doi: 10.1063/1.5031894.
- [53] M. Garcia-Perez *et al.*, « Fast Pyrolysis of Oil Mallee Woody Biomass: Effect of Temperature on the Yield and Quality of Pyrolysis Products », *Ind. Eng. Chem. Res.*, vol. 47, n° 6, p. 1846-1854, mars 2008, doi: 10.1021/ie071497p.
- [54] C. Mohabeer *et al.*, « Production of liquid bio-fuel from catalytic de-oxygenation: Pyrolysis of beech wood and flax shives », *Journal of Fuel Chemistry and Technology*, vol. 47, n° 2, p. 153-166, févr. 2019, doi: 10.1016/S1872-5813(19)30008-8.
- [55] A. Imran, E. A. Bramer, K. Seshan, et G. Brem, « Catalytic Flash Pyrolysis of Biomass Using Different Types of Zeolite and Online Vapor Fractionation », *Energies*, vol. 9, n° 3, p. 187, 2016, doi: 10.3390/en9030187.
- [56] I. Y. Mohammed, F. K. Kazi, S. Yusup, P. A. Alaba, Y. M. Sani, et Y. A. Abakr, « Catalytic Intermediate Pyrolysis of Napier Grass in a Fixed Bed Reactor with ZSM-5, HZSM-5 and Zinc-Exchanged Zeolite-A as the Catalyst », *Energies*, vol. 9, n° 4, p. 1-17, 2016.
- [57] S. Bilgen, S. Keleş, et K. Kaygusuz, « Calculation of higher and lower heating values and chemical exergy values of liquid products obtained from pyrolysis of hazelnut cupulae », *Energy*, vol. 41, n° 1, p. 380-385, 2012.
- [58] M. Atienza-Martínez, J. Ábrego, J. F. Mastral, J. Ceamanos, et G. Gea, « Energy and exergy analyses of sewage sludge thermochemical treatment », *Energy*, vol. 144, p. 723-735, févr. 2018, doi: 10.1016/j.energy.2017.12.007.
- [59] N. Ramesh et S. Murugavelh, « A cleaner process for conversion of invasive weed (*Prosopis juliflora*) into energy-dense fuel: kinetics, energy, and exergy analysis of pyrolysis process », *Biomass Conv. Bioref.*, mai 2020, doi: 10.1007/s13399-020-00747-5.
- [60] M. J. B. Fong, A. C. M. Loy, B. L. F. Chin, M. K. Lam, S. Yusup, et Z. A. Jawad, « Catalytic pyrolysis of *Chlorella vulgaris*: Kinetic and thermodynamic analysis », *Bioresource Technology*, vol. 289, p. 121689, oct. 2019, doi: 10.1016/j.biortech.2019.121689.
- [61] P. Basu et P. Kaushal, « Modeling of Pyrolysis and Gasification of Biomass in Fluidized Beds: A Review », *Chemical Product and Process Modeling*, vol. 4, n° 1, mai 2009, doi: 10.2202/1934-2659.1338.

- [62] V. S. Sikarwar *et al.*, « An overview of advances in biomass gasification », *Energy Environ. Sci.*, vol. 9, n° 10, p. 2939-2977, oct. 2016, doi: 10.1039/C6EE00935B.
- [63] M. Sui, G. Li, Y. Guan, C. Li, R. Zhou, et A.-M. Zarnegar, « Hydrogen and syngas production from steam gasification of biomass using cement as catalyst », *Biomass Conv. Bioref.*, vol. 10, n° 1, p. 119-124, mars 2020, doi: 10.1007/s13399-019-00404-6.
- [64] J. Udomsirichakorn et P. A. Salam, « Review of hydrogen-enriched gas production from steam gasification of biomass: The prospect of CaO-based chemical looping gasification », *Renewable and Sustainable Energy Reviews*, vol. 30, p. 565-579, févr. 2014, doi: 10.1016/j.rser.2013.10.013.
- [65] Y.-S. Jeong, K.-B. Park, et J.-S. Kim, « Hydrogen production from steam gasification of polyethylene using a two-stage gasifier and active carbon », *Applied Energy*, vol. 262, p. 114495, mars 2020, doi: 10.1016/j.apenergy.2020.114495.
- [66] C. Guizani, F. J. Escudero Sanz, et S. Salvador, « The gasification reactivity of high-heating-rate chars in single and mixed atmospheres of H₂O and CO₂ », *Fuel*, vol. 108, p. 812-823, juin 2013, doi: 10.1016/j.fuel.2013.02.027.
- [67] Y. Cheng, Z. Thow, et C.-H. Wang, « Biomass gasification with CO₂ in a fluidized bed », *Powder Technology*, vol. 296, p. 87-101, août 2016, doi: 10.1016/j.powtec.2014.12.041.
- [68] N. Sadhwani, S. Adhikari, et M. R. Eden, « Biomass Gasification Using Carbon Dioxide: Effect of Temperature, CO₂/C Ratio, and the Study of Reactions Influencing the Process », *Ind. Eng. Chem. Res.*, vol. 55, n° 10, p. 2883-2891, mars 2016, doi: 10.1021/acs.iecr.5b04000.
- [69] R. G. dos Santos et A. C. Alencar, « Biomass-derived syngas production via gasification process and its catalytic conversion into fuels by Fischer Tropsch synthesis: A review », *International Journal of Hydrogen Energy*, vol. 45, n° 36, p. 18114-18132, juill. 2020, doi: 10.1016/j.ijhydene.2019.07.133.
- [70] A. Ben Hassen Trabelsi *et al.*, « Hydrogen-Rich Syngas Production from Gasification and Pyrolysis of Solar Dried Sewage Sludge: Experimental and Modeling Investigations », *BioMed Research International*, août 09, 2017. <https://www.hindawi.com/journals/bmri/2017/7831470/> (consulté le juill. 27, 2020).
- [71] M. Miri, S. Shahraki, et M. Motahari-Nezhad, « Syngas production from gasification of high sulfur fuel oil using a CO₂ sorbent », *Petroleum Science and Technology*, vol. 37, n° 17, p. 1931-1937, sept. 2019, doi: 10.1080/10916466.2018.1463259.
- [72] A. Bernardi, J. E. A. Graciano, et B. Chachuat, « Production of chemicals from syngas: an enviro-economic model-based investigation », in *Computer Aided Chemical Engineering*, vol. 46, A. A. Kiss, E. Zondervan, R. Lakerveld, et L. Özkan, Éd. Elsevier, 2019, p. 367-372.

- [73]C.-L. Jin *et al.*, « Economic assessment of biomass gasification and pyrolysis: A review », *Energy Sources, Part B: Economics, Planning, and Policy*, vol. 12, n° 11, p. 1030-1035, nov. 2017, doi: 10.1080/15567249.2017.1358309.
- [74]A. V. Bridgwater, « The technical and economic feasibility of biomass gasification for power generation », *Fuel*, vol. 74, n° 5, p. 631-653, mai 1995, doi: 10.1016/0016-2361(95)00001-L.
- [75]A. M. Sepe, J. Li, et M. C. Paul, « Assessing biomass steam gasification technologies using a multi-purpose model », *Energy Conversion and Management*, vol. 129, p. 216-226, déc. 2016, doi: 10.1016/j.enconman.2016.10.018.
- [76]M. Di Marcello, G. A. Tsalidis, G. Spinelli, W. de Jong, et J. H. A. Kiel, « Pilot scale steam-oxygen CFB gasification of commercial torrefied wood pellets. The effect of torrefaction on the gasification performance », *Biomass and Bioenergy*, vol. 105, p. 411-420, oct. 2017, doi: 10.1016/j.biombioe.2017.08.005.
- [77]M. Prestipino, V. Chiodo, S. Maisano, G. Zafarana, F. Urbani, et A. Galvagno, « Hydrogen rich syngas production by air-steam gasification of citrus peel residues from citrus juice manufacturing: Experimental and simulation activities », *International Journal of Hydrogen Energy*, vol. 42, n° 43, p. 26816-26827, oct. 2017, doi: 10.1016/j.ijhydene.2017.05.173.
- [78]M. Zhai, L. Guo, Y. Wang, Y. Zhang, P. Dong, et H. Jin, « Process simulation of staging pyrolysis and steam gasification for pine sawdust », *International Journal of Hydrogen Energy*, vol. 41, n° 47, p. 21926-21935, déc. 2016, doi: 10.1016/j.ijhydene.2016.10.037.
- [79]*Gasification of Lignite and Wood in the Lurgi Circulating Fluidized-bed Gasifier: Final Report*. Electric Power Research Institute, 1989.
- [80]I. Narváez, A. Orío, M. P. Aznar, et J. Corella, « Biomass Gasification with Air in an Atmospheric Bubbling Fluidized Bed. Effect of Six Operational Variables on the Quality of the Produced Raw Gas », *Ind. Eng. Chem. Res.*, vol. 35, n° 7, p. 2110-2120, janv. 1996, doi: 10.1021/ie9507540.
- [81]H. Hofbauer, R. Rauch, G. Loeffler, S. Kaiser, E. Fercher, et H. Tremmel, « Six Years Experience with the FICFB-Gasification Process », *10th Eur. Conf. Technol. Exhib. Wurzburg, no. January*, janv. 2002.
- [82]X. Yao *et al.*, « Syngas production through biomass/CO₂ gasification using granulated blast furnace slag as heat carrier », *Journal of Renewable and Sustainable Energy*, vol. 9, n° 5, p. 053101, sept. 2017, doi: 10.1063/1.4993259.
- [83]N. Sadhwani, S. Adhikari, et M. R. Eden, « Biomass Gasification Using Carbon Dioxide: Effect of Temperature, CO₂/C Ratio, and the Study of Reactions Influencing the Process », *Ind. Eng. Chem. Res.*, vol. 55, n° 10, p. 2883-2891, mars 2016, doi: 10.1021/acs.iecr.5b04000.

- [84]T. Renganathan, M. V. Yadav, S. Pushpavanam, R. K. Voolapalli, et Y. S. Cho, « CO2 utilization for gasification of carbonaceous feedstocks: A thermodynamic analysis », *Chemical Engineering Science*, vol. 83, p. 159-170, déc. 2012, doi: 10.1016/j.ces.2012.04.024.
- [85]A. Dufour, *Thermochemical Conversion of Biomass for the Production of Energy and Chemicals*. Hoboken, New Jersey: ISTE Ltd and John Wiley & Sons Inc, 2016.
- [86]M. Hosseini, I. Dincer, et M. A. Rosen, « Steam and air fed biomass gasification: Comparisons based on energy and exergy », *International Journal of Hydrogen Energy*, vol. 37, n° 21, p. 16446-16452, nov. 2012, doi: 10.1016/j.ijhydene.2012.02.115.
- [87]C. S. Park, P. S. Roy, et S. H. Kim, « Current Developments in Thermochemical Conversion of Biomass to Fuels and Chemicals », *Gasification for Low-grade Feedstock*, juill. 2018, doi: 10.5772/intechopen.71464.
- [88]M. Pohořelý, M. Jeremiáš, K. Svoboda, P. Kameníková, S. Skoblia, et Z. Beňo, « CO2 as moderator for biomass gasification », *Fuel*, vol. 117, p. 198-205, janv. 2014, doi: 10.1016/j.fuel.2013.09.068.
- [89]S. Rupesh, C. Muraleedharan, et P. Arun, « Energy and exergy analysis of syngas production from different biomasses through air-steam gasification », *Front. Energy*, déc. 2016, doi: 10.1007/s11708-016-0439-1.
- [90]A. M. Parvez, I. M. Mujtaba, et T. Wu, « Energy, exergy and environmental analyses of conventional, steam and CO2-enhanced rice straw gasification », *Energy*, vol. 94, p. 579-588, janv. 2016, doi: 10.1016/j.energy.2015.11.022.
- [91]Z. Abu El-Rub, E. A. Bramer, et G. Brem, « Review of Catalysts for Tar Elimination in Biomass Gasification Processes », *Ind. Eng. Chem. Res.*, vol. 43, n° 22, p. 6911-6919, oct. 2004, doi: 10.1021/ie0498403.
- [92]D. Buentello-Montoya et X. Zhang, « An Energy and Exergy Analysis of Biomass Gasification Integrated with a Char-Catalytic Tar Reforming System », *Energy Fuels*, vol. 33, n° 9, p. 8746-8757, sept. 2019, doi: 10.1021/acs.energyfuels.9b01808.
- [93]Y. Zhang, B. Li, H. Li, et B. Zhang, « Exergy analysis of biomass utilization via steam gasification and partial oxidation », *Thermochimica acta*, 2012.
- [94]Y. Tang, J. Dong, Y. Chi, Z. Zhou, et M. Ni, « Energy and Exergy Analyses of Fluidized-Bed Municipal Solid Waste Air Gasification », *Energy Fuels*, vol. 30, n° 9, p. 7629-7637, sept. 2016, doi: 10.1021/acs.energyfuels.6b01418.
- [95]V. S. Stepanov, « Chemical energies and exergies of fuels », *Energy*, vol. 20, n° 3, p. 235-242, mars 1995, doi: 10.1016/0360-5442(94)00067-D.

- [96] Y. Wu, W. Yang, et W. Blasiak, « Energy and Exergy Analysis of High Temperature Agent Gasification of Biomass », *Energies*, vol. 7, n° 4, Art. n° 4, avr. 2014, doi: 10.3390/en7042107.
- [97] Z.-S. Chen et L.-Q. Wang, « Energy and exergy analysis of gas production from biomass intermittent gasification », *Journal of Renewable and Sustainable Energy*, vol. 5, n° 6, p. 063141, nov. 2013, doi: 10.1063/1.4857395.
- [98] C. C. Sreejith, C. Muraleedharan, et P. Arun, « Energy and exergy analysis of steam gasification of biomass materials: a comparative study », *International Journal of Ambient Energy*, vol. 34, n° 1, p. 35-52, mars 2013, doi: 10.1080/01430750.2012.711085.
- [99] H. Gu, Y. Tang, J. Yao, et F. Chen, « Study on biomass gasification under various operating conditions », *Journal of the Energy Institute*, vol. 92, n° 5, p. 1329-1336, oct. 2019, doi: 10.1016/j.joei.2018.10.002.
- [100] C. R. Vitasari, M. Jurascik, et K. J. Ptasinski, « Exergy analysis of biomass-to-synthetic natural gas (SNG) process via indirect gasification of various biomass feedstock », *Energy*, vol. 36, n° 6, p. 3825-3837, juin 2011, doi: 10.1016/j.energy.2010.09.026.
- [101] Y. Zhang, P. Xu, S. Liang, B. Liu, Y. Shuai, et B. Li, « Exergy analysis of hydrogen production from steam gasification of biomass: A review », *International Journal of Hydrogen Energy*, vol. 44, n° 28, p. 14290-14302, mai 2019, doi: 10.1016/j.ijhydene.2019.02.064.
- [102] M. Hosseini, I. Dincer, et M. A. Rosen, « Steam and air fed biomass gasification: Comparisons based on energy and exergy », *International Journal of Hydrogen Energy*, vol. 37, n° 21, p. 16446-16452, nov. 2012, doi: 10.1016/j.ijhydene.2012.02.115.
- [103] W. Paengjuntuek, J. Boonmak, et J. Mungkalasiri, « Energy Efficiency Analysis in an Integrated Biomass Gasification Fuel Cell System », *Energy Procedia*, vol. 79, p. 430-435, nov. 2015, doi: 10.1016/j.egypro.2015.11.514.
- [104] D. Panepinto, V. Tedesco, E. Brizio, et G. Genon, « Environmental Performances and Energy Efficiency for MSW Gasification Treatment », *Waste Biomass Valor*, vol. 6, n° 1, p. 123-135, févr. 2015, doi: 10.1007/s12649-014-9322-7.
- [105] C. M. van der Meijden, H. J. Veringa, et L. P. L. M. Rabou, « The production of synthetic natural gas (SNG): A comparison of three wood gasification systems for energy balance and overall efficiency », *Biomass and Bioenergy*, vol. 34, n° 3, p. 302-311, mars 2010, doi: 10.1016/j.biombioe.2009.11.001.
- [106] P. Chaiwatanodom, S. Vivanpatarakij, et S. Assabumrungrat, « Thermodynamic analysis of biomass gasification with CO₂ recycle for synthesis gas production », *Applied Energy*, vol. 114, p. 10-17, févr. 2014, doi: 10.1016/j.apenergy.2013.09.052.

- [107] T. Renganathan, M. V. Yadav, S. Pushpavanam, R. K. Voolapalli, et Y. S. Cho, « CO2 utilization for gasification of carbonaceous feedstocks: A thermodynamic analysis », *Chemical Engineering Science*, vol. 83, p. 159-170, déc. 2012, doi: 10.1016/j.ces.2012.04.024.
- [108] M. S. Rao, S. P. Singh, M. S. Sodha, A. K. Dubey, et M. Shyam, « Stoichiometric, mass, energy and exergy balance analysis of countercurrent fixed-bed gasification of post-consumer residues », *Biomass and Bioenergy*, vol. 27, n° 2, p. 155-171, 2004, doi: 10.1016/j.biombioe.2003.11.003.
- [109] Y. Kalinci, A. Hepbasli, et I. Dincer, « Biomass-based hydrogen production: A review and analysis », *International Journal of Hydrogen Energy*, vol. 34, n° 21, p. 8799-8817, nov. 2009, doi: 10.1016/j.ijhydene.2009.08.078.
- [110] R. Saidur, G. BoroumandJazi, S. Mekhilef, et H. A. Mohammed, « A review on exergy analysis of biomass based fuels », *Renewable and Sustainable Energy Reviews*, vol. 16, n° 2, p. 1217-1222, févr. 2012, doi: 10.1016/j.rser.2011.07.076.
- [111] X. Wang, W. Lv, L. Guo, M. Zhai, P. Dong, et G. Qi, « Energy and exergy analysis of rice husk high-temperature pyrolysis », *International Journal of Hydrogen Energy*, vol. 41, n° 46, p. 21121-21130, déc. 2016, doi: 10.1016/j.ijhydene.2016.09.155.
- [112] Y. Zhang, Y. Zhao, X. Gao, B. Li, et J. Huang, « Energy and exergy analyses of syngas produced from rice husk gasification in an entrained flow reactor », *Journal of Cleaner Production*, vol. 95, p. 273-280, mai 2015, doi: 10.1016/j.jclepro.2015.02.053.
- [113] G. Wang, J. Zhang, J. Shao, et P. Zhang, « Experiments and Kinetics Modeling for Gasification of Biomass Char and Coal Char under CO2 and Steam Condition », in *TMS 2016 145th Annual Meeting & Exhibition*, Cham, 2016, p. 375-382, doi: 10.1007/978-3-319-48254-5_45.
- [114] R. Reschmeier et J. Karl, « Experimental study of wood char gasification kinetics in fluidized beds », *Biomass and Bioenergy*, vol. 85, p. 288-299, févr. 2016, doi: 10.1016/j.biombioe.2015.05.029.
- [115] H. Zuo, P.-C. Zhang, J. Zhang, X.-T. Bi, W.-W. Geng, et G. Wang, « Isothermal CO2 Gasification Reactivity and Kinetic Models of Biomass Char/Anthracite Char », *BioResources*, vol. 10, juill. 2015, doi: 10.15376/biores.10.3.5242-5255.
- [116] C. Di Blasi, « Combustion and gasification rates of lignocellulosic chars », *Progress in Energy and Combustion Science*, vol. 35, n° 2, p. 121-140, avr. 2009, doi: 10.1016/j.pecs.2008.08.001.
- [117] J. Wang et S. Wang, « Preparation, modification and environmental application of biochar: A review », *Journal of Cleaner Production*, vol. 227, p. 1002-1022, août 2019, doi: 10.1016/j.jclepro.2019.04.282.

- [118] S. You *et al.*, « A critical review on sustainable biochar system through gasification: Energy and environmental applications », *Bioresource Technology*, vol. 246, p. 242-253, déc. 2017, doi: 10.1016/j.biortech.2017.06.177.
- [119] M. F. Irfan, M. R. Usman, et K. Kusakabe, « Coal gasification in CO₂ atmosphere and its kinetics since 1948: A brief review », *Energy*, vol. 36, n° 1, p. 12-40, janv. 2011, doi: 10.1016/j.energy.2010.10.034.
- [120] W. Klose et M. Wölki, « On the intrinsic reaction rate of biomass char gasification with carbon dioxide and steam », *Fuel*, vol. 84, n° 7, p. 885-892, mai 2005, doi: 10.1016/j.fuel.2004.11.016.
- [121] M. J. Groeneveld et W. P. M. van Swaaij, « 39 Gasification of char particles with CO₂ AND H₂O », *Chemical Engineering Science*, vol. 35, n° 1, p. 307-313, janv. 1980, doi: 10.1016/0009-2509(80)80101-1.
- [122] H. N. Nguyen, L. V. D. Steene, et D. D. Le, « Kinetics of rice husk char gasification in an H₂O or a CO₂ atmosphere », *Energy Sources, Part A: Recovery, Utilization, and Environmental Effects*, vol. 40, n° 14, p. 1701-1713, juill. 2018, doi: 10.1080/15567036.2018.1486900.
- [123] S. Yuan, X. Chen, J. Li, et F. Wang, « CO₂ Gasification Kinetics of Biomass Char Derived from High-Temperature Rapid Pyrolysis », *Energy Fuels*, vol. 25, n° 5, p. 2314-2321, mai 2011, doi: 10.1021/ef200051z.
- [124] M. Morin, S. Pécate, M. Hémati, et Y. Kara, « Pyrolysis of biomass in a batch fluidized bed reactor: Effect of the pyrolysis conditions and the nature of the biomass on the physicochemical properties and the reactivity of char », *Journal of Analytical and Applied Pyrolysis*, vol. 122, p. 511-523, nov. 2016, doi: 10.1016/j.jaap.2016.10.002.
- [125] L. Nowicki, A. Antecká, T. Bedyk, P. Stolarek, et S. Ledakowicz, « The kinetics of gasification of char derived from sewage sludge », *J Therm Anal Calorim*, vol. 104, n° 2, p. 693-700, mai 2011, doi: 10.1007/s10973-010-1032-1.
- [126] S. Porada, G. Czerski, P. Grzywacz, D. Makowska, et T. Dziok, « Comparison of the gasification of coals and their chars with CO₂ based on the formation kinetics of gaseous products », *Thermochimica Acta*, vol. 653, p. 97-105, juill. 2017, doi: 10.1016/j.tca.2017.04.007.
- [127] R. Murillo *et al.*, « Kinetic Model Comparison for Waste Tire Char Reaction with CO₂ », *Ind. Eng. Chem. Res.*, vol. 43, n° 24, p. 7768-7773, nov. 2004, doi: 10.1021/ie040026p.
- [128] A. Kr. Sharma, « Equilibrium and kinetic modeling of char reduction reactions in a downdraft biomass gasifier: A comparison », *Solar Energy*, vol. 82, n° 10, p. 918-928, oct. 2008, doi: 10.1016/j.solener.2008.03.004.

- [129] C. Dupont, G. Boissonnet, J.-M. Seiler, P. Gauthier, et D. Schweich, « Study about the kinetic processes of biomass steam gasification », *Fuel*, vol. 86, n° 1, p. 32-40, janv. 2007, doi: 10.1016/j.fuel.2006.06.011.
- [130] C. Dupont, J.-M. Commandré, P. Gauthier, G. Boissonnet, S. Salvador, et D. Schweich, « Biomass pyrolysis experiments in an analytical entrained flow reactor between 1073K and 1273K », *Fuel*, vol. 87, n° 7, p. 1155-1164, juin 2008, doi: 10.1016/j.fuel.2007.06.028.
- [131] S. Septien, S. Valin, C. Dupont, M. Peyrot, et S. Salvador, « Effect of particle size and temperature on woody biomass fast pyrolysis at high temperature (1000–1400°C) », *Fuel*, vol. 97, p. 202-210, juill. 2012, doi: 10.1016/j.fuel.2012.01.049.
- [132] A. Gómez-Barea, P. Ollero, et C. Fernández-Baco, « Diffusional Effects in CO₂ Gasification Experiments with Single Biomass Char Particles. 1. Experimental Investigation », *Energy Fuels*, vol. 20, n° 5, p. 2202-2210, sept. 2006, doi: 10.1021/ef050365a.
- [133] A. Gómez-Barea, P. Ollero, et A. Villanueva, « Diffusional Effects in CO₂ Gasification Experiments with Single Biomass Char Particles. 2. Theoretical Predictions », *Energy Fuels*, vol. 20, n° 5, p. 2211-2222, sept. 2006, doi: 10.1021/ef0503663.
- [134] A. Mueller, H. D. Haustein, P. Stoesser, T. Kreitzberg, R. Kneer, et T. Kolb, « Gasification Kinetics of Biomass- and Fossil-Based Fuels: Comparison Study Using Fluidized Bed and Thermogravimetric Analysis », *Energy Fuels*, vol. 29, n° 10, p. 6717-6723, oct. 2015, doi: 10.1021/acs.energyfuels.5b01123.
- [135] C. Chen, S. Zhang, K. Xu, G. Luo, et H. Yao, « Experimental and Modeling Study of Char Gasification with Mixtures of CO₂ and H₂O », *Energy Fuels*, vol. 30, n° 3, p. 1628-1635, mars 2016, doi: 10.1021/acs.energyfuels.5b02294.
- [136] S. Vyazovkin et C. A. Wight, « Model-free and model-fitting approaches to kinetic analysis of isothermal and nonisothermal data », *Thermochimica Acta*, vol. 340-341, p. 53-68, déc. 1999, doi: 10.1016/S0040-6031(99)00253-1.
- [137] R. García, C. Pizarro, A. G. Lavín, et J. L. Bueno, « Biomass proximate analysis using thermogravimetry », *Bioresource Technology*, vol. 139, p. 1-4, juill. 2013, doi: 10.1016/j.biortech.2013.03.197.
- [138] S. Tong, L. Li, L. Duan, C. Zhao, et E. J. Anthony, « A kinetic study on lignite char gasification with CO₂ and H₂O in a fluidized bed reactor », oct. 2018, doi: <https://doi.org/10.1016/j.applthermaleng.2018.10.113>.
- [139] J. Preciado-Hernandez, J. Zhang, M. Zhu, Z. Zhang, et D. Zhang, « An experimental study of CO₂ gasification kinetics during activation of a spent tyre pyrolysis char », *Chemical Engineering Research and Design*, vol. 149, p. 129-137, sept. 2019, doi: 10.1016/j.cherd.2019.07.007.

- [140] A. Galadima et O. Muraza, « Catalytic thermal conversion of CO₂ into fuels: Perspective and challenges », *Renewable and Sustainable Energy Reviews*, vol. 115, p. 109333, nov. 2019, doi: 10.1016/j.rser.2019.109333.
- [141] Sundmacher, *Fuel Cell Engineering*. Academic Press, 2012.
- [142] Y. Bai, Y. Wang, S. Zhu, L. Yan, F. Li, et K. Xie, « Synergistic effect between CO₂ and H₂O on reactivity during coal chars gasification », *Fuel*, vol. 126, p. 1-7, juin 2014, doi: 10.1016/j.fuel.2014.02.025.
- [143] T. R. Kosanić, M. B. Čeranić, S. N. Đurić, V. R. Grković, M. M. Milotić, et S. D. Brankov, « Experimental investigation of pyrolysis process of woody biomass mixture », *J. Therm. Sci.*, vol. 23, n° 3, p. 290-296, juin 2014, doi: 10.1007/s11630-014-0709-3.
- [144] U. Wolfesberger, I. Aigner, et H. Hofbauer, « Tar content and composition in producer gas of fluidized bed gasification of wood—Influence of temperature and pressure », *Environmental Progress & Sustainable Energy*, vol. 28, n° 3, p. 372-379, 2009, doi: 10.1002/ep.10387.
- [145] N. van Z.-S. Richard et H. Thunman, « General equations for Biomass Properties », 2003.
- [146] K. Manatura, J.-H. Lu, K.-T. Wu, et H.-T. Hsu, « Exergy analysis on torrefied rice husk pellet in fluidized bed gasification », *Applied Thermal Engineering*, vol. 111, p. 1016-1024, janv. 2017, doi: 10.1016/j.applthermaleng.2016.09.135.
- [147] J. Szargut, *Exergy Method: Technical and Ecological Applications*. WIT Press, 2005.
- [148] C. C. D. Mohabeer, « Bio-oil production by pyrolysis of biomass coupled with a catalytic de-oxygenation treatment », phdthesis, Normandie Université, 2018.
- [149] J. Honerkamp, *Statistical Physics: An Advanced Approach with Applications Web-enhanced with Problems and Solutions*, 2^e éd. Berlin Heidelberg: Springer-Verlag, 2002.
- [150] F. C. Eboh, P. Ahlström, et T. Richards, « Estimating the specific chemical exergy of municipal solid waste », *Energy Science & Engineering*, vol. 4, n° 3, p. 217-231, 2016, doi: 10.1002/ese3.121.
- [151] A. D. Pouwels, A. Tom, G. B. Eijkel, et J. J. Boon, « Characterisation of beech wood and its holocellulose and xylan fractions by pyrolysis-gas chromatography-mass spectrometry », *Journal of Analytical and Applied Pyrolysis*, vol. 11, p. 417-436, oct. 1987, doi: 10.1016/0165-2370(87)85045-3.
- [152] B. Rentsen, « Characterization of flax shives and factors affecting the quality of fuel pellets from flax shives », mars 2010.
- [153] L. Fan *et al.*, « Bio-oil from fast pyrolysis of lignin: Effects of process and upgrading parameters », *Bioresource Technology*, vol. 241, p. 1118-1126, oct. 2017, doi: 10.1016/j.biortech.2017.05.129.

- [154] S. Zhang *et al.*, « The conversion of biomass to light olefins on Fe-modified ZSM-5 catalyst: Effect of pyrolysis parameters », *Science of The Total Environment*, vol. 628-629, p. 350-357, juill. 2018, doi: 10.1016/j.scitotenv.2018.01.316.
- [155] K. A. Rogers et Y. Zheng, « Selective Deoxygenation of Biomass-Derived Bio-oils within Hydrogen-Modest Environments: A Review and New Insights », *ChemSusChem*, vol. 9, n° 14, p. 1750-1772, 2016, doi: 10.1002/cssc.201600144.
- [156] J. Li, Y. Li, Y. Wu, et M. Zheng, « A comparison of biochars from lignin, cellulose and wood as the sorbent to an aromatic pollutant », *Journal of Hazardous Materials*, vol. 280, p. 450-457, sept. 2014, doi: 10.1016/j.jhazmat.2014.08.033.
- [157] Y. Cui, W. Wang, et J. Chang, « Study on the Product Characteristics of Pyrolysis Lignin with Calcium Salt Additives », *Materials (Basel)*, vol. 12, n° 10, mai 2019, doi: 10.3390/ma12101609.
- [158] H. Kawamoto, « Lignin pyrolysis reactions », *J Wood Sci*, vol. 63, n° 2, p. 117-132, avr. 2017, doi: 10.1007/s10086-016-1606-z.
- [159] D. F. Arseneau, « Competitive Reactions in the Thermal Decomposition of Cellulose », *Can. J. Chem.*, vol. 49, n° 4, p. 632-638, févr. 1971, doi: 10.1139/v71-101.
- [160] C. Wan, F. Yu, Y. Zhang, Q. Li, et J. Wooten, « Material Balance and Energy Balance Analysis for Syngas Generation by a Pilot-Plant Scale Downdraft Gasifier », déc. 2013. doi/10.1166/jbmb.2013.1374.
- [161] B. Jin, H. Zhao, et Z. Liu, « Chapter 11 - System Integration and Optimization for Large Scale Oxy-fuel Combustion Systems », in *Oxy-Fuel Combustion*, C. Zheng et Z. Liu, Éd. Academic Press, 2018, p. 223-238.
- [162] J. G. Speight, « Chapter 13 - Upgrading by Gasification », in *Heavy Oil Recovery and Upgrading*, J. G. Speight, Éd. Gulf Professional Publishing, 2019, p. 559-614.
- [163] A. Ephraïm, V. Pozzobon, O. Louisnard, D. Pham Minh, A. Nzihou, et P. Sharrock, « Simulation of biomass char gasification in a downdraft reactor for syngas production », *AIChE Journal*, vol. 62, p. n/a-n/a, nov. 2015, doi: 10.1002/aic.15111.
- [164] B. D. Caprariis *et al.*, « Carbon Dioxide Reforming of Tar During Biomass Gasification », *1*, vol. 37, p. 97-102, juin 2014, doi: 10.3303/CET1437017.
- [165] N. Kaisalo, « Tar reforming in biomass gasification gas cleaning: Dissertation », 2017, Consulté le: févr. 21, 2020. [En ligne]. Disponible sur: <https://cris.vtt.fi/en/publications/tar-reforming-in-biomass-gasification-gas-cleaning-dissertation>.
- [166] K. J. : Laidler, N. H. : Sagert, B. W. Wojciechowski, et E. W. R. Steacie, « Kinetics and mechanisms of the thermal decomposition of propane I. The Uninhibited of reaction », *Proceedings of the Royal Society of London. Series A. Mathematical and Physical Sciences*, vol. 270, n° 1341, p. 242-253, nov. 1962, doi: 10.1098/rspa.1962.0215.

- [167] M. Back, « Mechanism of the Pyrolysis of Acetylene », *Canadian Journal of Chemistry*, vol. 49, p. 2199-2204, févr. 2011, doi: 10.1139/v71-359.
- [168] C. Guizani, M. Jeguirim, R. Gadiou, F. J. Escudero Sanz, et S. Salvador, « Biomass char gasification by H₂O, CO₂ and their mixture: Evolution of chemical, textural and structural properties of the chars », *Energy*, vol. 112, p. 133-145, oct. 2016, doi: 10.1016/j.energy.2016.06.065.
- [169] M. Morin, X. Nitsch, et M. Hemati, « Interactions between char and tar during the steam gasification in a fluidized bed reactor », *Fuel*, vol. 224, p. 600-609, juill. 2018, doi: 10.1016/j.fuel.2018.03.050.
- [170] C. Fushimi, T. Wada, et A. Tsutsumi, « Inhibition of steam gasification of biomass char by hydrogen and tar », *Biomass and bioenergy*, 2011.
- [171] A. M. Parvez, I. M. Mujtaba, et T. Wu, « Energy, exergy and environmental analyses of conventional, steam and CO₂-enhanced rice straw gasification », *Energy*, vol. 94, p. 579-588, janv. 2016, doi: 10.1016/j.energy.2015.11.022.
- [172] D. Buentello-Montoya et X. Zhang, « An Energy and Exergy Analysis of Biomass Gasification Integrated with a Char-Catalytic Tar Reforming System », *Energy Fuels*, vol. 33, n° 9, p. 8746-8757, sept. 2019, doi: 10.1021/acs.energyfuels.9b01808.
- [173] S. Pereira, F. Ribeiro, et M. M. Pereira, « Study of promoters to Reverse Boudouard reaction under regeneration step conditions of FCC process », 2015.
- [174] K. Palacio, A. Sanchez, et J. F. Espinal, « Thermodynamic evaluation of carbon dioxide gasification reactions at oxy-combustion conditions », *Combustion Science and Technology*, vol. 190, n° 9, p. 1515-1527, sept. 2018, doi: 10.1080/00102202.2018.1454916.
- [175] L. Wang, P. Maziarka, Ø. Skreiberg, T. Løvås, M. Wądrzyk, et A. Sevault, « Study of CO₂ gasification reactivity of biocarbon produced at different conditions », *Energy Procedia*, vol. 142, p. 991-996, déc. 2017, doi: 10.1016/j.egypro.2017.12.158.
- [176] M. Morin, S. Pécate, et M. Hemati, « Experimental study and modelling of the kinetic of biomass char gasification in a fluidized bed reactor », *Chemical Engineering Research and Design*, vol. 131, p. 488-505, mars 2018, doi: 10.1016/j.cherd.2017.09.030.
- [177] M. Kumar, R. C. Gupta, et T. Sharma, « Effects of carbonisation conditions on the yield and chemical composition of Acacia and Eucalyptus wood chars », *Biomass and Bioenergy*, vol. 3, n° 6, p. 411-417, janv. 1992, doi: 10.1016/0961-9534(92)90037-Q.
- [178] P. Basu, « Chapter 7 - Gasification Theory », in *Biomass Gasification, Pyrolysis and Torrefaction (Second Edition)*, P. Basu, Éd. Boston: Academic Press, 2013, p. 199-248.

- [179] X. Zeng, F. Wang, Y. Wang, A. Li, J. Yu, et G. Xu, « Characterization of Char Gasification in a Micro Fluidized Bed Reaction Analyzer », *Energy Fuels*, vol. 28, n° 3, p. 1838-1845, mars 2014, doi: 10.1021/ef402387r.
- [180] B. Cluet, « Évaluation de la ségrégation de la biomasse dans un lit fluidisé et modélisation globale du procédé de gazéification », Theses, Université de Lorraine, 2014.
- [181] G. Lardier *et al.*, « Gas and Bed Axial Composition in a Bubbling Fluidized Bed Gasifier: Results with Miscanthus and Olivine », *Energy Fuels*, vol. 30, n° 10, p. 8316-8326, oct. 2016, doi: 10.1021/acs.energyfuels.6b01816.
- [182] Y. Iqbal et I. Lewandowski, « Biomass composition and ash melting behaviour of selected miscanthus genotypes in Southern Germany », *Fuel*, vol. 180, p. 606-612, sept. 2016, doi: 10.1016/j.fuel.2016.04.073.
- [183] B. Sajjadi, W.-Y. Chen, et N. O. Egiebor, « A comprehensive review on physical activation of biochar for energy and environmental applications », *Reviews in Chemical Engineering*, vol. 35, n° 6, p. 735-776, juill. 2019, doi: 10.1515/revce-2017-0113.
- [184] Y. Hu, H. Yu, F. Zhou, et D. Chen, « A comparison between CO₂ gasification of various biomass chars and coal char », *The Canadian Journal of Chemical Engineering*, vol. 97, p. 1326-1331, janv. 2019, doi: 10.1002/cjce.23417.
- [185] H. Liu, C. Luo, S. Kato, S. Uemiya, M. Kaneko, et T. Kojima, « Kinetics of CO₂/Char gasification at elevated temperatures: Part I: Experimental results », *Fuel Processing Technology*, vol. 87, n° 9, p. 775-781, sept. 2006, doi: 10.1016/j.fuproc.2006.02.006.
- [186] C. Guizani, « Effects of CO₂ on the biomass pyro-gasification in High Heating Rate and Low Heating Rate conditions », Theses, Ecole des Mines d'Albi-Carmaux, 2014.
- [187] P. Ollero, A. Serrera, R. Arjona, et S. Alcantarilla, « The CO₂ gasification kinetics of olive residue », *Biomass and Bioenergy*, vol. 24, n° 2, p. 151-161, févr. 2003, doi: 10.1016/S0961-9534(02)00091-0.
- [188] M. Barrio et J. E. Hustad, « CO₂ Gasification of Birch Char and the Effect of CO Inhibition on the Calculation of Chemical Kinetics », in *Progress in Thermochemical Biomass Conversion*, John Wiley & Sons, Ltd, 2008, p. 47-60.
- [189] Q. Sun, W. Li, H. Chen, et B. Li, « The CO₂-gasification and kinetics of Shenmu maceral chars with and without catalyst », *Fuel*, vol. 83, n° 13, p. 1787-1793, sept. 2004, doi: 10.1016/j.fuel.2004.02.020.
- [190] A. Mianowski, T. Radko, et T. Siudyga, « The reactivity of cokes in Boudouard–Bell reactions in the context of an Ergun model », *J Therm Anal Calorim*, vol. 122, n° 2, p. 1013-1021, nov. 2015, doi: 10.1007/s10973-015-4761-3.

- [191] D. G. Roberts et D. J. Harris, « High-Pressure Char Gasification Kinetics: CO Inhibition of the C–CO₂ Reaction », *Energy Fuels*, vol. 26, n° 1, p. 176-184, janv. 2012, doi: 10.1021/ef201174k.
- [192] A. Diedhiou, L.-G. Ndiaye, A. Bensakhria, et O. Sock, « Thermochemical conversion of cashew nut shells, palm nut shells and peanut shells char with CO₂ and/or steam to aliment a clay brick firing unit », *Renewable Energy*, vol. 142, p. 581-590, nov. 2019, doi: 10.1016/j.renene.2019.04.129.
- [193] W. F. DeGroot et F. Shafizadeh, « Kinetics of gasification of Douglas Fir and Cottonwood chars by carbon dioxide », *Fuel*, vol. 63, n° 2, p. 210-216, févr. 1984, doi: 10.1016/0016-2361(84)90039-5.
- [194] L. Van de steene, J. P. Tagutchou, F. J. Escudero Sanz, et S. Salvador, « Gasification of woodchip particles: Experimental and numerical study of char–H₂O, char–CO₂, and char–O₂ reactions », *Chemical Engineering Science*, vol. 66, n° 20, p. 4499-4509, oct. 2011, doi: 10.1016/j.ces.2011.05.045.
- [195] I. Matsui, D. Kunii, et T. Furusawa, « Study of char gasification by carbon dioxide. 1. Kinetic study by thermogravimetric analysis », *Ind. Eng. Chem. Res.*, vol. 26, n° 1, p. 91-95, janv. 1987, doi: 10.1021/ie00061a017.
- [196] J. François *et al.*, « Modeling of a Biomass Gasification CHP Plant: Influence of Various Parameters on Energetic and Exergetic Efficiencies », *Energy Fuels*, vol. 27, n° 12, p. 7398-7412, déc. 2013, doi: 10.1021/ef4011466.
- [197] C. K. Law, *Combustion Physics*. Cambridge University Press, 2010.
- [198] Y. A. Çengel et M. A. Boles, *Thermodynamics: an engineering approach*. McGraw-Hill Higher Education, 2006.
- [199] R. U. Ayres, L. W. Ayres, et K. Martinàs, *Eco-Thermodynamics: Exergy and Life Cycle Analysis*. INSEAD, 1995.
- [200] K. T. Lee et C. Ofori-Boateng, *Sustainability of Biofuel Production from Oil Palm Biomass*. Springer Science & Business Media, 2013.
- [201] W. M. Haynes, *CRC Handbook of Chemistry and Physics, 95th Edition*, 95^e éd. Boca Raton; London; New York: CRC Press, 2014.
- [202] K. T. Lee et C. Ofori-Boateng, *Sustainability of Biofuel Production from Oil Palm Biomass*. Springer Singapore, 2013.
- [203] R. U. Ayres, L. W. Ayres, et K. Martinàs, *Eco-Thermodynamics: Exergy and Life Cycle Analysis*. INSEAD, 1995.
- [204] W. M. Haynes, *CRC Handbook of Chemistry and Physics, 95th Edition*, 95^e éd. Boca Raton; London; New York: CRC Press, 2014.

- [205] Y. Xu, X. Hu, W. Li, et Y. Shi, « Preparation and Characterization of Bio-oil from Biomass », *Progress in Biomass and Bioenergy Production*, juill. 2011, doi: 10.5772/16466.
- [206] H. Ben, F. Wu, Z. Wu, G. Han, W. Jiang, et A. J. Ragauskas, « A Comprehensive Characterization of Pyrolysis Oil from Softwood Barks », *Polymers (Basel)*, vol. 11, n° 9, août 2019, doi: 10.3390/polym11091387.
- [207] R. Lødeng et H. Bergem, « 7 - Stabilisation of pyrolysis oils », in *Direct Thermochemical Liquefaction for Energy Applications*, L. Rosendahl, Éd. Woodhead Publishing, 2018, p. 193-247.
- [208] H. Chen, « 4 - Lignocellulose biorefinery conversion engineering », in *Lignocellulose Biorefinery Engineering*, H. Chen, Éd. Woodhead Publishing, 2015, p. 87-124.
- [209] M. S. Talmadge *et al.*, « A perspective on oxygenated species in the refinery integration of pyrolysis oil », *Green Chem.*, vol. 16, n° 2, p. 407-453, janv. 2014, doi: 10.1039/C3GC41951G.
- [210] M. Khlewee, « Production of Bio-oil with Different Oxygen Content and Characterization of Catalytic Upgrading to Transportation Fuel », déc. 2017.
- [211] P. Giudicianni, G. Cardone, et R. Ragucci, « Cellulose, hemicellulose and lignin slow steam pyrolysis: Thermal decomposition of biomass components mixtures », *Journal of Analytical and Applied Pyrolysis*, vol. 100, p. 213-222, févr. 2013, doi: 10.1016/j.jaap.2012.12.026.
- [212] A. Demirbas et G. Arin, « An Overview of Biomass Pyrolysis », *Energy Sources*, vol. 24, n° 5, p. 471-482, mai 2002, doi: 10.1080/00908310252889979.
- [213] F. M. A. Geilen *et al.*, « Highly Selective Decarbonylation of 5-(Hydroxymethyl)furfural in the Presence of Compressed Carbon Dioxide », *Angewandte Chemie International Edition*, vol. 50, n° 30, p. 6831-6834, 2011, doi: 10.1002/anie.201007582.
- [214] X. Sheng, M. E. S. Lind, et F. Himo, « Theoretical study of the reaction mechanism of phenolic acid decarboxylase », *The FEBS Journal*, vol. 282, n° 24, p. 4703-4713, 2015, doi: 10.1111/febs.13525.
- [215] A. Saraeian, M. W. Nolte, et B. H. Shanks, « Deoxygenation of biomass pyrolysis vapors: Improving clarity on the fate of carbon », *Renewable and Sustainable Energy Reviews*, vol. 104, p. 262-280, avr. 2019, doi: 10.1016/j.rser.2019.01.037.
- [216] X. Li, W. Dong, J. Zhang, S. Shao, et Y. Cai, « Preparation of bio-oil derived from catalytic upgrading of biomass vacuum pyrolysis vapor over metal-loaded HZSM-5 zeolites », *Journal of the Energy Institute*, vol. 93, n° 2, p. 605-613, avr. 2020, doi: 10.1016/j.joei.2019.06.005.

- [217] X. Huang, J. M. Ludenhoff, M. Dirks, X. Ouyang, M. D. Boot, et E. J. M. Hensen, « Selective Production of Biobased Phenol from Lignocellulose-Derived Alkylmethoxyphenols », *ACS Catal.*, vol. 8, n° 12, p. 11184-11190, déc. 2018, doi: 10.1021/acscatal.8b03430.
- [218] P. Lahijani, Z. A. Zainal, A. R. Mohamed, et M. Mohammadi, « CO₂ gasification reactivity of biomass char: Catalytic influence of alkali, alkaline earth and transition metal salts », *Bioresource Technology*, vol. 144, p. 288-295, sept. 2013, doi: 10.1016/j.biortech.2013.06.059.
- [219] Z. Ravaghi *et al.*, « Influence of the effective parameters on H₂:CO Ratio Of Syngas At Low-Temperature Gasification », *Chemical Engineering Transactions*, vol. 37, p. 253-258, janv. 2014, doi: 10.3303/CET1437043.
- [220] T. A. Milne, R. J. Evans, et N. Abatzoglou, « Biomass Gasifier “« Tars »”: Their Nature, Formation, and Conversion », National Renewable Energy Laboratory, Golden, CO (US), NREL/TP-570-25357; ON: DE00003726, nov. 1998. doi: 10.2172/3726.
- [221] J. Kluska, P. Kazimierski, M. Ochnio, et D. Kardaś, « Characteristic of tar content and syngas composition during beech updraft gasification », *Eco-Energetics: technologies, environment, law and economy*, vol. 2, p. 63-78, juin 2019, doi: 10.24426/eco-energetics.v2i2.110.
- [222] X. Nitsch et J.-M. Commandre, *Tar cracking and reforming in fluidized-bed biomass gasification conditions*. .
- [223] J. Nie, B. Wang, L. Wei, et L. Sun, « Investigation on the Transformation Behavior of Nickel and Vanadium during Steam Gasification of Petroleum Coke », *Industrial & Engineering Chemistry Research*, vol. 57, oct. 2018, doi: 10.1021/acs.iecr.8b03310.
- [224] M. Tangstad, J. P. Beukes, J. Steenkamp, et E. Ringdalen, « 14 - Coal-based reducing agents in ferroalloys and silicon production », in *New Trends in Coal Conversion*, I. Suárez-Ruiz, M. A. Diez, et F. Rubiera, Éd. Woodhead Publishing, 2019, p. 405-438.
- [225] J. Hunt, A. Ferrari, A. Lita, M. Crosswhite, B. Ashley, et A. E. Stiegman, « Microwave-Specific Enhancement of the Carbon–Carbon Dioxide (Boudouard) Reaction », *J. Phys. Chem. C*, vol. 117, n° 51, p. 26871-26880, déc. 2013, doi: 10.1021/jp4076965.
- [226] E. E. Kwon, Y. J. Jeon, et H. Yi, « New candidate for biofuel feedstock beyond terrestrial biomass for thermo-chemical process (pyrolysis/gasification) enhanced by carbon dioxide (CO₂) », *Bioresource Technology*, vol. 123, p. 673-677, nov. 2012, doi: 10.1016/j.biortech.2012.07.035.
- [227] C. Guizani, F. J. Escudero Sanz, et S. Salvador, « Effects of CO₂ on biomass fast pyrolysis: Reaction rate, gas yields and char reactive properties », *Fuel*, vol. 116, p. 310-320, janv. 2014, doi: 10.1016/j.fuel.2013.07.101.

- [228] L. Chen, C. Dupont, S. Salvador, M. Grateau, G. Boissonnet, et D. Schweich, « Experimental study on fast pyrolysis of free-falling millimetric biomass particles between 800°C and 1000°C », *Fuel*, vol. 106, p. 61-66, avr. 2013, doi: 10.1016/j.fuel.2012.11.058.
- [229] D. Serrano, S. Sánchez-Delgado, C. Sobrino, et C. Marugán-Cruz, « Defluidization and agglomeration of a fluidized bed reactor during *Cynara cardunculus* L. gasification using sepiolite as a bed material », *Fuel Processing Technology*, vol. 131, p. 338-347, mars 2015, doi: 10.1016/j.fuproc.2014.11.036.
- [230] A. Juneja, A. Juneja, S. Mani, et J. Kastner, « Catalytic Cracking of Tar using BioChar as a Catalyst », *2010 Pittsburgh, Pennsylvania, June 20 - June 23, 2010*, Consulté le: août 05, 2020. [En ligne]. Disponible sur: https://www.academia.edu/31065318/Catalytic_Cracking_of_Tar_using_BioChar_as_a_Catalyst.
- [231] A. S. Al-Rahbi, J. A. Onwudili, et P. T. Williams, « Thermal decomposition and gasification of biomass pyrolysis gases using a hot bed of waste derived pyrolysis char », *Bioresource Technology*, vol. 204, p. 71-79, mars 2016, doi: 10.1016/j.biortech.2015.12.016.
- [232] Y. Zhang, Y. Luo, W. Wu, S. Zhao, et Y. Long, « Heterogeneous Cracking Reaction of Tar over Biomass Char, Using Naphthalene as Model Biomass Tar », *Energy Fuels*, vol. 28, n° 5, p. 3129-3137, mai 2014, doi: 10.1021/ef4024349.
- [233] Z. Y. K. A. El-Rub, « Biomass char as an in-situ catalyst for tar removal in gasification systems », mars 2008, Consulté le: juill. 28, 2020. [En ligne]. Disponible sur: <https://research.utwente.nl/en/publications/biomass-char-as-an-in-situ-catalyst-for-tar-removal-in-gasificati>.
- [234] X. Zeng *et al.*, « Recent progress in tar removal by char and the applications: A comprehensive analysis », *Carbon Resources Conversion*, vol. 3, p. 1-18, janv. 2020, doi: 10.1016/j.crcon.2019.12.001.
- [235] S. Hosokai, K. Kumabe, M. Ohshita, K. Norinaga, C.-Z. Li, et J. Hayashi, « Mechanism of decomposition of aromatics over charcoal and necessary condition for maintaining its activity », *Fuel*, vol. 87, n° 13, p. 2914-2922, oct. 2008, doi: 10.1016/j.fuel.2008.04.019.
- [236] F. Rodriguez-Reinoso, « Controlled Gasification of Carbon and Pore Structure Development », in *Fundamental Issues in Control of Carbon Gasification Reactivity*, J. Lahaye et P. Ehrburger, Éd. Dordrecht: Springer Netherlands, 1991, p. 533-571.
- [237] M. Molina-Sabio, M. T. Gonzalez, F. Rodriguez-Reinoso, et A. Sepúlveda-Escribano, « Effect of steam and carbon dioxide activation in the micropore size distribution of activated carbon », *Carbon*, vol. 34, n° 4, p. 505-509, janv. 1996, doi: 10.1016/0008-6223(96)00006-1.

- [238] K. Ajay, D. Jones, et M. Hanna, « Thermochemical Biomass Gasification: A Review of the Current Status of the Technology », *Energies*, vol. 2, sept. 2009, doi: 10.3390/en20300556.
- [239] H. Zhang *et al.*, « Biomass fast pyrolysis in a fluidized bed reactor under N₂, CO₂, CO, CH₄ and H₂ atmospheres », *Bioresource Technology*, vol. 102, n° 5, p. 4258-4264, mars 2011, doi: 10.1016/j.biortech.2010.12.075.
- [240] T. Kreitzberg, H. Haustein, B. Gövert, et R. Kneer, « Investigation of gasification reaction of pulverized char under N₂/CO₂ atmosphere in a small-scale fluidized bed reactor », *Journal of Energy Resources Technology*, vol. 138, févr. 2016, doi: 10.1115/1.4032791.
- [241] I. Matsui, T. Kojima, D. Kunii, et T. Furusawa, « Study of char gasification by carbon dioxide. 2. Continuous gasification in fluidized bed », *Ind. Eng. Chem. Res.*, vol. 26, n° 1, p. 95-100, janv. 1987, doi: 10.1021/ie00061a018.

Appendix

Appendix A1

This section included the additional tables, figures and data that were not included in chapter 2.

Table A1.1. Thermodynamics properties of gaseous compounds.

Element	a	b ($\times 10^{-2}$)	c ($\times 10^{-5}$)	d ($\times 10^{-9}$)	LHV (kJ/kmol) [197]
N ₂	28.90	-0.15	0.81	-2.87	---
H ₂	29.11	-0.19	0.40	-0.87	240420
CO	28.16	0.17	0.53	-2.22	282800
CO ₂	22.26	5.98	-3.50	7.47	---
CH ₄	18.89	5.02	1.27	-11.01	801280
C ₂ H ₂	21.80	9.21	-6.52	18.21	1253200
C ₂ H ₄	3.95	15.64	-8.34	17.67	1321600
C ₂ H ₆	6.90	17.27	-6.41	7.29	1425000
C ₃ H ₈	-4.04	30.48	-15.72	31.74	2037200
H ₂ O(g)	32.24	0.19	1.06	-3.60	---

*Coefficients were obtained from NIST Tables and Çengel and Boles [198]

Table A1.2. Specific enthalpy, entropy and chemical standard exergy for gases.

Element	h° (kJ/kmol) [198]	^b s° (kJ/kmol.K) [198]	ex _{ch} (kJ/kmol) [199], [200]
N ₂	8669	191.5	720
H ₂	8468	130.6	236100
CO	8669	197.5	275100
CO ₂	9364	213.7	19870
CH ₄	10019	186.2	831650
C ₂ H ₂	10012	200.9	1265000
C ₂ H ₄	10518	219.3	1361100
C ₂ H ₆	10900	229.5	1495000
C ₃ H ₈	14776	269.9	2152800
H ₂ O(g)	9904	188.8	10

^b Reference NIST Thermodynamic tables.

Appendix

Table A1.3. Thermodynamics properties of bio-oil major compounds.

Substance Group	Selected molecule	Phase change from 25°C to T °C	^a Cp_i (kJ/kmol.K)	^b Δh_{phase_change} (kJ/kmol)	^c LHV_i (kJ/kmol)
Acids	Acetic acid	liquid-Gas	123.65	23.70	874000.00
Alkanes	Nonane	Liquid-Gas	425.63	46.50	5683300.00
Alkenes	Toluene	Liquid-Gas	179.39	33.18	3908880.00
Alcohols	Catechol	Liquid-Gas	234.75	71.90	2874000.00
Aldehydes	Furfural	Liquide-Gas	188.18	47.60	2339000.00
Amides	Benzamide	Solid-Liquide-Gas	123.15	63.80	1182700.00
Ketones	2-Cyclopenten-1-one	Liquide-Gas	214.00	42.60	2873500.00
Esters	Allyl butyrate	Liquid- Gas	210.13	35.02	2256000.00
Furans	Furan	Liquid- Gas	141.77	27.71	2083500.00
Guaiaicol	4-Methylcatechol	Liquid- Gas	270.78	52.70	3590000.00
Phenols	Phenol	Solid-Liquide-Gas	209.53	46.80	3054000.00
Sugars	Levoglucozan	Solid-Liquide-Gas	353.93	87.25	2875000.00

^a Calculated from 25 °C to the boiling point; heat capacities from boiling point to operating temperature were calculated using Aspen Plus.

^{b, c} Obtained from NIST thermodynamics tables and CRC handbook [201].

Table A1.4. Chemical standard exergy for major bio-oil compounds.

Selected molecule	ex_{ch} (kJ/kmol) [202], [203]
Acetic acid	907200.00
Nonane	6064900.00
Toluene	4587900.00
Catechol	3126200.00
Furfural	1086711.00
Benzamide	1251000.00
2-Cyclopenten-1-one	3104060.00
Allyl butyrate	2278750.00
Furan	2123420.00
4-Methylcatechol	3701220.00
Phenol	3126200.00
Levoglucozan	2791262.00

Table A1.5. Thermodynamics properties of major tar compounds.

Substance Group	Element	Phase change from 25°C to T °C	^a Cp_i (kJ/kmol.K)	^b Δh_{phase_change} (kJ/kmol)	^c LHV_i (kJ/kmol)
Phenols	Phenol	Solid-liquid-Gas	209.18	46.80	3054000
Furans	Furan	Liquid-Gas	133.95	47.60	2339000
HAC	O-Cresol	Solid-Liquid-Gas	244.70	46.20	3705000
AC	Toluene	Liquid-Gas	179.39	33.18	3908880
Naphthalenes	Naphthalene	Solid-Liquide-Gas	264.23	47.60	5182700
LPAH	Indene	Liquid-Gas	191.44	45.30	4795500
HPAH	Pyrene	Solid-Liquide-Gas	472.81	76.00	7850700
Other	Acetic acid	Liquid- Gas	140.59	23.70	874000

^a Calculated from 25 °C to the boiling point; heat capacities from boiling point to operating temperature were calculated using Aspen Plus.

^{b, c} Obtained from NIST thermodynamics tables and CRC handbook [204]

Table A1.6. Chemical standard exergy for tars.

Element	ex_{ch} (kJ/kmol) [199], [200]
Acetic acid	907200
Phenol	3126200
Furan	1086711
O-Cresol	3763000
Toluene	3931000
Indene	5213000
Naphthalene	5251100
Pyrene	7218100

The following section is the interpretation of the mass balance and product distribution of the obtained results from the thesis of Mohabeer C. [148]. This discussion was not included in the principal sections of the manuscript as the results of mass balance and experimental runs came essentially from the previously mentioned thesis. Meanwhile, a detailed and self-interpretation of the results was included, in order to support additional questions about the subject, when employing thermodynamic analysis.

A1.1 Results and discussion

The following results presented an error margin of approximately 1% due to the experimental uncertainty and deviations. The errors surrounding the experimental test were those found in deviation calculations after experiment repetitions, mass weighting, values rounding and equipment tolerance. The uncertainty of values was added with error bars over the presented results. In gaseous components, the light hydrocarbons with more than one carbon molecule

were presented as C₂+ (including, C₂H₂, C₂H₄ and C₂H₆) and C₃+ (Including, C₃H₄, C₃H₆ and C₃H₈) in this work for convenience.

The mass balance and product distribution results obtained from the pyrolysis of beech wood, flax shives, cellulose, hemicellulose and lignin, with and without catalytic treatment were taken from the thesis work of Mohabeer C. [148], and summarized in **Table A1.7**.

A1.1.1 Pyrolysis of beech wood and flax shives

The results of mass balance obtained from the pyrolysis at 500°C for both biomasses, beech wood and flax shives were illustrated in **Figure A1.1**. As can be observed the highest yield of products corresponded to bio-oil in both cases. For the case of beech wood 69.7 wt. % was obtained and for flax shives 59.5 wt. %. Both raw materials corresponded to the classification of lignocellulosic biomass, while beech wood presented a higher bio-oil yield than flax shives. Explanation to this can be found by looking to the proximate analysis of both biomasses, beech wood accounted for values of 75.4% of volatile matter, while flax shives 69.2%. As can be observed the values of beech wood volatile matter by proximate analysis (**Section 1.2 of Chapter 2**) already manifested a tendency to release higher matter than flax shives.

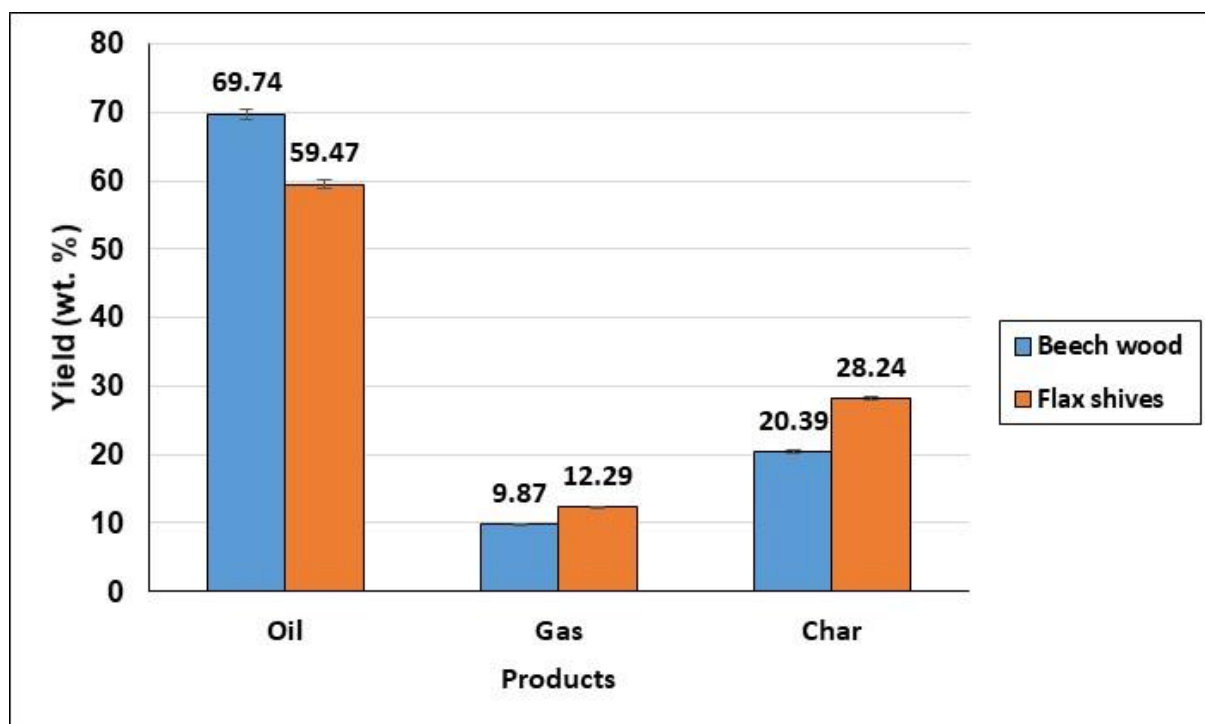


Figure A1.1. Products yield from the pyrolysis of beech wood and flax shives at 500°C.

Table A1.7. Mass balance of results in a semi-continuous reactor.

Raw Material	Oxygen content (%)	^a Gases components: % molar						^b Bio-oil concentration: % Vol.												Streams: Yield %		
		H ₂	CO	CO ₂	CH ₄	^c C ₂₊	^c C ₃₊	(a)	(b)	(c)	(d)	(e)	(f)	(g)	(h)	(i)	(j)	(k)	(l)	Bio-oil	Gas	Biochar
Beech Wood (no catalyst)	33.82	1.04	44.61	39.99	11.38	2.77	0.00	36.36	14.46	3.62	0.85	4.83	7.36	3.92	10.26	9.58	2.16	1.34	5.26	69.73	9.87	20.40
Beech Wood (HZSM-5)	18.4	0.93	49.6	32.36	5.26	7.12	4.73	7.50	46.92	1.75	0.00	13.28	7.47	3.82	6.21	5.42	4.56	3.06	0.00	49.67	28.48	21.85
Beech Wood (Fe-HZSM-5)	14.5	15.3	28.61	38.61	6.18	6.56	4.74	0.00	71.53	1.04	0.00	8.97	5.09	0.00	7.30	0.00	3.99	2.07	0.00	57.76	19.80	22.44
Flax Shives (no catalyst)	34.76	1.30	35.39	50.18	10.51	1.60	0.00	37.26	12.92	3.33	2.01	4.54	11.02	3.48	8.53	10.85	0.76	1.30	3.99	59.47	12.29	28.24
Flax Shives (HZSM-5)	14.42	1.35	42.34	35.79	7.29	7.66	5.56	0.00	65.50	0.57	0.00	10.51	9.27	3.22	5.35	1.49	3.04	1.05	0.00	50.67	22.67	26.66
Flax Shives (Fe-HZSM-5)	13.97	13.77	25.83	43.41	6.31	5.57	4.81	0.00	63.54	0.82	0.00	12.15	5.79	1.36	9.04	0.00	5.64	1.66	0.00	49.50	23.26	27.24
Cellulose	33.82	1.64	54.80	34.27	3.67	3.25	1.79	7.04	11.63	5.58	0.60	4.76	8.44	2.93	11.19	4.46	0.56	0.00	42.8	75.66	11.84	12.50
Xylan	28.05	1.60	46.59	43.78	5.37	2.41	0.00	24.68	9.91	3.46	7.39	3.58	17.13	8.43	10.61	8.54	2.27	1.19	2.82	78.54	8.58	12.87
Lignine	19.38	15.6	9.54	59.97	11.35	3.57	0.00	14.01	47.66	0.00	9.68	10.0	0.00	5.84	6.07	0.00	0.00	47.7	0.00	32.78	10.60	56.62

^a Dry basis.

^b a) Acids, b) Phenols, c) Aldehydes, d) Alkanes, e) Alkenes, f) Alcohols, g) Amides, h) Ketones, i) Esters, j) Furans, k) Guaiacols, l) Sugars.

^c C₂₊ represented: C₂H₂, C₂H₄ and C₂H₆. C₃₊ represented: C₃H₄, C₃H₆ and C₃H₈.

Biochar yield obtained from flax shives presented a variation of approximately 8%, from the one obtained from beech wood pyrolysis. Despite the understanding that both biomasses were not strictly the same, the proximate analysis (**Section 1.2 of Chapter 2**) showed that the fixed carbon value of flax shives (19.97 %) was higher than beech wood (17.54%). It can be considered that the lasted was one of the reasons for the difference in biochar yield from both biomasses. The yields obtained from the pyrolysis gases from both biomasses was very close, only a difference of 2.43% in the yield of products, for this reason, it can be considered that gaseous products did not present variation comparing both biomasses results, meanwhile, to complete this statement the individual gas component were analyzed.

Figure A1.2 showed the total volume of individual gases obtained from the pyrolysis of biomasses. As can be observed the total volume was very similar for both biomasses, the main difference was the produced volume of carbon dioxide in flax shives (126.7 ml) concerning beech wood (87.52 ml), for a difference of approximately 39.2 ml. This result contributed to the observed mass yield difference presented in the pyrolysis gases of both biomasses.

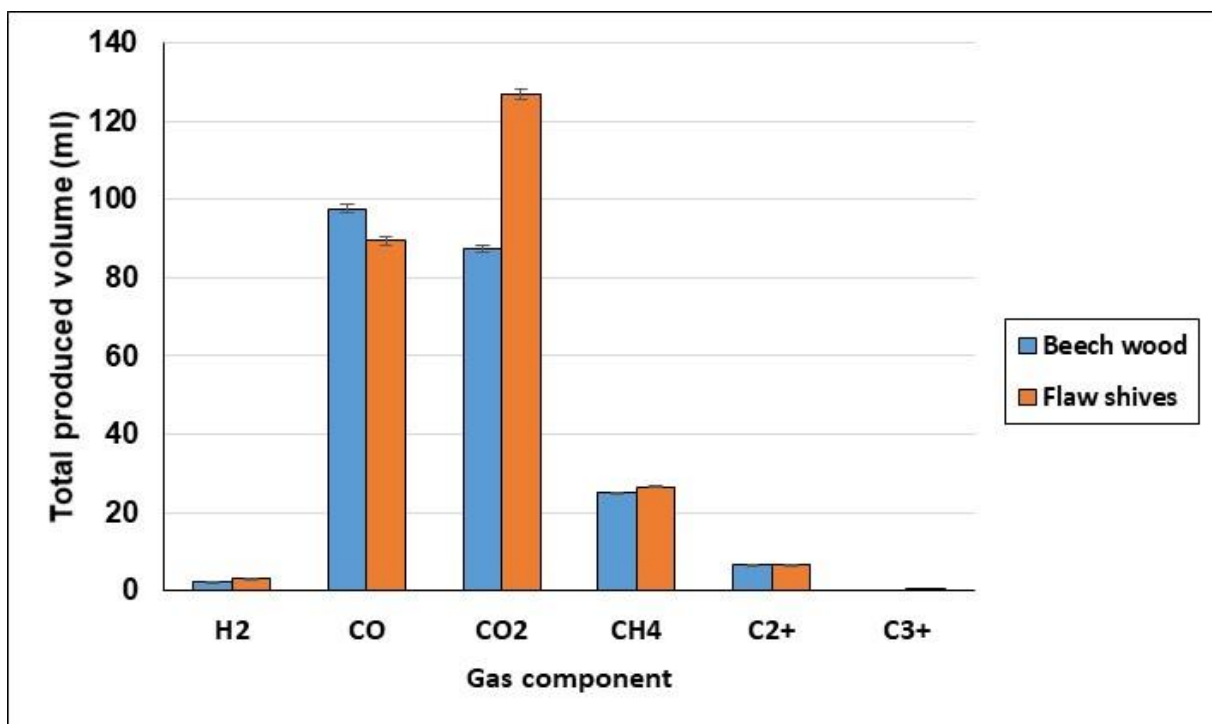


Figure A1.2. *The volumetric flow of individual gases from the pyrolysis of biomasses at 500°C.*

The obtained bio-oil compounds were also analyzed, **Figure A1.3** shows the molar fraction of the individuals chemical families presented in bio-oil. As can be observed, it was found 5 compounds to be the majority in the obtained results, by organizing these compounds in higher percentage order we found that acids, phenols, esters, ketones and alcohols were the most

significant components in bio-oil. These findings were coherent with literature, Xu et al. [205] characterized biomass pyrolytic oil in their work and it was found that the majority of oil compounds were organized in the following form, acids > alcohols > esters > ketones > phenols. The same was found by Ben et al. [206] who explained that lignocellulosic bio-oil is mainly constituted by aliphatic OH groups such as phenyl groups and by carboxylic acids.

In addition to the bio-oil characterization for both biomasses, it was also observed that they have approximately the same composition. Both mol fraction curves were almost superposed. This evidenced that the results were very similar and that although biomasses might not have the strictly same quantity of components (cellulose, hemicellulose and lignin), the obtained bio-oil of lignocellulosic biomass was almost the same. Also, the **oxygen content** obtained from both biomasses was very similar, for beech wood 33.8% was found and for flax shives 34.8%. These results were coherent with the values found in the literature for the bio-oil obtained from lignocellulosic biomasses [207]–[210], where between 35-40% were the values commonly found for intermediate and fast pyrolysis at a temperature between 450°C and 550°C.

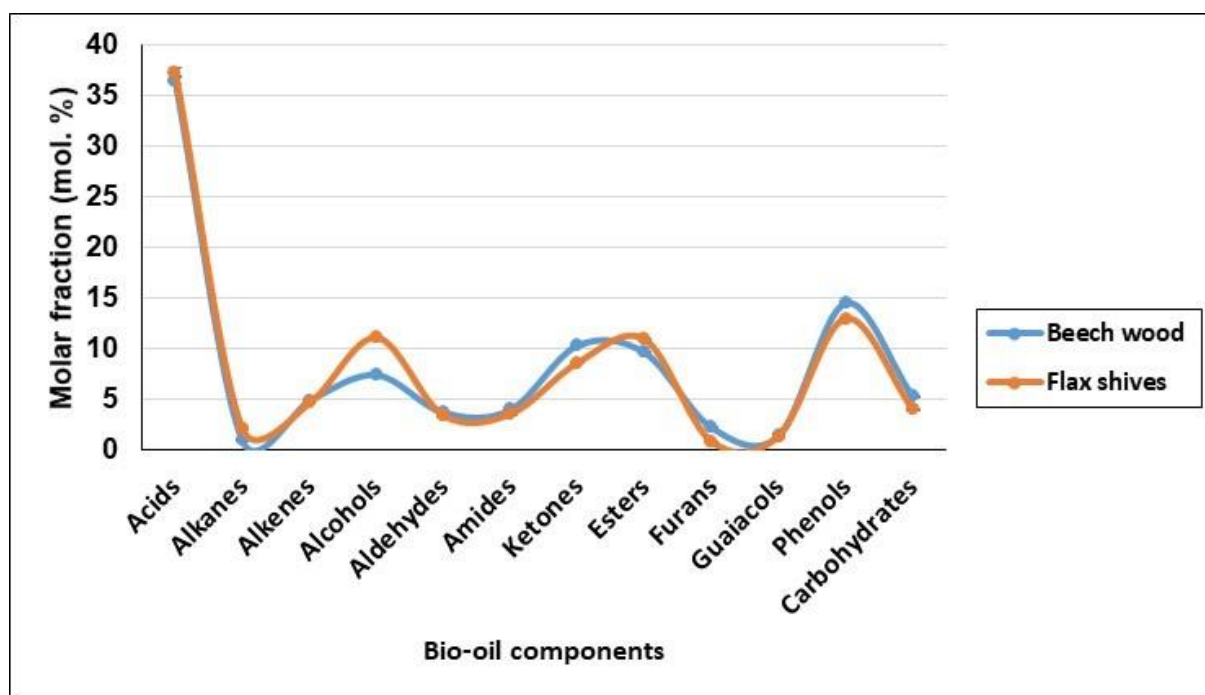


Figure A1.3. The molar fraction of individual chemical families in bio-oil at 500°C.

A1.1.2 Pyrolysis of the biomass pseudo-components

The mass balance results obtained from the pyrolysis of biomass components were shown in **Figure A1.4**. As can be observed for Cellulose and hemicellulose the amount of bio-oil represented the highest product yield, 75.7% and 78.6% respectively, as reported in the

literature [211], [212]. Due to the fact, these molecules were constituted of high content of volatile matter, the structure of the molecules was formed by chemical bonds that were very sensitive to thermal degradation, hence the amount of oil was superior to lignin (32.8%).

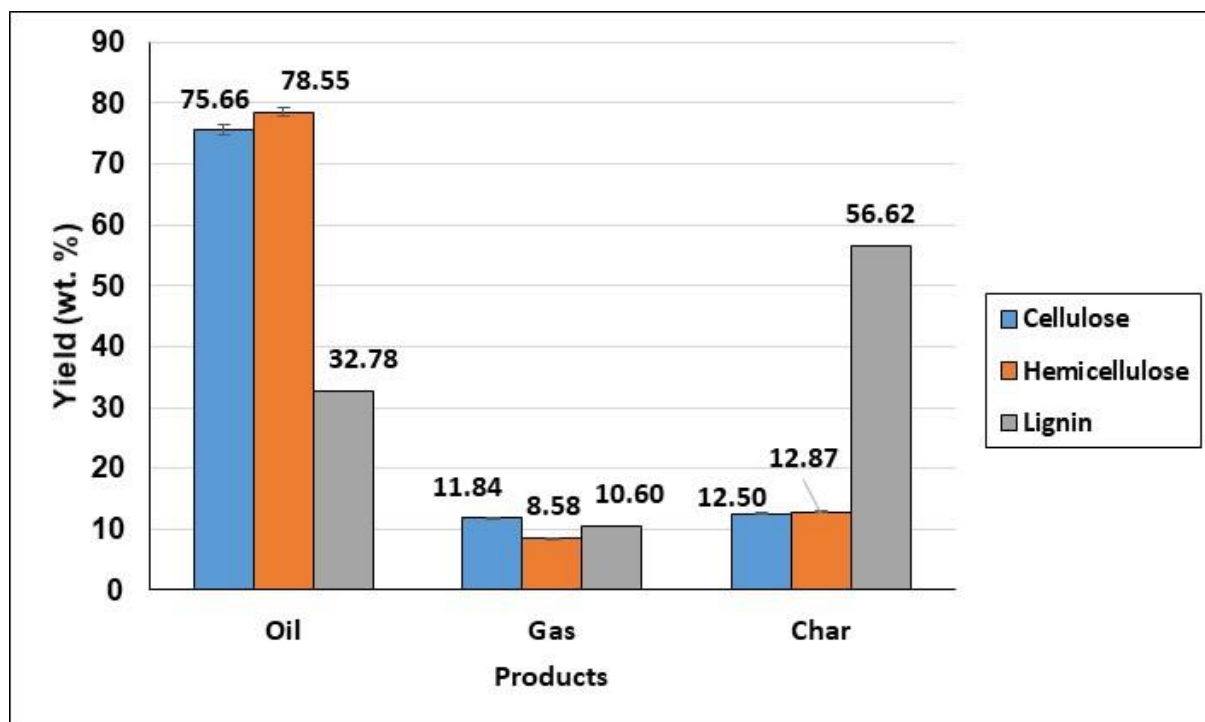


Figure A1.4. Mass balance of the pyrolysis of biomass components, cellulose, hemicellulose and lignin at 500°C.

Contrary to the oil content, the pyrolysis of lignin showed to maintain a high yield of char. This was due to the high fixed carbon yield presented by proximate analysis of lignin and also due to the high thermal resistance presented by lignin, phenomena also described by Qu et al. [28]. The obtained results can be interpreted as follows, in biomass pyrolysis, the amount of bio-oil obtained was strictly linked to the decomposition of cellulose and hemicellulose, as the pyrolysis of these two components showed to give bio-oil as the principal product. On the other hand, the yield of carbon in biomass pyrolysis could be attributed to the presence of lignin, as was observed lignin pyrolysis gave char as the main product (56.6%).

The pyrolysis gases obtained from the pyrolysis of the three components did not show a significant difference between components, the values were very close from 8.6% to 11.8%. Due to this, it was proposed to evaluate the total volume of produced gases after the pyrolysis of each component, it can be observed in **Figure A1.5**, that the volume of CH₄ and H₂ was very superior in the pyrolysis of lignin than cellulose and hemicellulose.

The most significant observation was the quantity of CO release by the cellulose (144 ml) compared to 81.3 ml and 22.9 ml, for hemicellulose and lignin, this was due to the decarbonylating routines that suffer carbon hydrates such as sugar when temperature increase [213], as was well known that cellulose presented a high amount of carbohydrates inside its structure. In addition to this, the volume of CO₂ release from lignin pyrolysis was 1.6 times higher than for cellulose and hemicellulose. The reason for this was the thermal effect on phenols presented in lignin structure leading to decarboxylation reactions and being reduced into smaller hydrogen-bonded molecules and CO₂ [214].

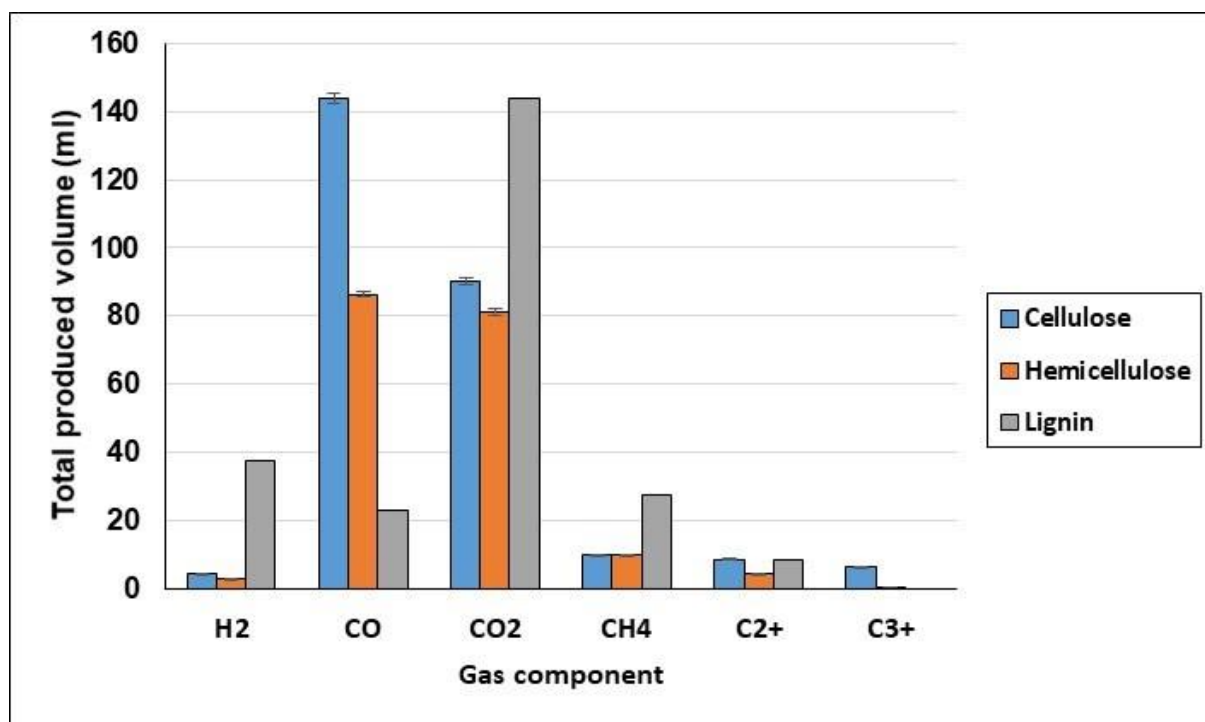


Figure A1.5. The volumetric flow of individual gases from the pyrolysis of cellulose, hemicellulose and lignin at 500°C.

Figure A1.6 shows the chemical family distribution of the obtained bio-oil after the pyrolysis. As can be seen for lignin no other family excelled more than phenols primary and acids. For hemicellulose also acids were the most significant yield and finally for cellulose phenols and carbohydrates presented the highest yields. Through these results it can be established that oil obtained from the individual component, did not show a strict image of the results of biomass pyrolysis, meanwhile, acids and phenolic compounds showed to be equally the most abundant chemical families. The **oxygen content** of the bio-oil was also calculated, cellulose presented the highest value with 33.82% of oxygenated molecules in the obtained bio-oil, followed by 28.05% for hemicellulose and 19.38% for lignin. These results evidenced that the oxygen

content could potentially be influenced by cellulose and hemicellulose, as these compounds presented similar values to biomass.

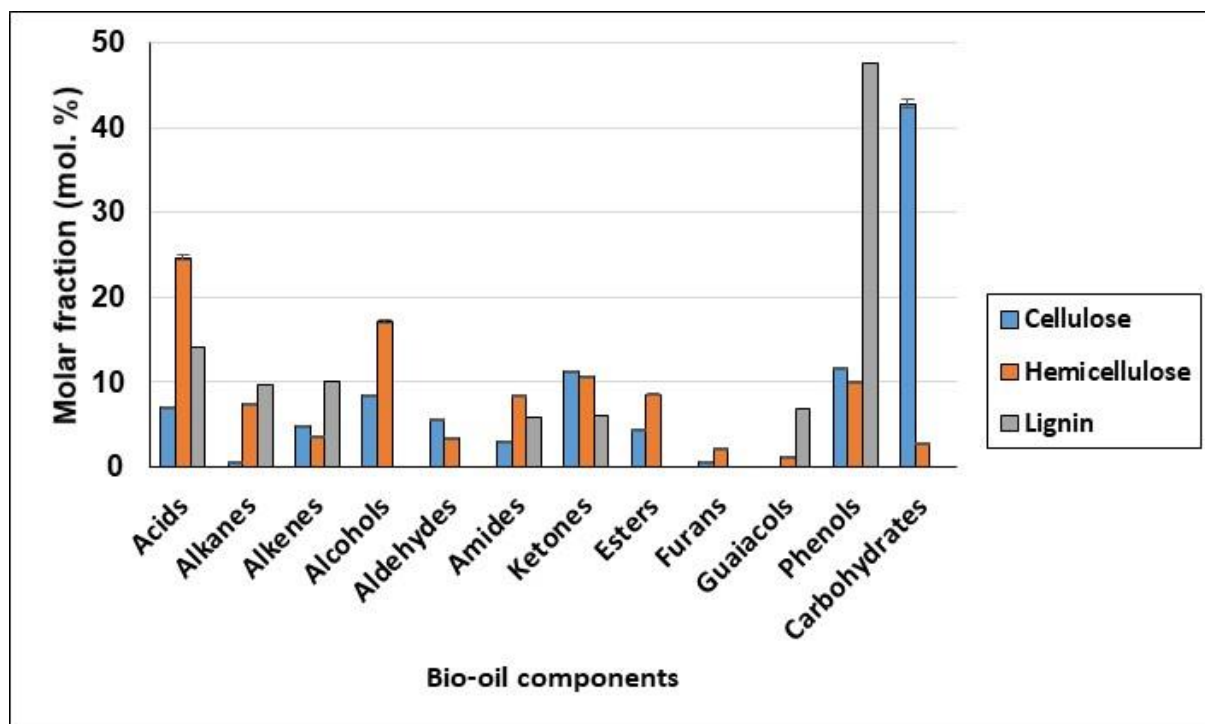


Figure A1. 6. The molar fraction of individual chemical families in bio-oil, from cellulose, hemicellulose and lignin at 500°C.

A1.1.3 Bio-oil upgrading

The effect of the catalytic pyrolysis of both biomasses and the three principal components was also evaluated. The use of the zeolite catalysts was investigated, in order to evaluate mass and product distribution in the bio-oil upgrading. As the oxygen content of pyrolytic bio-oil limits its use and valorization, deoxygenation reaction was the most appropriate routine to upgrade their properties.

A1.1.3.1 Upgrading biomasses bio-oil

It can be observed in **Figure A1.7** and **A1.8** the variation of mass balance by the use of a catalyst in the pyrolysis of beech wood and flax shives, respectively. As can be seen, there was a reduction in the yield of bio-oil due to the conversion of oxygenated compounds into lighter molecules. The presence of catalyst was capable to reduce the amount of bio-oil, by reducing the heavy molecules such as carboxylic acids into gaseous species and water, the same statement was also reported in the work of Saraeian et al. [215]. After the upgrading of pyrolysis oil, CO, CO₂ and water yields increased due to the cracking effect of the used

catalyst. It can be also observed that the total gas yield doubled its value after the catalytic treatment, this fact once again evidenced the formation of lighter molecules due to decarbonylation and decarboxylation reactions.

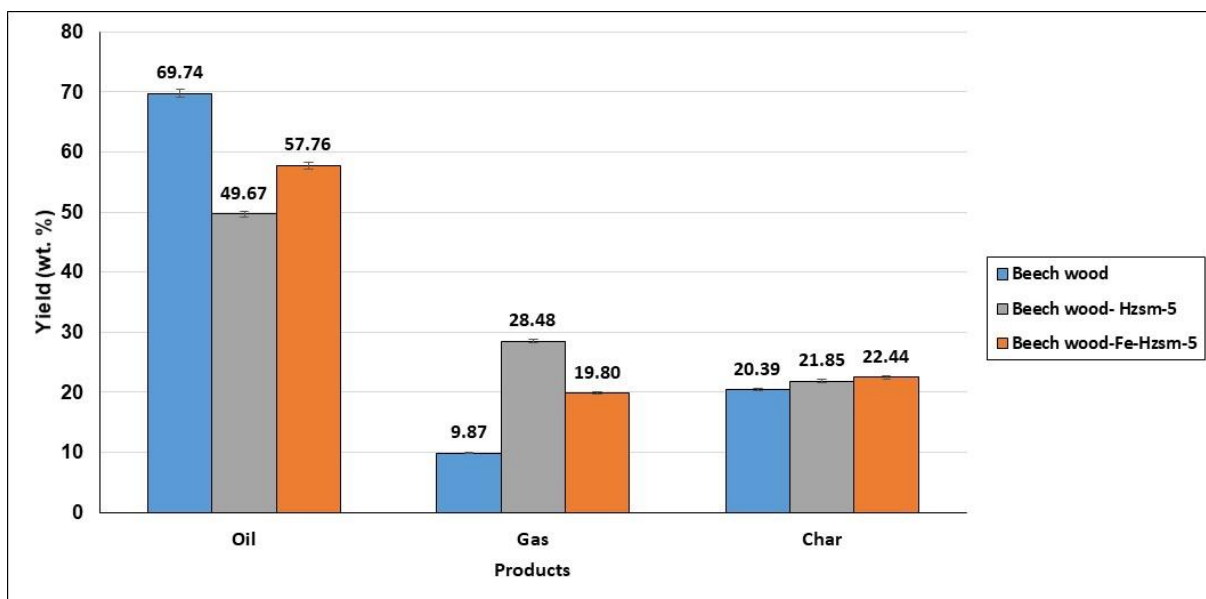


Figure A1.7. Mass balance of the obtained products from the catalytic treatment of beech wood at 500°C.

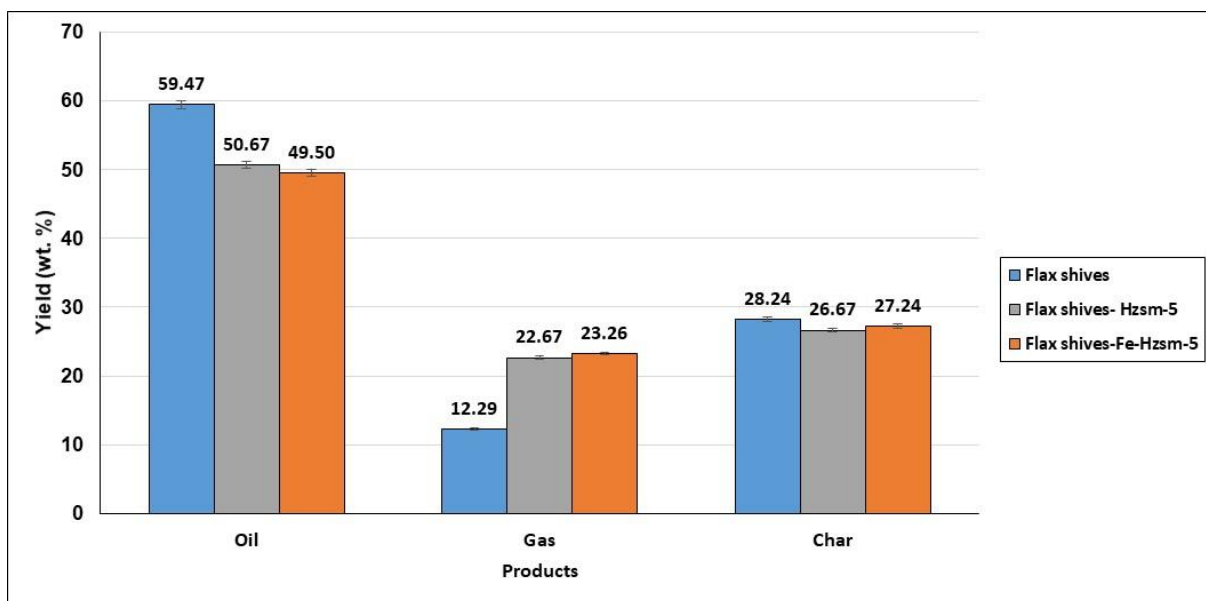


Figure A1.8. Mass balance of the obtained products from the catalytic treatment of flax shives at 500°C.

In order to evaluate the performance of the catalytic treatment, it was observed the oxygen content of the pyrolysis oil. **Figure A1.9** illustrated the percentage of oxygen by the total

molecules present in the bio-oil. As can be observed, all catalysts were able to reduce the oxygen content for both biomasses. Amid all the tested catalysts, zeolite HZSM-5 and its iron modification Fe-HZSM-5 were the two catalysts more efficient, in terms of oxygen content reduction. Catalyst HZSM-5 was able to reduce oxygen content approximately from 46 to 58.5 % the initial oxygen content. While, the iron modified zeolite HZSM-5 reduced oxygen content between 57.1 and 59.8% the initial oxygen content amount. These two catalysts were known to be very effective in reducing carboxylic acids molecules [216], and as shown previously (**Section A1.1.1**) the majority of pyrolytic bio-oil was conformed of acids.

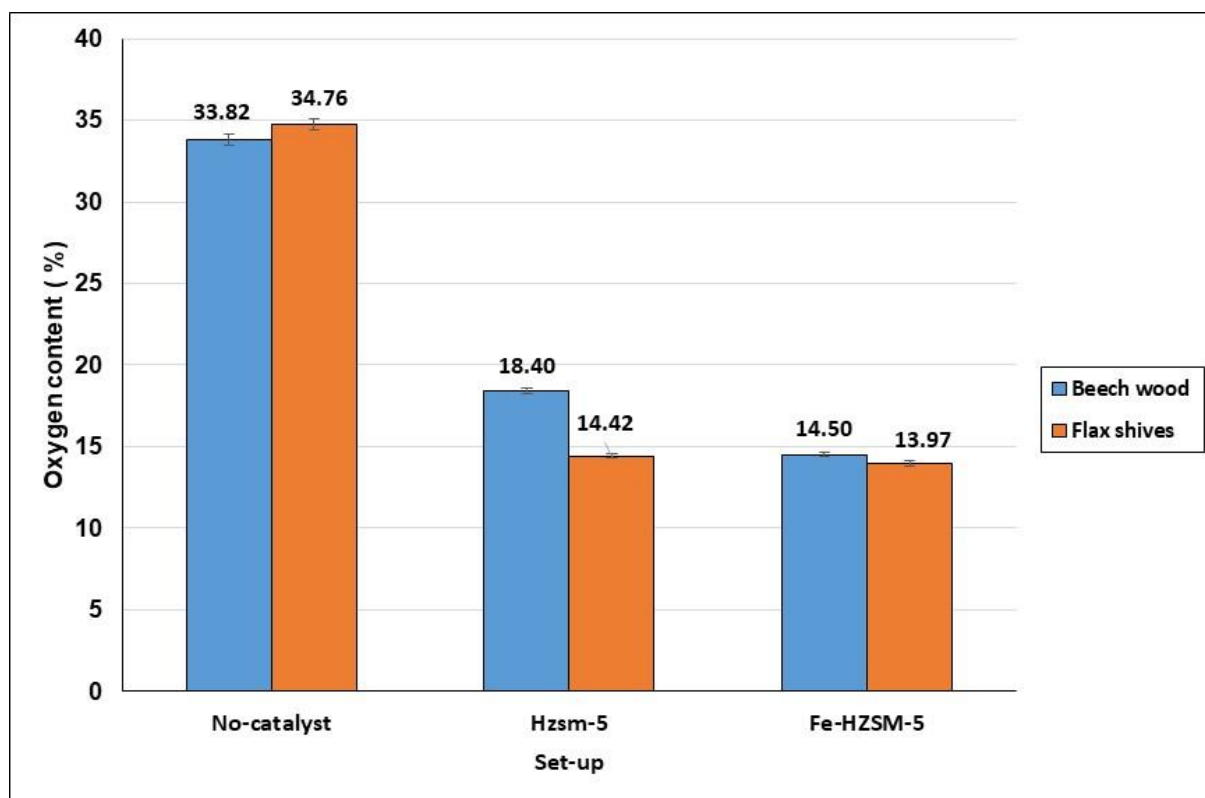


Figure A1.9. Oxygen content in bio-oil after catalytic treatment of beech wood and flax shives at 500°C.

A1.1.3.2 Upgrading biomass components bio-oil

In the **Figures A1.10, A1.11** and **A1.12** have illustrated the mass balance after the catalytic pyrolysis of cellulose, hemicellulose and lignin. For cellulose and hemicellulose, it was observed a reduction in the oil content as observed in the amount of oil of biomasses. These reductions corresponded to the cracking reaction of oxygenated molecules which led to the formation of lighter hydrocarbons and non-condensable gases, due to this it was observed an increase in the gas yield. Contrary to this, lignin liquids yield was reduced slightly as can be

seen. The catalytic treatment of these compounds separately did not emulate completely the behavior of biomasses, due to the fact that when these compounds are together a competitiveness environment is created.

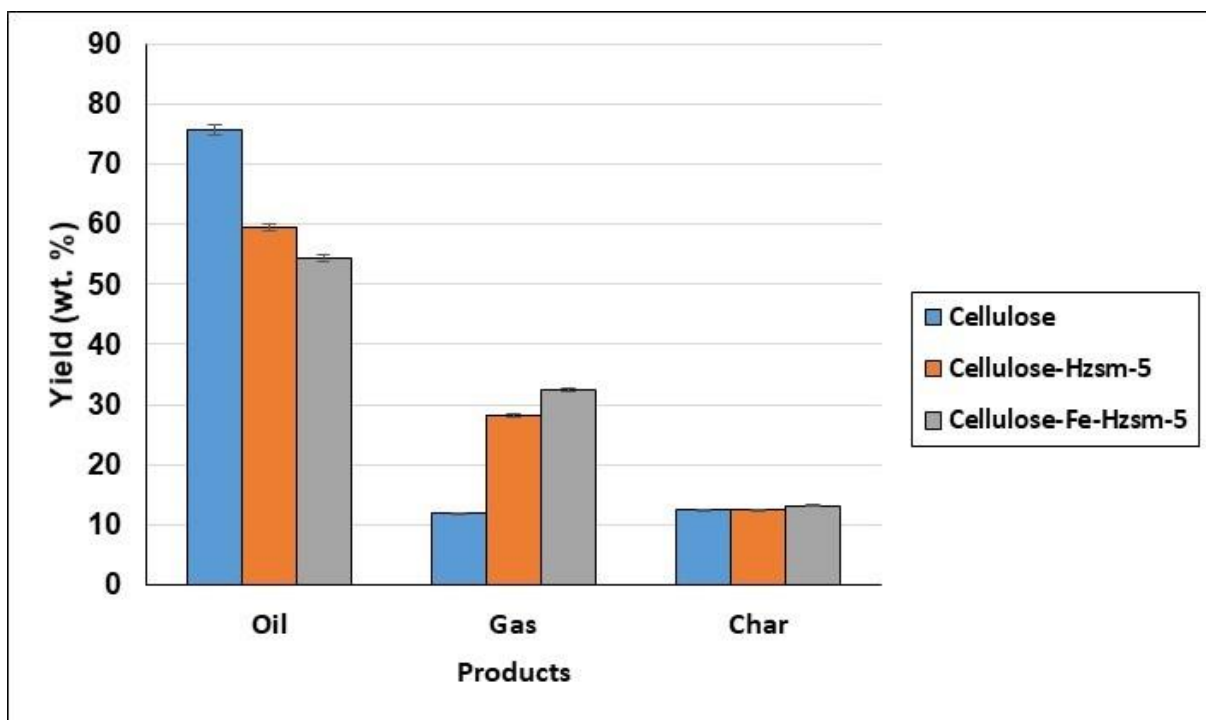


Figure A1.10. Mass balance of catalytic treatment of cellulose at 500°C.

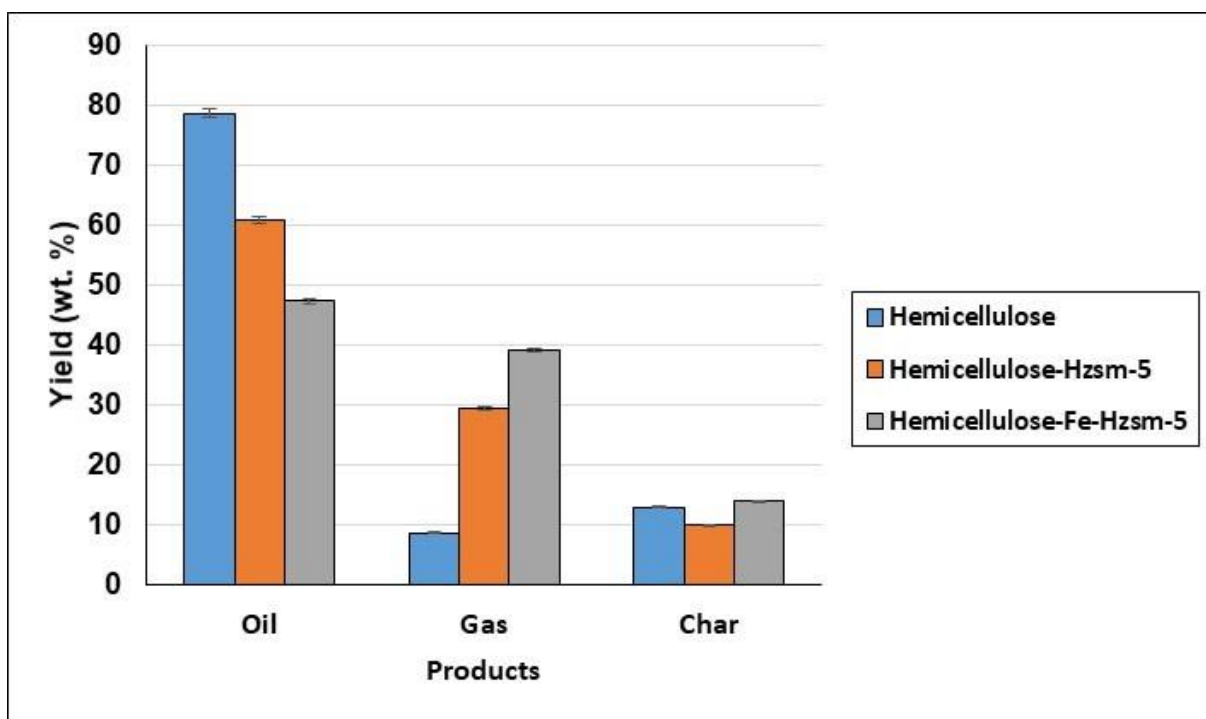


Figure A1.11. Mass balance of catalytic treatment of hemicellulose at 500°C.

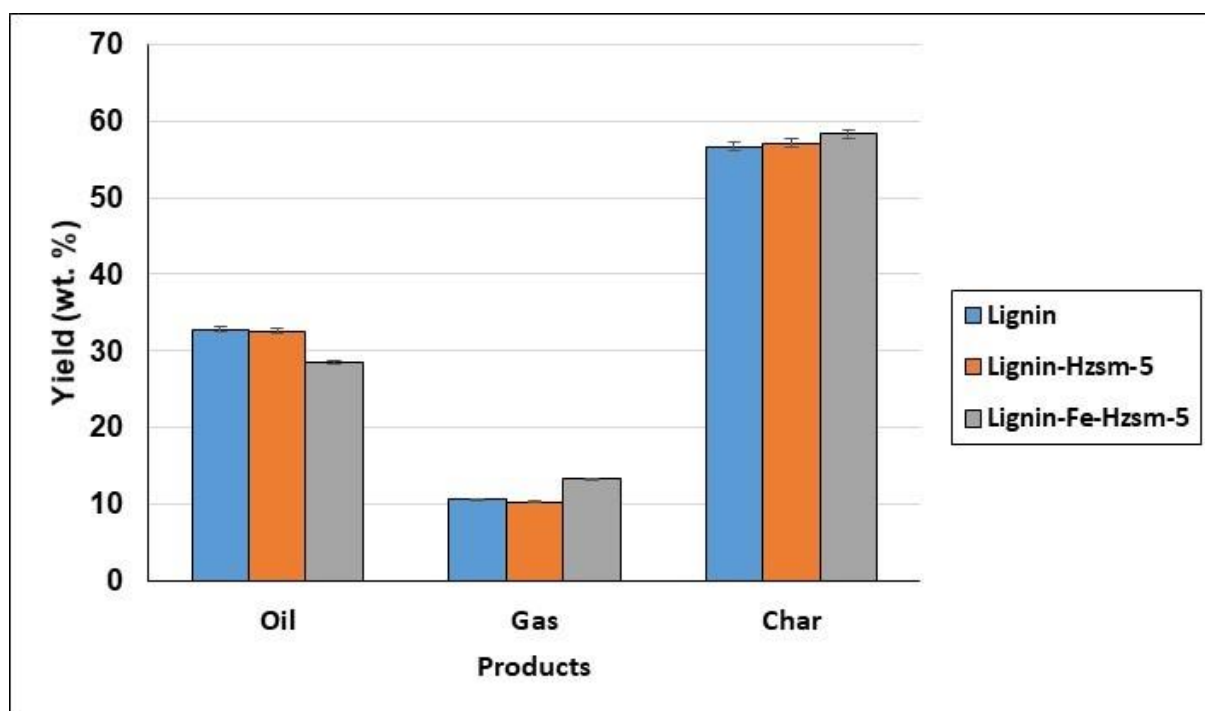


Figure A1.12. Mass balance of catalytic treatment of lignin at 500°C.

Figure A1.13 shows the effects of catalyst in the oxygen content for biomass components, instantly it can be seen that amid the two catalyst Fe- HZSM-5 was very effective in oxygen reduction. Lignin oxygen content was reduced to 0% with these catalysts, while for cellulose and lignin a reduction of 60% and 50%, respectively was achieved. These values were very similar to those obtained from biomasses, meaning that in terms of oxygen content the behavior of cellulose and hemicellulose was very familiar with biomasses.

These findings show that even for individual components the efficacy of this catalyst was proven as was for biomasses. Acids components were massively reduced in cellulose, hemicellulose and lignin. A formation of alkenes and phenolic compounds were also detected, Huang et al. [217] also observed this formation in their study, the authors referred that HZSM-5 zeolites favor trans-alkylation reactions to form phenols.

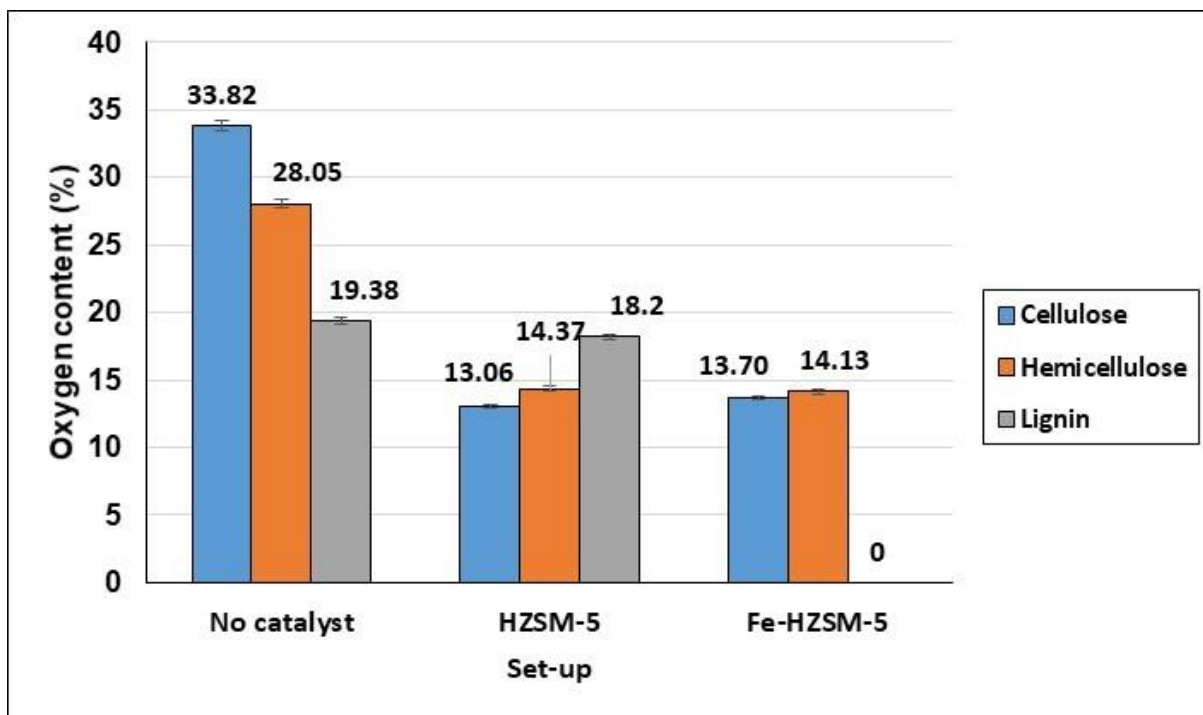


Figure A1.13. Oxygen content of pseudo-components after catalytic treatment at 500°C.

Appendix A.2

This section included additional data and comments that were not included in **chapter 3**.

Uncertainty Analysis

In order to calculate the uncertainty of the presented results in this work, the following procedure was employed, first of all, it was calculated the standard deviation of the selected results. This included the variations due to experiment repetitions.

Standard deviation of results (σ)

$$\sigma = [(U_i - \bar{U})^2/N]^{1/2} \quad \text{Eq. A2.1}$$

where U_i , \bar{U} and N represented the selected results, average values of experiment repetitions, and the number of experimental repetitions, respectively. Then it was added the uncertainty concerning, equipment tolerance such as Gas-Chromatography, furnace temperature controller, balance and values rounding. The final result was presented as,

$$U \pm (\sigma + \sum_i e_i) \quad \text{Eq. A2.2}$$

Where $\sum_i e_i$ represented the summary of all individual uncertainty values regarding equipment tolerance and values rounding. The uncertainty values were added to the standard deviation

Appendix

and represented the total uncertainty of the results. Standard deviation represented 1.47% of the uncertainty, while other uncertainty values ($\sum_i e_i$) represented approximately 0.23% of the total. $U \pm 1.7\%$

Table A2. 1. Energy product distribution of gases for beech wood and flax shives with catalytic treatment (MJ/kg_{gas}) at 500°C.

	Beech wood (no catalyst)	Beech wood (HZSM-5)	Beech wood (Fe- HZSM-5)	Flax shives (no catalyst)	Flax shives (HZSM-5)	Flax shives (Fe- HZSM-5)
H ₂	0.08	0.07	1.89	0.10	0.10	1.45
CO	4.14	4.22	4.13	3.02	3.80	3.16
CH ₄	2.88	1.22	2.43	2.45	1.79	2.11
CO ₂	0.37	0.28	0.56	0.43	0.32	0.53
C ₂₊	1.26	2.72	4.30	1.03	3.09	3.06
C ₃₊	0.00	2.66	4.53	0.01	3.30	4.14

Appendix A3

This section presents the additional data and results that were not included in **chapter 4**.

A3.1 Results and discussion

The following results presented an error margin of approximately 1.7% due to the experimental uncertainty and deviations. The errors surrounding the experimental test were those found in deviation calculations after experiment repetitions, mass weighting, the rounding of values and equipment tolerance. The uncertainty of values was added with error bars over the presented results.

A3.1.1 Effect of temperature in products distribution

The effect of temperature was investigated in beech wood gasification using CO₂ as gasification agent, sand as bed material and with a residence time of gases of 10.6 s. In **Figure A3.1** it is observed the evolution with the temperature of the obtained products. As can be seen syngas presented the highest product yield, followed by char and tar.

Biochar

The yield of biochar was reduced from 29.63% to 17.31%, due to the increase in temperature. The presence of the gasification agent favored the rapid conversion of biochar into gaseous compounds. The carbon present in the biochar reacted with CO₂ to form CO molecules, this Boudouard reaction was favored by the increase of temperature, this statement was also exclaimed by Lahijani et al. [218] which showed temperature as the most effective parameter

in carbon conversion. Regardless of the positive effect of temperature in reducing char content, the results showed that even at 900°C, a significant yield of carbon remained in the process. This evidenced the requirement of higher temperatures in order to turn this unconverted char into syngas.

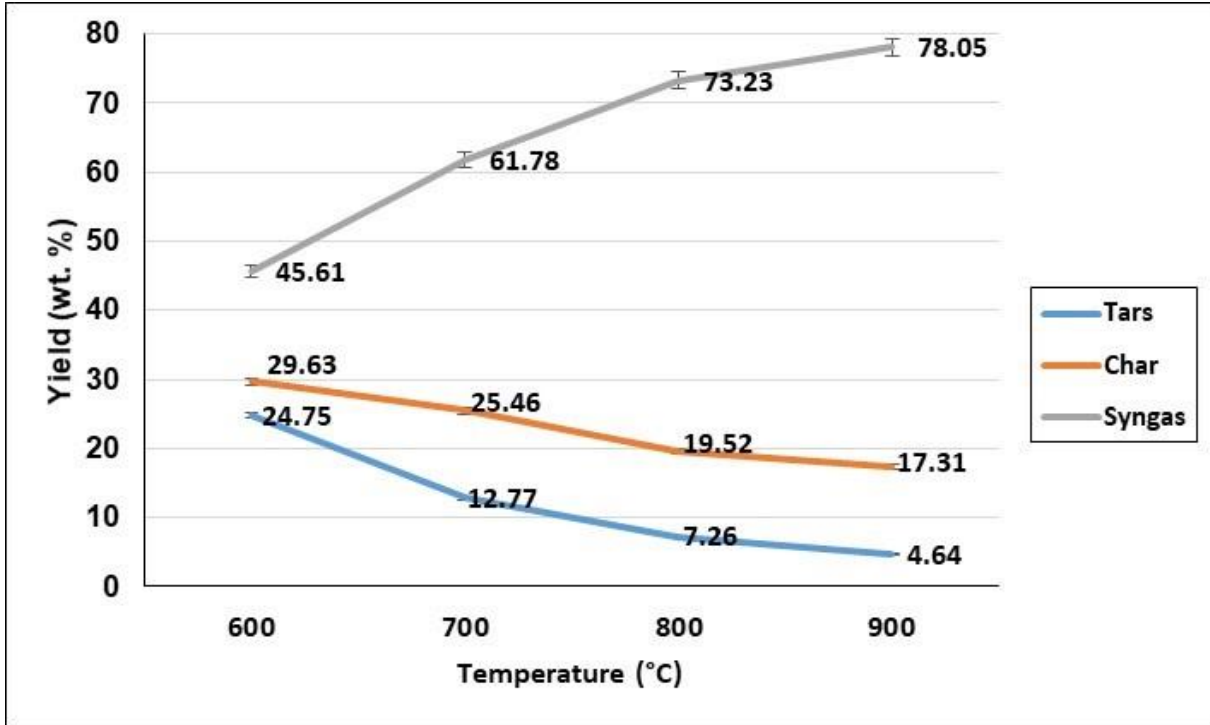


Figure A3.1. Effect of temperature in product yields obtained from gasification with CO₂.

Syngas

As it is illustrated the syngas yield was increased from 45.6% to 78.1%, from 600°C to 900°C. The two factors that attributed this increased were the carbon conversion and the tar thermal cracking reactions, both favored by the increase of temperature. The previously mentioned reactions led to the formation of lighter molecules such as CO, H₂, CH₄ and others, that form part of the syngas definition. The most significant increase in syngas yield was observed from 600°C to 700°C, this was due to the high production of H₂ and CH₄ as a result of the conversion of oxygenated molecules that stills present at this temperature. **Figure A3.2** shows the volumetric flow rate of individual syngas components as a function of the temperature.

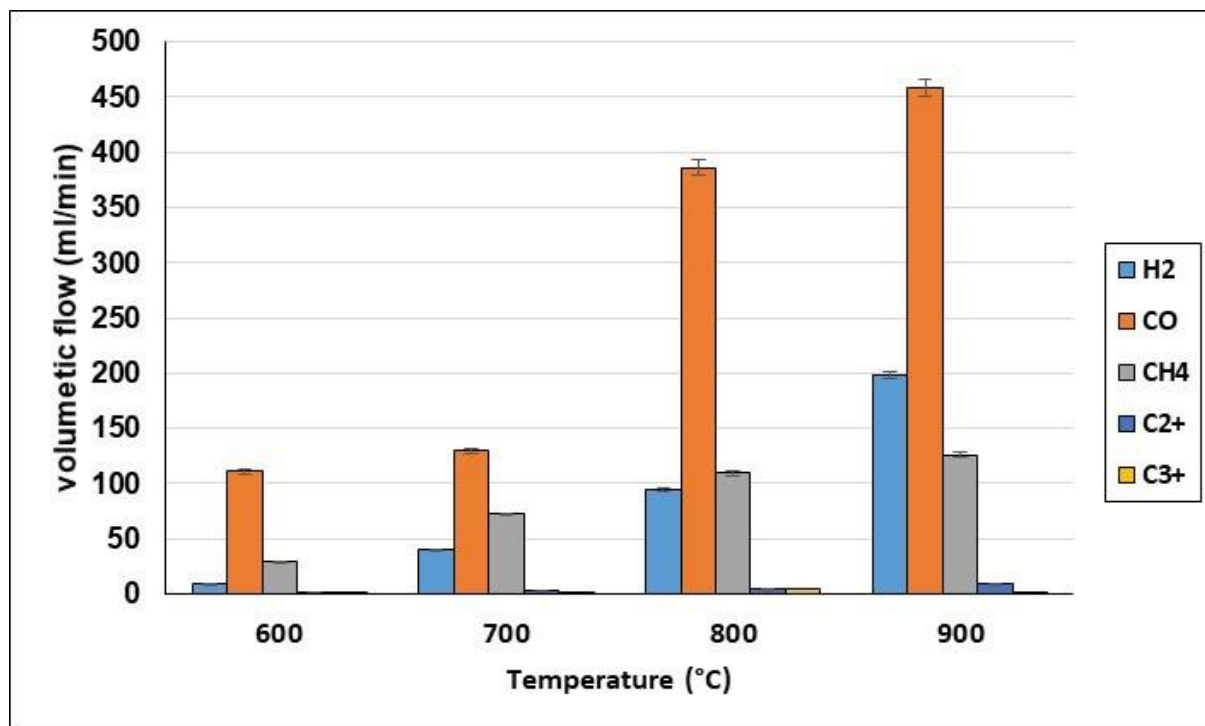


Figure A3.2. Effect of temperature in the volumetric flow of individual syngas components. Gasification with CO₂.

The volume rate of hydrogen was increased significantly from 600°C to 700°C, 9.5 ml/min to 39.9 ml/min respectively, for an increase of 4 times the value at 600°C. The major syngas components as H₂, CO and CH₄ increased the volume rate with temperature. Amid the three major syngas components, CO predominated due to the Boudouard reaction, while its presence was reduced at higher temperatures. In **Figure A3.3** it can be observed that the molar fraction of CO achieved 73% at 600°C, but with higher temperatures, these values decreased due to the increase of hydrogen yield because of tar cracking and shift reactions. The H₂/CO ratio was increased from 0.08 to 0.43 with the increase of temperature, the same behavior was observed by Ravaghi et al. [219].

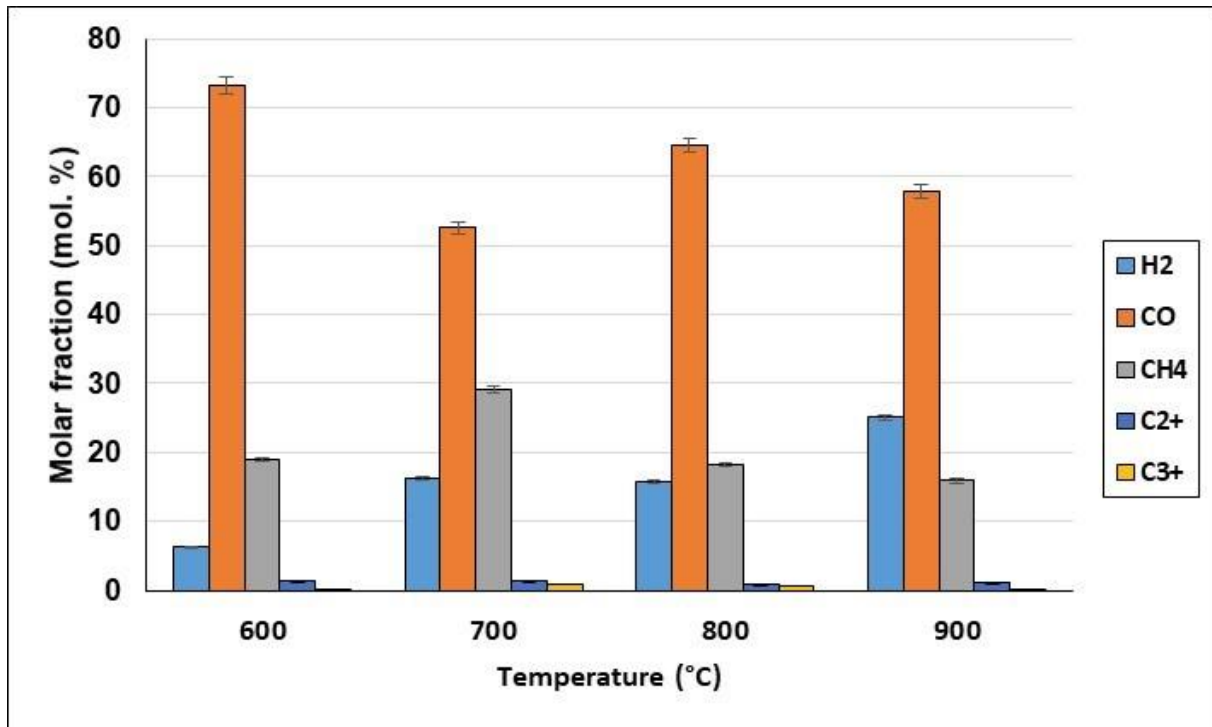


Figure A3.3. Effect of temperature in syngas molar concentration of individual gas components. Gasification with CO₂.

Tar

As observed in the mass balance figure, the amount of tar decreased with temperature. For uncountable reasons this was a good fact, meanwhile, the concentration of tar molecules in syngas still represents a problem. **Figure A3.4** illustrates the total concentration of tar molecules in the obtained syngas, in units of g/Nm³. At 600°C the concentration of tar in the syngas was exorbitant, 268.6 g/Nm³, as temperature increased this value was reduced to 10.9 g/Nm³. The latest value was coherent with the average limit value presented by Milne et al. [220] in the investigation of tar content in fluidized bed reactors. As can be seen, in order to achieve low tar concentration in syngas, higher temperature or optimization might be required.

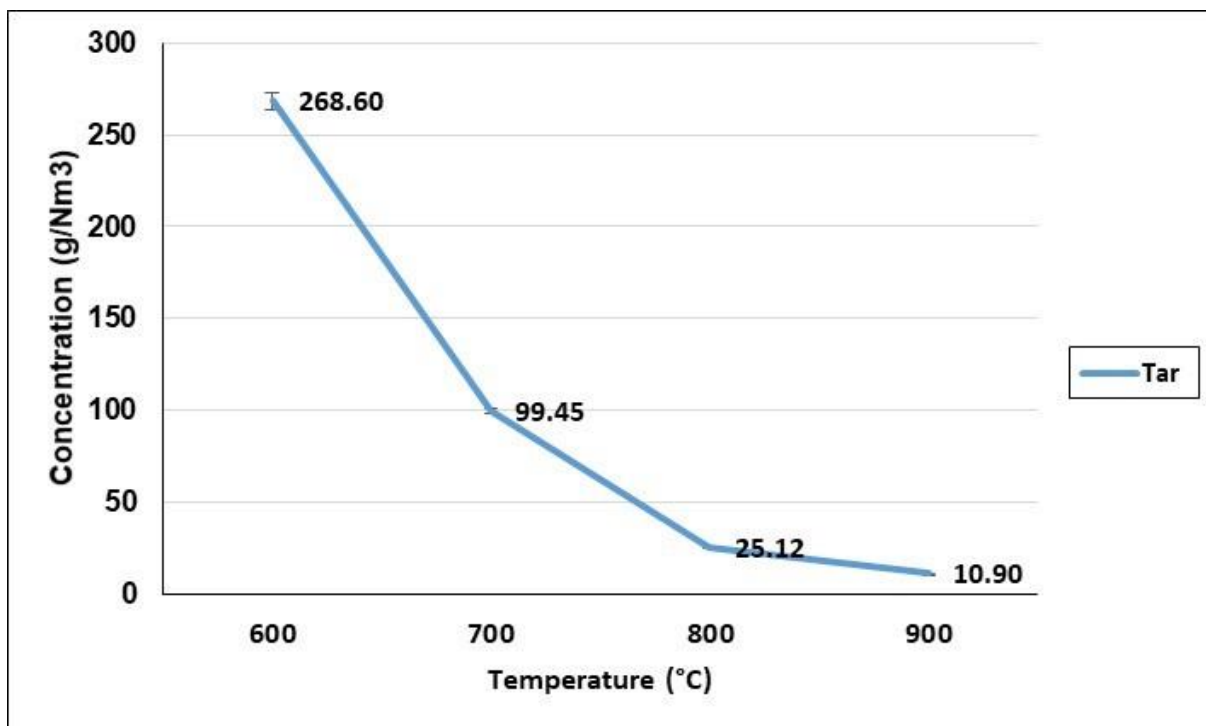


Figure A3.4. Effect of temperature in tar concentration in the syngas. Gasification with CO₂.

In **Figure A3.5** can be seen the concentration distribution of the tar by class type. As illustrated, classes 2 and 4 were the most dominant in the tar, meanwhile, all types were reduced as the temperature was increased. At 900°C class 2, mainly represented by phenols and heterocyclic aromatic compounds (HAC) showed the highest concentration, followed by naphthalene and light poly-aromatics compounds (LPAH), these findings were alike to those found by Kluska et al. [221] which showed phenolics derivatives and PAH as the principal compounds in beech wood tar. **Figure A3.6** shows the evolution with the temperature of phenols, HAC, and naphthalene. As can be seen phenolic compounds and HAC showed a significant reduction with temperature change, while naphthalene compounds were reduced but showed a notorious resistance with the temperature changes. Naphthalene compounds are known to have high thermal resistance [222], due to these reasons the concentration was not as significantly reduced as other compounds.

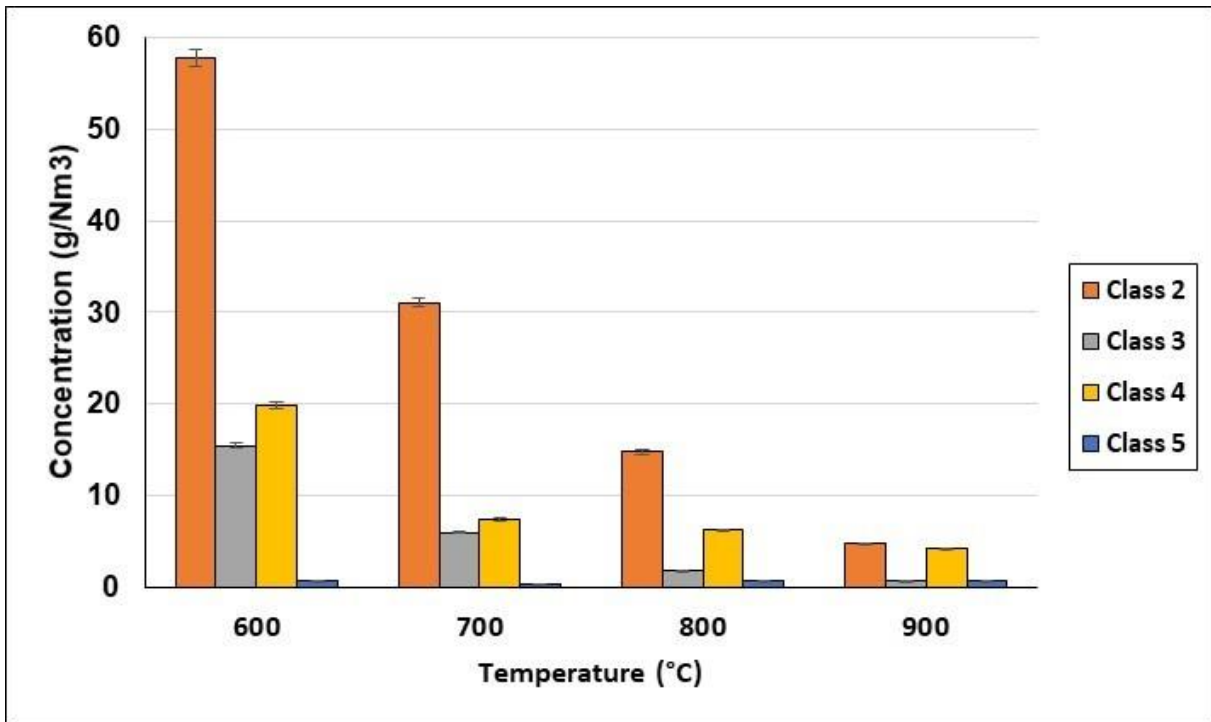


Figure A3.5. Effect of temperature in the concentration distribution of tars. Gasification with CO₂.

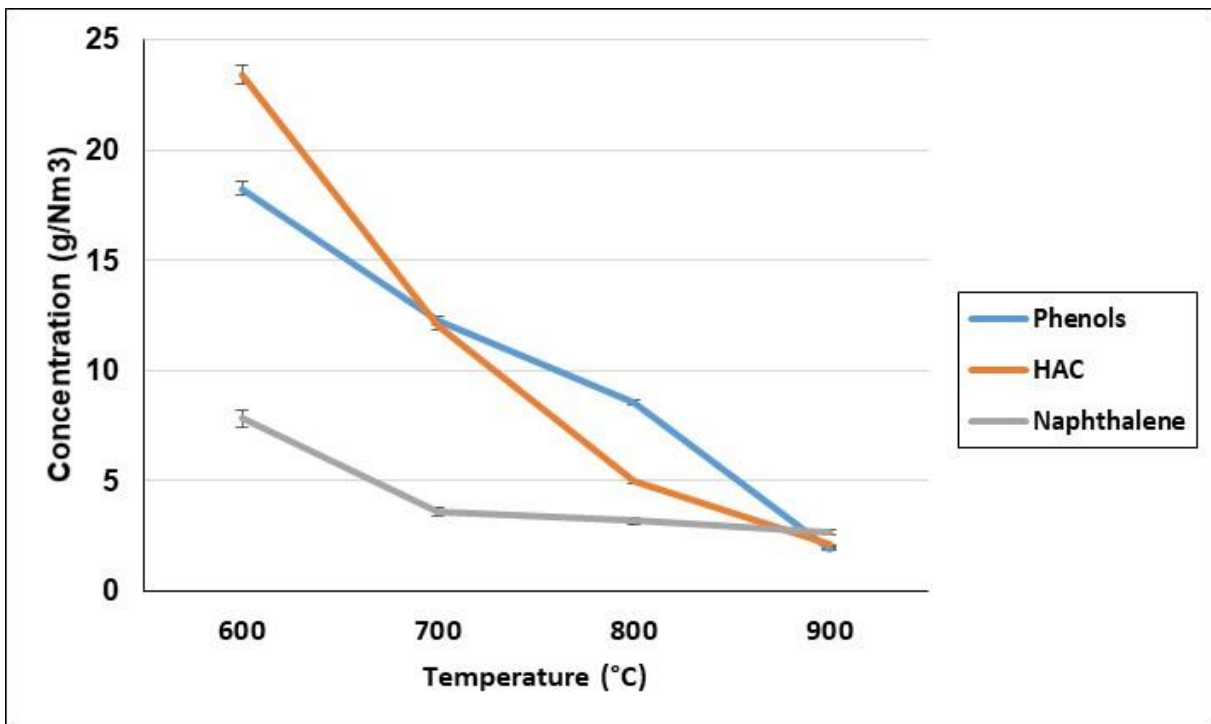


Figure A3.6. Evolution with the temperature of the major tar compounds. Gasification with CO₂.

After the observed phenomena and the obtained values, it was seen that temperature played an important role in order to increase syngas yield and reduced other products, meanwhile even 900°C remains not the sufficient temperature to favor syngas production and quality. Due to this fact, parameter optimization and study must be continued in order to improve the gasification process.

A3.1.2 Effect of the residence time of vapors in product distribution.

The residence time was the ratio between the volumetric flow of the gasification agent divided by the reacting zone of the reactor. Equation A3.1 illustrate the use formula for calculate the residence time (τ),

$$\tau \text{ (s)} = \text{flow rate of gasification agent (ml/s)} / \text{Reactor volume (ml)} \quad \text{Eq. A3.1}$$

For a temperature of 900°C, three residence time was selected for the test; 8.02 s, 10.6 s and 15.2 s. The selection of these values was taking into account the mechanical limitations of the installation. The minimal fluidization velocity of the installation was achieved with a residence time of approximately 27 s; hence an inferior value was chosen 15.2 s in order to avoid fixed bed limits. Then for the lowest residence time chosen 8.02 s, it was observed that below this value a turbulent fluidized bed was present provoking operational pressure to increase and potentially will damage the quartz reactor. **Figure A3.7** shows the fluidization regimes where the selected residence time was situated in the Geldart classification.

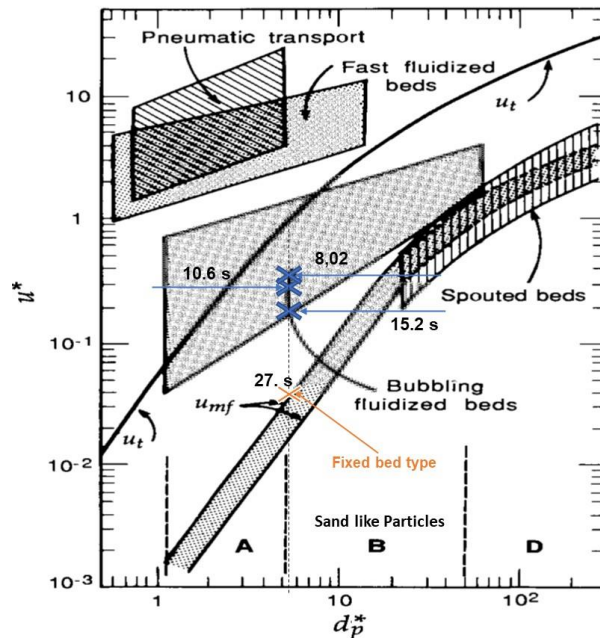


Figure A3. 7. Fluidized bed regimes for solid particles (adapted from Levenspiel et al.

[6]).

Figure A3.8 shows the mass balance of the obtained results for residence time evaluation at 900°C. It was observed that the variations of products yield were almost insignificant, the syngas and tar yield decreased slightly with the increase of the residence time. Meanwhile, low variations of char conversion were obtained with the increase of the residence time. The increase of the volumetric flow of the gasification was translated into a reduction of the residence time of vapors, consequently, the CO₂/C ratio was increased. The latest might be one of the reasons that with lower residence times values, more char was converted.

Though it was found in the literature that with the increase of residence time char conversion and tar yield decrease, due to the large exposition of char molecules with the oxidant, allowing a better mass diffusion. For the tar high resident times are translated into long exposition to the thermal condition that would lead to cracking reactions [223]. In order to avoid confusion in residence time statements Sikarwar et al. [62] recommended in their review of biomass gasification advances the use of a wide range of residence times in order to well evaluate this variable effect.

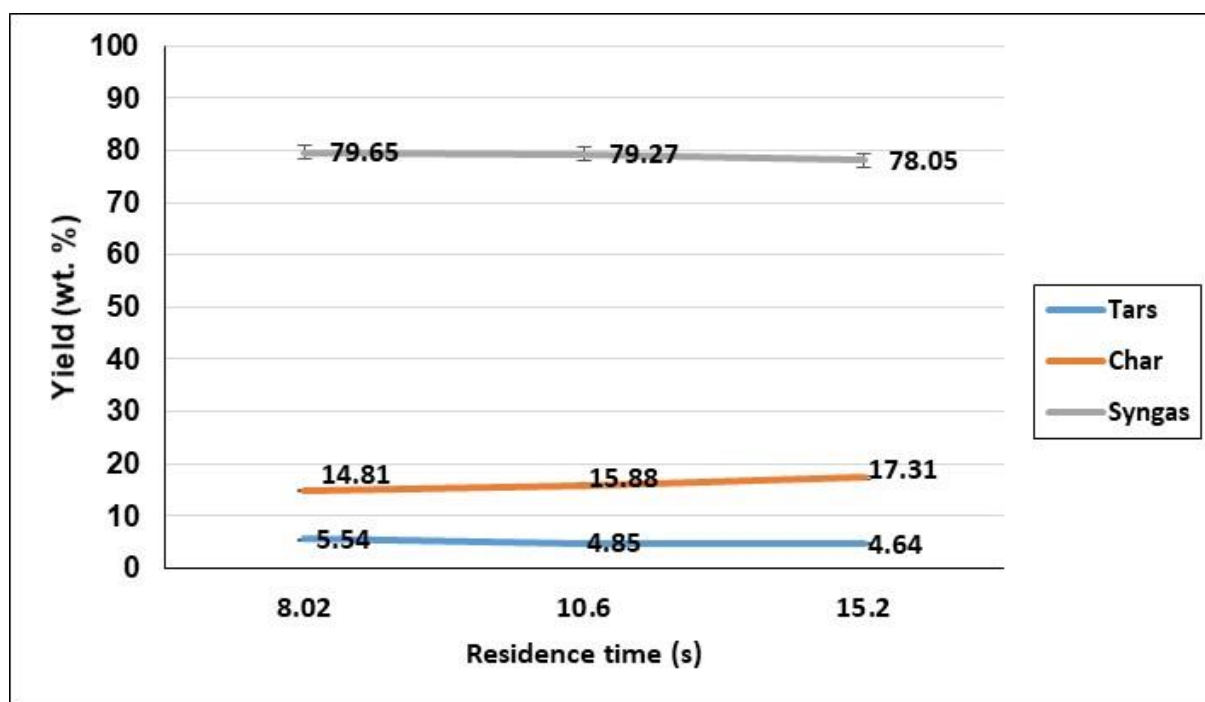


Figure A3.8. Effect of the residence time of gases in the mass balance of products. Gasification with CO₂.

Due to the low variations in mass balance, we are conscious that the selection of the used residence times was not more convenient to evaluate its effect. Meanwhile, due to mechanical

problems with the experimental set-up, this study was only evaluated in the previous conditions.

A3.1.3 Effect of the gasification agent in products distribution

In the following section, it was evaluated the effect of the presence of the gasification agent CO_2 in the distribution of the products. This evaluation was done by comparing the results of high-temperature pyrolysis (800°C and 900°C) with the results obtained from **Section A3.1.1** with the gasification of biomass with CO_2 , using sand as bed material and a residence time of 10.6 s. The pyrolysis test was done by using N_2 as a carrier gas in an inert atmosphere. **Figure A3.9** shows the results of the mass balance for pyrolysis and gasification at 800°C and 900°C.

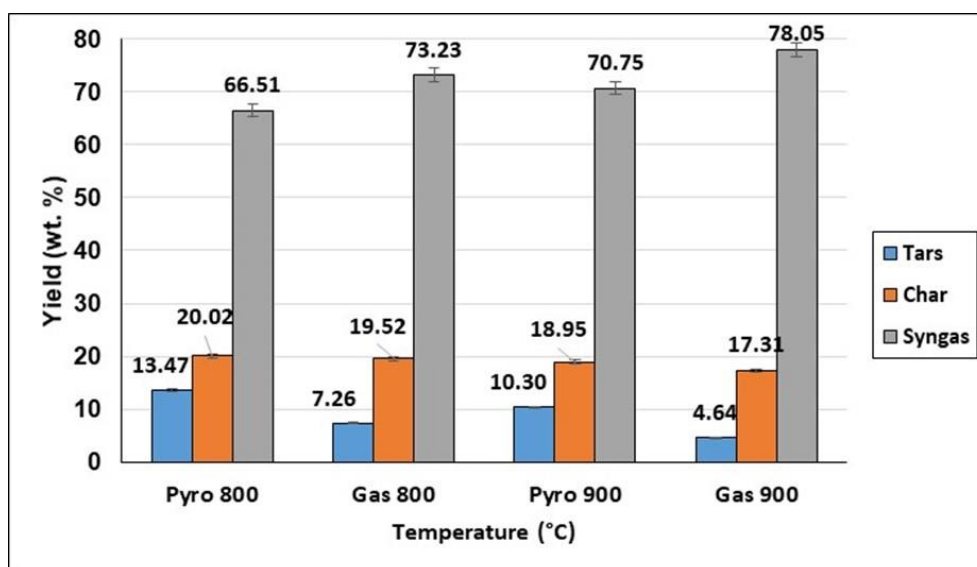


Figure A3.9. Mass balance comparison from high-temperature pyrolysis and gasification with CO_2 at 800°C and 900°C.

Biochar

For pyrolysis, it can be observed a reduction of the amount of biochar with the increase of temperature from 20.02 wt. % to 18.95 wt. %, this reduction might come due to the reactivity increase of biochar with temperature favoring conversions reactions. On the other hand, comparing the unconverted biochar from pyrolysis with gasification, the yield only presented a variation of 0.5 wt. % when CO_2 was used as a gasification agent. The latest showed that the gasification agent presented a low effect in char conversion at this temperature. Boudouard reaction can take place at a temperature between 500°C and 800°C, meanwhile, it is only at a higher temperature than mostly the equilibrium of the reaction goes to one side, letting high carbon conversion [224]. Hunt et al. [225] explained that at temperatures above >700°C,

Boudouard reaction free energy variation became negative, favoring CO formation progressively. Due to these statements, higher gaps in carbon conversion can be observed at 900°C, where the difference in carbon yield in pyrolysis and gasification began to rise (1.64 wt. %).

Syngas

The yield of syngas increased with the use of gasification agent, it can be observed in **Figure A3.9** with the use of CO₂ at 800°C and 900°C, syngas showed higher yields than the pyrolysis. This was due to the high reduction of tar molecules in the CO₂ atmosphere and secondly with a lower impact, the influence of gasification agents with carbon conversion. **Figure A3.10** shows the volumetric flow of individual syngas components obtained after the experimental tests.

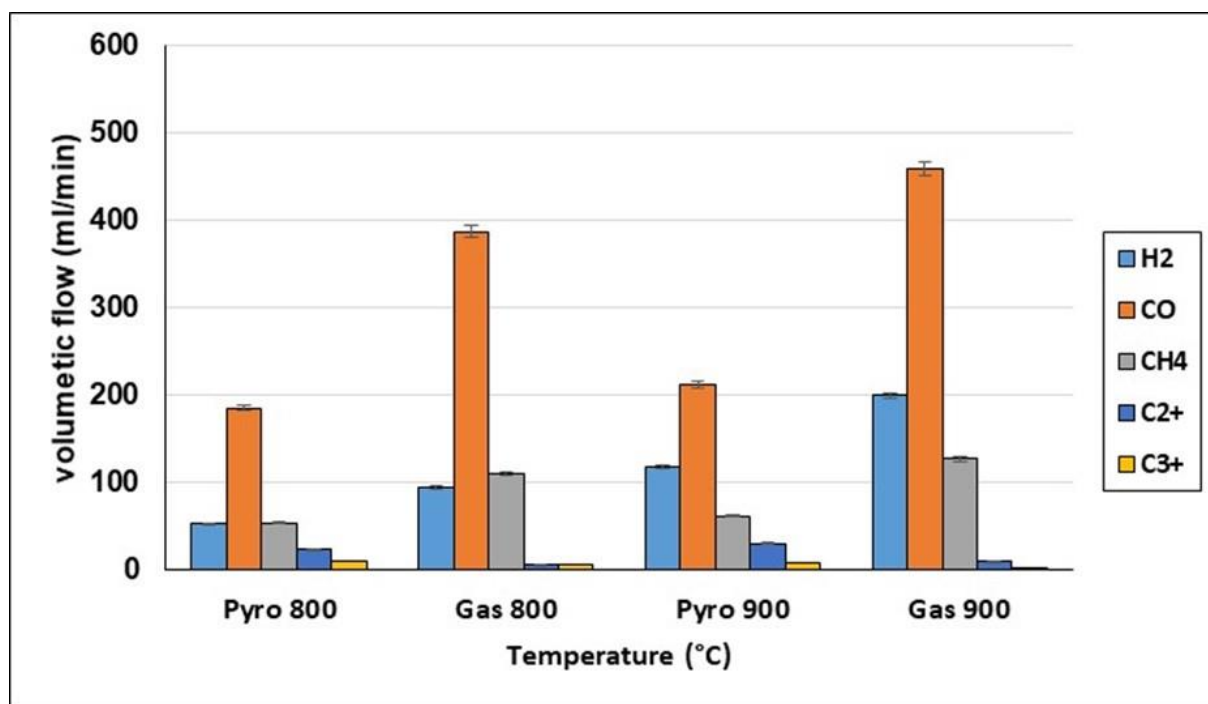


Figure A3.10. Volumetric flow rate comparison with pyrolysis and gasification with CO₂ at 800°C and 900°C.

As can be seen, CO was the component with the highest volumetric flow rate exiting the reactor for all experimental tests, the obtained CO values were increased 2 times when CO₂ was used as gasification agent (from 184.27 ml/min to 386.35 ml/min at 800°C and from 210.63 ml/min to 457.74 ml/min at 900°C), compared with pyrolysis. In addition to this, the molar fraction of CO was also reduced in pyrolysis with the increase of the temperature as hydrogen molecules were formed, as temperature increased the ratio H₂/CO was increased. **Figure A3.11** shows

the molar concentration of syngas components and the evolution of the H₂/CO ratio with temperature for pyrolysis and gasification.

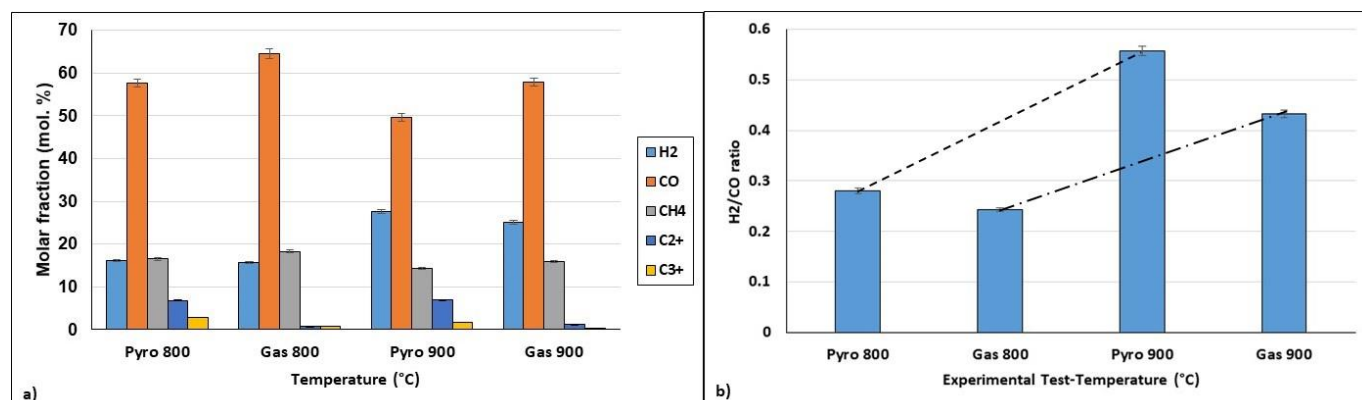


Figure A3.11. a) syngas molar concentration, b) H₂/CO ratio evolution for pyrolysis, and gasification with CO₂ at 800°C and 900°C.

Tar

The effect of introducing the gasification agent in the process affected the tar concentration at both temperatures. As can be observed in **Figure A3.12** the concentration of tar molecules was reduced significantly in the CO₂ atmosphere compared to pyrolysis. Class 2 and 4 represented the highest concentration values of tar in the syngas. As discussed previously, phenolic compounds, HAC, LPAH and naphthalene also represented the compounds with the higher concentration values in pyrolysis. The reduction of tar molecules can be explained due to the secondary reactions that may occur with tar and CO₂, tar dry reforming reaction. This reaction involved the conversion of tar molecules into light hydrocarbons such as H₂ and CO and it is highly favored at high temperatures. Kwon et al. [226] claimed that the introduction of CO₂ in the biomass conversion process, reduce the concentration of pyrolytic oil (in this case Tars) and enhanced the production of syngas. The same was observation was introduced by Guizani et al [227] in the study of the effect of CO₂ in the fast pyrolysis of biomass. The following reaction was presented as the dry reforming mechanism of tar with carbon dioxide,



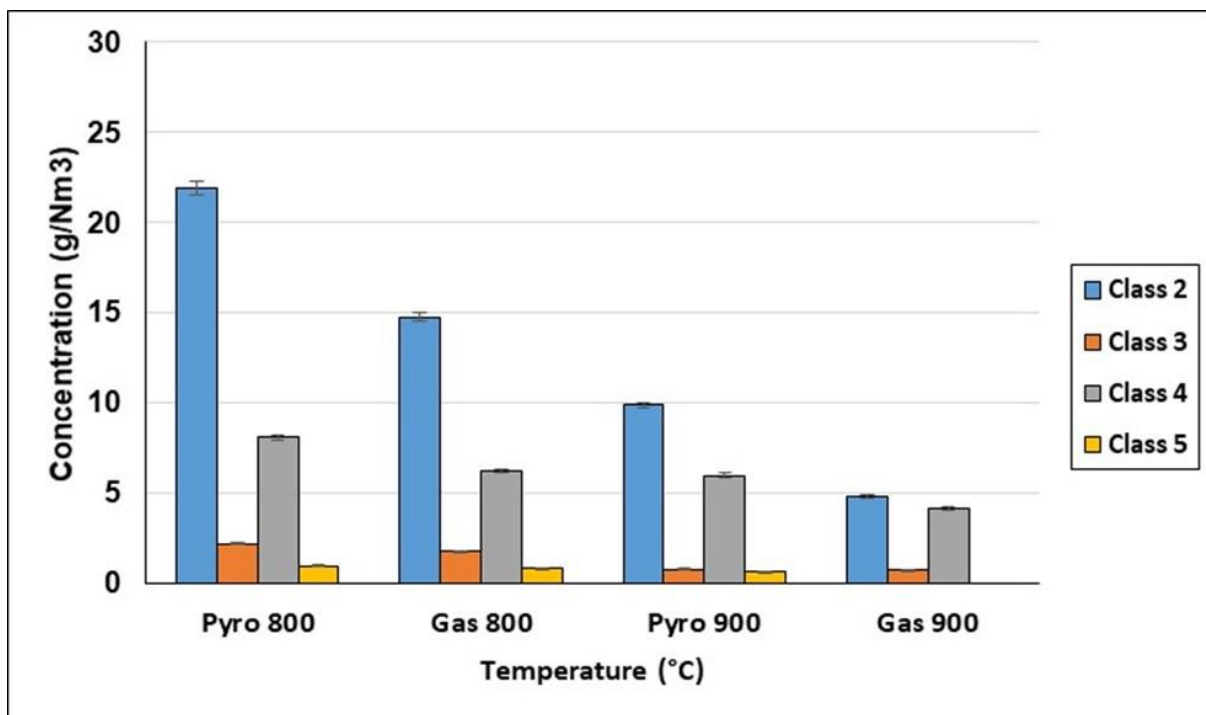


Figure A3.12. Tar concentration organized by class type for pyrolysis and CO₂ gasification at 800°C and 900°C.

In summary, the presence of the gasification agent favored the production of syngas by increasing the content of H₂ and CO due to the conversion of biochar and tar molecules. Despite this, the number of impurities and the remaining biochar still elevated. Due to this, the potential use of a catalytic bed in order to reduced tar concentration and the study of the effect of reducing the particle size might be evaluated in order to determine their influence in product distribution.

A3.1.4 Effect of biomass particle size in products distribution

An investigation of the effect of varying biomass particle size was performed in order to provide details of the product distribution and the optimum diameter of the particle. In **Figure A3.13** has presented the mass balance of the gasification of biomass in a diameter range from 1.5 mm to 6 mm (pellet size). The gasification was performed at the highest temperature of 900°C, using sand as bed material, CO₂ as a gasification agent and a residence time of 15.2 s. As can be seen, the principal variation was achieved with the lowest particle size to 4 mm, for syngas and biochar.

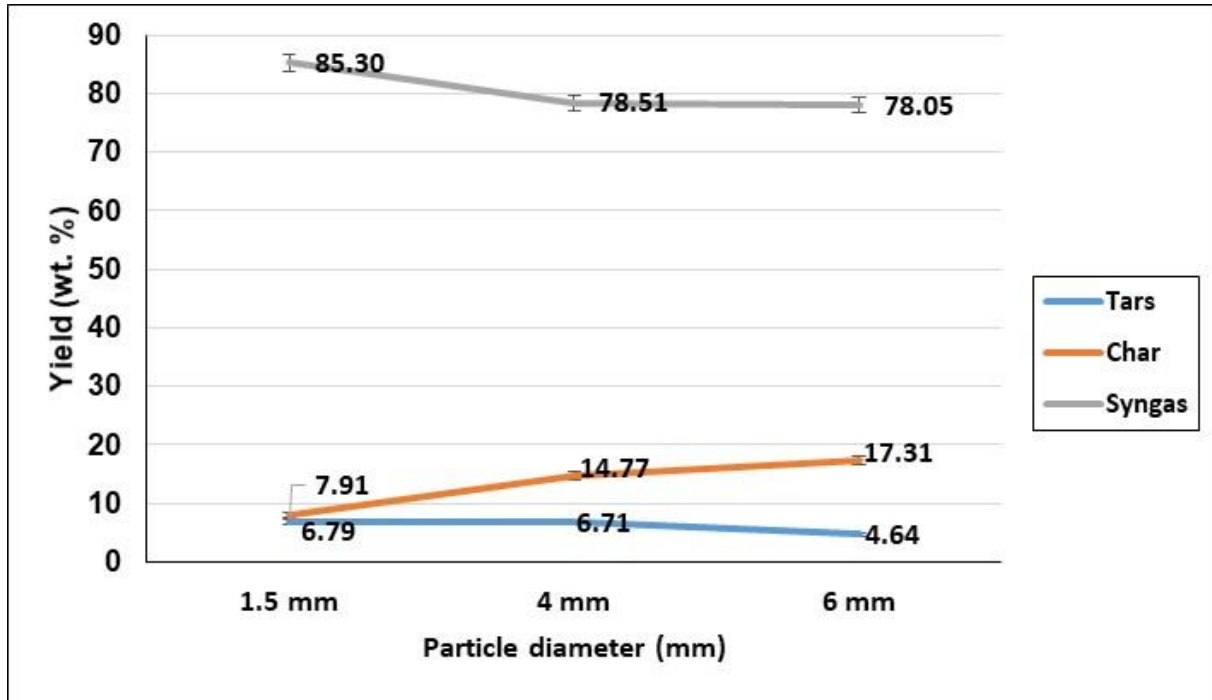


Figure A3.13. Effect of biomass particle size in product distribution in gasification with CO₂ at 900°C.

Biochar

As can be observed by reducing the diameter of the particle from pellet size (6 mm) to 1.5 mm, the biochar conversion was increased. At 900°C, the unconverted char was reduced from 17.31 wt.% to 7.91 wt. %. This meant that in terms of biochar conversion, the reduction of the particle size allows the gasification agent to rapidly penetrate particle structure due to the increase of the contact area between the agent and the fuel. Another explanation for this was that by reducing the particle size lower heat and mass limitations were present in the iteration due to the presence of porous and less fibrous biochar [228]. **Figure A3.14** shows the practical example of the CO₂ molecules surrounded biomass for high and low particle sizes. This evidence how CO₂ molecules could be limited by the internal and external diffusion effects contrary to a low particle size where CO₂ molecules have a shorter path in the particle and react faster due to lower thermal and mass resistance.

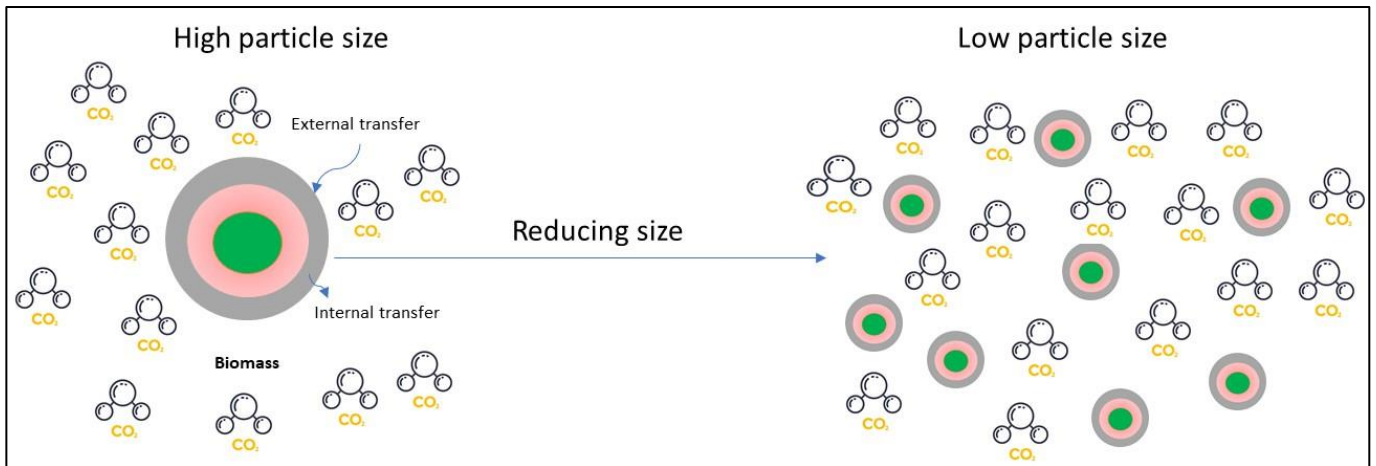


Figure A3.14. Example of gasification atmosphere for low and high particle size.

Syngas

Syngas yield was increased with the reduction of the particle size, for a diameter of 1.5 mm the syngas represented 85.3 wt. % of the mass balance of products. In **Figure A3.15** can be observed the volumetric flow rate of syngas components as a function of the biomass particle size. The volume rate of CO and H₂ reached the highest volume rate with the lowest particle size, in which CO represented the highest rate. The fact that syngas yield was increased with the reduction of biomass diameter can be explained by two statements. The first one is that by reducing the particle size the heat source penetrated efficiently into the particle structure provoking the high release of volatile matter, which included syngas components. The second statement is that the reduction of particle size favored the heterogeneous reaction of biochar and gasification agent, due to this higher conversion of biochar was obtained, hence syngas yields increased. **Figure A3.16** illustrates biomass particle structure schematic.

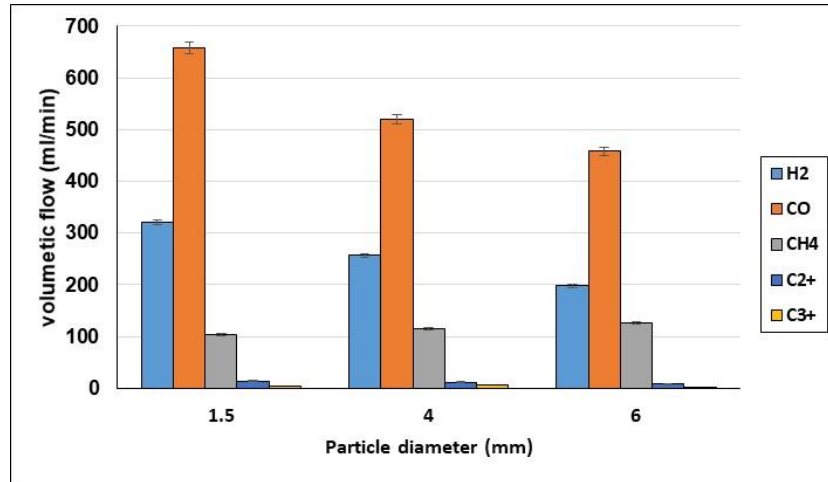


Figure A3.15. Effect of biomass particle size in the volumetric flow rate of syngas components. Gasification with CO₂ at 900°C.

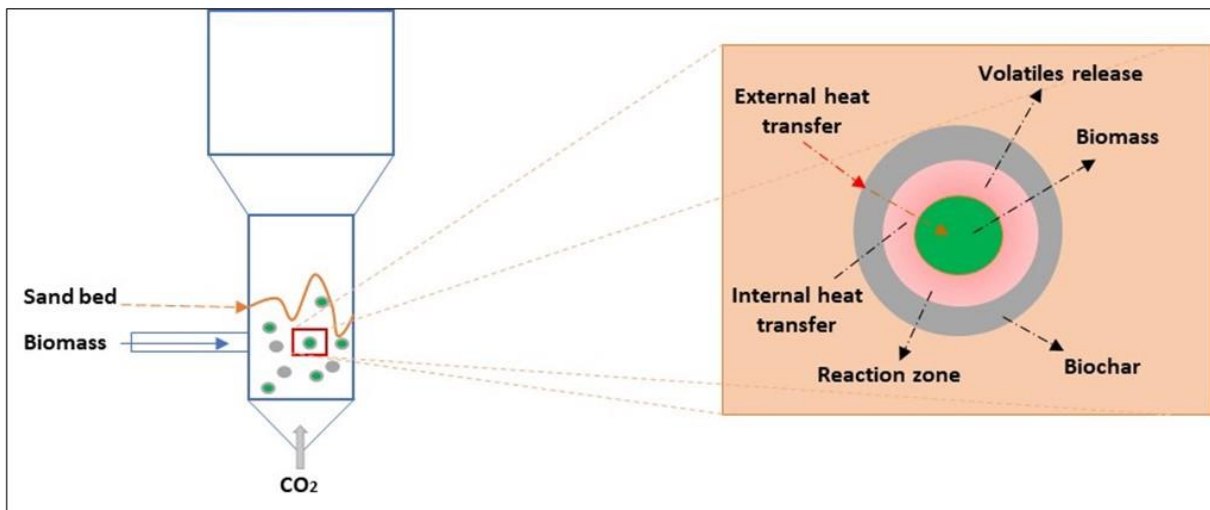


Figure A3.16. Schematic of biomass particle structure.

Tar

As the previous mention in the syngas discussion, the heat source penetrated efficiently into the biomass structure provoking a higher thermochemical conversion and at the same time a higher release of volatile matter. The release of volatiles comes with syngas components and organic molecules such as tar. Due to this, it was observed that the yield of tar was higher when the particle size was reduced. **Figure A3.17** and **A3.18** shows the evolution of the tar concentration in the syngas with the particle size. The conversion of biomass pellet size

showed the lowest concentration of tar molecules with 10.9 g/Nm³ at 900°C, on the other hand, 1.5 mm biomass results showed a concentration of 21.44 g/Nm³, approximately 2 times higher.

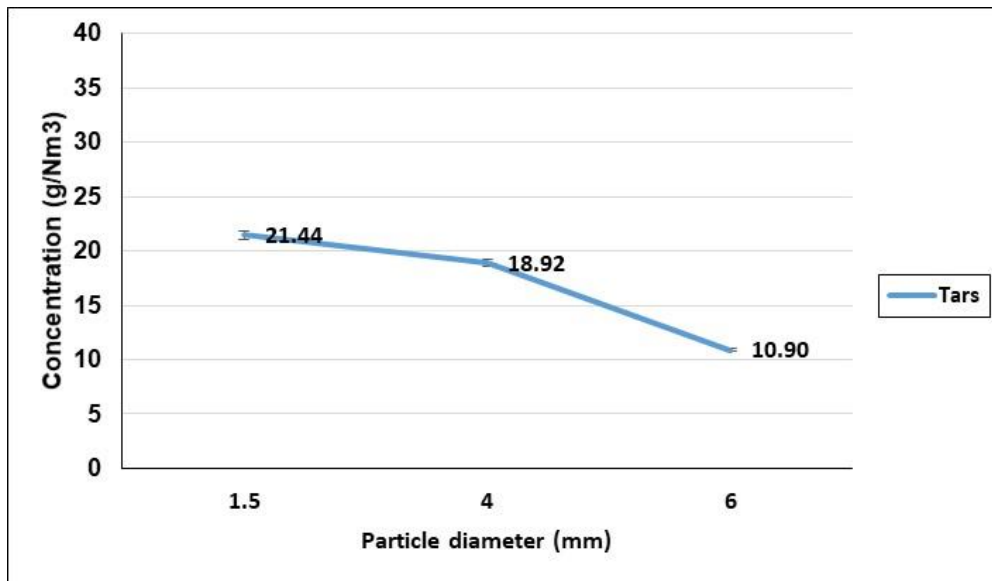


Figure A3.17. Effect of particle size in tar concentration in syngas.

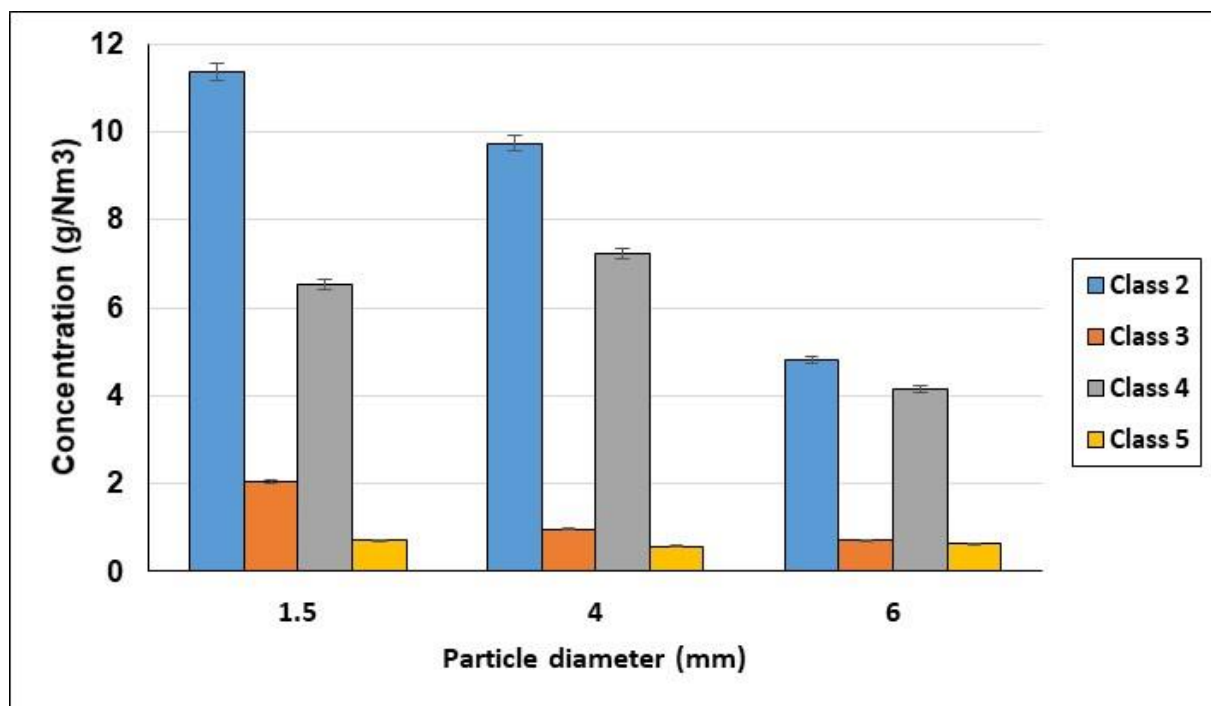


Figure A3.18. Effect of particle size in tar classification distribution. Gasification with CO₂ at 900°C.

In the optimization of biomass gasification parameters, the selection of the correct particle size requires very critical evaluation. As it was observed by reducing the particle size the syngas

yield was increased, and the biochar conversion was higher, meanwhile, the quality of the syngas was reduced to the presence of higher organic matter. Consequently, a choice must be done by selecting a higher production of syngas with low quality or lower syngas yield with higher quality. On the other hand are the mechanical operation conditions, the use of lower particle size in fluidized bed increase the probability of training particles out the reacting zone. The use of higher particle size can lead to the defluidization of the bed [229] and also requires high fluidization velocities.

A3.1.5 Effect of biochar bed quantity in products distribution

The effect of the use of biochar as a bed material in the gasification of biomass was investigated in the following section. The experimental test was performed at 900°C, with four different amounts of biochar in the fluidized bed, 0 g (only sand bed), 4 g, 8g and 12 g. The residence time of gases was 15.2 s, in order to assure good fluidization of biochar particles with biomass. In **Figure A3.19** can be observed the evolution of the yield of the products with the quantity of biochar. A uniform tendency was observed with the quantity of biochar from 0 g to 12 g, for syngas, biochar and tar.

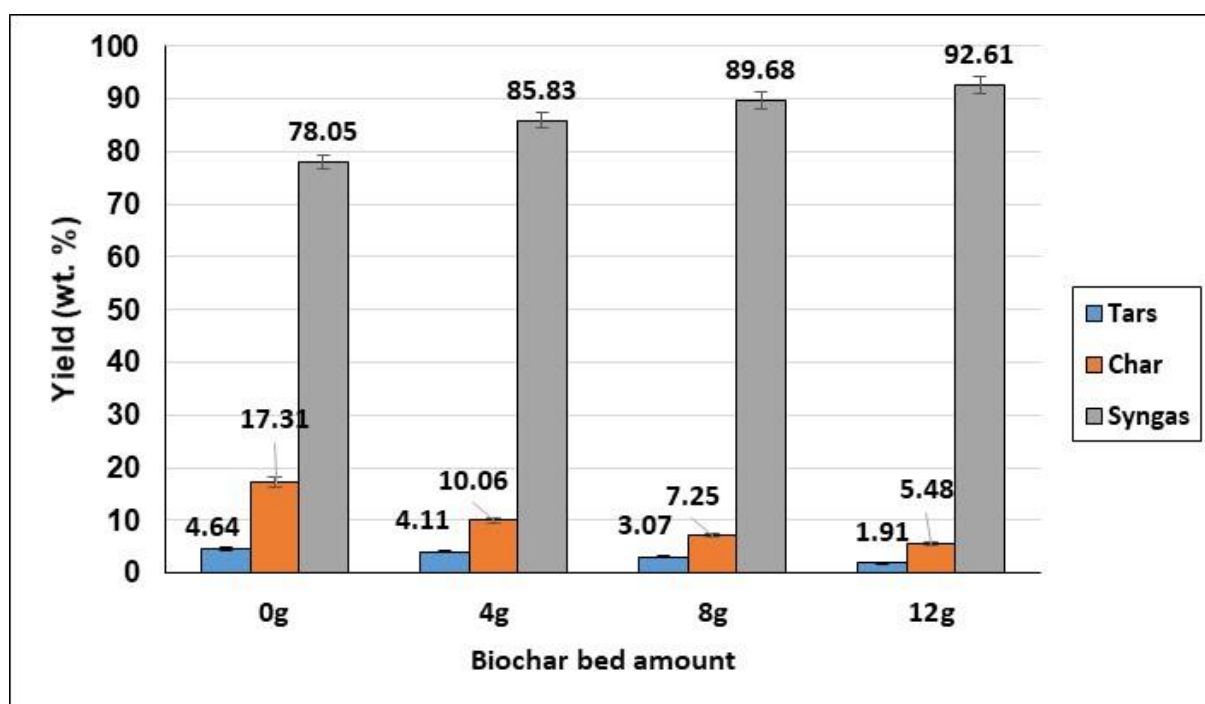


Figure A3.19. Effect of biochar bed quantity in product distribution. Gasification with CO₂ at 900°C.

Biochar

As biochar was also a product in the gasification of biomass, the following procedure was adopted in order to calculate the biochar yield,

$$\text{Biochar yield (wt.\%)} = [m_{\text{Final}} - m_{\text{bed}}] / m_{\text{biomass}} * 100 \quad \text{Eq. A3.3}$$

Where m_{Final} , m_{bed} and m_{biomass} , were the total mass of biochar obtained after the test, the initial mass of biochar bed and the total fed biomass in the experiment. This method was employed in order to facilitate the task of calculating biochar yield, by considering that a biochar make-up was present and only biomass biochar was consumed. As can be seen, the yield of biochar was reduced as a function of the amount of bed. This consumption of biochar was mainly due to the Boudouard reaction with the introduced char and the gasification agent and the possible gasification reactions with the newly formed gaseous components after the catalytic cracking of tar with the bed.

Syngas

The syngas yield increased significantly with the increase of the amount of biochar in the fluidized bed, from 78.05 wt. % to 92.61 wt. %. This meant that with a 12 g biochar bed the only 7.39 wt. % of the total biomass was not able to be converted into syngas. The obtained syngas was mainly represented by CO, and its molar concentration increased as a function of the biochar bed height as can be observed in **Figure A3.20**. The molar fraction of H₂ was significantly reduced with the increase of biochar mass, this meant that the Boudouard reaction was the most dominant chemical reaction. **Figure A3.21** illustrates the specific volumetric rate for individual syngas compounds obtained in the process. The highest volumetric flow rate of products was obtained with 12 g of biochar bed, 1115.12 ml/min compared to 424.5 ml/min with sand only as bed material. In general, there was an increase of the three principal syngas components, except that for H₂ and CH₄ the increase was not as significant as for CO.

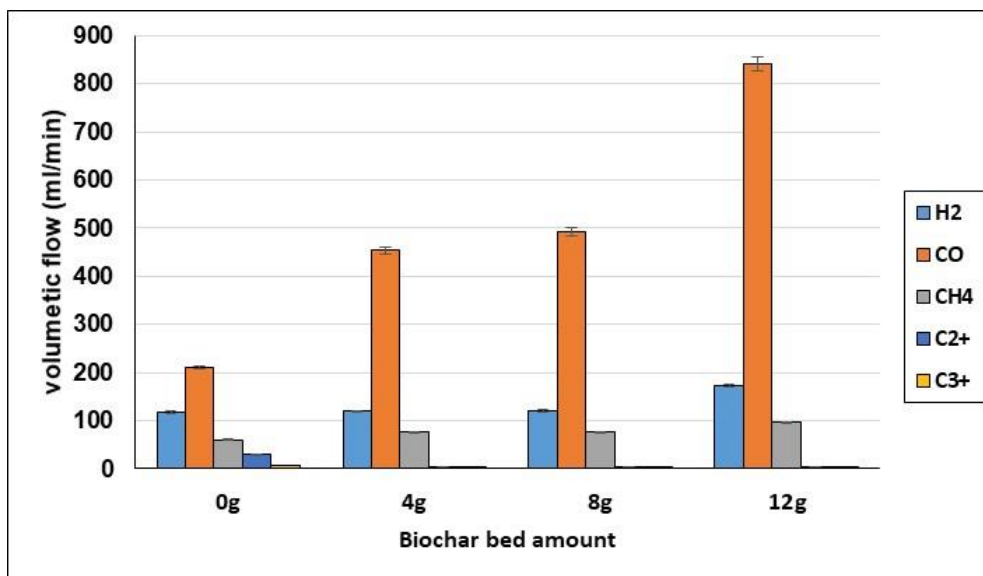


Figure A3.20. Effect of biochar bed quantity in syngas components molar fraction. Gasification with CO₂ at 900°C.

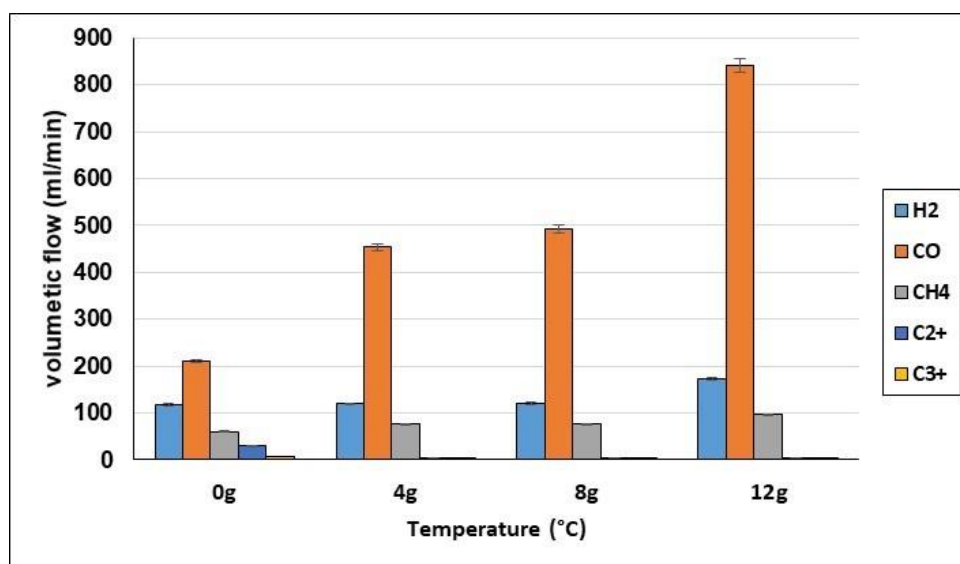


Figure A3.21. Effect of biochar bed quantity in syngas components volumetric flow rate. Gasification with CO₂ at 900°C.

Tar

The tar yield decreased from 4.64 wt. % to 1.91 wt. % with the increase in the amount of catalytic bed. The tar molecules were converted into lighter molecules and reduced their concentration in the produced syngas. **Figure A3.22** shows the evolution of the tar concentration in the syngas and the conversion values concerning sand bed. Normal fluidized bed gasification shows a concentration value of 15.24 g/Nm³ using sand as bed material, this

value was reduced to 5.73 g/Nm³ for the conversion of approximately 62.4 %. The value was coherent with the concentration range [at 900°C, 60 – 70 % conversion] claimed in the literature using biochar for catalytic cracking [230], [231].

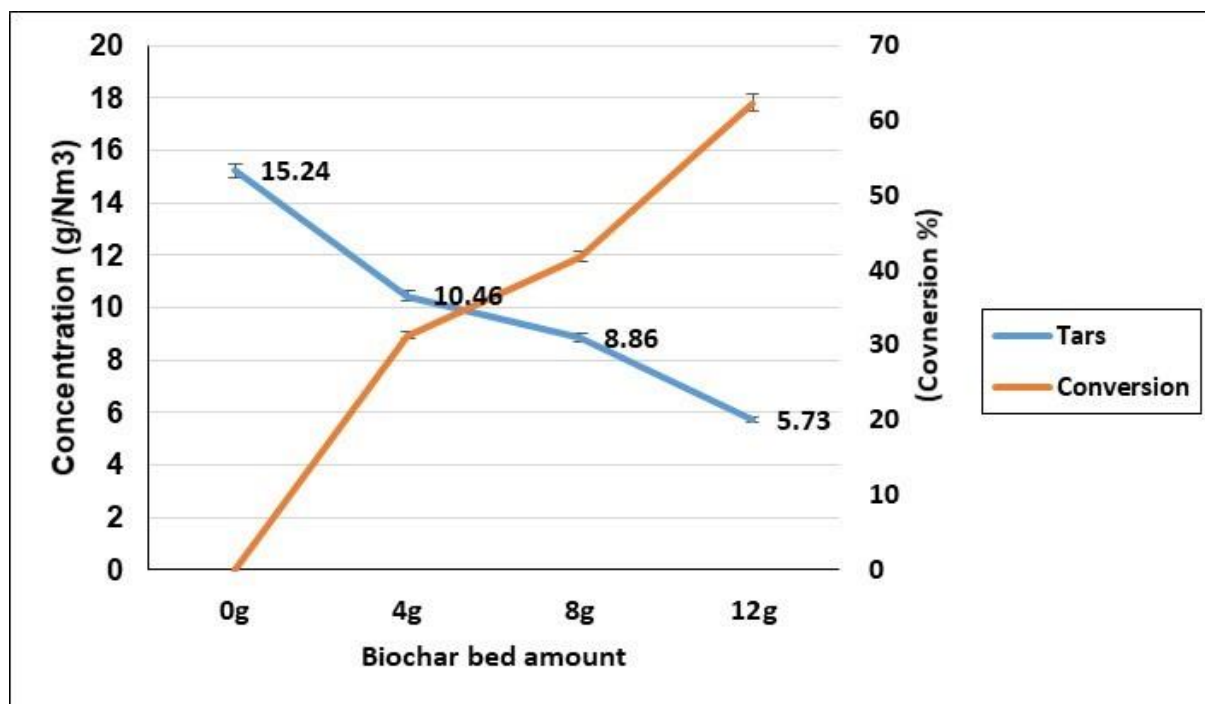


Figure A3.22. Effect of biochar bed quantity in tar concentration and conversion. Gasification with CO₂ at 900°C.

In **Table A3.1** was illustrated the complete liquids products obtained from the experimental tests. As can be observed with the increase of bed quantity the mainly tar compounds concentration decrease. Phenols, HAC and naphthalene remained as the main tar compounds present. It was found in the literature that these compounds individually can be highly cracked at this temperature (900°C) with the use of biochar [232]–[234], meanwhile, the presence of other molecules could generate competitiveness and inhibition in the cracking reaction [235].

Table A3.1. Effect of biochar bed quantity in tar groups concentration (g/Nm³) in syngas. Gasification with CO₂ at 900°C.

Group	Biochar bed quantity (g)				Class
	0	4	8	12	
Phenols	3.82	2.01	1.77	1.13	2
Furans	0.57	0.79	0.62	0.45	
HAC	3.17	1.82	2.16	1.35	
AC	0.99	0.34	0.76	0.23	3
LPAH	1.86	1.29	0.72	0.61	4
Naphthalene	3.35	3.53	1.90	1.02	
HPAH	0.87	0.39	0.25	0.19	5
Others	0.61	0.30	0.68	0.73	Others

As discussed in this section, the use of biochar as catalytic bed material favored the reduction of tar, showing its effectiveness. It was also able to increase syngas production due to the formation of lighter molecules from tar. On the other hand, a make-up reposition of biochar was needed due to its consumption with CO₂. The efficacy of biochar was now proven with an optimum amount of 12 g bed in presence of CO₂. It is well known that the CO₂ atmosphere activates biochar and increases its catalytic activity, the following section has of interest to evaluate the effect of varying temperature and also varying gasification agent to steam with a 12 g biochar bed. The latest was done in order to determine the most efficient gasification agent and the most effective thermal condition for tar conversion.

A3.1.6 Effect of varying gasification agents using biochar as bed material.

In this section it was investigated the effect of varying the gasification agents steam and CO₂ in a temperature range of 600°C and 900°C, using biochar as bed material. Both gasification agents are known as biochar activators [183] and favor the heterogeneous cracking of tar molecules. **Figure A3.23** and **Figure A3.24** show the obtained product distribution in the gasification of biomass at different temperatures using steam and using CO₂ with a 12 g biochar bed. The products obtained from the use of both gasification agents followed the same tendency. Tar and biochar yield decreased and syngas yield increased with the evolution of the temperature for both gasification agents.

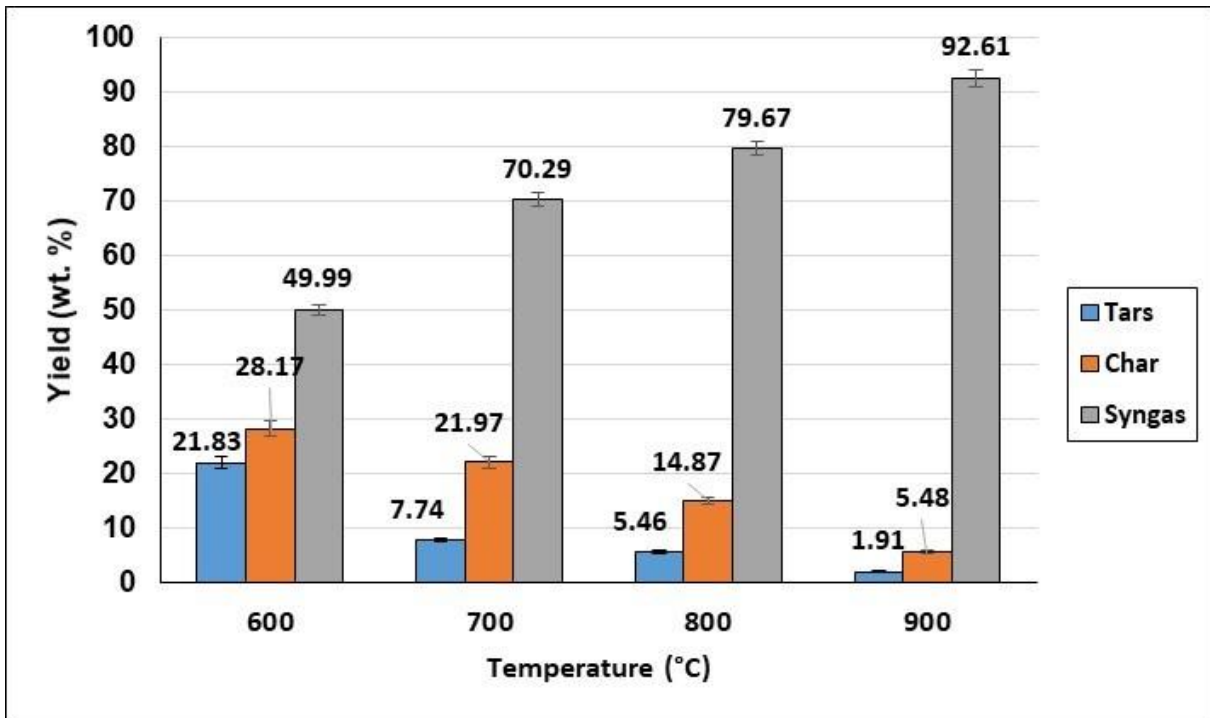


Figure A3.23. Effect of temperature in gasification with CO_2 using biochar as bed material.

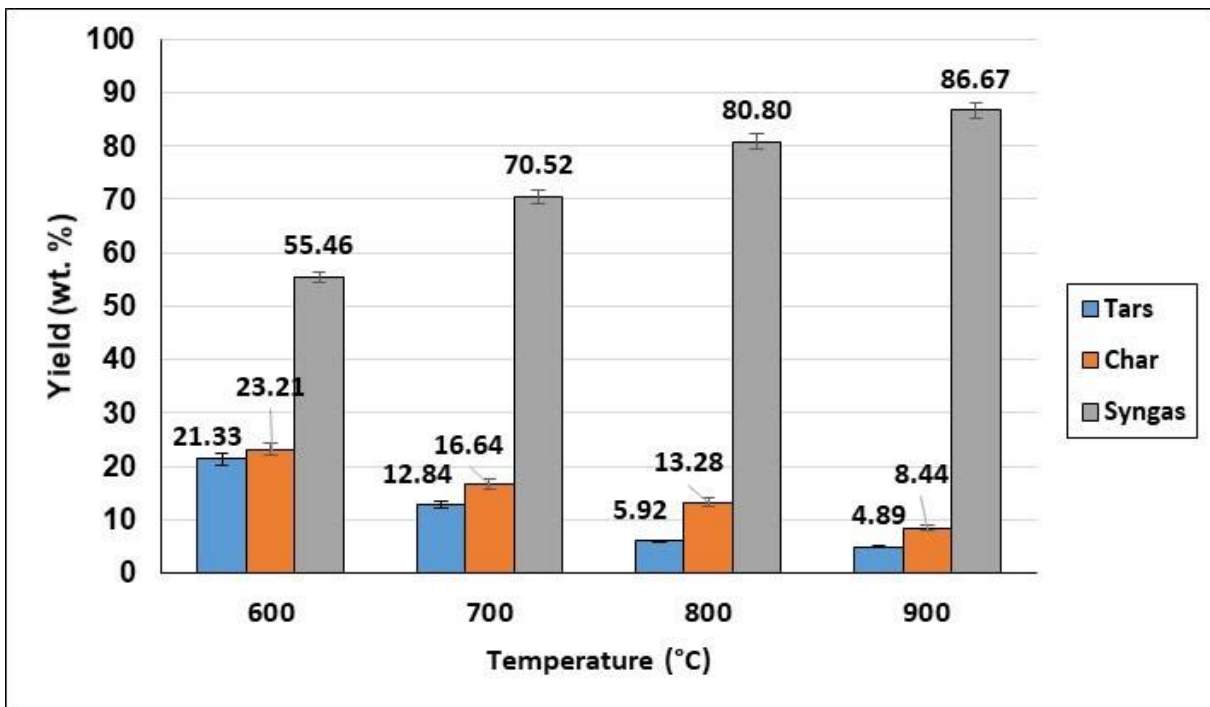


Figure A3.24. Effect of temperature in gasification with steam using biochar as bed material.

Biochar

Comparing both results it was observed that at a temperature from 600°C to 800°C, biochar conversion was higher with steam than with CO₂. Biochar reactivity was higher with steam than with CO₂ gasification, this statement has been widely studied in the literature [138], [236], [237] explaining that in steam gasification there is higher retention of Alkali and alkaline earth metals. These metals are known as catalyzers for carbon conversion in char gasification. Also, steam gasification leads to the formation of a char with higher porosity [168], allowing upcoming H₂O molecules a higher reactive atmosphere than CO₂ gasification.

Despite this, at 900°C higher char conversion was obtained for CO₂ gasification than for steam gasification which could be contradictory with the statement explained previously. Meanwhile, these statements have the supposition that only one principal reaction was taking place in the gasification atmosphere, carbon with the gasification agent. At this was not exactly the case in this study, secondary reactions were taking place in parallel with the gasification reaction. This could be one of the reasons for the inverted trend at this temperature.

Syngas

The syngas yield from both gasification agents showed to increase with the temperature as it was also observed in **Section A3.1.1**. The difference in total yield from both gasification agents was between 0.23 wt. % to 5.94 wt. %. Evidencing that in terms of syngas production both gasification agents have similar values. **Figure A3.25** shows the molar fraction obtained for both gasification agents at different temperatures. As illustrated CO₂ gasification produced practically a mono-component syngas in which the wide majority was CO, due to Boudouard reaction and tar dry reforming reaction. While for steam gasification the syngas product was more diversified, at low temperature 600°C – 700°C, CO showed significant mol fraction of approximately 60%, then with temperature increase, char and tar reforming was privileged and H₂ content increased meaningfully.

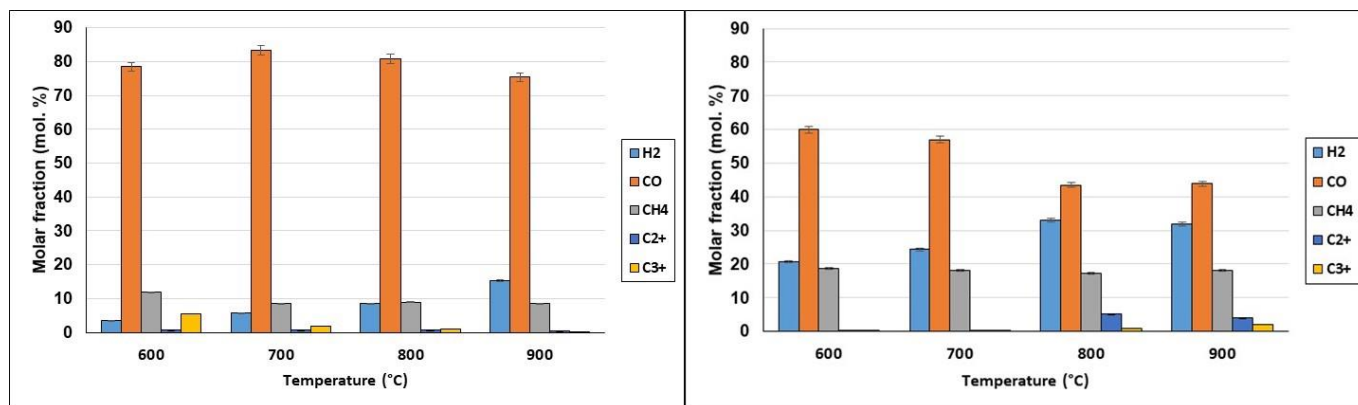


Figure A3.25. Effect of temperature in syngas components molar concentration with steam and CO₂ using biochar as bed material.

Table A3.2 shows the H₂/CO ratio for both gasification tests. As observed the tendency showed that the H₂/CO ratio increased with the temperature. Despite this, the molar rate of CO in CO₂ gasification stayed very significant and predominant, meanwhile, for steam gasification, the H₂ content became more important as temperature increased.

Table A3.2. Effect of temperature in H₂/CO ration for CO₂ and steam gasification.

Temperature (°C)	CO ₂ gasification	Steam gasification
600	0.05	0.35
700	0.07	0.43
800	0.11	0.76
900	0.20	0.73

Tar

The evolution of the tar concentration in the syngas with the temperature and the use of biochar as bed material was illustrated in **Figure A3.26** for both gasification agents. As can be seen, the amount of tar showed its highest value at a low temperature (600°C), 192.1 g/Nm³ and 130.89 g/Nm³, for CO₂ and steam gasification respectively. Tar was highly concentrated in CO₂ gasification at this temperature, due to the high amount of oxygenated aliphatic compounds compared to steam gasification. Aliphatic compounds such as acids, esters, alcohols and aldehydes represented approximately 70% (135.42 g/Nm³) of the tar concentration value, for CO₂ gasification. Meanwhile, for steam gasification, approximately 60 % of the tar value was represented by aliphatic compounds (81.73 g/Nm³).

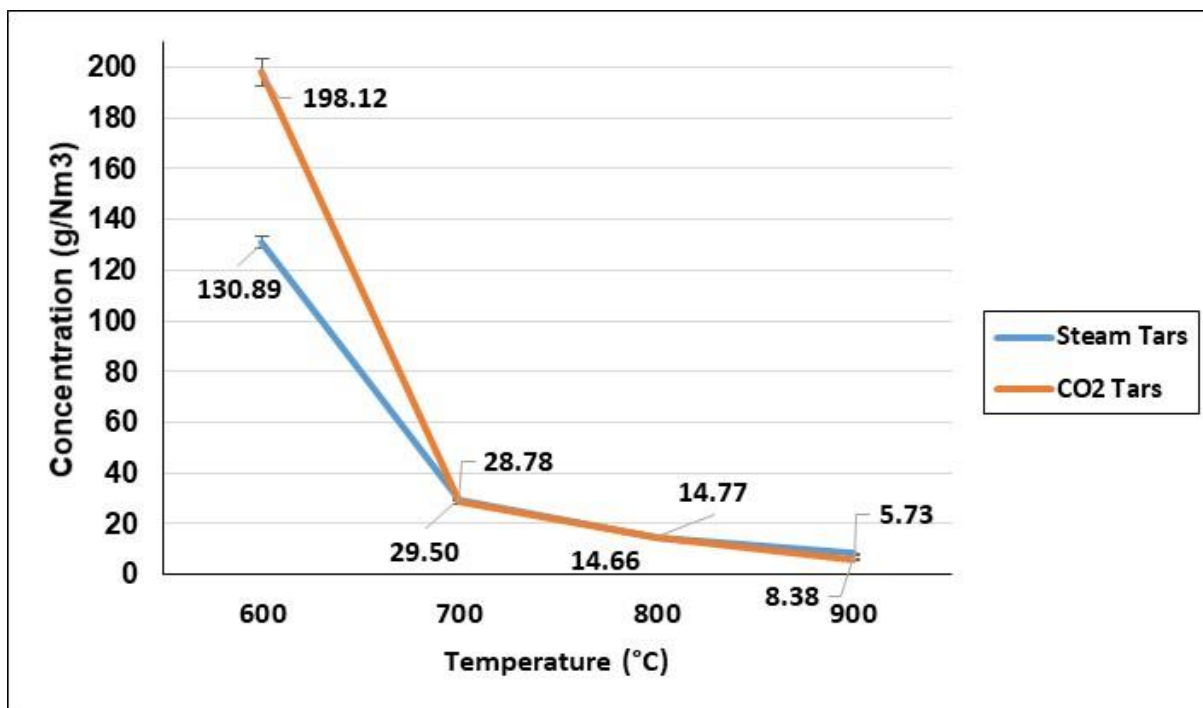


Figure A3.26. Effect of temperature in tar concentration for CO₂ and steam gasification.

At 600°C, the products obtained from thermochemical decomposition of biomass comprise a high content of oxygenated aliphatic molecules, such as acids, esters, phenols, alcohols, ketones and others. Meanwhile, as temperature increases these compounds were converted into lighter molecules, water and gases, due to the low thermal resistance [238]. The fact that at this temperature CO₂ gasification showed higher aliphatic compounds than steam gasification could be explained by the following reason: the presence of steam in gasification has been proven that improves the porous structure of the biochar and this helps to trap and remove OH groups (acids, ketones, aldehydes and others.) from the biochar surface, easier than with the presence of CO₂ [183]. Zhang et al. [239] studied the effect of biomass decomposition in different gaseous atmospheres in a fluidized bed, the authors also showed that the presence of CO₂ favored the formation of acids, aldehydes and ketones compared to the other conditions.

As the temperature increased from 700°C to 900°C, the concentration of tar in the syngas was very similar for both gasifications. This could mean that the effectiveness of both gasification agents with biochar was very similar at these temperatures, or that the gasification agent has a low impact in tar cracking in the presence of biochar. In order to validate the effectiveness of the use of both gasification agents and biochar, it was compared with the results of gasification when sand as bed material.

Figure A3.27 shows the conversion curve as a function of the temperature of gasification with biochar vs gasification with sand for both agents. As was illustrated a higher conversion was achieved with steam gasification at 600°C compared with CO₂. Meanwhile, this was the opposite at high temperature where CO₂ presence showed to have a higher impact on tar cracking. The maximum conversion was achieved at 700°C, where both gasification agents were able to crack approximately 70% of the tar molecules, compared with sand gasification. it was observed that the majority of the remaining aliphatic and oxygenated molecules were cracked at 700°C, due to this it was seen a high reduction of tar molecules.

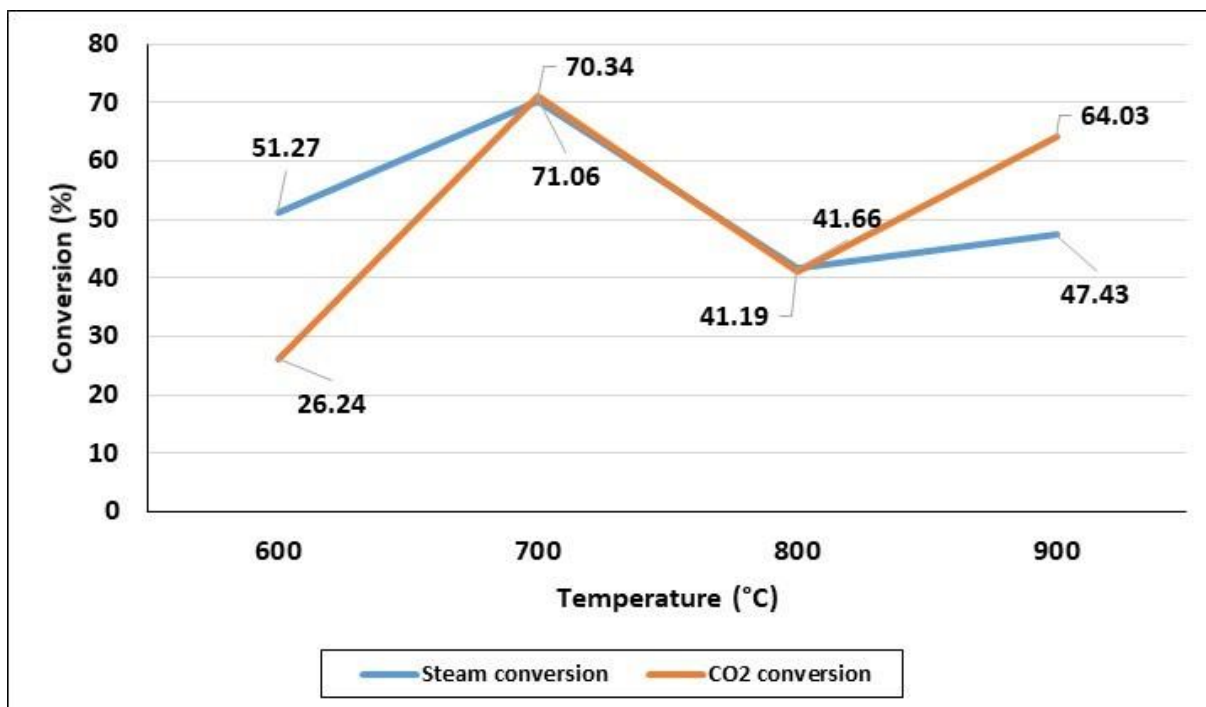


Figure A3.27. Effect of temperature in the conversion of tar molecules for steam and CO₂ gasification.

At 700°C and 800°C the conversion was identical for both gasification agents, which might be translated that the credits for the conversion of tar molecules could be mainly attributed to biochar. Despite this, a significant difference was observed at 900°C with the use of CO₂. The gasification atmosphere with CO₂ showed to be more efficient in tar cracking at this temperature compared with steam. This investigation proved that for high-temperature CO₂ with biochar gasification was more efficient than steam. Despite that the maximum conversion was achieved at 700°C, the most critical and thermal stable tar molecules are present at high temperatures. Hence it could be more valuable the evaluation of conversion at high than for low temperatures.

Appendix A4

This section included the tables and figures that were not included in **chapter 5**.

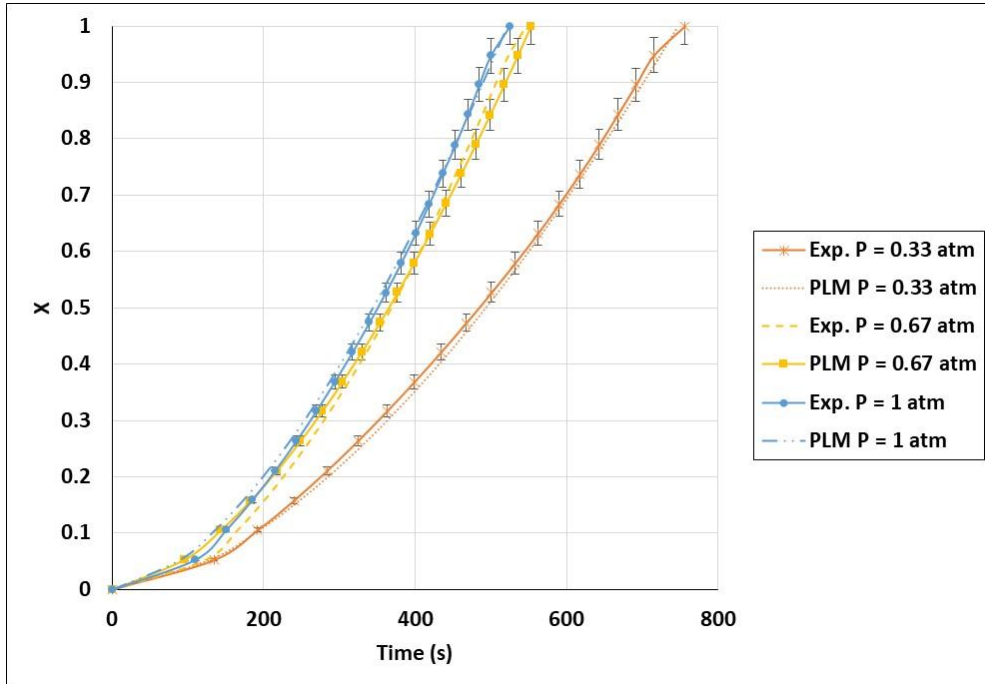


Figure A4.1. Validation of conversion curves of experimental test and power-law model (PLM), partial pressure effect, Temperature 1000°C and CO₂/C ratio 10.5.

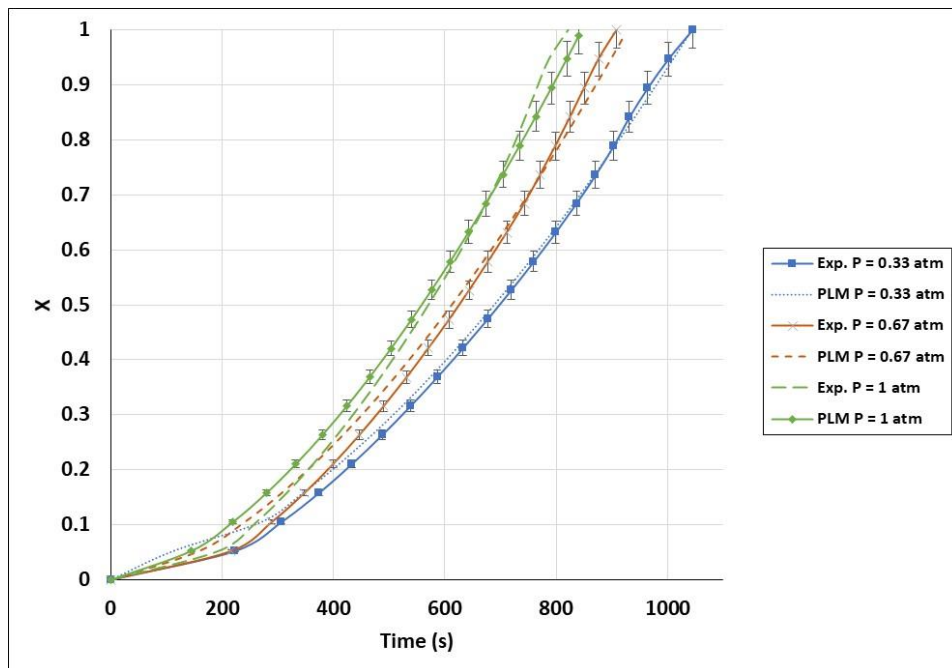


Figure A4.2. Validation of conversion curves of experimental test and power-law model (PLM), partial pressure effect, Temperature 1000°C and CO₂/C ratio 3.5

Table A4. 1. Kinetic models for biochar gasification with CO₂, in TGA and FBR.

Reference	Kinetic mode: dx/dt (s-1), A (atm-n s-1)	Char used	Type of reactor
Gomez-Barea (2006) [132]	$dx/dt = 1.993 \cdot 10^3 \exp(-129.79/RT) P_{CO_2}^{0.4} (1-x)$	Wood	TGA
Van de Steene (2011) [194]	$dx/dt = 1.2 \cdot 10^8 \exp(-245/RT) P_{CO_2}^{0.7} (90.90x^5 - 187.23x^4 + 135.12x^3 - 40.59x^2 + 5.55x + 0.65)$	Wood	TGA
Diedhiou (2019) [192]	$dx/dt = 7.7 \exp(-126.80/RT) P_{CO_2}^1 (1-x)$ $dx/dt = 53.3 \exp(-124.4/RT) P_{CO_2}^1 (1-x)^{2/3}$	Palm wood	TGA
De Groot (1982) [193]	$dx/dt = 2.59 \cdot 10^6 \exp(-221.75/RT) P_{CO_2}^{0.62} (1-x)$	Wood	TGA
Kreitzberg (2016) [240]	$dx/dt = \{[(1.43 \cdot 10^6 \exp(-236/RT) P_{CO_2})] / (1 + [(1.43 \cdot 10^6 \exp(-236/RT) / 4.33 \cdot 10^8 \exp(-163/RT)]) (1-x)^{2/3})\}$	Wood	FBR
Matsui (1987) [195], [241]	$dx/dt = \{[(4.89 \cdot 10^{13} \exp(-268/RT) P_{CO_2})] / [1 + (0.658 \cdot P_{CO_2})] (1-x)\}$	Wood/Coal	TGA/FBR
Yuan (2011) [123]	$dx/dt = 8.464 \cdot 10^5 \exp(-202.9/RT) P_{CO_2}^n (1-x) [1 - 12.60 \ln(1-x)]^{1/2} (1 + 1.29x)^{2.04}$	Pine Sawdust	FBR
Mueller (2015) [134]	$dx/dt = 3.88 \cdot 10^5 \exp(-175/RT) P_{CO_2}^{0.59} (1-x)$	Wood	FBR